

**Institut für  
Wasserwirtschaft und Kulturtechnik  
Universität Karlsruhe (TH)**

---

**Towards Decision Support Models for an Ungauged  
Catchment in India, the Case of Anas Catchment**

**Anupam K. Singh**

**Heft 225**

---

Mitteilungen des Instituts für Wasserwirtschaft und Kulturtechnik  
der Universität Karlsruhe (TH)  
mit "Theodor-Rehbock-Wasserbaulaborium"  
Herausgeber: Prof. Dr.-Ing. Dr. h. c. mult. Franz Nestmann, Ordinarius

---

**2004**

**Towards Decision Support Models for an Un-gauged Catchment  
in India, The case of Anas catchment**

Zur Erlangung des akademischen Grades eines

DOKTOR-INGENIEURS

von der Fakultät für  
Bauingenieur-, Geo und Umweltwissenschaft  
der Universität Fridericiana zu Karlsruhe (TH)

genehmigte

DISSERTATION

von  
M. Sc. Anupam K. Singh

aus Kanasi/ Indien

Tag der mündlichen Prüfung: 26. 05. 2004

Hauptreferent: Prof. Dr.-Ing. Dr. h.c. mult. Franz Nestmann  
Korreferenten: Prof. Dr.-Ing., Dr. rer. nat. Andras Bardossy

Karlsruhe, 2004

## **Acknowledgement**

Only the timely support of Prof. Dr.-Ing., Dr. h.c. mult. Franz Nestmann has enabled me to successfully perform this research work at Institute for Water Resources Management, Hydraulics and Rural Engineering (IWK). He has co-operated and motivated me during difficult moments and provided financial support in spite of no external research funding.

My thanks are due to Prof. Dr. rer. nat., Dr.-Ing. Andras Bardossy for his invaluable comments, in-depth understanding and moral support in improving several loosely written parts of this research work. His supervision strengthened my confidence and professional abilities.

Over the last 2-years the entire hydrology group at IWK provided a warm and friendly working atmosphere, be it exchange of professional ideas or introduction to new scientific tools. Dr.-Ing. Jurgen Ihringer and my colleagues Marcus Casper, Dr. Charlotte Kämpf, Falk Lindenmaier, Martin Helms, Wolfram Schädel, Rolf Becker, Jutta Szabadics, Oleg Evdakov, Andrea Blatter, Joachim Liebert, Bruno Buechle, and Patric Preuss for their day-to-day help related to Geographical Information System (GIS), hydrologic modelling, remote sensing and database management. Mrs. Kay Dietner took the responsibility of correcting my Indian English and Resources Engineering office including its current and former staff for their all time help for daily life. Besides the professional skills, I am grateful to all of them for the common time in which they introduced me with the fascinating nature and culture of German folks and particularly of the Baden and Black Forest region. Although this was a wondrous and lengthy journey, but will be fondly remembered in years to come.

I am very much thankful to Dr.-Ing. Erwin Zehe, Junior Professor at University of Potsdam (formerly at Institute of Hydraulics Engineering at University of Stuttgart) and Dr. Jens Lange, Institute of Hydrology, Albert-Ludwigs University of Freiburg im. Brs. for sharing the responsibility of translating my research vision through their professional support in explaining the complex models, model parameters and structures during our several untiring meetings in Stuttgart and Freiburg during 2002 and 2003 without asking any service in return. Also thanks for Dr. Thea Vogt from University of Strasbourg, France for introducing me the basics of remote sensing and the art of digital image classification.

My special thanks to Mr. Salilendra K. Shrivastav and Mr. A.N. Borbankar from State Water Data Centre, Water Resources Department at Bhopal for their efforts in organising the rainfall and discharge data and their encouragement for initiating water resources research in this virgin Anas catchment. Ms. Meera Shahi and Mr. P.S. Sodhi both from Gramin Vikas Trust Jhabua believed in my concept and established a pilot hydrological measurement station in Kanjawani mili-watershed since June 2002. Also due thanks to Prof. Dr. Eldho T. Iype from Civil Engineering Department at Indian Institute of Technology (IIT) Bombay for supporting my research ideas and exposing them to the larger research community in India. Our research co-operation has been recognised as we won the best poster award from Stockholm International Water Institute (SIWI) during 2002 World Water Week in Sweden. Thanks to Mr. Wasim Akhtar former District Collector of Jhabua for providing much needed logistics during two field visits.

I am thankful to Ministry of Science, Research and Culture (MWK) Baden-Württemberg for sponsoring my most of the stay in Karlsruhe, German Academic Exchange Service (DAAD) for sponsoring few field visits to India and Karlsruher Hochschulvereinigung (KHV) for partial financial assistance for buying digital satellite data of Landsat TM from United States Geological Survey (USGS).

Last but foremost appreciation to my wife Rachna Gangwar for her constant support, lot of sympathy and financial backing in completing this research work. Finally, this work is dedicated to late my father and teacher (1936-2003) who always dreamed best in me for improving the miserable life of rural folks in India.

Anupam K. Singh

Karlsruhe, May 2004

## Contents

Forward

Acknowledgement

Abstract

Page

### **Chapter 1: Introduction**

1.1	Research objectives and model structure	3
1.2	Research outline and end users	6
1.3	Decision support models	
1.3.1	Need for DSMs	8
1.3.2	Concept of DSM	9
1.3.3	Classification of decisions support models	10
1.4	Review of decision support models	11

### **Chapter 2: Research Project Settings**

2.1	General characteristics of India	
2.1.1	Climate and agro-climatic zones	16
2.1.2	Water resources distribution and drainage basins	17
2.1.3	Water resources use and potential	18
2.1.4	Socio-economic development	20
2.2	Characteristics of Anas catchment	
2.2.1	Location of Mahi basin	20
2.2.2	Location of Anas catchment	22
2.3	Topography and drainage profile	23
2.4	Rainfall and climate	24
2.5	Land cover and land-use	27
2.6	Soils and geology	27
2.7	Hydrology and water resources	30
2.8	Socio-economic characteristics	33

### **Chapter 3: Catchment Modelling and Database Development**

3.1	Catchment modelling	
3.1.1	Classification of catchment models	35
3.1.2	Structure of catchment model	36
3.1.3	Selection of catchment models	38
3.2	Catchment modelling with GIS and remote sensing	
3.2.1	SCS-CN runoff model	40
3.2.2	Catchment water balance model	42
3.3	Generation of thematic maps and GIS database	44
3.4	Surface modelling with TIN	
3.4.1	Data source and surface analysis	48
3.4.2	Conversion of TIN into DEM	48

3.5	Digital Elevation Model (DEM)	
3.5.1	Data for DEM modelling	49
3.5.2	Interpolation methodology and results	49
3.5.3	DEM uncertainty analysis	50
3.6	Geo-database management system	
3.6.1	Structure of database	53
3.6.2	Data query and analysis	54
3.7	Results and discussion	55

#### **Chapter 4: Remote Sensing for Hydrological Model Parameterisation**

4.1	Concept of remote sensing	58
4.2	Digital image processing and pattern recognition	60
4.3.1	Image segmentation and enhancement	61
4.3.2	Feature extraction	61
4.3	Multi-spectral Image classification	
4.3.1	Gaussian maximum likelihood classification	64
4.3.2	Fishers Linear-discriminant classification	65
4.3.3	ECHO classification	66
4.3.4	Principal component analysis	66
4.4	Accuracy assessment of classification image	67
4.5	Application for Anas catchment	
4.5.1	Selection of satellite remote sensing data	69
4.5.2	Pre-classification process	69
4.5.3	Preparation of false colour composite	70
4.5.4	Design of supervised land-use classification system	70
4.6	Results of image classification	
4.6.1	Extraction of training features	73
4.6.2	Classification of training fields	74
4.6.3	Image classification results	75
4.7	Image integration in GIS	76
4.8	Results and discussion	78

#### **Chapter 5: Rainfall Prediction based on Atmospheric Circulation**

5.1	Downscaling approaches	
5.1.1	Dynamic downscaling	83
5.1.2	Statistical downscaling	83
5.1.3	Statistical-Dynamic downscaling	84
5.2	Atmospheric circulation and statistical downscaling	
5.2.1	CP based approach to downscaling	85
5.2.2	State of art on CP-based downscaling	86
5.3	Modelling methodology and structure of downscaling model	
5.3.1	Classification of circulation types	87
5.3.2	Downscaling of rainfall	89
5.4	Materials and database	
5.4.1	Large scale circulation data	91
5.4.2	Station rainfall data	92
5.4.3	Spatial database	92
5.4.4	Rainfall data characteristics	93
5.5	Sensitivity analysis for rainfall model	93

5.6	Model simulation results	
5.6.1	Conditional rainfall probability and amount	95
5.6.2	CP frequency analysis	98
5.6.3	Objective circulation pattern	100
5.6.4	Observed and simulated rainfall	101
5.7	Prediction of long-term rainfall	105
5.8	Results and discussion	107

## **Chapter 6: Runoff Modelling for Prediction in Un-gauged Catchments**

6.1	Modelling with ZIN-model	
6.1.1	Development of catchment database	115
6.1.2	Rainfall parameter	116
6.1.3	Runoff generation parameters	119
6.1.4	Runoff concentration parameters	122
6.1.5	Channel routing parameters	124
6.2	Sensitivity analysis for distributed model	128
6.3	Model simulation results	
6.3.1	Model run for 07/09/1994	130
6.3.2	Model run for 06/09/1994	131
6.3.3	Analysis of volume check	132
6.4	Model validation, up-scaling discharge	133
6.4	Effect of input parameter variability	
6.4.1	Effect of cloud velocity	135
6.4.2	Effect of alluvium infiltration rate	136
6.4.3	Effect of reservoir storage	138
6.5	Results and discussion	139

## **Chapter 7: Conclusions and Perspectives**

7.1	Catchment decision support models	143
7.2	Hydrological modelling and database development	143
7.3	Remote sensing for hydrological model parameterisation	144
7.4	Rainfall modelling based on GCM	145
7.5	Runoff modelling for prediction in un-gauged catchments	146
7.6	Application of decision support models	148
	<b>References</b>	149

## **Appendix**

A.1		
	Annex 1.1	In depth overview of decision support model reviewed
		167
A.2		
	Annex 2.1	Major agro-ecological zones in India
	Annex 2.2	Average monthly flow of selected major rivers in India
	Annex 2.3	Scenario narratives and definition of term
		170
A.3		
	Annex 3.1	Algorithms
	Annex 3.2	Accuracy assessment of DEM
	Annex 3.3	Comparing TIN, grid and lattice
		171
		171
		172

A.4			
	Annex 4.1	Histogram and density function for April 6 2000 image	173
	Annex 4.2	Weighted inter-class distance for training classes	173
	Annex 4.3	Seperability index between training classes for October 15 2000 image	174
	Annex 4.4	Training class performance for October 15 2000 image	174
	Annex 4.5	Class distribution for image area for October 15 2000 image	174
	Annex 4.6	Seperability index between training classes for April 6 2000 image	175
	Annex 4.7	Class distribution for image area for April 6 2000 image	175
	Annex 4.8	Definition of terms	175
	Annex 4.9	The land-use classes distribution using GML and ECHO classifiers for April 6 2000 and October 15 images	176
A.5			
	Annex 5.1	Comparison of main strengths and weaknesses of dynamic and statistical downscaling	177
	Annex 5.2	Predictor variables and techniques on downscaling daily precipitation	177
	Annex 5.3	Topographic parameters of rain-gauge stations in Anas catchment India	177
	Annex 5.4	Yearly frequencies of CP occurrence during monsoon season for 1985-94 period	178
	Annex 5.5	Spatial distribution of 500hPa geo-potential heights anomalies for wet and dry CP's	178
	Annex 5.6	Conditional rainfall probability and conditional rainfall amount for various CP-types at rainfall station	178
	Annex 5.7	Mean monthly rainfall totals for observed and simulated series during 1985-94	179
A.6			
	Annex 6.1	Land-use classes, curve number and runoff coefficients derived from October 15 2000 image	180
	Annex 6.2	Manning's roughness coefficients for various channel types	180
	Annex 6.3	Modelling the effect of cloud velocity for size rainfall event on 02/08/1994 at Anterbeliya and Mod stations	180
	Annex 6.4	Modelling the effect of infiltration rate for small rainfall event on 02/08/1994 at Anterbeliya and Mod stations	180



## List of Figures

Fig. 1.1	Monthly rainfall anomalies for west-central India derived using KNMI climate explorer	3
Fig. 1.2	Scheme of decision support models for Anas catchment in Mahi basin in western India	4
Fig. 2.1	Topographic features of India	15
Fig. 2.2	Major climatic regions and major river basins in India	16
Fig. 2.3	Long-term average monthly flow of selected Indian rivers	17
Fig. 2.4	Location of Mahi basin in India	21
Fig. 2.5	Anas catchment and its river network	22
Fig. 2.6	Yearly rainfall variability for five stations in Anas catchment during 1965-99	23
Fig. 2.7	Probability plotting of monsoon rainfall totals for station Jhabua derived from observed 40 years rainfall	24
Fig. 2.8	The rainfall recurrence interval and monsoon season rainfall for Thandla and Ranapur stations	24
Fig. 2.9	Mean monthly minimum and maximum temperature at meteorological station Alirajpur	25
Fig. 2.10	Properties of soil type in Anas catchment	26
Fig. 2.11	Geology in Anas catchment	28
Fig. 2.12	Stage-discharge curve for discharge station Anterbeliya for various years (1992-95) during monsoon season	29
Fig. 2.13	Stage-discharge relationship for two discharge stations Anterbeliya and Mod catchment for 1994 monsoon season	30
Fig. 2.14	Stage-discharge curve Anterbeliya station at different water levels	30
Fig. 3.1	A flow chart and sketch of integrated watershed model	35
Fig. 3.2	The structure of coupled GIS and hydrological model	39
Fig. 3.3	A manual procedure adopted for digitisation of topographic maps in Arc/Info platform	42
Fig. 3.4	Getting data into attribute data table and related data tables	43
Fig. 3.5	A TIN generated from input contour lines, geodetic points and drainage network	45
Fig. 3.6	DEM generated using TIN model and Arc-view 3D Analyst	47
Fig. 3.7	A 3D-digital elevation model for Anas catchment	48
Fig. 3.8	A plot of DEM uncertainty between two datasets	49
Fig. 3.9	The structure of relational database in catchment context	50
Fig. 3.10	Performing query and analysis from simple geo-database system for model parameter identification to distributed hydrologic model	51
Fig. 4.1	Electro-magnetic spectrum and percentage reflectance for grasses and soils in Landsat TM	55
Fig. 4.2	The process of pattern recognition for multi-spectral satellite image	57
Fig. 4.3	Multi-spectral image classification process	60
Fig. 4.4	False colour composite of Landsat ETM+ of Anas catchment	66
Fig. 4.5	Histogram and density function for April 6 200 image describing various training classes	68
Fig. 4.6	A comparison of feature extraction algorithms for April 6 2000 image	69

Fig. 4.7	Results obtained from ECHO and aximum-likelihood classifier for 6 <sup>th</sup> April 2000 image	71
Fig. 4.8	Land-use classes derived from 6 <sup>th</sup> April 2000 image	72
Fig. 4.9	Distribution of land-use classes in each watershed for 6 <sup>th</sup> April 200 image	73
Fig. 5.1	A typical representation of statistical rainfall downscaling model	79
Fig. 5.2	Location of Anas catchment in atmospheric circulation window at 5°x5° grid over Indian ocean	85
Fig. 5.3	Model sensitivity analysis for the effect of shifting atmospheric circulation window on the rainfall probability and rainfall amount	87
Fig. 5.4	Conditional rainfall probability and rainfall amount for all stations using 12CP and 10CP types during 1985-94	89
Fig. 5.5	Analysis on conditional rainfall probability and conditional rainfall amount for individual stations in Anas catchment	91
Fig. 5.6	Mean frequency of CP-type occurrence and wetness fraction for 12CP and 10CP types during monsoon for a period 1985-94	92
Fig. 5.7	Spatial distribution of mean 500hPa geo-potential height anomalies over Indian ocean for dry and wet CP-types respectively	94
Fig. 5.8	Mean monthly observed and simulated rainfall for selected stations in Anas catchment	96
Fig. 5.9	A comparison between observed and simulated number of rain-days during monsoon season of 1985-94	97
Fig. 5.10	Observed and simulated number of rain-days during monsoon season of 1985-94	97
Fig. 5.11	Observed and simulated monthly rainfall time series for Jhabua and Thandla stations for a period of 1961-94 during monsoon season	98
Fig. 5.12	Observed and simulated monsoon seasonal rainfall totals for Jhabua and Thandla stations for a period 1961-94	99
Fig. 5.13	Mass curve for observed and simulated rainfall at station Jhabua	99
Fig. 6.1	Rainfall runoff in the L'Avic and La-Teula catchments in Spain	104
Fig. 6.2	The schematic representation of ZIN model, spatial sub-divisions and hydrological process	105
Fig. 6.3	Spatial locations of reaches with deep river alluvium	107
Fig. 6.4	Spatial distribution of rainfall volume for 02.08.1994 event	108
Fig. 6.5	Hovmoller diagram derived from INSAT satellite images for 1994 monsoon season	109
Fig. 6.6	Clouds movement derived from INSAT cloud images	110
Fig. 6.7	Response of catchment to hill-slope flow process, lag times and peak runoff rates with respect to catchment size	111
Fig. 6.8	A sketch of runoff generation process and bank-full storage in main channel with deep groundwater level	111
Fig. 6.9	Discretisation scheme for application of distributed model	113
Fig. 6.10	Spatial sub-division of Anas catchment and hydrological time-lag response function	113
Fig. 6.11	Illustration of distributed flow routing model using Muskingum-Cunge method	115
Fig. 6.12	Simplified representation of cross-section geometry	116
Fig. 6.13	Determination of channel parameters from Landsat-TM remote sensing image	117
Fig. 6.14	Results obtained in the simulation for 06-07/09/1994 events for both Anterbeliya and Mod stations	121

Fig. 6.15	Results obtained in the simulation for 06/09/1994 events for Anterbeliya and Mod stations	122
Fig. 6.16	Up-scaling the model time scale to compare simulation results from ZIN-model, SCS-CN runoff model, lumped model	124
Fig. 6.17	Comparison between simulated and observed discharge at monthly time scale	125
Fig. 6.18	Modelling the effects of cloud velocity for a large size event of 07/09/1994 at Anterbeliya and Mod stations	126
Fig. 6.19	Modelling the effects of transmission losses for a large size event of 07/09/1994 at Anterbeliya and Mod stations	128
Fig. 6.20	Modelling the effects of reservoir storage for a large size event of 07.09.1994 at Anterbeliya and Mod stations	129

## List of Tables

Tab. 2.1	Profile of main topographic zones of India	14
Tab. 2.2	Water withdrawal and share of total renewal water	18
Tab. 2.3	Basin efficiency and reservoir storage for irrigation and water supply under 3 scenario's for 1995 and 2025	18
Tab. 2.4	Spatial characteristics of Mahi river basin	20
Tab. 2.5	Geographical area occupied by each watershed in Anas catchment	22
Tab. 2.6	Properties of various soil groups and geographical coverage in Anas catchment	26
Tab. 2.7	Tabulated area under each geological group and their properties	26
Tab. 3.1	Classification of watershed models based on under-lying physical process	34
Tab. 3.2	Basic criteria for evaluation of watershed model	36
Tab. 3.3	Details of various spatial and hydrological datasets used in research study	42
Tab. 3.4	Specifications of remote sensing datasets used in research study	435
Tab. 4.2	Landsat TM feature space transformation coefficients	63
Tab. 4.3	Properties of satellite data used for classification	65
Tab. 4.4	Landsat data product characteristics	65
Tab. 4.5	Selection of training classes and area for Landsat ETM+ images of 6 <sup>th</sup> April 2000	67
Tab. 4.6	Statistics on training classes for each channel for 6 <sup>th</sup> April 200 image	67
Tab. 4.7	Seperability index between training classes for 6 <sup>th</sup> April 200 image	68
Tab. 4.8	The eigenvalues and percentage component explained for 6 <sup>th</sup> April 200 image using DAFE and DBFE algorithms	69
Tab. 4.9	Eigenvalues of co-variance matrix obtained for 6 <sup>th</sup> April 2000 image using DAFE and DBFE algorithms	70
Tab. 4.10	Training class performance (redistribution method)	70
Tab. 4.11	Class distribution for image area	71
Tab. 4.12	Distribution of land-use classes in each watershed for 6 <sup>th</sup> April 200 image	73
Tab. 5.1	Statistical properties of daily rainfall data for various stations of Anas catchment during the monsoon season	86
Tab. 5.2	Sensitivity analysis of parameters affecting the rainfall probability and rainfall amount	87
Tab. 5.3	The mean occurrence frequency, rainfall probability, rainfall amount and wetness fraction at 12 CP-types during monsoon season	92
Tab. 5.4	Statistics of observed and simulated seasonal rainfall totals for various stations in Anas catchment	95
Tab. 5.5	Correlation between observed and simulated monthly rainfall totals	96
Tab. 6.1	Characteristics of different channel types	118
Tab. 6.2	Statistics on segment parameters and their variability range	118
Tab. 6.3	Sensitivity index of parameters affecting peak discharge and time to peak	119
Tab. 6.4	Rainfall-runoff events selected for ZIN model run	121
Tab. 6.5	Volume check for simulated runoff at Anterbeliya for three independent events	123

## List of Symbols Used

<i>Symbol</i>	<i>meaning</i>	<i>Units</i>
$\beta$	Positive exponent for large scale predictor ( $\beta \geq 1$ )	-
$\Delta$	Slope of saturation vapour pressure	hPa/°C
$\Delta s$	Change in soil moisture	mm
$\Delta t$	Time step for flood-routing within channels	min
$\Delta x$	Space step for flood-routing within channels	m
$\phi(x)$	Cumulative distribution function of the normal distribution	-
$\Sigma_i$	Covariance matrix for class $i$	-
$\gamma$	Psychometric constant	hPa/°C
$\mu$	Mean vector for all training classes	-
$\mu_i$	Mean vector for training class $i$	-
$\sigma_b$	Coefficient of variance between training classes	-
$\sigma_p$	Standard deviation of daily pressure data	-
$\sigma_w$	Coefficient of variance within training classes	-
$\tilde{A}_t$	Mean circulation pattern	-
$B$	Width of water surface in the channel	m
$c_p$	Heat capacity of air	kJ/kg/°C
$CN$	curve number	-
$C_1, C_2, C_3$	Constants for diffusion wave equation	-
$d_{ij}$	Decision point between class $i$ and $j$	-
$DOF(k, t)$	Degree of fulfillment of membership rule	-
$e_a$	Actual vapour pressure	hPa
$e_s$	Saturated vapour pressure	hPa
$E_a$	Absorbed energy	kg.m <sup>2</sup> /s <sup>2</sup>
$E_i$	Incident energy	kg.m <sup>2</sup> /s
$E_r$	Reflected energy	kg.m <sup>2</sup> /s
$E_t$	Transmitted energy	kg.m <sup>2</sup> /s
$E_{tcrop}$	Potential transpiration for crops	mm
$E_{tp}$	Potential evapotranspiration	mm
$\mathcal{G}_s(x)$	Probability of value $x$ for given class	-
$G$	Soil heat-flux in water depth equivalent	mm/day
$I_a$	initial abstraction	mm
$k_c$	Crop coefficient (a function of growing season)	-
$K$	A storage constant for flood routing	min
$\hat{K}$	Kappa index or kappa variance for class accuracy	-
$L_v$	Specific latent heat	kJ/kg
$n$	Manning's roughness coefficient	-

$O_1(\mathcal{G})$	Objective function for conditional rainfall threshold of $\mathcal{G}$	-
$O_2$	Objective function for conditional rainfall amount at given station	-
$Q$	discharge/ runoff	mm
$p_a$	Density of dry air	kg/m <sup>3</sup>
$p(x w_i)$	Conditional probability of sample $x$ belonging to class $w_i$	-
$\bar{P}$	Average pressure during time $t$ having $N$ observation	-
$P$	Rainfall in the catchment	mm
$P_c$	Overall classification accuracy	%
$P_{cr}$	Classification accuracy	%
$Q_{ref}$	Reference discharge in the channel	m <sup>3</sup> /s
$r_a$	Aerodynamics resistance due to plants	s/m
$r_s$	Surface resistance (a function of wind velocity)	s/m
$R$	Hydraulic radius (ration of cross-section area to wetted perimeter)	m <sup>2</sup> /m
$R_b$	Base line variable or typical value for most cases	-
$R_i, R_d$	Model variable being increased or decreased	%
$R_n$	Net radiation expressed in water depth equivalent	mm/day
$s$	Slope of hydraulic grade line	m/m
$S_0$	Energy slope	m/m
$S$	potential retention	mm
$S_b$	Scatter matrixes between the classes	-
$S_i$	Seperability index for training classes	-
$S_T$	Total scatter of training class data	-
$S_w$	Scatter matrixes within the classes	-
$T_c$	Time of concentration	hr
$T_t$	Travel time	hr
$v(i)^k$	Indices of membership function for CP-type classification	-
$v_k$	Kinematic wave celerity for channel flow	ms <sup>-1</sup>
$V$	Flow velocity	ms <sup>-1</sup>
$w_i$	Training feature class weight	-
$W(t, u)$	Large scale predictor, such as geo-potential heights at time $t$ and station $u$	-
$X$	Weighting factor for expressing relative importance to inflow and outflow	-
$Y(x)$	Known parameter such as rainfall at point $x$	mm
$Z(t, u)$	Local predictant, such as rainfall at time $t$ and station $u$	-
$Z(x)$	Interpolated parameter such as rainfall at point $x$	mm

## List of Acronyms Used

AML	Arc Macro Language
C-DAC	Centre for Development of Advance Computing
CP	Circulation pattern (also referred CP-type)
CSRE	Centre for Study of Resources Engineering
DAFE	Discriminant Analysis Feature Extraction
DANIDA	Danish International Development Assistance
DBFE	Decision Boundary Feature Extraction
DBMS	Database Management System
DEM	Digital Elevation Model
DFID	Department for International Development UK
DML	Data Manipulation Language
DN	Digital numbers
DRDA	District Rural Development Agency
DSM	Decision Support Model
DSS	Decision Support System
DTM	Digital Terrain Model
EC	European Community
ECHO	Extracting and Classification of Homogeneous Objects
ESRI	Environmental System Research Institute Inc.
FAO	Food and Agricultural Organisation
FCC	False Colour Composite
GCM	Global Circulation Model
GDP	Gross Domestic Product
GIS	Geographical Information System
GML	Gaussian-Maximum Likelihood
GUI	Geographical User Interface
HEC-HMS	Hydrological Modelling System of Hydrologic Engineering Centre
HRU	Hydrological Response Units
HSU	Hydrological Similar Units
IAHS	International Association of Hydrological Sciences
IDW	Inverse Distance Weighting
INR	Indian Rupees

INSAT	Indian National Satellite
IPCC	Intergovernmental Panel on Climate Change
KfW	Kreditaufwiederbau Frankfurt
KMS	Knowledge Management System
Landsat-TM	Landsat-Thematic Mapper
MIS	Management Information System
MSL	Mean Sea Level
MVPMC3	Modified Three Point Variable Parameter Method
NCAR	National Centre for Atmospheric Research
NCHSE	National Centre for Human Settlements and Environment
NGO	Non-governmental Organisation
NRDMS	Natural Resources Data Management System
NRSA	National Remote Sensing Agency
PCA	Principal Component Analysis
PRMS	Precipitation Runoff Modelling System
PUB	Prediction in Un-gauged basins
QDA	Query, Display and Analysis
RCM	Regional Climate Models
RMSE	root-mean square error
SAC	Space Application Centre
SCS-CN	Soil Conservation Service- Curve Number method
SST	Sea Surface Temperature
SWDC	Surface Water Data Centre
TIN	Triangular Irregular Network
UH	Unit Hydrograph
UNEP	United Nations Environment Program
USGS	United States Geological Survey
UTM	Universal Transverse Mercator
WALMI	Water and Land Management Institute



## **ABSTRACT**

The present research work deals with the decision support modelling methodologies and system concepts are being developed for a semi-arid catchment under limited hydro-meteorological and spatial data. The goal has been to initiate a decision support system concept at catchment scale for water resources planning and development in the course of possible climate change. Understanding the processes and feedbacks of complex natural systems, quantitative resources assessment are prerequisite to enhance the carrying capacity of semi-arid regions. To begin with the task of decision support models, for this purpose a physical based distributed hydrologic model (ZIN) and stochastic rainfall model based on atmospheric circulation pattern have been evaluated. Advances in geographical information system (GIS) and remote sensing made it possible to enhance the model parameter estimation, physical process modelling and support decision making. This research study has been first of its kind in the Anas catchment and begun from basic database development to adoptive model identification.

The goal of the research study have been to develop decision support models for quantification of water availability in view of stochastic nature of rainfall from no or poor quality observed discharge data. The research area has been Anas catchment (1750 km<sup>2</sup>) a head-watershed of Mahi basin in the semi-arid region of western India. The region receive a mean rainfall of 750mm per annum falling during June-September somewhere between 30-50 rainfall events. The soils are derived from basaltic rocks with shallow depth on ridges and deep alluvium in channel sections. The region has been currently affected by sever droughts which affected agriculture productivity and caused economic loss.

The catchment database for thematic coverages such as contour lines, drainage pattern and land-use has been developed in Arc/Info GIS platform from the paper maps of various spatial scale and resolution. Raster based digital elevation model (DEM) at 50m cell size has been produced for research area using triangulated irregular network (TIN) based modelling in Arc-Grid. As TIN is more efficient to represent a surface defined by the elevation of three corner points. The DEM constructed after converting from TIN into raster have shown mean error of 11.4% for elevation. A set of geomorphic parameters were examined between DEM and vector data found to have good fit. All the thematic coverages (with info tables) were stored in central

database system linked to ACCESS. The possibility of using digital remote sensing for preparation of land cover maps and GIS database development given a new possibility for identification of distributed hydrological model parameters. Few image classification algorithms have been compared and tested for the verification of training fields and classification accuracy. Later the raster data have been converted into vector for determination of land-use types and also for the runoff coefficients for each sub-catchment.

The potential of circulation based approach for rainfall downscaling has been explored using statistical method. The methodology has been applied in highly seasonal semi-arid environment. An automatic circulation pattern (CP) classification model in which daily rainfall occurrence has been conditioned on CP-type using a fuzzy-rule based process. Then rainfall is generated as stochastic process coupled to circulation pattern. For calibration and validation of the downscaling model the observed and simulated daily rainfall amounts for 10 rainfall recording stations spread over Anas catchment have been used. The model was calibrated for 10 years period between 1985-94 and also validated. The long term yearly monsoon rainfall during 1961-94 for Jhabua and Thandla rainfall recording stations have been generated. The seasonal rainfall shows a good fit within a variability range of 25% and may considered to be more plausible than raw GCM data.

The model performance is affected by long term rainfall data availability and reliability of global climate model (GCM). The period of data availability and GCM model have been important factors on which parameter determination for rainfall generations are based. Both a marked increase or a decrease in rainfall trends can be assumed depending upon the data origin of GCM such as NCEP/NCAR Reynolds reanalysis data or ECMWF data. The downscaling model have well simulated the monthly rainfall but few suggestions have been made to refine the downscaling model for possible input into distributed model.

Spatial fragmentation of catchment area into sub-catchments and/or segments enabled identification of gauged and un-gauged nodes and derivation of model parameters which have been used as an input for ZIN model. The ZIN model applied in this study composed of process based approach mainly based on field derived parameters. The runoff generation input for the model capture in particular the terrain and land-use characteristics. The lateral hydrological process for each sub-catchment is modelled through hydrograph response curve for runoff concentration at each node point and channel routing has been done using

Muskingum-Cunge flow routing model. Small scale variability is not represented as single hydrograph response curve have been taken for all sub-catchments. The most ZIN model parameters have been derived from field based data hence no calibration has been conducted. The independent model validation has been hindered due to poor quality of observed discharge data at both stations.

The simulation results have been characterised by uncertainties of input data; a) the uncertainty of rainfall data due to spatial pattern and rainfall intensity, b) the uncertainty of topographic parameters and remote sensing derived land-use, c) the uncertainty in individual model parameters such as cloud velocity, infiltration rate and recharge dynamics of alluvium. These parameters usually may differ over years and even during various events of the same year. But the ZIN model is particularly useful for simulating runoff for un-gauged catchments in semi-arid environment where limited physical data on catchment properties exists.

## **Kurzfassung**

In der vorliegenden Arbeit werden Methoden zur Entscheidungsfindung und Verfahrenskonzepte entwickelt, die im Rahmen möglicher Klimaänderungen in einem semi-ariden Einzugsgebiet, für das nur eingeschränkte hydro-meteorologische und geographische Daten vorliegen, wasserwirtschaftliche Planung und Entwicklung ermöglichen. Mit dem Verständnis komplexer natürlicher Systeme wird eine quantitative Abschätzung der Wasservorräte ermöglicht, so dass die Ausnutzung bestehender Kapazitäten in semi-ariden Regionen verbessert wird. Es wurde ein stochastisches Niederschlags-Generierungsmodell, das auf atmosphärischen Großwetterlagen basiert, mit einem physikalisch basierten hydrologischen Modell (ZIN-Modell) verknüpft. Durch Einsatz von Fernerkundungsdaten und geographischen Informationssystemen (GIS) konnte eine größere Datenbasis geschaffen werden, die zur Verbesserung des ZIN-Modells und somit einer verbesserten Entscheidungsfindung führen konnte. Die Arbeit beruht dabei auf der erstmaligen Untersuchung des Anas-Einzugsgebietes in Indien und umfasst die Arbeiten von der Daten-Akquisition bis zur adaptiven Modell-Bestimmung.

Ziel der Untersuchungen war es, eine Grundlage für ein Entscheidungssystem (decision support system) zu schaffen, um eine Quantifizierung des Wasserdargebotes im Blick auf die stochastische Natur des Niederschlags und auf der Basis von fehlenden bzw. nur bedingt beobachteten Abflussdaten zu erreichen. Als Untersuchungsgebiet wurde das Anas-Einzugsgebiet, mit einer Fläche von 1750 km<sup>2</sup> gewählt, das zum Einzugsgebiet des Mahi Beckens in der semi-ariden Klimazone Indiens gehört. Diese durch Monsun geprägte Region erhält ihre Niederschläge vorwiegend in den Monaten Juni-September, mit einem durchschnittlichen Jahresniederschlag von 750 mm. Während an den Hängen und Höhenzügen die in der Regel aus Verwitterung von Basalten entstandenen, Böden nur geringe Mächtigkeiten besitzen, erreichen in den Flusstälern auf fluviatilen Ablagerungen entstandene Böden (Alluvium) im Gegensatz dazu höhere Mächtigkeiten. Die Region wurde in jüngster Zeit von starken Dürren erfasst, was Auswirkungen auf die landwirtschaftliche Produktion hatte und zu wirtschaftlichen Verlusten führte.

Im geographischen Informationssystem (GIS) Arc Info wurden die geographische Grundlage des Einzugsgebiets aus Kartenwerken mit unterschiedlichen Maßstäben und Auflösungen digitalisiert und aufbereitet, wie unter anderem die thematischen Einheiten der Höheninformation, dem Entwässerungsnetz und der Landnutzung. Ein rasterbasiertes digitales Höhenmodell (DHM) mit einer Rasterweite von 50 m wurde für das Einzugsgebiet mit Hilfe des Triangulated Irregular Networks (TIN) erstellt, die eine effiziente Darstellung von Höhendaten auf Grundlage dreier Eckpunkte darstellt. Das aus dem TIN konstruierte DHM zeigte einen mittleren Fehler von 11.4% in der Höhendarstellung. Geomorphologische Strukturen aus dem DHM und vektorielle Daten zeigten dabei eine gute Übereinstimmung. Die thematischen Informationen wurden zusätzlich zum GIS in einer auf Access basierenden Datenbank zusammengefasst. Fernerkundungsdaten wurden zur Bestimmung raumverteilter hydrologischer Parameter genutzt. Dazu wurden verschiedene Klassifikations-Algorithmen verglichen und an Trainings-Feldern angepasst sowie deren Genauigkeit verglichen. Dann wurden diese Raster-Daten zur Bestimmung der Landnutzungsparameter und Abflussbeiwerte jeweiliger Untereinzugsgebiete in Vektor-Daten umgewandelt.

Das Potential eines auf globalen Großwetterlagen basierten Modells für das Downscaling von Niederschlagsdaten wurde mit einem statistischen Ansatz genutzt, unter Berücksichtigung einer stark saisonalen semi-ariden Umgebung. Das automatisch konditionierbare Modell für globale Großwetterlagen wurde auf der Grundlage von Fuzzy-Regeln für Tagesniederschläge konditioniert. Dann wurde der Niederschlag als stochastischer Prozess in Bezug auf die Großwetterlagen generiert. Zur Kalibrierung und Validierung des Downscalings wurden die 10-jährigen Beobachtungszeitreihen (1985-1994) der Tagesniederschläge von 10 Niederschlagsstationen aus dem Anas Einzugsgebiet verwendet. Daraus wurden die langzeitlichen Jahresniederschläge des Monsuns für die Jahre 1961-94 für die Stationen Jhabua und Thandla generiert. Die saisonalen Niederschlagsdaten zeigen eine gute Übereinstimmung innerhalb einer 25%-igen Schwankungsbreite, und werden als plausibler angenommen als die Rohdaten des globalen Klimamodells.

Die Qualität von hydrologischen Modellen wird durch die Verfügbarkeit langjähriger Niederschlagszeitreihen bzw. durch die Qualität der globalen Klimamodelle (GCM) beeinflusst. Die Zeitspanne, in der diese Daten für das Anas-Gebiet vorliegen bzw. das GCM angewendet werden kann, war daher ein wichtiger Faktor bei der Niederschlags-Generierung.

Je nachdem ob die Klimadaten aus der National Centre for Atmospheric Research (NCAR) Reynolds Reanalysis oder vom European Centre for Medium Range Weather Forecast (ECMWF) stammen, kann ein deutlich positiver bzw. negativer Trend in den generierten Niederschlagsdaten erwartet werden. Bei der Generierung monatlicher Niederschlagssummen zeigte das Downscaling Modell eine gute Performance. Für die verbesserungswürdige Performance auf der Ebene täglicher Niederschläge werden für semi-aride Bereiche noch weitere Verbesserungsvorschläge gegeben.

Die Aufteilung in Untereinzugsgebiete und Teileinzugsgebiete ermöglicht die Ausweisung von Punkten mit und ohne Messeinrichtungen, die dann im physikalisch basierten, verteilten hydrologischen Modell (ZIN-Modell) Verwendung finden. Ein Großteil der Parameter für das ZIN Modell wurden im Untersuchungsgebiet bestimmt, wie z.B. Gewässerdurchschnitte oder die Verbreitung der infiltrationsfreudigen Flusssedimente (Alluvium). Die Eingangsdaten für die Abflusssimulation setzen sich in erster Linie aus der Geländebeschaffenheit und Landnutzungsfaktoren zusammen. Die hydrologischen Prozesse jedes Untereinzugsgebietes werden durch Niederschlagskonzentration und Anwendung des Einheitsganglinienverfahrens an jedem Knotenpunkt berechnet, die Wellenfortpflanzung im Gewässer wird durch das Muskingum-Cunge Verfahren beschrieben. Eine kleinräumige Variabilität wird nicht repräsentiert, da die genutzten Einheitsganglinien für alle Untereinzugsgebiete gleich angesetzt werden müssten. Ein Hauptteil der Parameter wurde aus im Gelände erhobenen Daten gewonnen, so dass keine Kalibration notwendig wurde. Eine unabhängige Validierung des Systemmodells war nicht möglich, da die Zeitreihen der beiden Pegel keine beobachteten Abflussereignisse mit ausreichender Qualität besitzen.

Die Simulationsergebnisse sind durch große Unsicherheiten der Eingangsdatensätze geprägt. A) die Ungenauigkeit der Niederschlagsdaten aufgrund der geographischen Ungleichheit und der Niederschlagsintensität. B) die Ungenauigkeit der topographischen und der durch Fernerkundung erworbenen Landnutzungsparameter, C) der Unsicherheit, die aus den einzelnen Modellparametern wie Wolkengeschwindigkeit, Infiltrationsrate oder Auffüllungsrate der Flussbetsedimente herrührt. Diese Parameter können über Schwankungsbreiten verfügen, die im Jahresverlauf schwanken können bzw. innerhalb von Ereignissen. Aber das ZIN-Modell ist verhältnismäßig brauchbar, um den Abfluss in nicht bemessenen Einzugsgebieten in einer semi-ariden Umgebung zu simulieren, in dem limitierte physikalische Datensätze der Gebietsparameter bestehen.

## 1. INTRODUCTION

The Indian subcontinent is extremely sensitive to the water resources problems, floods during several weeks during monsoon season and water scarcity during many months during summer. Drought is a periodic phenomenon in almost for 60% of the geographical area which falls under arid and semi-arid agro-climatic region of India. The southern and western parts of the country are considered drought-prone due to inter-annual variation of rainfall followed by erratic and irregular monsoon seasons. During the year 1999-2000 due to inadequate monsoon the majority of the agricultural community in this region have suffered reductions in consecutive annual harvests. The most at-risk populations are small and subsistence farmers living in the remote areas who typically have no access to secured irrigation water supply. For the third consecutive year the monsoon has failed to arrive so region is experiencing extreme regional drought conditions. The National Calamity Contingency Fund of India responsible for emergency aid for natural disaster mitigation has allocated approximately 60 million Euro (€1 = 50 INR as on 2001) during this year alone. The recent estimates from Government of India reports that over 125 million people in about 152 districts in eight states namely Andhra Pradesh, Chhattisgarh, Gujarat, Karnataka, Madhya Pradesh, Maharashtra, Tamilnadu, Rajasthan have been affected. This means that economic and agricultural activities within the Mahi basin, Sabarmati basin, Tapi-Narmada basin, Godavari basin, Krishna and Kaveri basin have been severely at halt.

Government of India's strategies to avert famine through increased irrigated agricultural production have lowered groundwater tables. Efforts to curb area under irrigation have reduced the acreage of cultivated land resulting in fewer agricultural jobs and the loss of livelihoods for wage labourers. This led to implementation of watershed development program in various federal states under national government sponsored and multi-lateral agency assisted programs since mid 1990's. An impact assessment study of European funded namely DANIDA, DFID, EC and KfW watershed development program by Ninan (1998)

shows that program have been failed to address natural resources, environment and economic identification concerns. In identifying and implementing the watershed development programs a systematic resources assessment and hydrological process modelling studies have been missing. This led to minimal program effectiveness and impact on proper utilisation of water resources. The growing urgency for watershed management in arid and semi-arid regions to sustain livelihood and maintain ecosystem has created a need for reliable, applicable and relevant catchment decision support models.

Most catchments in developing world are un-gauged and rather limited spatial and temporal information for complex decision support models and model parameters are available. Thus the key issues to be answered are; What predictions are needed? What are major decision support parameters? on which spatial and temporal scale? and at which degree of impact may have on decision making? How our research efforts can be linked with other international initiatives such IAHS decade (2003-2012) on predictions in un-gauged basins (PUB)?

The new approaches and knowledge on available in the form of measurement and data processing need to be explored. The current approaches for prediction in un-gauged basins (PUB) includes method such as extrapolation of basin response information, measurement by remote sensing, application of process based hydrological models and application of coupled meteorological-hydrological models without the need to specify rainfall inputs (Sivapalan 2003).

The purpose of the present research study are to development decision support model parameters for Anas catchment which may assist in decision making. It should be kept in mind that decision models should be relatively simple to apply, do not need large amount of observed data and are flexible enough to adopt to other regions of similar hydro-meteorological conditions. Ideally these models and model parameters should reflect the underlying physical mechanisms and be easy to validate and be capable of creating scenarios for a range of variables. Thus combining the Geographical Information System (GIS) for catchment water resources database with rainfall and runoff prediction models to select optimal strategy for water resources development.



The situation in Anas catchment with a geographical area of 1750 km<sup>2</sup> a head-watershed of Mahi basin in Western India is no more different where limited hydro-meteorological and spatial data are available. The catchment have never been explored before either for any scientific study for water resources quantification or hydrological process modelling. The annual rainfall amounts ranges between 350mm to 1300mm with a long term mean of 750 mm/annum. Large spatial and temporal variability have been observed in rainfall anomalies for several stations during 1960-2000 period in this region (refer figure 1.1). According to latest summary on future climate change with the global warming rainfall tend to increase or decrease between 10-20% (IPCC 2001). The persistent drought conditions led to the rural out-emigration to the tune of 57% to metropolitan areas in search of employment as far away as Bombay and Delhi (NCHSE 1993).

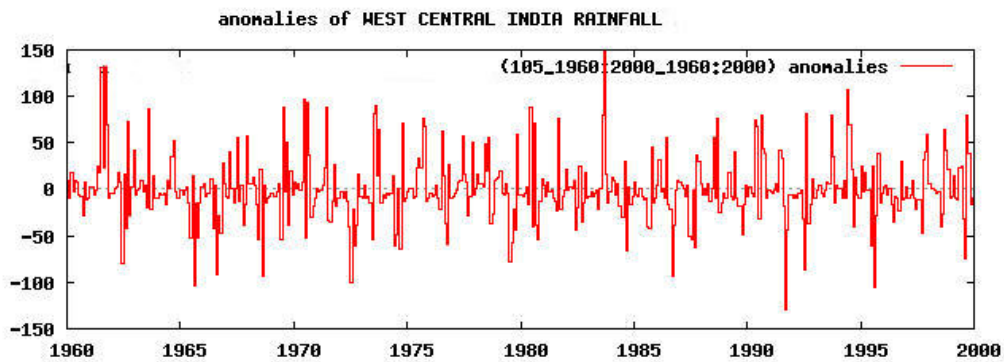


Figure 1.1 Monthly rainfall anomalies for west-central India derived using KNMI climatic explorer (source: <http://climexp.knmi.nl/>)

Also in this area rather limited hydrological data exists but the sound assessment of water resources is vital for life. Flexible assessment tools and decision support models are needed to cope with the problem of limited data (Lange and Singh 2003) but can also link with climate, water resources, agriculture sector and socio-economic system.

### 1.1 Research Objective and Model Structure

The objective of this research study is to identify models which can help in making informed decision for a macro catchment in semi-arid environment of India. This general objective is specified according to the requirements of decision support parameters such as rainfall

prediction and the scientific interest in the field of hydrology and water resources for a semi-arid environment.

1. To develop a catchment database for identification of spatial heterogeneity using the GIS and remote sensing tools. Since spatial and temporal data features on catchment properties are limited and if available represent different scale. This will help in homogenisation of features and utilisation of available information.
2. To apply a fuzzy-rule based statistical rainfall downscaling model using atmospheric circulation pattern for rainfall forecasting. The economic activities and ecological environment depends solely upon rainfall amount and its probability, reliable prediction are needed for decision making.
3. To develop a non-calibrated, distributed rainfall-runoff model which can provide maximum information on hydrological process. There is a need for paradigm change in hydrology from calibration based models to process based models. Since runoff generation and production in semi-arid catchments is event-based and non-linear, at a same time little is know over this issue.
4. To perform a model uncertainty analysis both for rainfall and hydrological model. Uncertainty in the modelling results need to be identified for interpretation and goodness of results. Model prediction in un-gauged catchments can not be verified with confidence but a range of parameters variability can be suggested.

The basic elements for decision support models in Anas catchment are the four modelling modules namely statistical downscaling of rainfall prediction, non-calibrated distributed hydrological model, water resources planning and development model, river and reservoirs management model together with the spatial and hydrological database sub-system and the query-display-analysis sub-system for decision making. Figure 1.2 shows the conceptual layout of various models for catchment level decision support management.

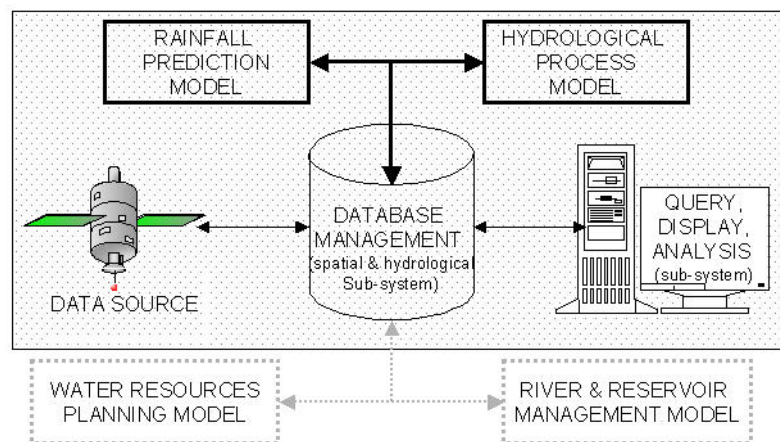


Figure 1.2 Scheme of decision support models for Anas catchment in Mahi basin of Western India. For current research study our focus is limited to rainfall prediction and hydrological models

**Rainfall Prediction Model:** Rainfall as a source of water supply for agriculture and ecosystem management is one part of the water scarcity. The forecasting of station rainfall and its conditional rainfall probability and rainfall amount are important information for decision making. The coupling of station rainfall to atmospheric circulation pattern based on conditional analysis and assessing rainfall amount and probability can be also be an important parameter for future water resources assessment or climate change modelling.

**Distributed Hydrological Model:** Hydrological modelling is undertaken in order to understand the runoff generation process and dynamics of water resources. Historically it has been the dominant methodology for catchment planning and development. The application of simulation models may be for water resources quantification or for decision on construction of retention pond and check dams.

**Water Resources Planning and Development Model:** Optimisation and prioritisation of water resources development measures at sub-watershed scale may benefit from water harvesting and water conservation in a selected sub-watershed using existing knowledge and tools.

**River and Reservoir Management Model:** Reservoir management model is used to analyse the water distribution in rivers and reservoirs for operation, irrigation scheduling and planning.

The main sub-system of the modelling modules is a GIS database library. This is a main database of spatially referenced data which may be queried and manipulated to calculate

parameters for input into the given models. In addition the query and results can be used for formulating decision rules or making final decisions. It consists of loosely coupled GIS and simulation models that connects them. The GIS employed here is Arc/Info (ESRI) which provides the primary means of storing, maintaining and manipulating the spatial data. The GIS data library consists of raster data sets such as land use maps derived from remote sensing data, vector data sets such as streams, contour lines and attribute files in ASCII or \*.dbf formats. Additional spatial attribute files are created by way of decision support modules. The attribute files can be transformed into GIS format or can directly be used for map generating.

Database management systems (DBMS) and GIS have enhanced potential of terrain and elevation modelling. The application of remote sensing data for construction of thematic maps and regionalisation of hydrologic feature and identifying suitable locations for water resources development is an interesting research work for regions with limited data records. The key feature of watershed-based decision making is flexible and bottom up approach in establishing common goals, actions plans and investments at community level.

The primary software and development tools employed for decision support models were chosen for a combination of their capabilities, affordability and ability to run on the personal computers. Appropriate commercial development tools to maintain the catchment database such as Microsoft Access, FORTRAN and C/C++ are affordable. The revised and precompiled software packages that were incorporated for Anas catchment modeling were Arc/Info UNIX version (ESRI, 1997), ArcView 3.2a (ESRI, 2001), Multispec W3.2 (Purdue University), fuzzy rainfall model with modified code (FORTRAN, Bardossy and Plate, 1991) and ZIN model with modified code (C++, Lange 1999).

## **1.2 Research Outline and End Users**

The results of my research are organised around several distinct research activities from GIS database development to catchment based modelling. All activities share a common spatial and temporal database for number of parameters. The research area characteristics are described in chapter 2. The development of GIS based data management system for various

attributes is given in Chapter 3 while chapter 4 gives a detailed explanation on the remote sensing application in creating catchment specific database and regionalisation of hydrological data. The output can be used in establishing time series database be it for land-use change detection or preparation of geological maps.

Chapter 5 explains a stochastic downscaling model developed to generate rainfall time series at point scale. The station rainfall is linked to the circulation patterns of geo-potential heights using conditional model parameters. The results from distributed rainfall pattern has application generate rainfall for any point within the catchment. Chapter 6 presents the application of distributed rainfall-runoff models (ZIN) in Anas catchment. Finally the results are summarised giving an outlook for possible improvements and future research (see chapter 7).

The major goal of the watershed decision support models is to deliver, exchange and integrate river basin information for various actors (state and local government agencies, public, NGOs) decision makers and planners. Since the task of developing a full decision support system for a river catchment is a complex multi-disciplinary task which would require over many years of research for an individual to start from scratch.

The research study for Anas catchment India is innovative with respect to the following challenges: a) Integration of spatial data from various sources into temporal-scale information with substantial degree of accuracy, e.g. topographic map at 1:50000, geology map at 1:250000 and land-use map derived from Landsat raster data imageries at 30m cell size. b) Application of methods of data acquisition by remote sensing (such as detection of land use change) processing by GIS and translation of this knowledge for hydrological model parameterisation and visualisation. c) Stochastic downscaling of rainfall generation based on atmospheric circulation pattern for predicting rainfall probability and amount. This will further help in predicting occurrence of monsoon, which will be an important information for crop growth and hence optimal agricultural yield. d) Improved understanding of hydrological process based on spatial and geo-morphological parameters and knowledge on prediction in un-gauged catchments. This will form a basis for developing a spatially distributed water resources assessment methodology at sub-catchment scale.

The end users of results obtained from watershed decision support models in India are State Water Data Centre (SWDC) of Ministry of Water Resources, Government of M.P. at Bhopal. A World Bank assisted project on hydrological data collection and strengthening the capabilities of SWDC is under implementation since 1996. The District Rural Development Agency (DRDA) of State Authority at Jhabua, a prime agency solely responsible for the implementation of watershed management activities has distinct interest in research results. Other institutions that may use research results for field level implementation are Natural Resources Data Management System (NRDMS) of Ministry of Science and Technology, Government of India at New Delhi; Space Application Centre (SAC) of Ministry of Space, Government of India at Ahmedabad; Water and Land Management Institute (WALMI) of Department of Rural Development at Bhopal.

### **1.3 Decision Support Models (DSM)**

#### 1.3.1 Need for DSMs

The emphasis of decision support models have been on the use of existing knowledge and tools for sustainable catchment management and to reach an appropriate decision. Simonovic and Bender (1996) for a research study in Canada state that decision support system (DSS) allowed to reduce costs associated with promotion of strategies by seeking an adequate level of consensus before proceeding with design and project implementation. They propose that DSS are likely to increase the efficiency of data collection through early clarification of issues in the planning process. Watershed decision support modelling is used by Hann et al. 1982 to simulate the hydrological process and system dynamics that takes place in a natural watersheds. Thus the objectives of watershed decision modelling may be; to gain a better understanding of hydrological phenomena occurring in the watershed and to generate synthetic sequences of hydrologic data for forecasting for future decisions.

There is increasing pressure from engineers, water managers and decision makers to allocate less water to agriculture which uses almost 90 percent of currently available water supplies and more to life support and economic activities. This caused an increasing conflict between agriculture to sustain food production and direct human needs to support the fresh water

ecosystems. The consideration of watershed as the basic unit in hydrological planning is necessitated by the fact that downstream is often affected due to development in the upstream. Watersheds are also convenient units for performing economic analyses and optimisation of natural resources (FAO 1977). Further a catchment is a convenient unit for analysis that overlaps and integrates the sectoral concerns of foresters, hydrologists, economists, engineers and agriculturists. National Water Policy of Government of India (1987) also stresses the need for planning of water use and related activities on a catchment basis.

Thus this research study on towards decision support models for un-gauged catchment in India, intends to improve our understanding of hydrological processes and modelling the rainfall probability in un-gauged catchments which is important for both the water resources planning and conservation management. It is postulated that a watershed decision support system if developed with all the sub-system models, will be a helpful tool in water resources development, water allocation and water policy formulation for semi-arid Anas catchment.

### 1.3.2 Concept of DSM

Decision support models are computer programs or a set of interlinked modelling modules that utilises analytical methods, such as decision analysis, optimisation algorithms, program scheduling routines. These models can help decision makers to describe modelling process, formulate options, analyse their impacts and select appropriate alternatives and if possible implement them (Adelman 1992). Little (1970) proposed in one of the earliest works on computer based decision support that a decision support system (DSS) be a model based on a set of procedures for processing data and judgements to assist managers in their decision making. A detailed literature review on DSS for watershed management shows that a DSS is composed of several sub-system models such as database management system (DBMS), data sources system, knowledge management system (KMS) and includes query, display and analysis system for decision makers.

A definition of a decision support systems (DSS) or decision support models that is acceptable to everybody is not available at this moment. The reason being that DSS are being studied by various scientific disciplines and each emphasise different aspects of DSS based on their background to the subject. In general the main goal of a DSS is to improve the

quality of the decisions to be made. Thus DSS are seen as information management systems or database management systems. Such computerised systems are desirable in those situations in which the solution of a complex decision making problem calls for a comprehensive input of insights, expertise and preferences of decision makers (Vellekoop et al. 1987). Moore and Chang (1980) define a DSS in terms of its features and use. They view a DSS as a system that is extendable, capable of supporting ad-hoc analysis and decision modelling, oriented towards future planning, and of being used at irregular, unplanned intervals.

Decision support models are used to support decision processes like management information systems (MIS), data base management systems (DBMS), and some knowledge-based systems (KBS). All these systems may support decision makers in an interactive mode so that this feature does not distinguish DSS from other systems (e.g. real-time flood forecasting). The main difference between DSS and other information systems lies in the numeric model component: formal quantitative models such as statistical, simulation, logic and optimisation models are an integral part of a DSS (Emery 1987, Bell 1992). These models are used to represent the decision problem, their solutions are decision alternatives.

### 1.3.3 Classification of decision support models

Because there is no single definition for decision support system models, their classification is equally difficult. Given the increasing use of computer-based numerical models and geographical information system (GIS), support methodologies given by De May (1992) for classification purpose has been considered. In principle there are three major groups based on query, display and analysis (QDA) module:

First, the Monadic methodology involves pattern recognition with the use of simple cases or set of procedures. There is no complex analysis, as pre-processed inputs are compared with pre-defined parameters. Second, the Structural methodology involves analysis of specific aspects of information input and decision criteria's. For example, the optimisation of atmospheric circulation pattern based on station rainfall, i.e. chapter 5 of this research study can be cited as a typical example. Third, the Contextual methodology involves complex systems where the input parameters are assessed on the basis of their context and use. For example, the sensitivity analysis for digital elevation model, i.e. chapter 3 of this research



study can be cited to support this methodology. In general, decision support models may be grouped into two major categories based on their possible support mechanism, i.e. model oriented and data oriented as defined by Kersten (2000).

Model-oriented decision support: Model-oriented decision support assumes that models exist prior to decision making. A decision opportunity or a problem identified in the intelligence phase leads to the selection of a modelling technique. A model is constructed in the design phase and used to select decision alternatives. The alternative model parameters are calculated using data stored in data bases and the user's input. This type of support is centred on user model interaction.

Data-oriented decision support : In contrast the case of data-oriented support, no prior model is given rather it is constructed from the analysis of available data. Data mining and knowledge discovery techniques are used to extract knowledge and formulate models. This approach depends on the accessibility of large data sets often stored in a database warehouse. The data-oriented support, however, may be initiated by the user but it may also originate with the system itself.

Thus the functions of DSS can be put as, a) assist decision makers in formulation of decision process, b) support management judgement and c) improve the effectiveness of decision making. Model-based decision support system have been selected for the present research study although few models have been modified in order to fit them with the existing data.

#### **1.4 Review of Decision Support Models**

The development of decision support system methodology at catchment scale is still a subject of research and debate. Dhar and Stein (1997) view that data-oriented DSS are used to construct models and obtain knowledge about ill-defined problems rather than simply condensing and summarizing large amount of data. Model-based decision support system for resources management have been discussed for a considerable time (Fedra and Reitsma 1990, Fedra 1996, Crausaz and Musy 1997, Gijsbers 1998, Krejcek and Vanecek 1999, Todini et al. 1999, Welp 2000, Billib et al. 2003, Breuer et al. 2003).

There have been several efforts in Europe during 90's on development of DSS, from flood operations (Todini et al. 1999) to integrated water management (Crausaz et al. 1999, Crausaz and Musy 1997). Todini et al. (1999) developed a DSS aimed at analysing flood events and mitigating their effects on the social environment for Reno river basin in Italy. The support system includes a set of mathematical models linked to a databank, to a GIS, to a Knowledge Base System (KBS) and to a Geographical User Interface (GUI). In case of GESREAU (GEStion des Ressources en EAU) a decision support system developed by Crausaz et al. (1999) is a GIS based information system that stores water management related data. It also contains the data used for strategic and operational decisions. Some links to simulation models are defined in order to evaluate the dynamic behaviour of spatial objects. In case of GESREAU it should be noted that simulation models (hydrologic and hydraulic models) and decision support system are working independently. The resulting data files from one system can be transferred into other system and vice-versa.

The NELUP decision support system (Dunn et al. 1996), used for predicting the impact of agricultural land-use change at Cam basin in England, consists of a series of models (ecology and hydrology) which are integrated with relational and spatial databases, thereby permitting interactive evaluation of future scenarios through GUI. The models are coupled by means of data transfer via the database and allow to make impact assessment queries. The hydrological modelling module is based on SHETRAN program developed by the Danish Hydraulic Institute and Institute of Hydrology (Abbott et al. 1986). The model data needs for running SHETRAN program are extensive that NELUP is in direct conflict with the very essence of DSS objective.

Andreu et al. (1996) designed a decision support system for water resources planning in Segeru river basin in Spain. The system consists of basin optimisation and simulation modules, an aquifer flow modelling tool and a module for risk assessment during the operational management of system. Although the system is capable to calculate time series values of basin release, the development of decision rules has been left upon model developer and engineers, which may render replication for other catchments difficult.

WaterWare (Jamieson and Fedra 1996) decision support system had the objective of developing a comprehensive, easy to use decision support system for river basin planning. By combining the capabilities of GIS, database technology, modelling techniques and expert system, it aims to improve the quality of decision making. In essence, the software system comprises a set of standards to ensure compatibility, shared tools for displaying results, a common language for problem representation thereby providing greatest flexibility for future updates and continuing development.

The HYDRA (Jacucci et al. 1994) is an information modelling and decision support system for irrigation water management for European Mediterranean agriculture. The main components of the HYDRA are a set of soil water balance and crop growth simulation models, a database management system, a agro-meteorological information module, a soil information module, and advanced GUI and an expert system which moderates model control for a number of decision oriented scenarios.

In India no single DSS for catchment management has been working, as per my knowledge. Although decision support systems for disaster management (C-DAC, 2003) and for natural resource planning and management (Bothale et al., 2002) have been gaining momentum. The Geo-Smart (Bothale et al., 2002) has been developed over Arc/Info GIS platform and consists of thematic maps with built-in query builder. In this case spatial data are stored in GIS data library and accessible for spatial data query. Such systems are term as spatial decision tools (Adinarayan et al. 2000) as per the intensity of the definition of decision support system. A fully functional decision support systems at catchment scale are still at their infancy within India and not only differs on methodological approach but also on range of decisions to be addressed. In depth overview of various decision support system reviewed given in annex 1.1, this comparative review is based on model structure, sub-system components, integration with other model sub-systems and coupling with geographical uses interface (GUI).



## 2. RESEARCH PROJECT SETTINGS

India is crowned by the great Himalayas in the northern and surrounded by huge oceans on the other three sides. It lies to the north of the equator between  $8.4^{\circ}$  and  $37.6^{\circ}$  north latitude and  $68.7^{\circ}$  and  $97.3^{\circ}$  east longitude, measuring 3214 km from north to south and 2933 km from east to west. It has a surface area of 3,287,263 sq. km. As we are talking about the India's variety of terrain, it is unmatched by any single country in this world. From the high altitude plains of Ladakh in north to the sweltering heat at the sand dunes of Thar desert in north-west. We have the Andaman's tropical rain forests in south-east and dry semi-arid regions in the west.

The Indian landscape has been modified over time by earthquakes, rifting and climate change. Major crust movements have been responsible for the sharply demarcated four broad structural and physiographic divisions, each with its own characteristic features; a) Northern Himalayas mountains, which form an indomitable physical barrier as world's biggest and largest mountain range. The mountain range also contain cold arid deserts and fertile valleys, b) Indo-Gangetic plains, an intermediate tectonic rift valley, is filled with a thick deposit of alluvium (Pichamuthu, 1967). These plains comprises one of the world's greatest stretches of flat and deep alluvium and are among the most populated areas of the world (456 persons per sq. km), c) the Deccan peninsula, consists mainly of Pre-cambrian rocks in a stable shield area and are separated by hill-ranges (such as Aravali, Vindhyan etc.) from Indo-Gangetic plains, and d) the coastal plains and islands lies between Western Ghats and Arabian sea whereas eastern coastal plain face the bay of Bengal in the east. These major topographic features have given rise to a mosaic of features, which are unique to the various geographical areas.

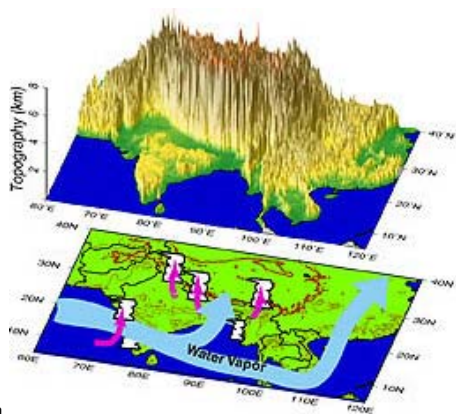
### 2.1.1 Climate and agro-climatic zones

The Indian climate may be broadly described as tropical monsoon type, but vary between hot deserts in north-west to cold deserts in north. Because of the wind, humidity, latitude and differences in altitude, there are considerable number of micro-climatic patterns. India's climate is formed by the north-east monsoon (January-February i.e. winter monsoon) winds which blow from land to sea and the south-west monsoon (June-September i.e. summer monsoon) winds blow from sea to land after crossing the Indian ocean. Almost 75-80% of the yearly rainfall in India is caused by summer monsoon.

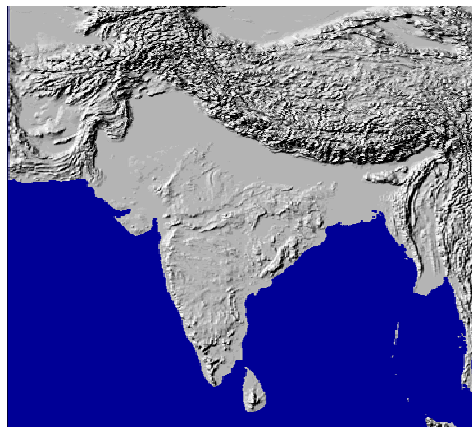
Table 2.1 Profile of main topographic zones of India

Zone	Area [km <sup>2</sup> ]	Population [million] [%]	Density [pers./km <sup>2</sup> ]	Urban [%]	Rural [%]
Northern mountain	322,158	28.04 (3.3)	87		
The great plains	730,955	333.43 (39.8)	456	8.8	31.0
The Deccan Plateau	1,525,279	307.49 (36.7)	202	9.3	27.4
The Coastal plains & Islands	486,635	169.61 (20.2)	349	7.0	13.2

Source: Census of India, 1991.



a.



b.

Figure 2.1: **Topographic features** of India. [Sources a) after NASDA Japan 2002 and b) after NASA USA 1998]

The variability of underlying physical features and seasonal changes in the atmospheric pressure circulation pattern has been creating considerable variations of rainfall distribution in various seasons and regions of the country. Also the rainfall is highly variable among the 35 meteorological sub-divisions as classified by Indian Meteorological Department (IMD). The yearly rainfall is as low as 100 mm in western Rajasthan to as high as 9000 mm in north-eastern Meghalaya. This results tremendous run-off during few months and the country remain dry for almost the rest year.

India has been divided into 6 major climatic zones based on rainfall, moisture index and crop growing period. This classification is based on Thornthwaite index (Hyper arid  $>-0.95$ , Arid  $-0.95$  to  $-0.80$ , Semi-arid  $-0.80$  to  $-0.50$ , Dry sub-humid  $-0.50$  to  $-0.35$ , Humid  $>0.65$ ) as laid down by National Bureau of Soil Science and Land Use Planning (Velayutham et. al., 1999). Later 20 agro-ecological regions on a 1:4 million scale map based on topography, soils, climate and rainfall, crop growing period and available water capacity of soils were further classified. Subsequently 60 agro-ecological sub-regions (refer annexure 2.1) for regional level planning using the detailed soil information at subgroup level, physiography at land form level, bio-climate (refined limits of arid, semi-arid and sub-humid), types and length of crop growing period at 30-days class interval. The information of length of growing period as well as agro-ecological zoning supported by moisture availability index can act an excellent base for water resources modelling and crop suitability evaluation.

### 2.1.2 Water resources distribution and drainage basins

The distribution of water and its availability has strong relationship with rainfall and topography. India is divided into 20 river basins- comprising of 12 major river basins, each having a catchment area exceeding 20,000 km<sup>2</sup> based on drainage pattern (Sharma and Paul, 1999). In addition, other water resources includes reservoirs, tanks and lakes which cover about 70,000 km<sup>2</sup> of the surface area of the India. The Ganga basin is the largest and Mahi basin is one among the smallest basins having a drainage area of 34,482 km<sup>2</sup> and river length of 583 km as shown in figure 2.2b.

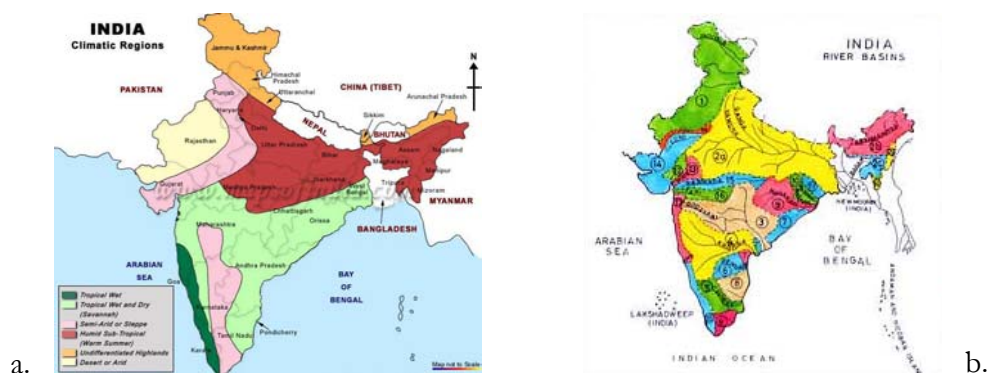


Figure 2.2 a) Major **climatic regions** in India (based on Thornthwaite moisture index) adopted from Source: Velayutham et. al., 1999 and b) major **river basins** in India (Source: Ministry of Water Resources)

Flood and drought affect vast areas of the country and one-third of the country is drought prone. The ground water potential varies in different basins. Due to heavy extraction of

ground water and its limited recharge, it is getting depleted at a fast rate. Sivaramakrishnan (1993) has estimated around 1,870,000 million m<sup>3</sup> of surface water availability, of this only about 50% can be put to beneficial use because of topographical constraints. Because of the uneven rainfall, the availability of renewable freshwater varies enormously in different river basins. The peninsular rivers are rainfed and therefore fluctuate in volume while the coastal rivers are short in length with limited catchment area. The yearly distribution of the flow of various rivers is highly dependent on rainfall.

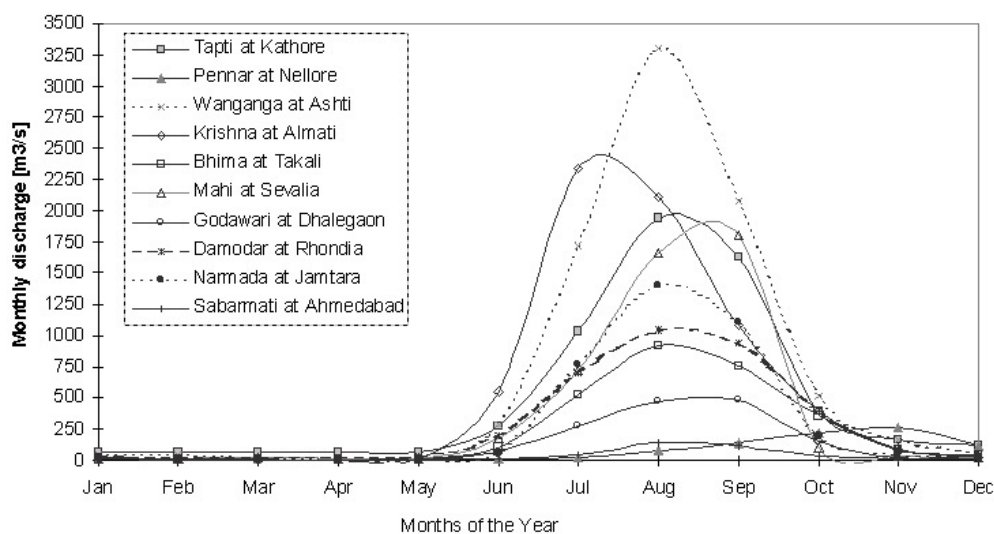


Figure 2.3 Average **monthly flow of selected Indian rivers** (Source: National Centre for Atmospheric Research, Boulder, Colorado state)

The catchment area for various rivers varies between 13,000 km<sup>2</sup> (Sabarmati river at Ahmedabad) to 61,500 km<sup>2</sup> (Tapti at Kathore) at various gauge sections, as shown in the Figure 2.3. It is clear that almost 95% of flow for Narmada river at Jamtara occurs between July and October (4 months), while more than 91% in case of Mahi river at Sevalia takes place between July and September (3 months). The July to October (monsoon seasonal flow) for rivers exceeding 90% of total yearly flow are includes Mahi at Sevalia (93.5%), Wanganga at Ashti (92.1%), Godavari at Dhalegaon (90.4%) and Bhima at Takali (90.2%). From this observation it may be concluded that reservoir storage measures have to be undertaken to enable significant use of water resources throughout the year for conjunctive water needs and demands.

### 2.1.3 Water Resources Use and Potential



Water development is critical for food security in many river basins of India. Basin models has taken advantage of recent developments in hydrological science and system modelling technologies, to assess regional water resources quantity and water movement over the land surface (Maidment 1999). Rosegrant et. al. 2002 through IMPACT-WATER model have worked on water withdrawal, basin efficiency and reservoir storage for various development scenarios (refer annexure 2.3 for detail on scenario definitions). The model results for various basins in India for the year 1995 and projected scenarios for the year 2025 are presented below in table 2.2 and table 2.3.

Table 2.2 Water withdrawal and the share of total renewal water

Name of river basin	Total water withdrawal [km <sup>3</sup> ]			Ratio of withdrawal to total [number]		
	1995	2010	2025	1995	2010	2025
Sahyadri ghats basin	14.9	18.7	20.8	0.14	0.17	0.19
Eastern ghats basin	10.5	13.7	11.6	0.67	0.87	0.74
Cauvery river basin	11.8	12.8	13.1	0.82	0.89	0.91
Godavari river basin	30.2	33.3	38.8	0.27	0.30	0.35
Krishna river basin	46.2	51.4	57.5	0.51	0.57	0.63
Coastal drainage basin	34.8	46.9	43.6	1.08	1.45	1.35
Chhotanagpur plateau basin	7.2	10.9	14.3	0.17	0.26	0.34
Brahmari river basin	25.5	27.2	31.0	0.24	0.22	0.26
Luni river basin	41.9	43.1	50.8	1.48	1.40	1.66
Mahi, Tapi, Narmada river basin	31.4	34.3	36.3	0.36	0.39	0.42
Brahmaputra river basin	5.5	7.2	9.2	0.01	0.01	0.01
Indus river basin	159.1	178.7	198.6	0.72	0.81	0.90
Ganges river basin	255.3	271.9	289.3	0.50	0.54	0.57
India	674.4	750.0	814.8	0.30	0.33	0.35

Source: Ministry of water resources, Government of India (1998-2000) as quoted in Rosegrant et. al. 2002.

Table 2.3 Basin efficiency and reservoir storage for irrigation and water supply under three scenario's for 1995 and 2025

Name of river basins	Basin efficiency [%]				Reservoir storage [km <sup>3</sup> ]			
	1995 estimate	2025 projections			1995 estimate	2025 projections		
		BAU	CRI	SUS		BAU	CRI	SUS
Sahyadri ghats basin	0.57	0.63	0.43	0.71	16	23	16	19
Eastern ghats basin	0.52	0.56	0.41	0.64	9	14	9	11
Cauvery river basin	0.52	0.57	0.41	0.69	7	11	7	9
Godavari river basin	0.53	0.58	0.42	0.65	24	35	24	29
Krishna river basin	0.53	0.58	0.41	0.67	23	34	23	28
Coastal drainage basin	0.60	0.66	0.45	0.76	19	33	19	25
Chhotanagpur plateau basin	0.55	0.61	0.43	0.69	4	5	4	4
Brahmari river basin	0.60	0.66	0.45	0.77	21	36	21	27
Luni river basin	0.61	0.67	0.45	0.77	21	36	21	27
Mahi, Tapi, Narmada river basin	0.55	0.61	0.42	0.69	17	30	17	22
Brahmaputra river basin	0.55	0.60	0.42	0.66	2	3	2	3
Indus river basin	0.55	0.61	0.43	0.75	21	31	21	25
Ganges river basin	0.59	0.65	0.44	0.75	50	74	50	59
India					232	367	233	287

Terms described above refers to water projection for 2025, BAU-business as usual, CRI-water crisis scenario and SUS-sustainable water use scenario. Source: Rosegrant et. al. 2002

Table 2.2 shows that some of the river basins such as Luni (arid climatic zone) and coastal basins (tropical wet and dry climatic zone) are withdrawing more than the total renewal water. The other river basins such as Cauvery (tropical wet and dry climatic zone) and Indus (semi-arid climatic zone) are expected to exceed their total water withdrawal in the year 2025. The other basin will also remain under stress due to increased water demand and limited water supply. It is clear from the table 2.3 that rapid improvement in basin efficiency for each river basin is needed. For arid and semi-arid climatic zones improved basin efficiency to be followed by higher degree of reservoir storage in order to meet the increased water demand. In case of Mahi, Tapi and Narmada river basin an average basin efficiency of 0.55 has been estimated which will improve up-to 0.61 (for BAU scenario) and 0.69 (for SUS scenario) in 2025. An added reservoir storage capacity of the 13 km<sup>3</sup> (76.5% increase for BAU scenario) and 5 km<sup>3</sup> (29.4% increase for SUS scenario) is estimated. In general, additional reservoir storage need to be created for various basin and sub-basins in India.

#### 2.1.4 Socio-economic development

Agriculture contributes to 29.3% of India's GDP employing almost 64.9% of total workforce. The overall growth of Indian economy has depended much on the performance of agriculture and on consistent irrigation for plant production. Expansion of irrigation has played an important role in the development and prosperity of various regions. Most irrigation projects are operating at a low efficiency in the range of 30-40%. It is estimated that even after achieving the full irrigation potential, nearly 50% of the total cultivated area will remain rainfed. This needs a more decentralised planning for water resources and process modelling at catchment or sub-catchment scale. The agricultural sector continue to receive the attention and priority during the successive Five-Year Plans. India today is not only self-sufficient in grain production, but also has substantial reserves, which help in overcoming the effects of drought and occasional failure of monsoon. In 1998-99 the primary sector comprising agriculture and allied activities have contributed 29% to the countries GDP and provided livelihood for almost two-third of work force.

## **2.2 Characteristics of Anas Catchment**

### 2.2.1 Location of Mahi basin

The Mahi basin extends over an area of 34,482 km<sup>2</sup> which covers nearly 1.1% of total geographical area of India. The basin lies in the three states of western India namely Rajasthan (47.7%), Gujarat (33.9%) and Madhya Pradesh (19.4%) as given in Table 2.4 below. Mahi river rises from an elevation of 560m above mean-sea-level for an about 583 km before falling into Arabian sea through the Gulf of Cambay refer figure 2.5 below.

The principle tributaries of the Mahi river basin are Anas, Hiran, Som, Goma and the Panam. The river basin is mostly hilly and its shape is double fanned, which gives rise to high intensity flash floods. The upper part of the basin comprises mostly hills and degraded forests while the central part consists of developed lands including well developed alluvium tract on lower part. On an average the river is about 100-130 m wide and mostly flows through rocky terrain. The mean annual rainfall over the Mahi river basin is around 790 mm, of which about 85% falls during the four monsoon months (i.e. June-September)

Table 2.4 Spatial characteristics of the Mahi river basin

State	Length of river course [km]	Sub-basin area [km <sup>2</sup> ] (% of total)	Mean annual rainfall [mm]
Madhya Pradesh	0 to 167	6695 (19.4)	750
Rajasthan	167 to 341	16453 (47.7)	778
Gujarat		11694 (33.9)	804
a) until Wanakbori weir	341 to 428	10322	
b) until confluence point	428 to 583	1372	

Source: Indian Agriculture Research Institute, 1983

An average yearly surface water potential of 11,000 million m<sup>3</sup> has been assessed by MoWR (anonymous), out of which 47.27% is utilisable water. Present use of surface water in the basin is 2,500 million m<sup>3</sup> which is below the utilisable water potential. The ground water utilisation is about 25% of the utilisable potential. The hydropower potential of the basin has been assessed as 68.6 MW at 60% load factor. In the Rajasthan part of Mahi river basin, there are 3 major surface water resources projects (viz. Bajaj sagar, Jhakhlam, Jaisamand), 2 medium and 220 minor irrigation projects having an irrigation potential of 224,870 ha of cultivable land. A 4529 million m<sup>3</sup>/annum of total surface water potential has been estimated of which only 853 million m<sup>3</sup>/annum is utilised. Similarly a 968 million m<sup>3</sup>/annum of ground water potential is estimated of which only 266 million m<sup>3</sup>/annum found its use. Som Kamala Amba a major irrigation project with a storage capacity of 333 million m<sup>3</sup> are under construction along with 38 minor irrigation projects during the years 1997 and 2015. In the Madhya Pradesh part of the Mahi river basin, there are 2 medium and 406 minor irrigation

projects, with an irrigation potential of 13,870 ha of cultivable land. A total surface water potential of the order 759 million m/annum has been estimated.

For resolving the water sharing conflicts between riparian states like Madhya Pradesh, Rajasthan and Gujarat in Mahi river basin, specific agreements for sharing of water, sharing of costs of land acquisition, resettlement and rehabilitation, and sharing of benefits exists since 1966. There is also a provision for cost reimbursement by Rajasthan to Gujarat state, subsequent to the development of the Narmada river to provide water for Mahi at a later data. Till now these agreements are working well and fair understanding exists.

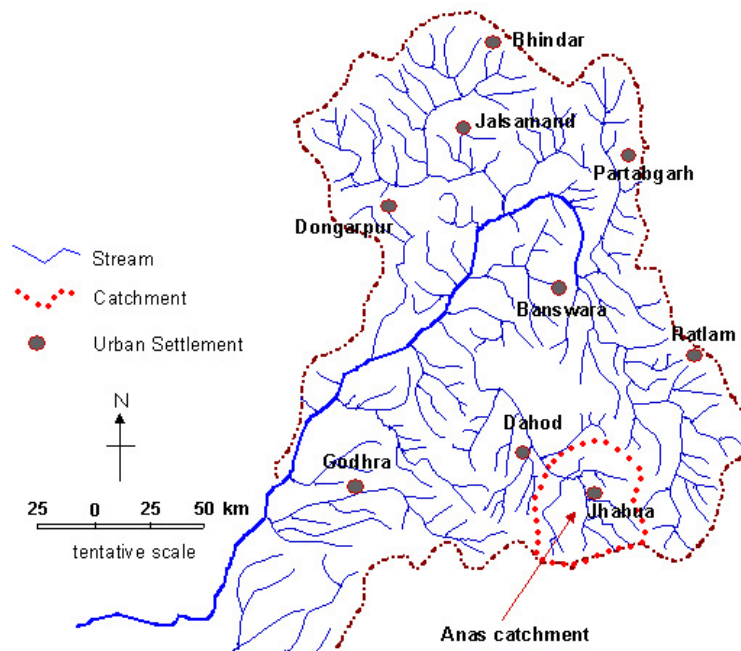


Figure 2.4 Location of Mahi basin in India

### 2.2.2 Location of Anas catchment

Anas catchment a part of Malawa Plateau in Mahi basin taken for the research study is classified as drought prone based on agro-climatic classification as explained in section 2.1.2. The average altitude of the catchment varies between 280 meter at downstream and goes as high as 540 m at upstream above the mean sea level. Anas catchment lies at the west edge of the state of Madhya Pradesh between 22°50'N 74°20'E and 22°30'N 74°50'E, bordering with the Dahod district of Gujarat state and Banswara district of Rajasthan state. Anas river and its tributaries such as Negari, Sunar, Span and Mod flow northward, and joins Mahi river in the Dakar village of Banswara district of Rajasthan state. The catchment is predominantly

occupied by the tribal population, and economically among one of the most backward regions of India.

### 2.3 Topography and drainage profile

Anas is mainly an undulating catchment, covered with a chain of low and medium hills and extended up to Vindhayachal hill range. The catchment covers an area of approximately 1750 km<sup>2</sup> highly undulating and rolling in nature with a mixture of hills and valleys. The maximum elevation of 561 meter above MSL is recorded in S-E direction at catchment boundary between Anas and Mahi catchments. The catchment may be sub-classified into 19 major watersheds based on the drainage pattern and elevation (refer figure 2.6a & 2.6b). The list of watersheds along with their respective geographical area is given below in table 2.5.

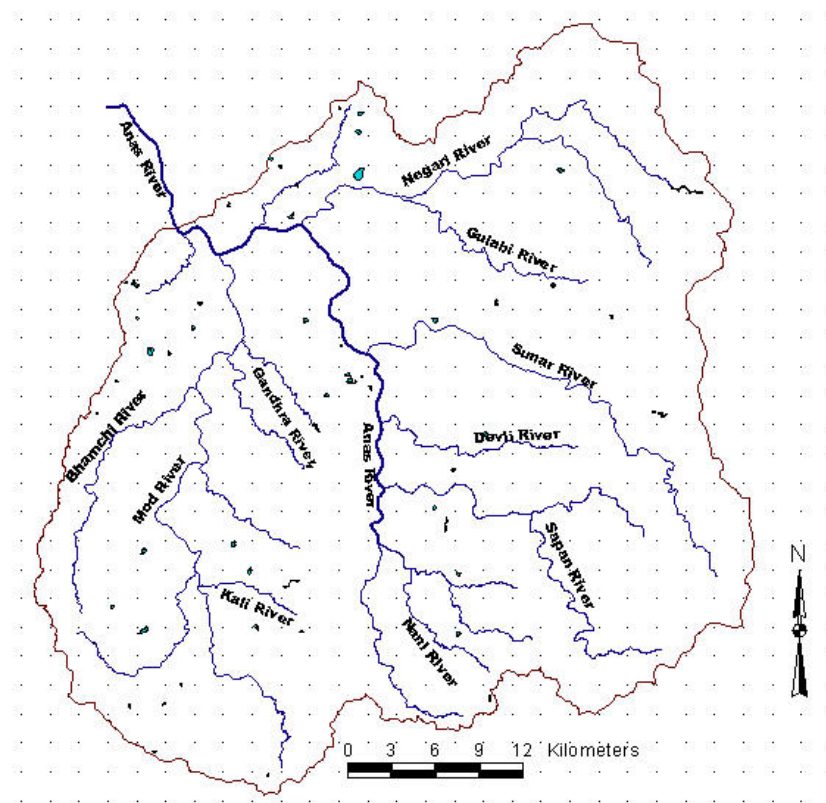


Figure 2.5 Anas catchment and its river network

Table 2.5 Geographical area occupied by each watershed in Anas catchment

Serial	ID	Name of watershed	Geographical area in [km <sup>2</sup> ]	Remarks (if any)
A.		<b><i>Mod sub-catchment</i></b>	<b><i>536.125</i></b>	Mod sub-catchment occupies
1	101	Upper Mod-Kali river	138.864	30.5% of total catchment area
2	102	Dhobada river	87.912	
3	103	Bhamachi river	77.970	
4	104	Middle Mod river	112.627	
5	105	Gandhro river	34.164	
6	106	Lower Mod river	84.586	
B.		<b><i>Anas sub-catchment</i></b>	<b><i>1220.339</i></b>	Anas sub-catchment occupies
7	201	Upper Anas river	63.441	69.5% of the total catchment
8	202	Prithviraj-Dhobariya river	118.708	area
9	203	Upper Sapan river	110.767	
10	204	Lower Sapan river	86.697	
11	205	Anas-Devli river	110.395	
12	206	Sunar-Harkiyakhal river	111.917	
13	207	Lower Sunar river	111.964	
14	208	Gulabi river	83.111	
15	209	Upper Negari river	71.073	
16	210	Side Negari river	89.712	
17	211	Lower Negari river	85.468	
18	212	Lower Anas river	73.781	
19	213	Anas-Mod river	103.299	
Total Anas catchment area			1756.464	100.0%

## 2.4 Rainfall and climate

The magnitude of rainfall in the research study areas varies with time and space. It is this variation in rainfall which is responsible for the hydrological problems including period droughts and sudden floods. The catchment receive a mean annual rainfall of 750 mm having an annual fluctuations between 350mm and 1300mm depending upon wet and dry years. Two distinct rainfall seasons were recognised in most of the semi-arid zones of India followed by two transitional periods. About 75-85% of the rainfall have been concentrated during monsoon season, just during four months from June to September typically in 30-50 rainfall events. Although monsoon has not been a period of continuous rainfall but has been responsible for majority of surface runoff as well as groundwater recharge.

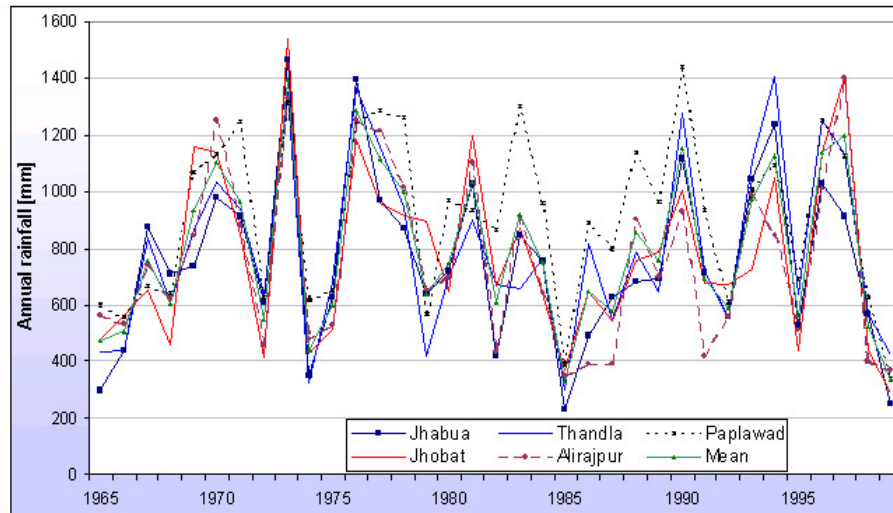
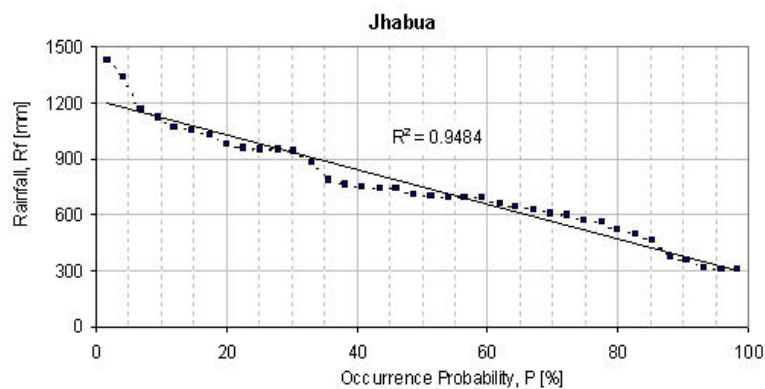
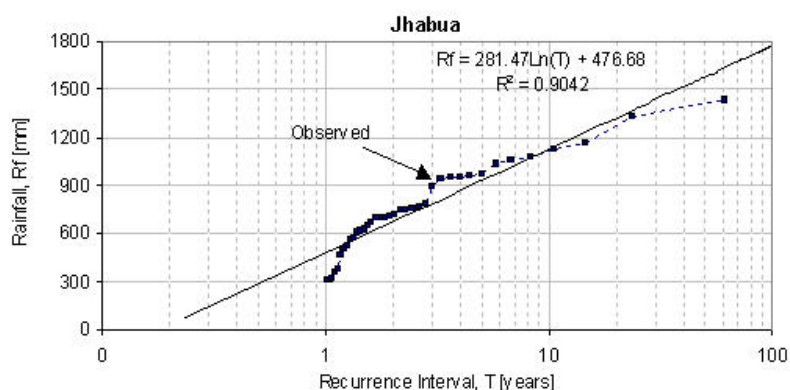


Figure 2.5 **Yearly rainfall variability** for 5 stations between 1965-99 in Anas catchment

The annual rainfall variation for various rainfall gauges in Anas catchment are given in figure 2.5 above. The probability and recurrence interval analysis of seasonal rainfall data for the station Jhabua during 1961-2000 for a 40 years period has been shown in figure 2.6a & 2.6b. It is expected that Jhabua may receive at least 705mm and 570mm of seasonal rainfall with a 50% and 75% probability of occurrence. A seasonal rainfall amount of 705mm will be equalled or exceeded every second year while the amount of 950mm every fourth year. Thus the significance of statistics have the chances of poor rainfall once in eight years leading to crop failures.



a.



b.

Figure 2.6 Probability plotting of monsoon rainfall totals for station Jhabua derived from observed 40 years rainfall data (1961-2000)

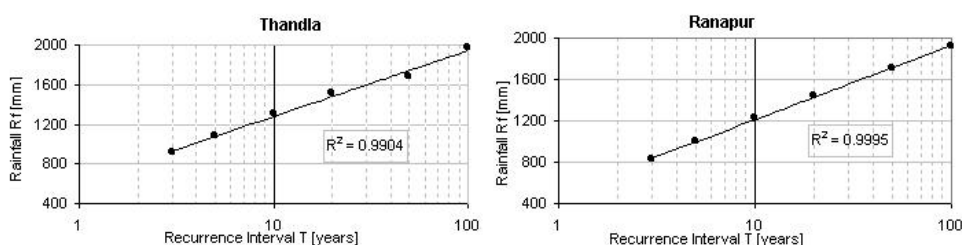


Figure 2.7 The rainfall recurrence interval and monsoon season rainfall for Thandla and Ranapur stations

Similarly the rainfall recurrence interval for Thandla and Ranapur stations have been calculated using observed monsoon rainfall (refer Figure 2.7). Interestingly some spatial variation have been observed for various stations but their variability range remain close to catchment mean.

The temperature variation within Anas catchment shows a diurnal variation in the maximum as well as in minimum temperature. The warm period of the year is between March to June where average monthly maximum remain between 36°C to 41°C. During the winter season between December to February the average monthly minimum temperature varies between 9°C to 12°C. Figure 2.8 below shows the average monthly maximum and minimum temperature recorded at meteorological station at Alirajpur, located somewhere 30-35km south of Anas catchment. The average monthly values have been obtained from daily temperature recorded at Alirajpur meteorological station during the years 1956-1998 with partial missing records between 1981-92 years. Thus high value of monthly temperatures



have been recorded pre- and post-monsoon season. During the normal rainfall years it may be assumed that soils are dry before and after rainy season.

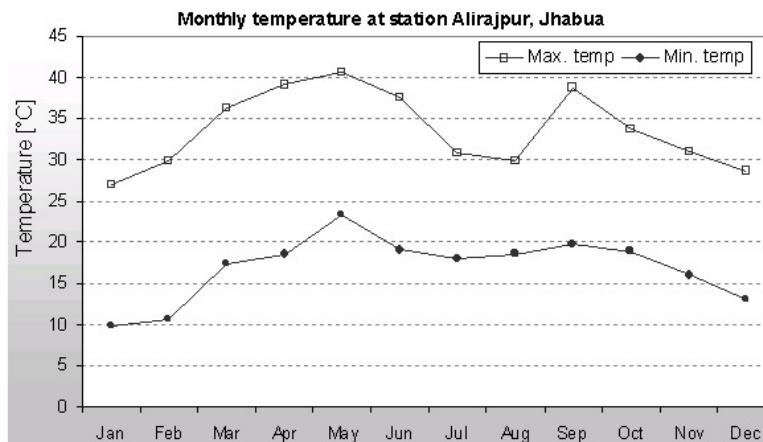


Figure 2.8 Mean **monthly maximum and minimum temperature** [°C] at Alirajpur meteorological station during 1956-98 (source: Indian Meteorological Department)

## 2.5 Land cover and land use

The forest cover is sparsely distributed on sloping lands and most of the area is under thin vegetation cover. The supervised classification of satellite image of 6<sup>th</sup> April for land cover identification shows that almost each 25% of land area has been under forest, range land and agriculture. Out of 25% forest cover, 18% has been notified as forestland but with thin forest cover. A detail study on land-use classification has been conducted in chapter 4 of this research work. The major agricultural crops grown in the catchment during monsoon season (Kharif crops) are maize, cotton, groundnut, pulses, soybean, peas and during the non-monsoon season (Rabi crops) are wheat, gram, black beans, oil seeds and vegetables. The double cropping area during non-monsoon season has been limited to just 20% of the net sown area. The limited area under double cropping mainly attribute due to the absence of supplementary irrigation during non-monsoon period.

## 2.6 Soils and geology

The major soil types found the catchment have been described in figure 2.9 and table 2.6 with their physical properties. The catchment has poor soil depth varying between 0.25-

0.50m on the hilly tracks and 1.5- 2.5m in the alluvium plains. The soils in the area are mainly of medium black cotton soils along river banks and valleys, loamy with gravel on well drained low lying areas, and laterites (red-yellow texture) on uplands and slopes. The fertility of black cotton soils is high due to ferro-magnesian lava and ash beds. They are poor in phosphorus and nitrogen, but still suitable for agricultural production. The red-yellow soils consist of granite, gneisses and schists deficient in humus, nitrogen, phosphoric acid and lime. They have low fertility and often used a for pasture or grass-lands (NCHSE, 1993).

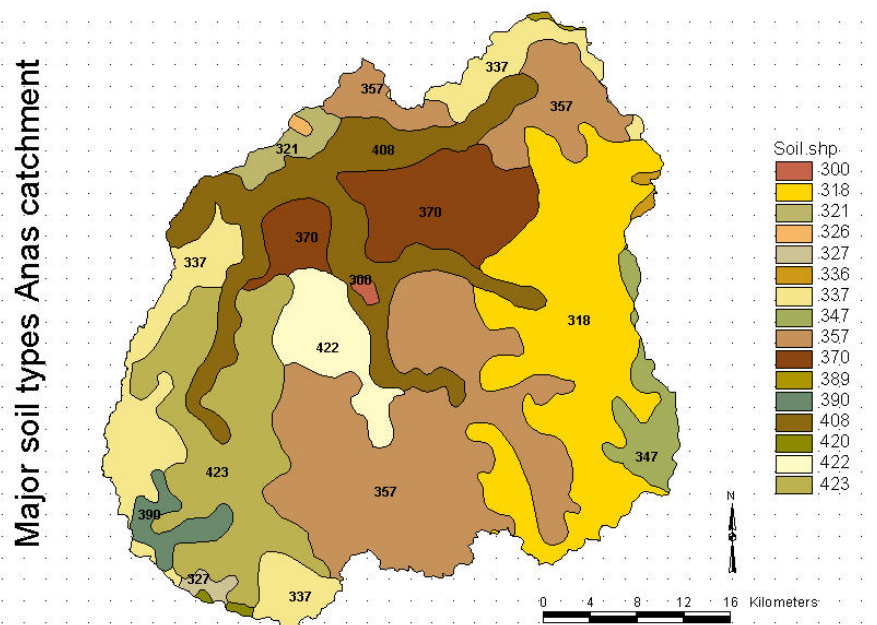


Figure 2.9 Properties of **soil types** in Anas catchment (300-urban area; 318, 321, 326 & 327- clay skeletal and stony; 336, 337, 347 & 357- clay to fine-clay; 370, 422 & 423- fine clay to loamy-clay; 389 & 392- fine clay; 408 & 420- loamy mixed)

Table 2.6 Properties of various soil groups and geographical coverage in Anas catchment

Group	Code	Soil type	Description of properties	Area [km <sup>2</sup> ]
Class 1: Stony and concrete surface, well drained				
	300	Urban area		3.497
Class 2: Soils of hills with escarpments (moderately steep sloping hills with escarpments)				
	318	Clayey-skeletal	shallow, excessively drained, very severe erosion, moderate stony	330.794
	321	Loamy	very shallow, well drained, severe erosion	23.133
Class 3: Soils of undulating plateau (clay-skeletal soils on gently sloping undulating plateau)				
	326	Clay-skeletal	shallow, excessively drained, severe erosion, moderate stony	2.259
	327	Fine loamy	Deep, moderate drained, moderate erosion	7.263
Class 4: Soils of plateau (excessively drained, clay-skeletal soils)				
	336	Clay-skeletal	very shallow, moderately sloping plateau with severe erosion	4.357
	337	Clay	Shallow, gently sloping plateau with moderate erosion	169.620
	347	Fine-Clay	Deep, moderate drained, gently sloping,	45.511

	(montmorillonitic)	moderate erosion	
Class 6: Soils of dissected plateau			
357	Fine-clayey	Slightly deep, well drained, gently sloping plateau, moderate erosion	478.411
Class 7: Soils of plains			
370	Fine-clay (montmorillonitic)	Deep, well drained, gently sloping plain land, moderate erosion	150.092
422	Loamy-clay (kaolintic)	Shallow, excessively drained, gently sloping uplands, severe erosion	70.581
423	Fine loamy-clay (kaolintic)	Slightly deep, well drained, gently sloping plain land, moderate erosion	215.508
Class 8: Soils of undulating plains with mounds			
389	Fine-clay (montmorillonitic)	Slightly deep, well drained, gently sloping, moderate erosion	1.775
390	Fine-clay (montmorillonitic)	Slightly deep, moderately drained, gently sloping, moderate erosion	27.597
Class 9: Soils on plateau with mesas and buttes			
408	Loamy-mixed	Shallow, excessive drained, loamy soils on gently sloping, moderate erosion	223.309
Class 10: Soils of hilly terrain			
420	Loamy-kaolintic	shallow, excessively drained, gently sloping hills, sever erosion	3.013

The rock types found to occur in the southwest part of the study area consists of Phyllite, quartzite, muscovite quartzite, feldspathic quartzite, gneiss and migmatites of Lower Proterozoic Aravalli group, pink granites of Upper Proterozoic granite. The igneous and metamorphic terrains, developed a thick array of fracture and joint systems, through which meteoric water could pass through. Over time these zones have promoted deep weathering, thick soil formation and thus could support dense vegetation cover. On the contrary the dissected plateau regions in view of highly varied characteristics of volcanic flows, influenced by high altitude and monotonous flat topography have promote ground water transport along the bedding planes. This effect can be found visible due to promotion of lesser stream formation within this zone. This zone too supported the weathering and soil formation but in a restricted way compared to igneous and metamorphic terrains. The land area found under each group can be summarised in table 2.7 below.

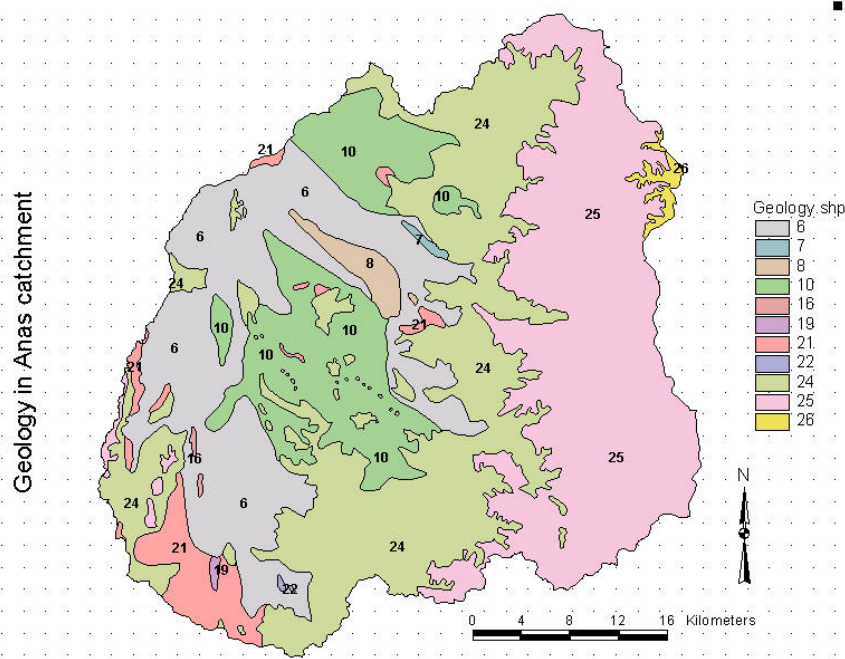


Figure 2.10 **Geology** in Anas catchment (6-quartzite; 7& 21-limestone; 8 &10-muscovite quartzite; 16-migmatite; 19-granite; 22-sandstone; 24,25 & 26- hard rock with feldspar)

Table 2.7 Tabulated area under each geological group and their properties

Code	Name	Description	Area [km <sup>2</sup> ]
6	Phyllite, Quartzite	Dark grey fine grained metamorphic rocks	367.644
7	Dolomitic limestone	Dirty white to dark grey stromatolitic fine grained hard compact rock	2.582
8	Muscovite Quartzite	White, flacky soft rocks	23.025
10	Feldspathised quartzite	Coarse grained hard metamorphic- sedimentary rock	242.030
16	Migmatite	Pink and grey hybrid coarse grained hard granite	1.506
19	Pink granite	Pink medium to coarse grained hard granite	1.990
21	Nodular limestone	Yellow and red medium to coarse grained rock, white and	68.483
22	Nimar sandstone	light pink hard compact rock	0.861
24	Vesicular pahoehoe flows	Dark and greyish, highly porphyritic hard rock with crystal of feldspar	525.752
25	Pahoehoe flows	Dark and light greenish, highly porphyritic hard rock with crystal of feldspar	511.173
26	Pahoehoe flows	Dark fine grained, moderately porphyritic hard rock with crystal of feldspar	11.674

## 2.7 Hydrology and water resources

The rivers in the research catchment are seasonal and flow during monsoon season only. In the head-watershed river channels often gets dry shortly after the end of the rainfall events. On the sloping plateau having low soil depths are excessively drained and runoff coefficients are in general higher than soils of dissected plateau and soils of plain regions. The mean

runoff coefficients vary between 20-25% depending upon terrain and soil depths. In the alluvium plains, the infiltration rates and soil permeability are high reaching as much as 200mm/hr depending upon intensity and distribution of rainfall event. Number of small storage surface water reservoirs having mean storage capacity between 0.2 to 0.3 million-m<sup>3</sup> have been constructed in the catchment in last 10-years. There existed about 150 reservoirs with wide range of storage capacity between 0.2 million-m<sup>3</sup> to as much as 3.8 million-m<sup>3</sup> for Gulabpura tank close to Jhabua town. The total storage capacity of these reservoirs found close to 55 million-m<sup>3</sup> in total. Thus the effect of storage reservoirs on runoff generation and infiltration can be an interesting parameter in hydrological modelling.

The inter-annual variability of discharge is very high and even vary between events of similar intensity. Limited discharge data from two discharge measurement stations during the period 1992-95 has been made available by State Water Data Centre at Bhopal collected during World Bank assisted Hydrology Project. The discharge data time series are of mixed resolution between 6hr (3 measurements each at 6:00 hr, 12:00 hr and 18:00 hr) to daily. The quality of available discharge data has not been found good due to manual measurements. The data reliability test for Anaterbeliya station has been performed as depicted in figure 2.11 for various years. The observed discharge varies considerably between years for the same discharge height. This shows that various calibration curves which have been used on year to year basis. Although arid and semi-arid catchments with intermittent runoff conditions, the measurement error may be expected to be rather high.

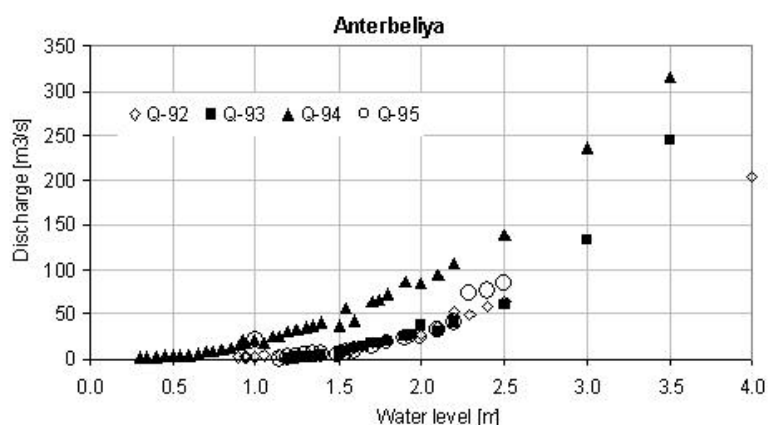


Figure 2.11 State-discharge curve for various years 1992-95 during monsoon seasons

The detailed review of measurement data for Anterbeliya and Mod stations for stage-discharge curves is conducted. As a matter of fact there is always some degree of error in stage-volume relationship. But the main source of error found for Anterbeliya and Mod discharge measurements present quite different situation during all the years.

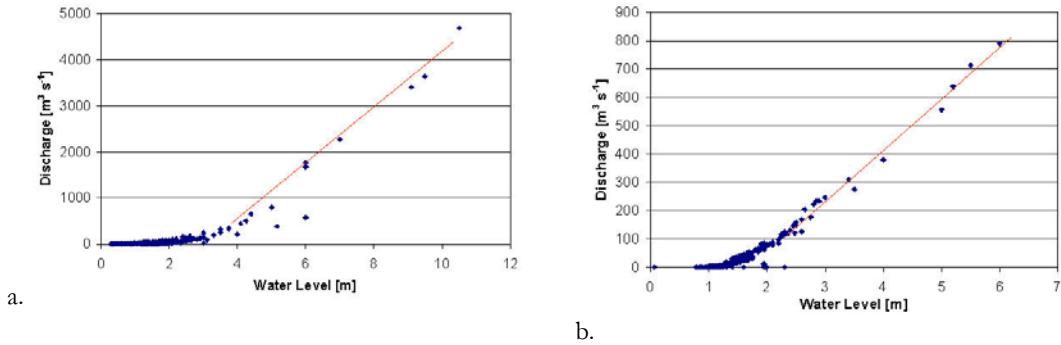


Figure 2.12 **Stage-discharge relationship** for two discharge stations a.) Anterbeliya, catchment area 1150 km<sup>2</sup> and b.) Mod, catchment area 550 km<sup>2</sup> in Anas catchment for 1994 monsoon season

The detailed analysis for the discharge data for the year 1994 shows gross anomalies in discharge with respect to water levels. It is difficult to derive relationship between stage and discharge curve which are often linear in the beginning and tending to take parabolic shape later. The observed data for various water levels (stages) have been depicted in figure 2.13 below.

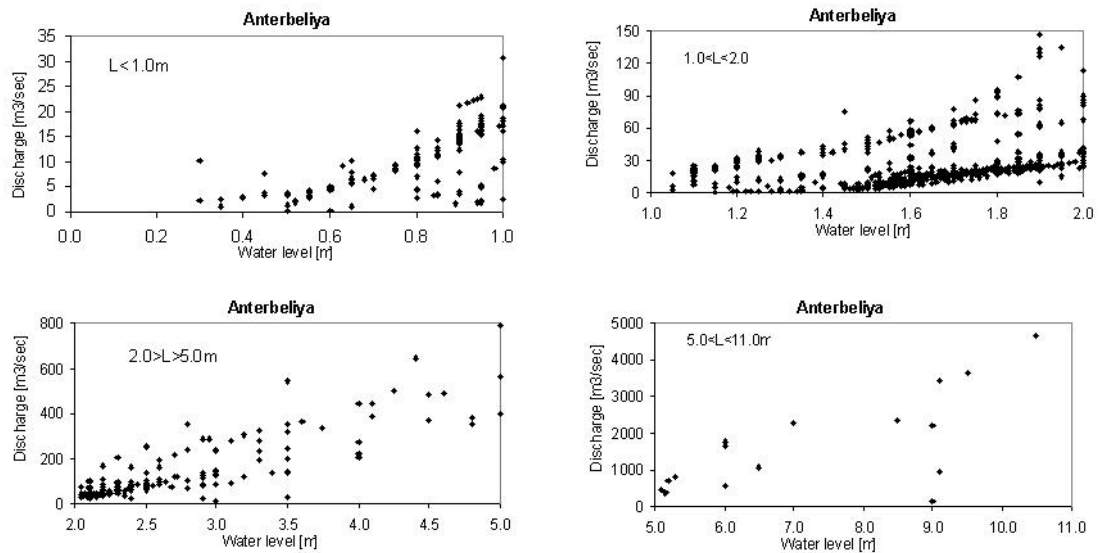


Figure 2.13 Stage-discharge curve Anterbeliya station at different water levels

The Large data uncertainty persists between stage-discharge as well as with measured rainfall. The calibration of distributed model based on measured discharge will lead to erroneous model parameter identification, thus alternative methods need to be explored and tested.

## **2.9 Socio-economic Characteristics**

The socio-economic characteristics of the population living in the Anas catchment can be categorized as disadvantaged group living below poverty line. Approximately the 90% of the total work force have been primarily engaged in agriculture which has been based on rainfed farming. The recent statistics shows that the allied agriculture activities and household industry has been very limited in the catchment. The dependence of masses on agriculture and have been making them vulnerable and dependent on monsoon season. The rainfall had played a significant role in seasonal out migration in search of jobs to nearby urban centres during dry years. A socio-economic study by NCHSE (1993) reported that as much as 50% of the households are seasonal migratory household and go as high as 70% during some dry monsoon years. This pattern has been an integral part of the survival strategy of the tribal people living in Anas catchment.





### **3. CATCHMENT MODELLING AND DATABASE DEVELOPMENT**

#### **3.1 Catchment Modelling**

The catchment modelling and database development on catchment properties forms an important elements for decision support model building. The term catchment modelling refers to the simulation of a hydrological process that take place in the certain time and given space. While the database development can be referred as the representation of spatial and temporal catchment properties and related parameters. The challenges faced in catchment modelling in recent years have reflected the need to deal with spatial variability, scaling and linkages among multi-disciplinary hydrology, meteorology, environmental biology and climatology. In recent years, the research advances in catchment modelling have employed geographical information system (Maidments, 2002), remote sensing data (Schultz and Engman, 2000) and environmental tracers (Leibundgut, 1995) for process modelling as well as water resources assessment tools. The usefulness of spatial properties of catchment for hydrological model parameters become much more important for un-gauged or poorly gauged basins where limited historical time-series data or catchment response information is available. The purpose of this chapter is to review and provide knowledge about the behaviour of hydrological systems under semi-arid environment for catchment modelling and in the decision support systems. Based on the review of scientific knowledge and data availability in the Anas catchment, the choice of appropriate hydrological models and decision support parameters have been made.

A review of literature on catchment science classified the some of the emerging research fields pertinent to catchment modelling includes the need for improved understanding of; how space and time scales are linked in process that converts rainfall into runoff (e.g. Gupta et al, 1986)? how the bio-physical and land-use mechanisms that determine evaporation from

a catchments can be parameterised (Band, 1993)? how the flow and storage of water within a catchment affects the water quality in streams and underlying rocks (Turner et al, 1991)? and how advanced technologies such as remote sensing (Schultz & Engman, 2000) radar and circulation pattern (Bardossy et al, 1992) may help to better understand the catchment behaviours and predict the water resources potential?

### 3.1.1 Classification of catchment models

Catchment models may be classified into various categories based on physical process description, spatial and temporal model scale, and type of data used as model input. Singh (1995), Black (1991), McCuen (1989) and Larson (1982) have primarily grouped them into distributed models, lumped models, stochastic and deterministic model. The physically based distributed models use general non-linear partial differential equation which involve some form of discretisation of space coordinates and of the time ordinate. Solutions are then found for the nodes defined by space time discretisation (Beven , 1985). The arid and semi-arid rivers are characterised by flow extreme flow variability and flood dominated regime while significant runoff events tend to be physically independent of one another (Kisiel et al., 1971). The level of runoff event independence will vary based on hydrological diversity, characteristics of runoff producing conditions and size of drainage network (Knighton & Nonson, 1997). Despite ths diversity, the general distinctiveness of runoff period suggests that event-based approach provides a most appropriate means for analysing the hydrology of arid and semi-arid regions. The following catchment models for dry land rivers can be identified based on runoff process;

- a) Peak discharge models can be classified into 2-type; i.e. calibrated models (single return period equations, index flood, moment estimation) and non-calibrated models. These models are used when storage is not a significant factor in the design.
- b) Single event hydrograph models consists of design storm and actual storm models. These models are more complex and reflect the effects of watershed and channel storage on the hydrologic response of the catchment. Single event models are particularly useful where a watershed is subdivided into various land cover type or soil conditions, and design can be based on average watershed conditions.
- c) Continuous multiple-event models are actual record and synthetic record types. There is a criticism for peak discharge and single event hydrograph model because they reflect only average watershed conditions. Thus, it has been suggested to use

multiple-event models which are more physically realistic and provide for continuous accounting of hydrologic process and water availability.

A general classification of watershed models according to physical process and based on hydro-dynamic models and empirical models can be summarised as in table 3.1.

Table 3.1 Classification of watershed models based on underlying physical process and scale

Physical process	Hydro-dynamic models	Empirical models
1. Surface runoff	<ul style="list-style-type: none"> <li>• Kinematic wave models</li> <li>• Diffusion wave models</li> <li>• Dynamic wave models</li> <li>• Conceptual models based on system approach</li> </ul>	<ul style="list-style-type: none"> <li>• SCS method</li> <li>• Tennessee Valley double triangular UH-method</li> <li>• UH-method based on orthogonal function</li> <li>• Rational formula</li> </ul>
2. Infiltration at a point under ponding	<ul style="list-style-type: none"> <li>• Richard's equation</li> <li>• Kinematic wave models</li> <li>• Green-Ampt model</li> <li>• Phillips 2-term model</li> </ul>	<ul style="list-style-type: none"> <li>• SCS model</li> <li>• HEC model</li> <li>• Holton model or Hortonian flow</li> </ul>
3. Base flow	<ul style="list-style-type: none"> <li>• Models based on Poisson equation</li> <li>• Models based on Laplac equations</li> </ul>	<ul style="list-style-type: none"> <li>• Hydrograph separation models</li> <li>• Algebraic equations (exponential or power decay functions)</li> </ul>
4. Evapo-transpiration	<ul style="list-style-type: none"> <li>• Penman-Monteith method</li> <li>• Morten method</li> <li>• Brutsaert method</li> </ul>	<ul style="list-style-type: none"> <li>• Algebraic equations (Blaney-Criddle, Jensen-Haise, Thornthwaite, Turc method, Hargreaves).</li> </ul>
5. Flow routing in channels	<ul style="list-style-type: none"> <li>• Kinetic wave models</li> <li>• Diffusion wave models</li> <li>• Dynamic wave models</li> <li>• Conceptual models based on system approach</li> </ul>	<ul style="list-style-type: none"> <li>• Muskingum or Muskingum-Cunge method</li> <li>• Volterra series integral method</li> <li>• Convex method</li> <li>• Hydrograph analysis method</li> </ul>

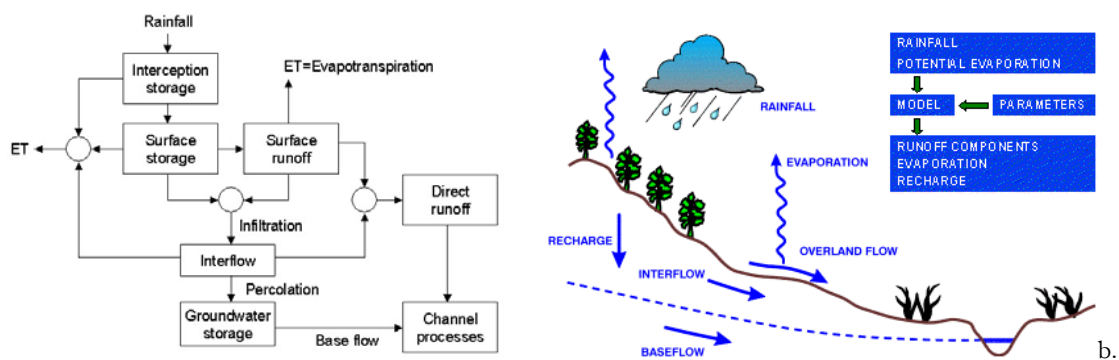
Source: modified Singh (1995), Blöschl & Sivapalan (1995), Black (1991), McCuen (1989), Beven (1985), Larson (1982)

Watershed and hydrologic modelling comprises following four steps: a) model formulation, b) parameters determination, c) model calibration/ verification, and d) model application. In general no model calibration needed if the model parameters have been derived from field based data.

### 3.1.2 Structure of catchment models

The structure of catchment models varies with type of input parameters, boundary conditions and output function. Woolhiser and Brakensiek (1982) identified four levels of catchment model structures based on scale properties includes; individual process, component models, integrated watershed models, and global watershed models. Hydrologic watershed model works on the principle that the demand of interception storage to be filled

before the rainfall can be used to generate runoff (McCuen, 1989). The runoff generation in semi-arid environment has been dominated by fast runoff components (Yair & Levee 1985, Pilgrim et al. 1988). The rainfall is then used to satisfy the soil infiltration capacity and later the Horton-type direct surface runoff is generated (Horton 1933). The temporal sequence of surface runoff may be estimated with the help of an infiltration function based on the soil moisture levels to determine the infiltration capacity. Most often in semi-arid regions, due to limited vegetation the infiltration capacity of soil often found to be low (Berndtsson and Larson, 1987). In two research study by Valentin and Bresson (1992), Casenave and Valentin (1992) on classification of surface-crusts according to their morphology and physical properties found that soils with shallow depths often have lower infiltration capacity up to 20mm/hr and in some cases even much lower. But for Anas catchment the crust formation have not been so dominant as the case with Sahel but still low infiltration capacity on rock outcrops as well in sloping land will be much common. Model parameters that govern the groundwater flow and percolation through the unsaturated zone partially estimate the computed runoff rates. Channel processes described in the model on the direct runoff and base flow estimate the computed stream-flow. Water is also lost from the system through evapotranspiration in addition to stream-flow. In case of dry-land catchments the interflow process is rather negligible as compared to other components.



a. Figure 3.1 a) A flow chart and b) sketch of **integrated watershed model for simulation** of runoff in a closed catchment (after McCuen 1989)

### 3.1.3 Selection of catchment models

The users of the watershed models are generally faced with the problem of selecting from among many best hydrologic models available with the research community. Many hydrologic models are site specific and therefore it appears to be very difficult for selecting an appropriate model which could efficiently provide the answers to all questions. General guidelines for model selection have been presented by Weber et al. (1973), Duckstein (1974)

and Lovell (1975). Jennings et al. (1976) developed a technique to select models for use in stream-flow and reservoir release studies. The model selection problem was viewed by Baker and Carder (1976) as an interactive question-choice process as shown in table 3.2.

The major challenge for selection of catchment models for semi-arid hydrology should be based on process description as suggested by Beven (2002) and Pilgrim et al. (1988). Since hydrological models for semi-arid regions differs with models from humid regions. Most often the catchment models for semi-arid regions have been based on empirical equations which relate catchment characteristics with to the runoff. Casenave and Valentin (1992) in a study in Africa derived infiltration and runoff classes according to soil and vegetation characteristics. They modelled depth of surface runoff as a function of rainfall and initial soil moisture. Others used rainfall, soil type, vegetation and surface storage for regionalisation.

Table 3.2 Basic criteria for evaluating watershed models

1. Ease of use: skill required, ease of interpreting results, assumption required by model
2. Availability of data: ability to use readily available data, ability to handle small and variable time increments, data accuracy and data resolution
3. Availability of models: cost to operate in terms of computing time and hardware system
4. Applicability to management activities: number of parameters predicted, sensitivity to change in management activities
5. Broad regional coverage: ability of a model to operate in diverse hydrological areas, extrapolation of model
6. Accuracy of prediction: ability to predict relative change and absolute effects, need to calibrate model, repeatability of model predictions, error between actual and predicted values for volumes

Source: as quoted in Haan et al. (1982)

The hydrological models for semi-arid environment often include infiltration excess-runoff and transmission losses as given by Lange et al. (1999) Sharma & Murthy (1996), Lane (1982) which are not included in humid models. Lange et al. (1999) for non-calibrated rainfall-runoff model computed the overland flow using initial infiltration loss and temporal decay of infiltration from existing field experiments. Lane (1982) presented a distributed model using SCS-CN method for runoff estimation and including transmission losses. On model comparison Ye et al. (1997) have been of the view that for monthly flow volumes a simple model is sufficient to satisfactorily represent the non-linear of low yielding catchments.

### **3.2 Catchment Modelling with GIS and Remote Sensing**

GIS and remote sensing has wide application in the field of natural resources, hydrology and water resources engineering, environmental and geo-planning, climate impact assessment. Specifically focusing on catchment modelling and water resources planning, GIS helped in distributed hydrological parameter identification to hydrological process description. The spatial variability on the catchment characteristics and land-use change can be well explained with GIS (refer chapter 6). Remote sensing technique because of its capability of repetitive coverage provides useful information of land dynamics and soil moisture parameters. With the advancement of GIS, the hydrological models have been more physically based and distributed considering the spatial heterogeneity of the catchment. In lumped model it may be dangerous to forecast events that are outside the range of catchment conditions over which the parameter values were calibrated. With the physically based parameter values which have been less dependent on model structure, an independent calibration by experimentation is possible (Beven 1985). Similar considerations holds good in forecasting the response of un-gauged catchments where information on hydrologic soil group and land-use has been available.

#### 3.2.1 SCS-CN runoff model

SCS-CN runoff model has been one of the most popular method for computing runoff for rainfall events in un-gauged basins. The model involves the use of curve number (CN) that relates to land-use, soil type, hydrological conditions and soil moisture. In the determination of runoff for a catchment, land-use information have been obtained from Landsat-ETM+ satellite before and after the monsoon season. The GIS and SCS-CN model have been combined to model runoff and the watershed parameters have been estimated using remote sensing and topographic characteristics. Schumann (1993) estimated hydrological parameters with the help of GIS for use in conceptual semi-distributed hydrological model. Kite and Kauwen (1992) performed runoff modelling using land-use classification and CN-number.

The SCS-CN curve number method starts with determination of CN as described in USGS (1986). The hydrological similar units based on land-use, hydrological soil groups (soil type, hydrological conditions, soil moisture) and topography have been delineated. The land-use information has been derived from Landsat-ETM satellite imagery while the topographical

information from digital elevation model (DEM). Appropriate CNs are assigned to each HSUs considering the antecedent moisture conditions. The direct runoff quantity from each HSU are estimated using SCS-CN model. In developing the SCS-CN runoff equation, the relationship between runoff depth and rainfall can be expressed as:

$$Q = \frac{(P - I_a)^2}{(P - I_a) + S} \quad \text{for } P > I_a \quad \dots\dots\dots (3.1)$$

$$\text{and } Q = 0 \quad \text{for } P \leq I_a \quad \dots\dots\dots (3.2)$$

where,  $P$  rainfall,  $I_a$  initial abstraction,  $S$  potential retention and  $Q$  runoff respectively.

The study of several small agricultural catchments in US suggested an approximation for initial abstraction  $I_a$ , by the following empirical equation.

$$I_a = 0.2S \quad \dots\dots\dots (3.3)$$

Thus by substituting the equation (3.3) into equation (3.1) gives the runoff ;

$$Q = \frac{(P - 0.2S)^2}{(P + 0.8S)} \quad \dots\dots\dots (3.4)$$

and the potential retention  $S$ , can be expressed as a function of CN;

$$S = 254 \cdot \left( \frac{100 - CN}{CN} \right) \quad \dots\dots\dots (3.5)$$

where the CN values are in range between 0 to 100. The higher CN values are associated with higher runoff potential. The soils of the basin are classified into four HSG based on their infiltration characteristics as given in table 2.6.

The other parameters such as travel time ( $T_t$ ) and time of concentration ( $T_c$ ) depends on the surface roughness, channel shape and channel slope. Time of concentration influences the shape and peak of runoff hydrograph.

The travel time is the ratio of flow length  $L$ , to the flow velocity  $V$ , thus;

$$T_t = \frac{L}{3600 \cdot V} \text{ [hr]} \quad \dots\dots\dots (3.6)$$

where average flow velocity is computed using Manning's equation

$$V = \frac{1}{n} R^{\frac{2}{3}} S^{\frac{1}{2}} \quad \dots\dots\dots (3.7)$$

where  $R$  hydraulic radius, and  $s$  slope of hydraulic grade line. The hydraulic radius can be calculated by dividing cross-sectional flow area to wetted perimeter.

Thus the time of concentration  $T_c$  is the sum of all  $T_t$  values for various channel flow segments:

$$T_c = \sum_{i=1}^n T_{t_i} \dots\dots\dots (3.8)$$

Figure 3.2 below depicts the conceptual structure of coupled GIS and SCS-CN runoff hydrological model used in runoff modelling for Anas catchment.

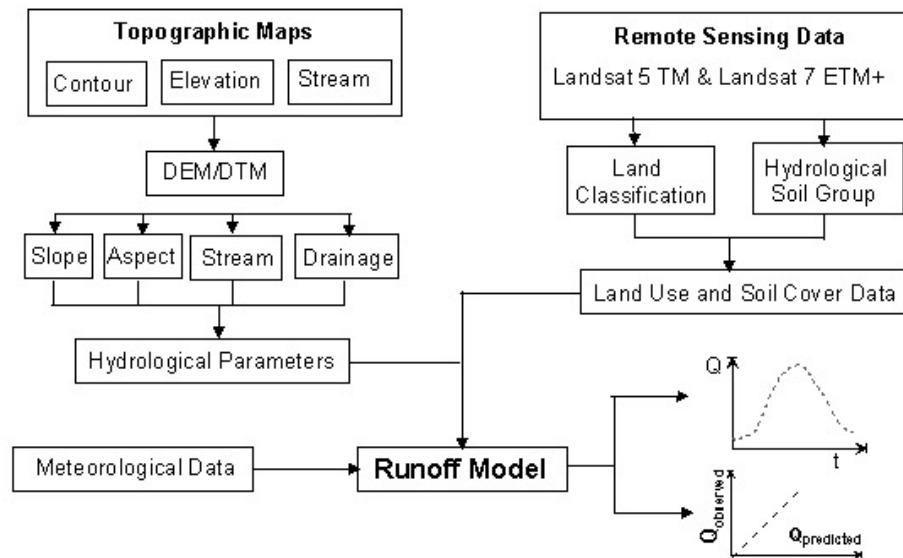


Figure 3.2 The structure of **coupled GIS and hydrological model** (after Awulachew 2001)

3.2.2 Catchment water balance model

Atmospheric processes on all spatial and temporal scales are sensitive to variation in land-surface properties and soil characteristics. The exchange of heat and moisture between earth’s surface and atmosphere is controlled by the vegetation and soil type (Mengalkamp et al., 1997). Therefore an appropriate description of basic water balance model can be expressed in terms of this equation;

$$Q = P - E_{tp} - \Delta S \dots\dots\dots (3.9)$$

where  $Q$  runoff,  $P$  rainfall,  $E_{tp}$  evapotranspiration,  $\Delta S$  change in soil moisture.



Thus the rainfall applied to the catchment must be utilised for evapotranspiration, stored in the catchment and must have gone out of catchment as channel flow. It is generally assumed that measurement of catchment runoff, rainfall and evaporation can be utilised to index those hydrological conditions which are needed to describe the catchment water balance. In other words, for an appropriate temporal time scale, equation 3.9 can be applied to estimate the runoff at monthly or yearly scale for know rainfall and evapotranspiration.

The evapotranspiration component which is the sum of moisture flux from bare surface and of evapotranspiration from vegetated surface. The potential evaporation has been dependent on temperature, sunshine hours, net-radiation and soil heat flux. On the comparison of three evapotranspiration models, Hatfield et al. (1996) reported a better fit for Penman-Monteith model for daily meteorological data in Davis, Lubbock and Logan catchments. The general form of evapotranspiration equation can be described as;

$$E_{tp} = \frac{\Delta \cdot (R_n - G) + c_p \cdot p_a \cdot \frac{(e_s - e_a)}{r_a}}{\left\{ \Delta + \gamma \cdot \left( 1 + \frac{r_s}{r_a} \right) \right\} \cdot L_v} \dots\dots\dots (3.10)$$

where  $\Delta$  slope of saturation vapour pressure [hPa/°C],  $R_n$  net radiation expressed in water depth equivalent [mm/day],  $G$  soil heat flux in water depth equivalent [mm/day],  $e_s$  and  $e_a$  are saturation and actual vapour pressure [hPa],  $L_v$  specific latent heat [KJ/kg], and the terms  $c_p$ ,  $p_a$ ,  $r_s$ ,  $r_a$  and  $\gamma$  are constants with know value for given climatic conditions.

The potential evaporation for crops and plants is calculated using crop-factor ( $k_c$ ) during various crop growing seasons. Thus

$$E_{tpcrop} = k_c \cdot E_{tp} \dots\dots\dots (3.11)$$

In case of arid and semi-arid regions it has been assumed that there is no significant change in soil moisture before and after the monsoon season. This assumption has been found somewhere close to reality.

### 3.3 Generation of Thematic Maps and GIS Database

As we have above in section 3.2, for distributed hydrological modelling catchment thematic data are needed such as topography for slope, stream network for channel nodes and other information. The availability of digital coverages for water resources modelling have been essential for coupling the decision support models. The use of GIS makes the relationship between parameter estimates and model more evident. In spite of continued efforts the spatial information in digital format for various developing regions has yet not been available. In case of Anas catchment India no digital data for the hydrological process modelling and water resources planning have been available. Generation of digital database and thematic coverages (vector and raster) from the topographic maps and deriving information from remote sensing have been considered a priority step, not only for integrating the hydrological model, but also bridging the scale gaps between various data-types.

The topographic maps at 1: 50,000 scale, geology map at 1: 250,000 and soil map at 1: 500,000 have been obtained from Survey of India, Geological Survey of India and National Bureau of Soil Survey and Land Use Planning respectively. The digital data has been developed at Arc/Info platform and coordinate system has been projected from decimal-degree into Universal Transverse Mercator (UTM) map projection system. Various thematic datasets (refer table 3.3 for complete list) have been manually digitised and transferred into ACCESS database for data query and analysis. The different datasets used in the research study with their data source has been described in table 3.3. The following steps may represent a systematic procedure to convert the topographic maps into the digital maps has been as follows:

Step 1: After scanning the various sections of topographic maps join all of them in one single image file using any image processing software which supports photo function.

Step 2: Register or define the geographic control points in Arc/Info using registry function and project decimal degree map into UTM. An Arc/Info AML algorithm has been written and used for this purpose.

Step 3: Convert the spatial features on a map into digital format through on screen digitising as coverage in Arc/Info. Once digitising have been over use CLEAN or

BUILD command to clean coverage and remove possible errors in order to make spatial data usable. This is done by defining FUZZY TOLERANCE and DANGLE LENGTH TOLERANCE, removing pseudo nodes and extra arc intersections. Later reconstruct topology.

Step 4: Get attribute data for each coverage type through TABLE MANAGER and TABLE EDITOR functions or relate the tables if data tables have been already existing before.

Step 5: Perform spatial analysis of database directly in Arc/Info or convert it into SQL format for data query and analysis which may allow better management and presentation of database.

The thematic information obtained from various maps have not been found sufficient to estimate the land-surface model parameters, additional remote sensing images were procured. The remote sensing images has been successfully used for hydrological modelling and spatial data analysis in regions with limited field data on an appropriate scale. Satellite images for Anas catchment taken from Landsat system have been obtained for the years 1990 and 2000. Thus the cloud free images on 4<sup>th</sup> April and 15<sup>th</sup> October 2000 and 19<sup>th</sup> April and 28<sup>th</sup> October 1990 for the study area have been obtained from USGS and NRSA India respectively. The properties of remote sensing data images are described in table 3.4. below. Further details on satellite system data product availability can be read directly from <http://landsat7.usgs.gov/> web URL. The table 3.4 lists basic properties of remote sensing data for Landsat-7ETM+ and Landsat-5TM.

Table 3.3 Details of various spatial and hydrological data sets used in research study

Type of data	Details of data	Source of data	Conversion tools
Drainage network, Contour lines, river alluvium, watershed boundary map	Topographic sheets 46J/5, 46J/6, 46J/9, 46J/10, 46J/13, 46J/14 (at 1:50,000 scale)	Survey of India (SOI), Dehradun	Arc-edit tools in Arc/Info 8.0
Geology, geomorphology, Soil map	District resources map Jhabua (at 1:250,000 scale) NBSS sheet 59 (at 1:500,000 scale)	Geological survey of India (GSI), Calcutta National Bureau of Soil Survey and Land use Planning, Nagpur	Arc-edit tools in Arc/Info 8.0 Arc-edit tools in Arc/Info 8.0
Groundwater level depth	Depth of water level for January, May and September months	State Water Resources Department, Bhopal	Arc-edit tools in Arc/Info 8.0
Rainfall	Daily station rainfall (10 stations) during 1985-99	Office of Land Records, Jhabua	Arc-edit tools in Arc/Info 8.0
Discharge	6-hourly discharge (2 stations) during 1992-94	Director, Hydro-meteorology, Bhopal	Arc-edit tools in Arc/Info 8.0

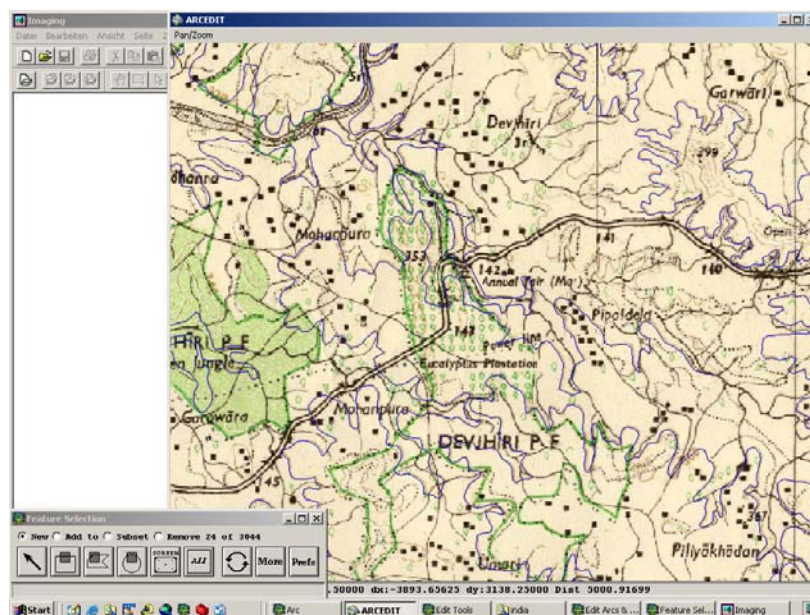


Fig. 3.3 A manual procedure adopted for digitisation of topographic maps in Arc/Info platform

Table 3.4 Specification of remote sensing data sets used in research study

Satellite type & sensor	Landsat 5 TM (NASA)	Landsat 7 ETM+ (NASA)
Bands	7 bands	8 bands
Spectral resolution	1 <sup>st</sup> band: 0.45-0.52 2 <sup>nd</sup> band: 0.52-0.60 3 <sup>rd</sup> band: 0.63-0.69 4 <sup>th</sup> band: 0.76-0.90 5 <sup>th</sup> band: 1.55-1.75 6 <sup>th</sup> band: 10.4-12.5 7 <sup>th</sup> band: 2.08-2.35	1 <sup>st</sup> band: 0.45-0.52 2 <sup>nd</sup> band: 0.53-0.61 3 <sup>rd</sup> band: 0.63-0.69 4 <sup>th</sup> band: 0.78-0.90 5 <sup>th</sup> band: 1.55-1.75 6 <sup>th</sup> band: 10.40-12.50 7 <sup>th</sup> band: 2.09-2.35 8 <sup>th</sup> band: 0.52-0.90
Spatial resolution	30 m (120 m for band-6)	30 m (60 m for band-6, 15 m for band-8)
Circulation (pass time over equator)	Polar, Sun-synchronous (9:30 hr)	Sun-synchronous (10 :00 hr)
Inclination to equator	98.2°	98.2°
Altitude	705 km	705 km
Orbit cycle repetivity	16 days	16 days
Scene size	185 x 172 km	183 x 170 km
Principal application	Vegetation, land use, soil and geomorphological mapping	Vegetation, land use, soil and geomorphological mapping

The information which describes and quantifies the spatial features in the Arc/Info GIS is stored in INFO files and optionally in externally in database management system (DBMS) tables. Each Arc/Info module (such as arc-edit, arc-grid, arc-command) provides tool to create, edit and delete attribute table definitions. In DBMS the commands which operate on

data are called Data Manipulation Language (DML) commands. Commands which operate on the structure and definition of database are called Data Definition Language (DDL) commands.

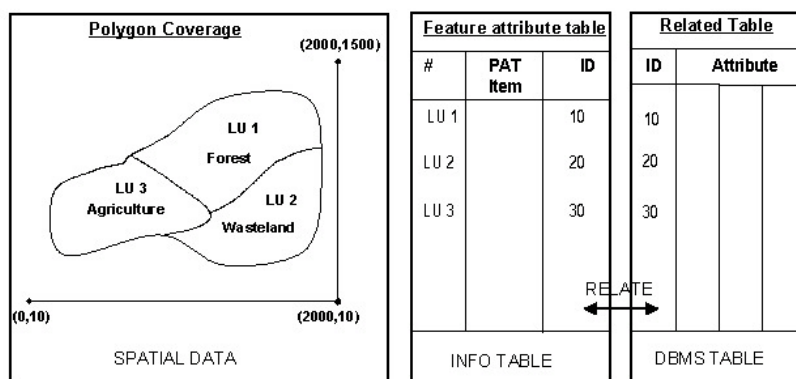


Figure 3.4 Getting spatial data into **attribute data table and relational database tables**

The Arc/Info stores information which quantifies and describes the geographic features in attribute tables which are connected to related tables (Figure 3.4). Feature attribute tables must be in INFO file format while related tables are either stored in INFO file or external DBMS tables. These tables can be unpacked in ASCII or SQL database format using Arc Macro Language (AML) commands of Arc/Info.

### 3.4 Surface Modelling with TIN

Triangulated Irregular Network (TIN) is a surface modelling package used to create, store, analyse and display surface information. The TIN model stores the topological relationship between triangles and their adjacent neighbourhood. This data structure allows efficient generation of surface models for analysis and display of terrain. The TIN data structure is based on irregularly spaced points, lines and polygon data interpolated as mass points and break lines as against DEM where data are stored in regular grid arrays. The data derived from paper map may contain systematic and random errors. Due care has been taken in system-specific pattern while converting to digital data.

### 3.4.1 Data source and surface analysis

The TIN surface model can be created from wide variety of data sources feature coverages to randomly distributed points in ASCII format. Since most of Anas catchment spatial and topological data were in map analogue format which were converted into Arc/Info digital feature format as point, line and polygon coverages. The arc/Info coverages prepared for Anas catchment includes; contour lines (as arc), height level points (as point), stream network (as arc), catchment boundary (as polygon). The data input have a line coverage containing isolines representing contours and a point coverage containing surface values for peaks and pits. The TIN surface thus converted has been shown in figure 3.5. This data can be supplemented with a polygon break-line coverage containing lakes and reservoirs, and boundary coverage to define the limits of catchment area.

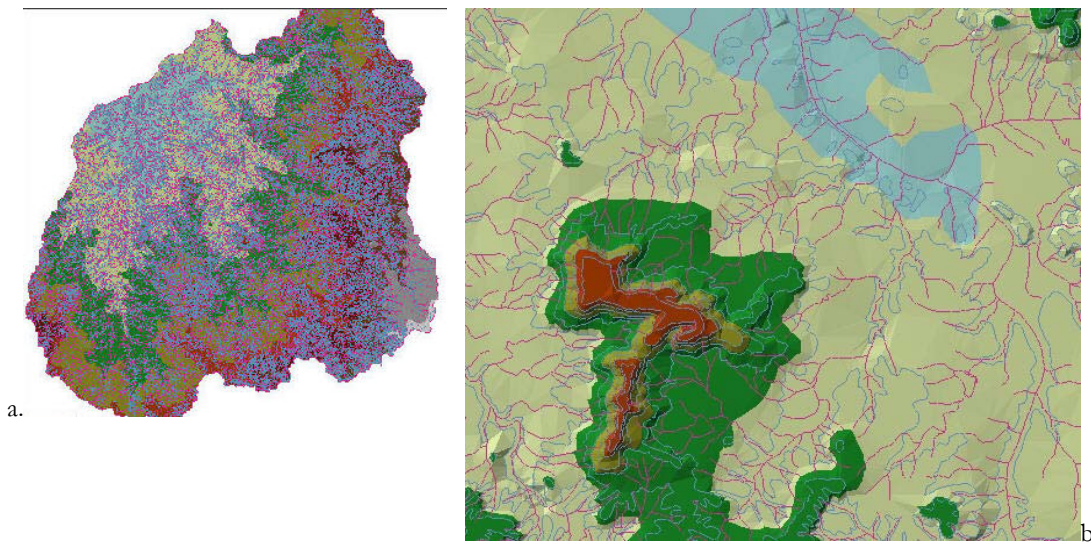


Fig. 3.5 A **TIN generated** from input contour lines, geodetic points and stream lines for the a) Anas catchment and b) part of the area from thematic data layers as hard and soft break-lines

### 3.4.2 Conversion of TIN into DEM

Once a TIN surface model is created it can be analysed, displayed or can be converted into other data models such as DEM or LATTICE for additional GIS processing. The most common analytical capabilities of TIN includes; a) Interpolation of surface height (z-value), b) Calculation of slope, aspect, surface area and surface length, c) Extraction of important surface features, d) Generation of contour isolines, and e) Analytical hill-shading.

But for integration of GIS and hydrological model since GRID based DEM has been recognised common tool. So the application of surface modelling with TIN remain limited to

generation of high quality DEM. In spite of better characterisation of physical parameters the further scope has been curtailed.

### **3.5 Digital Elevation Model**

Digital elevation model (DEM) is an ordered array of regular grid patterns that represents the spatial distribution of elevations above an arbitrary datum in a landscape. DEM may consist of elevations sampled at discrete points or the average elevations over a specified segment (Moore et al. 1993) of the earth surface. In most cases DEM has grid data with elevation attribute which are suitable to use for analysis in raster GIS. It does not only include representation of relief but also its description as slope, aspect, contour lines, break lines, peaks, and the other characteristics points (Podobnikar et al. 2000).

Traditionally the DEM data source has been the USGS at spatial resolution of 1km x 1km (30'' x 30'') whose scale found to be much smaller for the research analysis in Anas catchment. As number of thematic data layers and TIN have been available for Anas catchment, the GRID based digital terrain model (DTM) was generated from TIN. DTM is a modelled surface structure which contains other data of terrain as ridgelines, peak points which is synonymous to DEM.

#### 3.5.1 Data for DEM modelling

For DEM generation available thematic maps (as described in section 3.3) such as contour lines, geodetic points, drainage pattern and catchment boundary obtained from topographic maps at 1:50000 scale have been used for converting first into triangular irregular network (TIN). A detail description of surface modelling with TIN has been referred in section 3.4 above.

#### 3.5.2 Interpolation methodology and results

Digital elevation model can be structured in three principal ways to represent the elevation of surface depending upon the process adopted in the generation. Moore et al. 1993 ; Beven and Moore 1993 defined them as:

- a) In a grid based model the surface is described by a regularly spaced point networks. Data can be stored in several format, the most efficient being stored as  $z$ -coordinates.
- b) In a Triangular Irregular Network (TIN) model, the point network is irregular and consists of samples of surface specific points. Meaning thereby that TIN are represented by planes joining three adjacent points in the network whose  $x$ ,  $y$  and  $z$ -coordinates are known.
- c) Contour based models use contour as base in the polygonal network formation. Contour lines are stored as digital line graph in the form of  $x$ ,  $y$  coordinate pairs along each contour of specified elevation.

For the generation of GRID based DEM the TIN model has been used. The results thus obtained from conversion has been described in figure 3.6and figure 3.7.

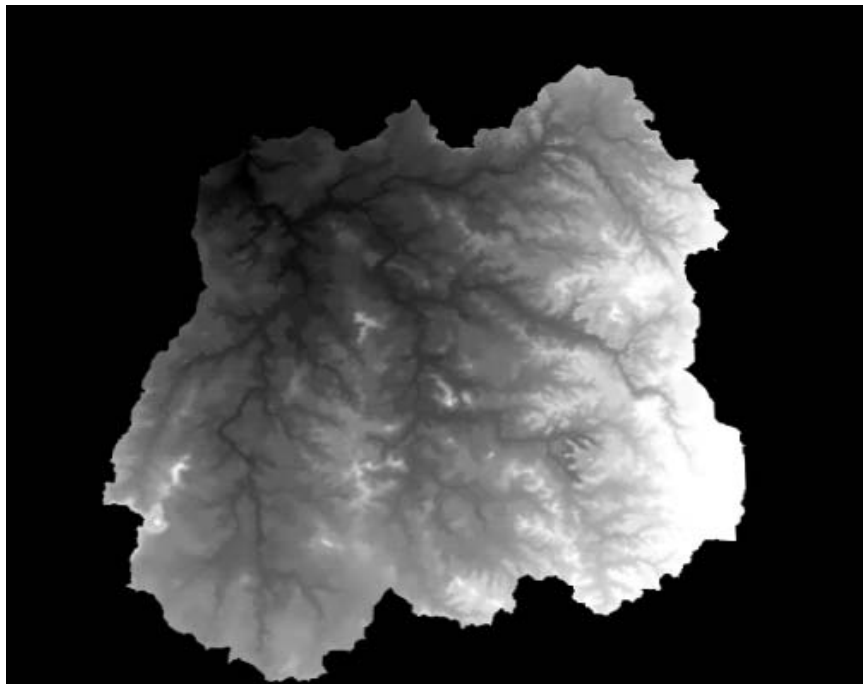


Fig. 3.6 DEM generated using TIN model for Anas catchment developed using Arc-View 3D Analyst

### 3.5.3 DEM uncertainty

The certainty with which we can represent a DEM is a function of input data quality and Arc/Info AML conversion model. The systematic errors of the DEM which can be measured depends on the source and resolution of the data samples. The conventional



description of a frequency distribution that include measures of central tendency and dispersion may be used to describe the pattern of deviation between two sets of elevation data (Miller and Kahn 1962).

Most widely used measure for reporting accuracy is the root mean-square error (RMSE). It is dispersion measure which may be equivalent to the average deviation between two datasets. The root mean-square error can be defined as (USGS 2000):

$$RMSE = \sqrt{\left(\frac{1}{n} \sum (h_{map} - h_{dem})^2\right)} \dots\dots\dots (3.12)$$

where,  $n$  - number of elevation pair modelled,

$h_{map}$  - height obtained from topographic map from Survey of India at 1:50,000 scale.

$h_{dem}$  - height obtained from DEM after transformation into grid.

The DEM data accuracy has been derived by comparing linear interpolation elevations and corresponding map location elevations and comparing the RMSE. The RMSE has been used to describe the uncertainty of DEM data. Larger the value of RMSE greater the difference between two set of measures of same phenomena. Annex 3.5 shows the results obtained from randomly selected 38 points having known elevation. The care have been made to select points through out the catchment from all elevation classes. A root mean-square error between DEM elevation and map elevation found to be 2.35m for 20m vertical resolution with 50m horizontal cell size. Thus the DEM has much better accuracy range as proposed by US Geological Survey. For DEM derived from vector hydro-graphic source data an RMSE of one-half of contour interval is required (USGS 2000).

The graphical plot between DEM elevation and topographic elevation has also been plotted which shows a good correlation having standard deviation of 0.99 that is good fit (refer figure 3.8). For quality control of input data not only statistical parameters have been sufficient but also visual control have been essential. Thus the best choice is a combination of objective (statistical) and subjective (visual) methods. Primary attributes such as hill shade relief, slope and aspect, flow path length and specific catchment area can be calculated directly from a DEM. All of these primary terrain attributes can be used when assessing the

hydrological response of a catchment to the rainfall. In additional, some secondary attributes such as soil moisture in a landscape level can be calculated from the primary ones.

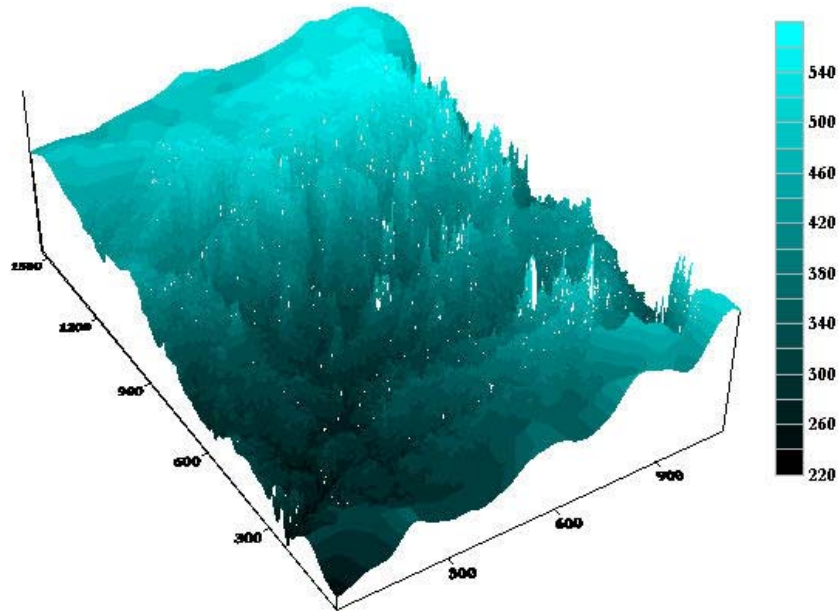


Figure 3.7 A 3-D Digital Elevation Model for Anas catchment

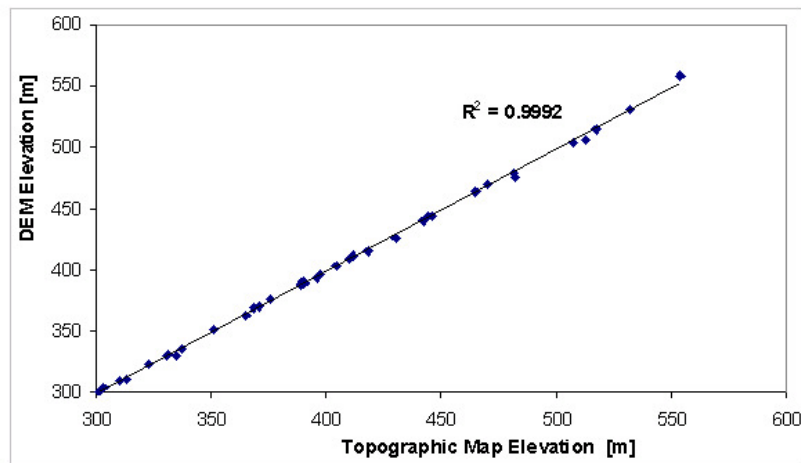


Figure 3.8 A plot of DEM uncertainty between two data sets (one selected elevations on DEM versus elevation on topographic map)

### 3.6 Geo-database Management System

Geo-database management system can be defined as storage system or platform used for storage of attribute data. GIS contains the ability to translate implicit spatial and hydrologic data into an explicit map location. As discussed under section 3.2 above GIS include a database manager usually linked to relational database management system. They also include query and analysis program to perform various mathematical or subjective search. Arc Hydro by Maidment (2002) and Elbe databank by Becker and Nestmann (2001) have been good examples of Geo-database for hydrologic and water resources modelling. For the purpose of Geo-database for an un-gauged catchment the following steps can be considered:

Step 1: GIS database design, refers to assigning the various thematic features such as land-use, rainfall station or discharge station an unique ID's.

Step 2: GIS database creation, based on the step 1 the GIS database is created with the consideration of resources, time scale and standard.

Step 3: GIS database updating and management has been considered to be a key factor to handle the right and updated data.

#### 3.6.1 Structure of database

Integrating spatial GIS data and dynamic hydrologic modelling involves linking spatial data with time series. Most of the GIS tools support static database generation linked to dynamic process. Merwade and Maidment (2002) described following structure for Arc Hydro which combined the geo-spatial and time series data in a relational database format (refer figure 3.9).

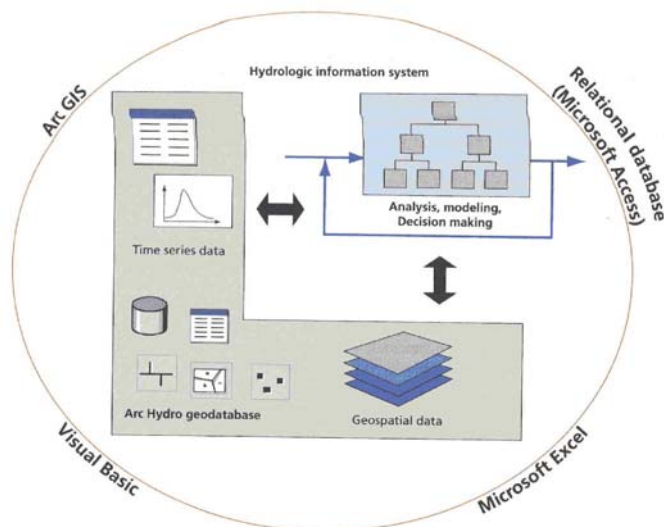


Fig. 3.9 The structure of relational database in catchment context (Source: after Merwade and Maidment 2002)

For development of Anas catchment, geo-database has been built in Arc/Info format and Arc-View format while the time series data have been stored under Microsoft excel and Statistica format. Later all the info tables from Arc/Info (in \*.aat and \*.pat) and Arc-View (\*.dbf) have been exported into ACCESS database format (\*.mdb) independent query and analysis. Section 3.6.2 below describes the further procedure.

### 3.6.2 Data query and analysis

A simple database has been constructed for Anas catchment in individual supported ACCESS formats with the aim to efficient query processing on local geo-spatial and geo-referenced collections stored under one file. The geo-database has much supported the complex query and analysis for large remote sensing land-use data for distributed hydrologic model parameterisation (refer figure 3.10). In additional the spatial analysis have been much easier for building queries and performing basic mathematics.

The screenshot shows the Microsoft Access interface. On the left, the 'Objekte' pane lists several queries: 'rfc1015\_area\_ratio', 'rfc1015\_area1', and 'rfc1015\_area2'. The main window displays two data tables. The top table, 'rfc1015\_area1 : Auswahlabfrage', has columns 'SEGNO', 'AREA', 'GRID\_CODE', and 'Summe von AREA'. The bottom table, 'rfc1015\_area2 : Auswahlabfrage', has columns 'SEGNO' and 'Summe von AREA'.

SEGNO	AREA	GRID_CODE	Summe von AREA
1006	10892993	1	1800
1006	10892993	2	24300
1006	10892993	3	697614.188
1006	10892993	4	92700
1006	10892993	5	1508400
1006	10892993	6	79444295.223
1006	10892993	7	3107912.192
1007	3504644.5	0	45900
1007	3504644.5	2	1800
1007	3504644.5	3	346500
1007	3504644.5	4	5400
1007	3504644.5	5	439200
1007	3504644.5	6	89404660
1007	3504644.5	7	2399400
1008	5566516	0	39600
1008	5566516	1	1800
1008	5566516	2	6300
1008	5566516	3	808200
1008	5566516	4	27000
1008	5566516	5	701100
1008	5566516	6	89905060
1008	5566516	7	2412900
1009	2494941	0	23400
1009	2494941	1	900
1009	2494941	2	9000
1009	2494941	3	1217700
1009	2494941	4	3600
1009	2494941	5	139500
1009	2494941	6	12292200
1009	2494941	7	866700
1010	1559775.5	0	19800
1010	1559775.5	1	900
1010	1559775.5	2	18000
1010	1559775.5	3	3304600
1010	1559775.5	5	9900
1010	1559775.5	6	1787400
1010	1559775.5	7	1004400

SEGNO	Summe von AREA
900	94500
1000	108000
1001	45290260
1002	49657960
1003	7748100
1004	17840571
1005	14728371
1006	85078608.705
1007	92642860
1008	93901960
1009	14553000
1010	6145200
1011	7414200
1012	3646800
1013	26329500
1014	25942500
1015	15264000
1016	46534500
1017	48563100
1018	14427000

Fig 3.10 Performing query and analysis in simple geo-database system for model parameter identification to distributed hydrologic model

### 3.7 Results and Discussion

Catchment modelling under GIS environment offers great potential for un-gauged catchments where limited topographic and spatial data exists. The analysis of catchment under GIS enabled to delineate 330 sub-catchments with relatively accurate and reliable information. The TIN model and DEM have been used as basic information to derive slope and aspect information of the catchment and to identify the development potential. The 3D representation of DEM using Arc-View 3D-Analyst is an interesting tools for visualisation.

Application of remote sensing data such as land-use for SCS-CN runoff model simulation found to be rather interesting. The SCS-CN runoff model can be used a semi-distributed hydrological model if combined with GIS database system. The scope of simple water balance model at larger temporal scale found to be appropriate tool for validating the performance of SCS-CN model or distributed ZIN-model.

In the context of river catchment, one issue of information management is the issue of designing, creating and managing the spatial data. This needs a carefully thought concept and continuous resources for updating. The concept of GIS and database management specifically for un-gauged catchment is must in order to avoid the negative impact of development activities. The geo-database provide additional functionality and capability over existing GIS data models. The future advancement of geo-data will support custom topologies and TIN into their database which will be an extra tools for prediction in catchments with limited spatial database.

## **4. REMOTE SENSING FOR HYDROLOGICAL MODEL PARAMETERISATION**

Remote sensing can be used for various hydrological and water resources management applications from spatial analysis and forecasting to decision making including flood control, drought management and irrigation planning. Schultz (2000) has successfully implemented the optimum release policy for two reservoirs in a tributary of Danube in South Germany. Spatial analysis and hydrological regionalisation have been compiled in a GIS environment by combining hydrological terrain, land use and land cover, geological maps and slope (Meijerink and Mannaerts 2000). For distributed hydrological modelling of the Paddle river in Alberta, Biftu and Gan (2001) used remotely sensed data in a semi-distributed approach. They derived the spatial distribution of land use classes from vegetation index and evapotranspiration using leaf-area index for Landsat-TM data. In other research work Fluegel (1995) used remote sensing and GIS data for identification of hydrological response units (HRU's) based on topography, soil and land-use information.

Remote sensing derived classification together with GIS data (such as DEM) can be used for defining a basin into hydrological similar units (HSU's). Ott et al. 1991 Bhaskar et al. 1992, Schumann 1993, Mohan and Shrestha 2000 successfully carried out rainfall-runoff modelling applying HSU's concept under varying hydro-meteorological zones. Runoff water harvesting potential sites have been selected in Sahel region by Tauer and Humborg 1992, using Landsat-TM and SPOT data for Kanguessanou valley in Mali. The determination of potential sites for runoff water harvesting have been based upon rainfall regime characteristics and evaluation of surface topography, soil properties and other environmental parameters.

Ground water recharge and discharge zones has been identified using Landsat-TM colour composite and areal photograph for Salt river system of western Australia (Salama et al. 1994). Geo-morphological features such as sand plains, dissected etchplain, colluvium and

rock outcrop, and hydro-geomorphological units such as streams, lakes and palaeochannels and structural features have been identified. Recharge was found to occur in the highly permeable areas of the sand plains. Soil erosion modelling and soil moisture mapping have been researched by Gomer and Vogt (2000) in Oued Mina catchment of Algeria. While the physical soil parameters (soil type and soil moisture) were derived from Landsat-TM, besides the DEM and rainfall pattern were calculated from GIS.

Remote sensing has high relevance for un-gauged catchments where data availability have been limited. The ultimate goal of remote sensing study in the context of this research work is to derive land-use and land cover information for input into hydrological models. SCS-CN runoff number method as discussed in chapter 3 can employ remote sensing directly to forecast the runoff within a catchment. Land use information can further help in assigning runoff coefficients for distributed segments as possible input for ZIN model. Thus remote sensing may be considered to be an important tool for database development, hydrological process modelling and water resources planning in un-gauged or poly-gauged catchments.

#### 4.1 Concept of Remote Sensing

In remote sensing the electromagnetic energy is classified by its wavelength and interacting with earth's surface. As shown in figure 4.1(a) that visible light is an small band of frequency range between 0.4-0.7  $\mu$  m. The frequency range below visible such as UV, X-rays do not penetrate atmosphere hence are not useful for remote sensing. Infrared and microwave (radar) frequency range are used in remote sensing measurement together with visible based on conservation of energy principle.

$$E_i = E_r + E_a + E_t \quad \dots\dots\dots (4.1)$$

where,  $E_i$ =the incident energy ,  $E_r$ =reflected energy,  $E_a$ =absorbed energy,  $E_t$ =transmitted energy.

The interaction of incident energy with earth's surface such as soil, land use, geology, water and settlements governs how much energy is absorbed and reflected. This can be expressed in terms of reflectance index ( $n = E_r/E_i$ ), which is a ratio of reflectance energy to



incident energy. These values (% reflectance) can then be compared to remote sensing data in order to identify which materials are present in the area of image. Randy-Keller 2003 plotted the reflectance index (% reflectance) for Landsat TM sensor as shown in the figure 4.2(b) below.

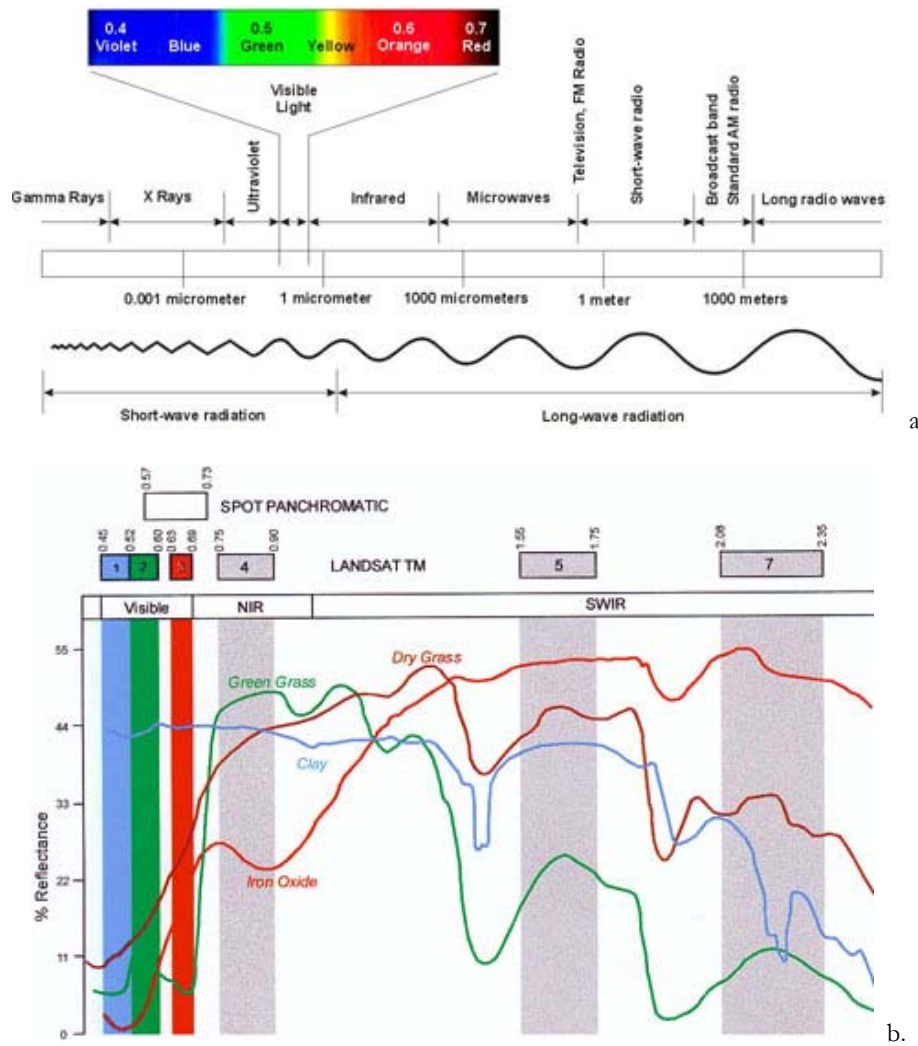


Figure 4.1 (a) Electromagnetic spectrum and (b) percentage **reflectance for grasses and soils** in Landsat TM (source: after Randy-Keller 2003)

Meaning thereby that the raw data collected from remote sensing sensor has to undergo radiometric and geometric corrections before it can be used for analysis. The current Landsat images supplied by various agencies (such as USGS or NRSA) are of processing level 1G (radiometric and geometric corrected). Thus, the obtained images directly can be used for analysis.

In case of Landsat-TM remote sensing data which have multi-spectral data in seven channels may have following applications (Sabins, 1997 as quoted in Belz, 2000):

Channel 1: 0.45-0.52  $\mu\text{m}$  (visible range, blue) For discrimination between soil/vegetation, oceanography.

Channel 2: 0.52-0.60  $\mu\text{m}$  (visible range, green) maximum of green reflection for vegetation. To make distinction between various vegetation type.

Channel 3: 0.63-0.69  $\mu\text{m}$  (visible range, red) The upper limit of spectral resolution 0.69  $\mu\text{m}$  has special meaning because of crossover vegetation reflectance, and impair exactness of vegetation classification. To discriminate between soil/vegetation.

Channel 4: 0.76-0.90  $\mu\text{m}$  (near infrared) This band shows a positive co-relation for biomass. Mainly used to calculate normalised difference vegetation index, and useful for land and water studies.

Channel 5: 1.55-1.75  $\mu\text{m}$  (middle infrared) Shows vegetation wetness or humidity, and can be used for soil moisture mapping.

Channel 6: 10.40-12.50  $\mu\text{m}$  (thermal infrared) Normally used for measure surface temperature and kinematic behaviour of it.

Channel 7: 2.08-2.35  $\mu\text{m}$  (middle infrared) Used for making distinction between mineral and geology including hydrothermal change.

## 4.2 Digital Image Processing and Pattern Recognition

Digital image processing of remote sensing data have found wide application in natural resources management including hydrological modelling, land use planning and soil moisture studies. It is the technique of interpreting and manipulation of digital images with the aid of algorithms and mathematic equations. Lillesand and Kiefer (2000) proposed following broad steps from a) image rectification, b) enhancement, c) classification, d) data merging and GIS integration, to e) bio-physical modelling for application. The ultimate aim is to identify patterns in an image to use them as thematic maps for decision support modelling.

The pattern recognition is the science and art of finding meaningful patterns in digital data, which can be extracted through, image classification (ERDAS 1997). Statistics are derived from the spectral characteristics of image and then each pixel is sorted by set of decision rule

criteria's. The pattern recognition process may consists of image segmentation, feature extraction and image classification as shown in figure 4.2 below.

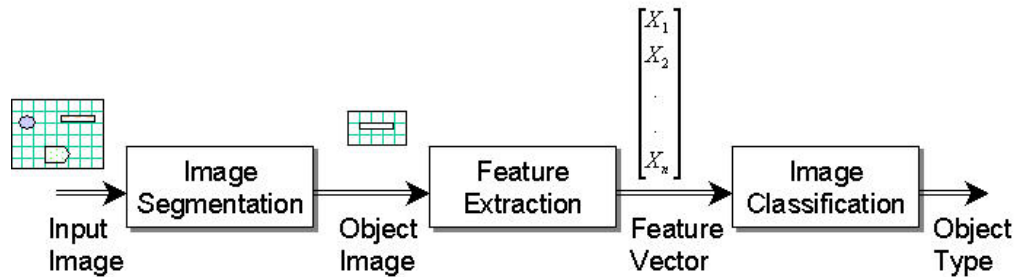


Figure 4.2 The process of **pattern recognition** for multi-spectral satellite image (source: after Castleman 1996)

#### 4.2.1 Image segmentation and enhancement

Image segmentation is a process of partitioning a digital image into disjoint sub-images. The objective of image optimisation is to achieve the best representation of original data to enable one to interpret the content of image. Using linear histogram stretching, the contrast and differentiability of the image can be improved. A linear contrast stretch assigns new digital numbers to an output image based on lowest and highest DN values between 1 and 256. The  $DN$  in the stretch image ( $DN_{st}$ ) for any input is given by:

$$DN_{st} = 256 \cdot \frac{(DN - DN_{min})}{(DN_{max} - DN_{min})} \dots\dots\dots (4.2)$$

where,  $DN_{min}$  and  $DN_{max}$  are the minimum and maximum  $DN$ 's in the original image.

Due to advancement of computing capabilities edge approach is one among the most common approach for image segmentation. Some of the popular image processing software such as ERDAS imagine, ENVI or MultiSpec have in-built image segmentation options. All relevant data such as brightness, colour, texture, pattern, shape, size, location and shape are included in the image. Tauer and Humborg (1994) used this type of satellite image assessment for hydrographical network and terrain structure analysis in Sahel zone of arid Africa. Water courses and reservoirs can be easily identified using supervised classification technique.

#### 4.2.2 Feature extraction

The purpose of feature extraction<sup>1</sup> is to provide some of the information needed for a classification decision rule to operate successfully (Castleman 1996). It is a crucial stage in pattern recognition because the performance of classification rule will depend on how well feature detector can capture the feature of an image to be classified. For multi-spectral feature extraction two reliable algorithms such as discriminate analysis feature extraction (DAFE) and decision boundary feature extraction (DBFE) are used (Lee and Landgrebe 1993; Hsieh and Landgrebe 1998).

#### Discriminate Analysis Feature Extraction (DAFE)

The discriminate analysis feature extraction (DAFE) algorithm is to form a linear combination of the original features so as to maximise the ratio of between-class and within-class variance which is a measure of class separability:

$$\frac{\sigma_b^2}{\sigma_w^2} = \frac{\text{variance between classes}}{\text{variance within classes}} \approx \text{maximum} \quad \dots \dots \dots (4.3)$$

Let  $x$  describe the  $n$ -dimensional feature vector as  $x = (x_1, x_2, \dots, x_n)$ . Then the scatter matrixes  $S_w$  within the classes and  $S_b$  between the classes can be expressed as:

$$S_w = \sum_{i=1}^n p_i \cdot E[(x_i - \mu_i)(x_i - \mu_i)^T] = \sum_{i=1}^n p_i \cdot \text{COV}(x_i) \quad \dots \dots \dots (4.4)$$

$$S_b = \sum_{i=1}^n p_i \cdot (\mu_i - \mu)(\mu_i - \mu)^T \quad \dots \dots \dots (4.5)$$

where  $\mu_i$  is the mean vectors of class  $i$  and  $\mu$  is the mean vector for all the classes.

#### Decision Boundary Feature Extraction (DBFE)

The theoretical basis for the DBFE algorithm is to use the decision boundary location of each class pair to determine discriminately informative and discriminately redundant features. DBFE determines an optimum linear transformation directly using training classes to determine discriminately informative and discriminately redundant features, this results in eigen-functions which define the required transformation. Hsieh and Landgrebe (1998) gave the following theorems for DBFE algorithm:

*Theorem 1:* For  $L$  univariate normal distributions with a common mean and different variances,  $\sigma_1^2 < \sigma_2^2 < \sigma_3^2 \dots \sigma_L^2$ , the probability of correct classification under the maximum likelihood can be bounded as:

$$\frac{1}{L} \left[ 1 + 2\phi\left(\frac{d_{1L}}{\sigma_1}\right) - 2\phi\left(\frac{d_{1L}}{\sigma_L}\right) \right] \leq P_{cr} \leq \frac{1}{L} \left[ 1 + (2\pi e)^{-0.5} \ln\left(\frac{\sigma_L^2}{\sigma_1^2}\right) \right] \dots (4.6)$$

where,  $P_{cr}$  = classification accuracy,  $d_{ij}$  = decision point between class  $i$  and  $j$  on the side

of  $x > 0$ ,  $d_{ij}^2 = \left[ \frac{\sigma_i^2 \sigma_j^2}{(\sigma_j^2 - \sigma_i^2)} \right] \ln\left(\frac{\sigma_j^2}{\sigma_i^2}\right)$   $\phi(x)$  = cumulative distribution function of

the standard normal distribution,  $\phi(x) = 2\pi^{-0.5} \int_{-\infty}^x \exp\left(-\frac{t^2}{2}\right) dt$

*Theorem 2:* Let us assume that the covariance matrices of equally-probable classes share the same eigen-vectors, then the overall classification accuracy ( $P_c$ ) is bounded by:

$$P_c = L^{n-1} \prod_{k=1}^n P_{cr,k} \dots (4.7)$$

where,  $P_{cr,k}$  = classification accuracy along the  $k$ -th eigenvector.

It is clear from equation 4.6 that larger the ratio of variances, the higher the classification accuracy along the features. Therefore, it can be stated that the best  $m$  features can be selected from the eigenvectors corresponding to  $m$  largest variance ratios. Thus the transformation has the advantage of showing the analyst directly that how many features must be used.

### 4.3 Multispectral Image Classification

Multi-spectral image classification<sup>2</sup> is the process of sorting pixels into number of classes, based on their data value are identified and assigned a unique colour. Classification implies the use of a decision rule and involves establishing mathematical basis for classification algorithm for the classification procedure. Many mathematical algorithms have been developed for the classification of multi-spectral satellite imagery. They range from statistical approaches based on mathematical formulation such as minimum distance classifier, parallel-

piped classifier, Gaussian maximum likelihood to pure artificial intelligence such as layered neural network. Several researchers and research studies (Landgrebe 2003, Gibson and Power 2000, Belz 2000, Sabins 1997, Castleman 1996, Tauer and Humborg 1992) focused predominantly on spectral classifier as the most commonly used classification method. Landgrebe (1997) introduced a class-conditional pre-processing algorithm based upon a projection pursuit. The modified classification procedure is given in figure 4.3 below.

Image classification is often used to smooth out small, insignificant variations and simplify an image into a thematic map such as land cover types. Supervised and unsupervised image classifications are two main spectral pattern recognition approaches commonly cited in literature.

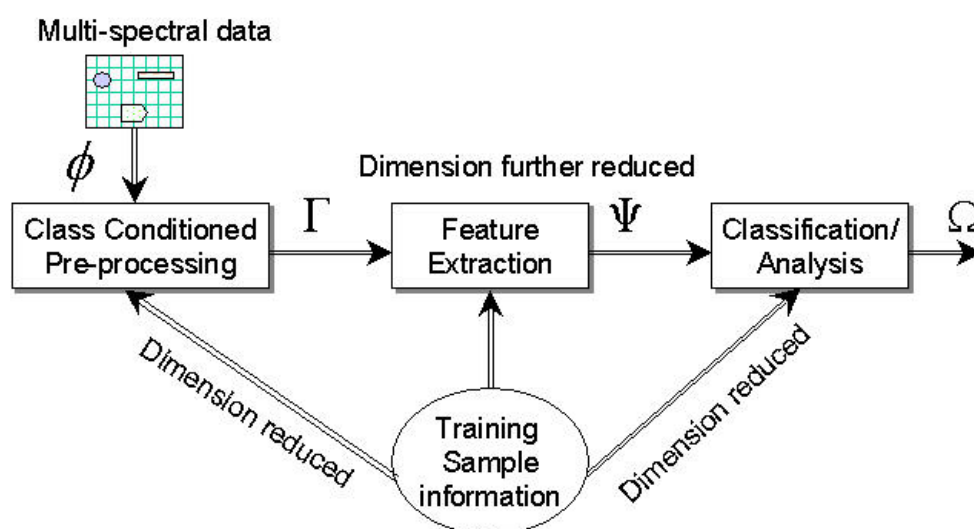


Figure 4.3 Multi-spectral images classification process (Source: modified Landgrebe, 1997)

In supervised classification, the spectral features of individual classes are pre-determined by the use of training fields. The pixel class assignments are based on classifier algorithm (minimum distance or maximum likelihood refer figure 3.6) and the parameters of such model are estimated from training areas. The three feature classifier algorithms (Landgrabe 2003) used in this research work for Landsat TM and ETM+ images are described below.

#### 4.3.1 Gaussian Maximum-likelihood (GML) classifier

In maximum likelihood strategy, the class of a pixel at location  $(x_i, y_j)$  is decided solely based on the digital number of that individual pixel. Thus, for the probability of value  $\vec{x}$  for

given class  $w_i$  can be written as (assuming that the data is normal distributed in each feature class  $w_i$ ):

$$g_s(\vec{x}) = p(\vec{x}|w_i) \dots\dots\dots (4.8)$$

the equation (4.8) yields the most likely class and referred as Gaussian maximum likelihood classifier.

The conditional probability  $p(\vec{x}|w_i)$  for equation (4.9) of a sample  $\vec{X}$  belonging to class  $w_i$ , can be estimated by:

$$p(\vec{x}|w_i) = \frac{1}{\sqrt{(2\pi)^n \Sigma_i}} \exp\left[-\frac{(\vec{x} - \vec{\mu}_i)^T (\vec{x} - \vec{\mu}_i)}{2\Sigma_i}\right] \dots\dots\dots (4.9)$$

where  $\vec{\mu}_i$  is mean vector and  $\Sigma_i$  the covariance matrix for that class. The term  $(\vec{x} - \vec{\mu}_i)^T$  is the transposition of  $(\vec{x} - \vec{\mu}_i)$  matrix. The parameters  $\vec{\mu}_i$  and  $\sigma_{jk}$  of the co-variance matrix  $\Sigma_i$  of class  $w_i$  from  $n$  samples can be calculated as:

$$\vec{\mu}_j = \frac{1}{n} \sum_{j=1}^n \vec{x}_j, \quad \vec{x}_j \in w_i \dots\dots\dots (4.10)$$

and

$$\sigma_{jk} = \frac{1}{n} \sum_{l=1}^n (\vec{x}_{jl} - \vec{\mu}_j)(x_{kl} - \mu_k) \text{ and } j, k = 1, 2, \dots, n \dots (4.11)$$

here the mean vector  $\vec{\mu}_j$  defines the location of the density while the covariance  $\sigma_{jk}$  provides information on shape of distribution.

4.3.2 Fisher’s linear discriminant classifier

In this classification algorithm, the classes  $w_i$  are assumed to have density functions with a combined covariance  $\Sigma$ , meaning that all classes have same variance and correlation structure. The decision boundary in this algorithms will have linear feature space, but location and orientation between class mean values will depend on combined covariance  $\Sigma$ , for all the classes. Thus the linear discriminant strategy:

$$g_i(\vec{x}) = (\vec{x} - \vec{\mu}_i)^T \Sigma^{-1} (\vec{x} - \vec{\mu}_i) \dots\dots\dots (4.12)$$

having the boundary condition to choose the class  $w_i$  if,

$$g_i(\vec{x}) \leq g_j(\vec{x}) \text{ for all } j = 1, 2, \dots, m \quad \dots\dots(4.13)$$

#### 4.3.3 Extraction and classification of Homogeneous objects (ECHO) classifier

Extraction and classification of homogeneous objects (ECHO) has been first introduced by Kettig and Landgrebe (1976) for classification of multi-spectral image data. The homogeneous regions termed as “objects” from the image scene are identified based on statistical properties of the cell.

The algorithm is based on a decision criteria, i.e.

$$g_j = (\vec{x} - \mu_j)^T \Sigma_j^{-1} (\vec{x} - \mu_j) \quad \dots\dots\dots (4.14)$$

and choose the class  $j$  by  $\underset{j}{Max} p(x_1, x_2, \dots, x_n | j) \quad \dots\dots\dots (4.15)$

In other words if  $g_j > c$ , where  $c$  is class threshold then cell is singular and will be rejected to classify in same class  $j$  and accept in case of vice-versa. The basic premise of this technique is that the objects of interest are large compared to the size of a pixel.

Training areas are employed in a sampling of representative class brightness values (Landgrebe 2003, Tauer and Humborg 1992). The training areas for supervised classes should be uni-modal and conform to a normal distribution (Campbell 1996). The statistical parameters (such as mean and standard deviation) for each training class are few important parameters. The training class areas may either be marked on each band or over false colour composite<sup>3</sup> image. Supervised classification provides optimum results for sub-areas and desired classes who agree with the training class definition.

#### 4.3.4 Principal component analysis

Principal component analysis (PCA) is a technique which allows the production of images where the correlation between them is zero. An important advantage of PCA is that most of the information within all channels (6 channels for Landsat) can be compressed into smaller number of channels (3 principal channels for Landsat) with little loss of information. This procedure may reduce processing and classification time. The first three principal components (PC1 in red, PC2 in green, PC3 in blue) typically contains between 95-98% of the variance. In other words, the main concept in PCA is to transform the multi-spectral



image channels in such a way to yield a new coordinate description by establishing a diagonal form of covariance matrix (Gibson and Power, 2000). There are two effects from PCA transformation, one; the new channels are orthogonal with each other two; the variance implicit in the original channels is packed in transformed channels such that eigenvector with the highest eigenvalues (PC1) contains high variance than the PC2 (Richards, 1993). PCA is used to maximise the total scatter of data, and can be defined as:

$$S_T = \sum_{k=1}^n (x_k - \mu)(x_k - \mu)^T \dots\dots\dots (4.16)$$

where,  $x_k$  = data value,  $\mu$  = mean value and  $T$  is between 1 to 6 for Landsat TM.

Tasseled Cap Transformation algorithm for Landsat TM (Crist and Cicone 1984) with the purpose of maximising information for agricultural regions became an important tool for PCA. The linear coefficients are the result of statistical modification of PCA to measure soil (brightness), vegetation (greenness) and canopy moisture (wetness). The index fit a linear transformation to 6 channels using a set of empirical derived coefficients presented in 3 channels (brightness, greenness, wetness) based on following formula:

$$Feature = \alpha_1.TM1 + \alpha_2.TM2 + \alpha_3.TM3 + \alpha_4.TM4 + \alpha_5.TM5 + \alpha_6.TM6 \dots\dots (4.17)$$

The feature space transformation coefficients obtained by Crist and Cicone (1984) for Purdue Agronomy Farm in United States are given in table 4.2.

Table 4.2 Ladsat TM feature space transformation coefficients

Feature	Channel					
	1	2	3	4	5	6
Brightness	0.33183	0.33121	0.55177	0.42514	0.48087	0.25252
Greenness	-0.24717	-0.16263	-0.40639	0.85468	0.05493	-0.11749
Wetness	0.13929	0.22490	0.40359	0.25178	-0.70133	-0.45732

Source: after Crist and Cicone, 1984

#### 4.4 Assessment of Image Classification Accuracy

Conventional multi-spectral classifiers perform well over limited area where spectral signatures remain within threshold limit of training areas. However, as the size of the

classification images increases, the classification accuracy decreases (Carlotto 1998). Two major factors are responsible for image misclassification; a) noise contained in the image causes the spectral response of a particular land cover or soil moisture to deviate from its ideal response, and b) inadequate spatial resolution of imaging sensors causes the geographical area sub-divided by a pixel to contain a mixture of land use types.

Number of techniques for measuring accuracy of remote sensing image are classification error matrix and Kappa statistic. Error matrix compare on a class-by-class basis the relationship between reference data and the corresponding results for automatic classification. The overall accuracy is calculated by:

$$\frac{\sum (\text{number of correctly classified pixels})}{\sum (\text{number of reference pixels})} \dots (4.18)$$

The degree of seperability between the training classes is an important step to check the modality of classes by examining the cluster map or clustering the training area. The training class seperability index between classes  $i$  and  $j$  can be calculated as:

$$S = \frac{|\mu_i - \mu_j|}{\sigma_i + \sigma_j} \dots (4.19)$$

where,  $\mu$  = mean field pixel value and  $\sigma$  = standard deviation of a pixel value within a field. For Gaussian distribution the value of seperability index should be  $S \cong 1.5$  (Dobson et al. 1992).

Kappa index or statistic is rather a preferred way (as compared to seperability index) to compute classification accuracy. The Kappa index or variance (given by Congalton, 1991) can be written in the form of:

$$\hat{K} = \frac{N \sum_{i=1}^n x_{ii} - \sum_{i=1}^n (x_{i0} x_{0i})}{N^2 - \sum_{i=1}^n (x_{i0} x_{0i})} \dots (4.20)$$

where,  $N$  is the total number of observation,  $n$  is number of rows in the accuracy matrix,  $x_{ii}$  is the number of observations in row  $i$  and column  $i$ ,  $x_{i0}$  and  $x_{0i}$  are the marginal totals of row  $i$  and column  $i$ . Foody (1992) estimated that Kappa index in fact underestimates true accuracy in the data.

## 4.5 Application for Anas catchment

The Anas catchment research area is a head watershed of Mahi basin in Jhabua district of Western India. A detailed description on study area has been given in chapter 2.

### 4.5.1 Selection of satellite remote sensing data

The selection of satellite remote sensing images were mainly based upon the cloud free scenes each before and after the monsoon season as to classify the hydrological parameters such as land-use correctly and the level (level 1G) of pre-processing performed on the raw image.

In summary following Landsat ETM+ and TM images of level 1G were selected (refer table 4.3).

Table 4.3 Properties of satellite data used for classification

Satellite	Sensor	Path .Row	Date of acquisition	Scene ID
Landsat 7	ETM+	147 x 044	6th April 2000	L71147044_04420000406
Landsat 7	ETM+	147 x 044	15th October 2000	L71147044_04420001015
Landsat 5	TM	147 x 044	19th April 1990	TML5_147044_19900419
Landsat 5	TM	147 x 044	28th October 1990	TML5_147044_19901028

A short explanatory note on acquired Landsat data product characteristics are given below:

Table 4.4 Landsat data product characteristics

Product type:	Standard, 185x172 km	Format:	GeoTIFF on CD-ROM
Data correction:	Systematic, Level 1G	Enhancement:	No data enhancement
Map projection:	UTM, Universal Transverse Mercator	Resampling method:	Near neighbourhood
Datum:	WGS84, World Geodetic system 1984		

### 4.5.2 Pre-classification process

Anas catchment has been clipped from the whole image (185 x 172 km) using AML subroutine in Arc/Info. The images has been converted into suitable format which can be read by GIS software Arc/Info as well as image classification software. The header and geo-referenced world files contain following information

Raster data header file (\*.hdr)  
 BYTEORDER M  
 LAYOUT BIL

Geo-referenced world file (\*.blw)

NROWS	2058	30.000000000000000	▶ <i>x-cell size</i>
NCOLS	1882	0.000000000000000	▶ <i>rotation</i>
NBANDS	1	0.000000000000000	▶ <i>rotation</i>
NBITS	8	-30.000000000000000	▶ <i>y-cell size</i>
BANDROWBYTES	1882	432795.000000000000000	▶ <i>x- in meter</i>
TOTALROWBYTES	1882	2547525.000000000000000	▶ <i>y- in meter</i>
BANDGAPBYTES	0		

The common information in the header file includes row and column number, the depth of each cell, the byte order, the number of bands for raster data retrieval. The geo-referenced raster file contains information about cell size, the  $(x, y)$  coordinates of upper left cell which talk about map projection. Arc/Info fully supports raster data format presented above and can easily convert using Arc/Info AML subroutine in Arc/Info.

#### 4.5.3 Preparation of False colour composite (FCC)

A false colour composite of Landsat image of 6<sup>th</sup> April 2000 (as shown in figure 3.7) is formed by projecting/merging various channels. Three channel layers of values between 0 to 255 have been used by merging the channel 4 (0.76-0.90  $\mu m$ ) in red, channel 3 (0.63-0.69  $\mu m$ ) in green and channel 2 (0.52-0.60  $\mu m$ ) in blue as suggested by Sabins (1997). Three optional fields has been used to indicate the weighting factor to be applied to the values in the channel assigned to the corresponding colour channel (red, green, blue). To disable a channel, a weight of 0 may be assigned to that layer. 4 bit precision is assigned, allowing each channel to contribute 16 levels of intensity information with the potential of generating 4096 output options.

#### 4.5.4 Design of supervised land cover classification system

A classification process begins with defining a classification system for training classes and areas. A hierarchical structure for the training classes and sub-classes (fields) have been developed. Thus the seven categories of land use classes and 21 fields in the second level were identified. The details classes and field for classification of 6<sup>th</sup> April 2000 imagery are described below in table 4.5 below

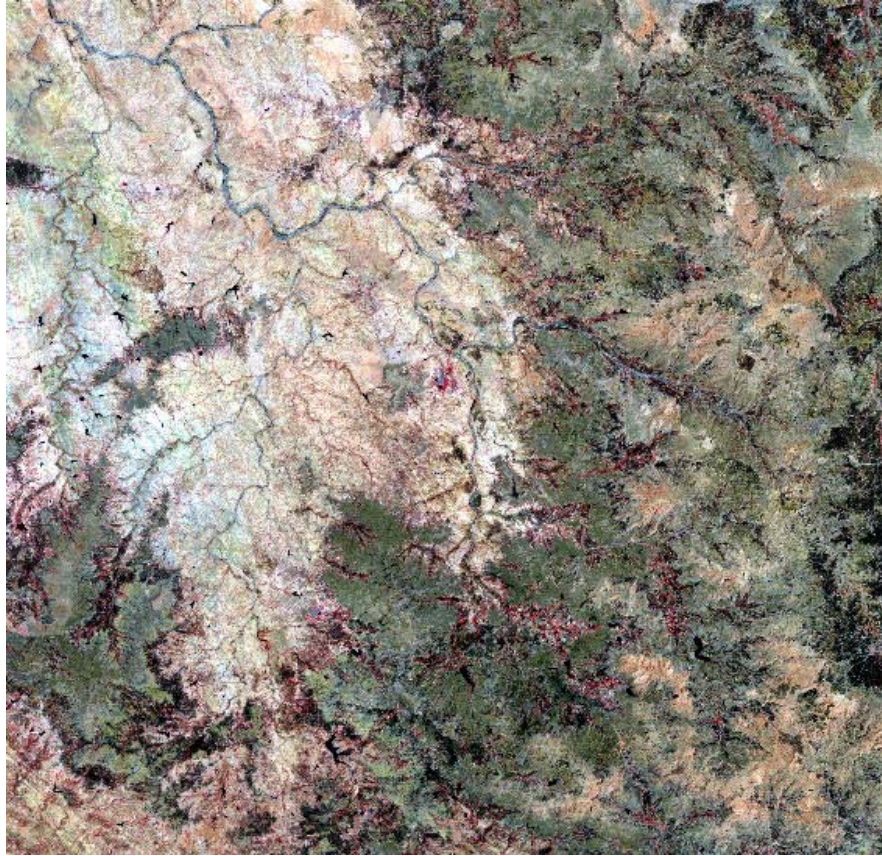


Figure 4.4 **False colour composite** of Landsat ETM+ of Anas catchment formed by projecting band 4 in red, band 3 in green and band 2 in blue.

Table 4.5 Selection of training classes and areas for Landsat ETM+ image of 6<sup>th</sup> April 2000

No.	Class name	Field (sub-class) Name of field	Number of pixel	Coordinates ( $x_1, y_1$ ); ( $x_2, y_2$ )
1.	Water bodies	Reservoir	560	(128,1682); (155,1701)
		Medium reservoirs	266	(1540,879); (1558,892)
		Small reservoirs	280	(1680,619); (1699,632)
		Ponds & tanks	96	(857,218); (868,225)
2.	River channel	Main river (4-5 <sup>th</sup> order)	205	(362,198); (366,238)
		Main river (2-3 <sup>rd</sup> order)	297	(705,520); (713,552)
		Tributaries	225	(857,1056); (883,1080)
		Sub-tributaries	208	(1159,503); (1184,510)
3.	Forest	Permanent forest	850	(1081,1595); (1114,1619)
		Regenerated forest	638	(1321,679); (1349,700)
		Planted forest	156	(1532,160); (1557,185)
4.	Range land	Shrub land	682	(1523,1226); 1544,1256)
		Mixed range land	420	(1171,964); (1198,978)
5.	Built-up area	Urban/ City	136	(986,847); (1002,854)
		Rural/ villages	144	(1423,637); (1434,648)
		Rural/ villages	130	(099,779); (111,788)
		Road/ paved river courses	696	(1134,1177); (1157,1205)
6.	Agricultural land	Harvested fields	744	(1116,377); (1139,407)
		Double cropped area	336	(676,180); (689,203)
		Rainfed farming	675	(494,887); (520,911)
		Irrigated lands	500	(458,050); (482,069)
7.	Barren land	Exposed bare rocks	1140	(257,607); (286,644)
8.	Others	Unclassified pixels will fall under this category		

## 4.6 Results of Image Classification

The training classes statistics for 6<sup>th</sup> April 2000 image is also calculated, as given in table 4.6.

Table 4.6 Statistics on training classes for each channel for 6<sup>th</sup> April 2000 image

Class name	Channel	Channel					
		1	2	3	4	5	6
Water bodies	$\mu$	92.7	81.1	87.0	47.0	78.2	64.5
	$\sigma$	11.4	15.7	28.3	24.0	60.7	49.0
River	$\mu$	109.6	101.5	128.5	74.3	154.4	132.3
	$\sigma$	8.0	11.1	18.4	13.6	45.6	41.7
Forest	$\mu$	94.8	81.1	98.6	56.7	107.9	90.0
	$\sigma$	4.8	6.7	12.7	8.0	21.1	16.4
Range land	$\mu$	105.0	97.7	128.7	79.8	145.5	110.4
	$\sigma$	6.6	9.1	13.1	9.9	23.3	13.5
Built-up area	$\mu$	99.4	88.4	107.5	73.7	137.6	106.1
	$\sigma$	6.9	10.3	18.6	13.8	37.1	30.2
Agriculture land	$\mu$	109.0	105.6	143.0	86.1	196.1	162.0
	$\sigma$	6.2	8.9	14.0	7.7	22.4	19.8
Barren land	$\mu$	111.0	106.4	147.5	92.5	205.5	153.4
	$\sigma$	4.6	6.8	9.4	3.9	11.4	16.3

Where,  $\mu$  and  $\sigma$  are mean and standard deviation for the training class.

Feature selection assist in determining the best subset of channels or features to be used for a given training set. The separability index between training classes is also calculated as given in table 4.7.

Table 4.7 Separability index between training classes for 6<sup>th</sup> April 2000 image

Training class ID's	Channel	Channel					
		1	2	3	4	5	6
1	2	0.87	0.76	0.89	0.73	0.72	0.75
	3	0.13	0.00	0.28	0.30	0.36	0.39
	4	0.68	0.67	1.01	0.97	0.80	0.73
	5	0.37	0.28	0.44	0.71	0.61	0.53
	6	0.93	1.00	1.32	1.23	1.42	1.42
	7	1.14	1.12	1.60	1.63	1.77	1.36
2	3	1.16	1.15	0.96	0.81	0.70	0.73
	4	0.32	0.19	0.01	0.23	0.13	0.40
	5	0.68	0.61	0.57	0.02	0.20	0.36
	6	0.04	0.21	0.45	0.55	0.61	0.48
	7	0.11	0.27	0.68	1.04	0.90	0.36
3	4	0.89	1.05	1.17	1.29	0.85	0.68
	5	0.39	0.43	0.28	0.78	0.51	0.35
	6	1.29	1.57	1.16	1.87	2.03	1.99
	7	1.72	1.87	2.21	3.01	3.00	1.94
4	5	0.41	0.48	0.67	0.26	0.13	0.10
	6	0.31	0.44	0.53	0.36	1.11	1.55
	7	0.54	0.55	0.84	0.92	1.73	1.44
5	6	0.73	0.90	1.09	0.58	0.98	1.12
	7	1.01	1.05	1.43	1.06	1.40	1.02
6	7	0.19	0.05	0.19	0.55	0.28	0.24

Symbols for training class ID's: 1-Water bodies, 2- River, 3- Forest, 4- Range land, 5- Built-up area, 6- Agriculture, 7- Barren land

A distinct training class separation index between barren land and forest ( $S = 3.00$ ) for channel 4 and 5, agriculture and forest ( $S = 2.03$ ) for channel 4, range land and forest ( $S = 1.29$ ) for channel 4, forest and river ( $S = 1.16$ ) for channel 1 have been found. The training classes water bodies and river are somewhat over lapping with other training classes in spite of several trials classification results could not be improved.

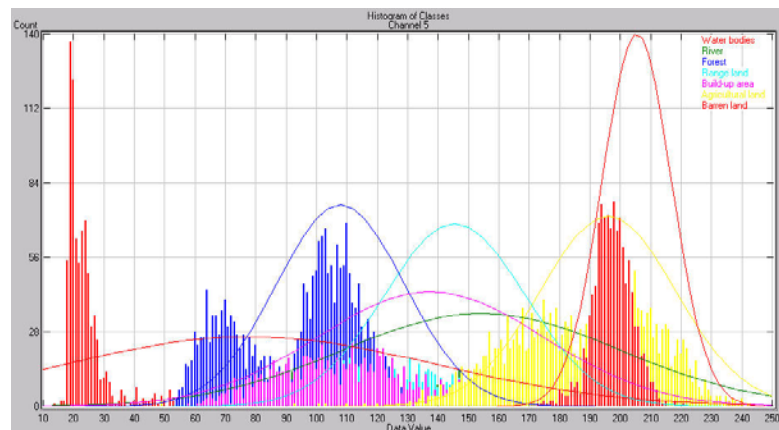


Figure 4.5 **Histogram and density function for various training classes** (channel 5: 1.55–1.75  $\mu$ m) of 6<sup>th</sup> April 2000 image

This is due to the existence of many small number of reservoirs in the catchment which are also used for cultivation during dry periods. Plantation along stream channels and river networks also hindered the supervised classification, which has been corrected using topographic maps and field verification. The class histogram and density function for channel 5 of 6<sup>th</sup> April 2000 image are presented above.

#### 4.6.1 Extraction of training features

The performance analysis for two feature extraction algorithms (DAFE and DBFE) is conducted for training classes on 6<sup>th</sup> April 2000 image. The results, thus obtained are given in table 4.8 below. The statistic for the six principal components using six Landsat ETM+ channels shows that the PC1 contains over 55.0% of variance while PC5 and PC6 combined contains over 2.5% of variance. For the individual components DBFE algorithm has shown better results as compared with DAFE except for PC2 as depicted in figure 4.6 below. The eigenvalues of co-variance matrix obtained from transformation using DAFE and DBFE algorithms are given in table 4.8.

Table 4.8 The eigenvalues and % component explained for 6<sup>th</sup> April 2000 image using discriminant analysis and decision boundary feature extraction algorithms

PC	Eigen-values		% component explained				Determinant		Feature Mean	
	DAFE	DBFE	Individual		Cumulative		DAFE	DBFE	DAFE	DBFE
			DAFE	DBFE	DAFE	DBFE				
PC1	0.808	3.249	55.895	56.444	55.895	56.444	0.808	3.249	17.66	-17.87
PC2	0.446	1.335	30.849	23.195	86.744	79.639	0.360	4.339	-2.67	-27.31
PC3	0.102	0.603	7.080	10.479	93.824	90.119	0.037	2.618	13.26	57.64
PC4	0.055	0.415	3.811	7.210	97.635	97.330	0.002	1.086	35.53	-59.95
PC5	0.020	0.132	1.386	2.300	99.022	99.630	0.000	0.144	15.13	13.39
PC6	0.014	0.021	0.977	0.369	100.00	100.00	0.000	0.003	-19.91	258.38

Terms here refers to; PC= Principal components; DAFE= Discriminant Analysis Feature Extraction algorithm, DBFE= Decision Boundary Feature Extraction algorithm.

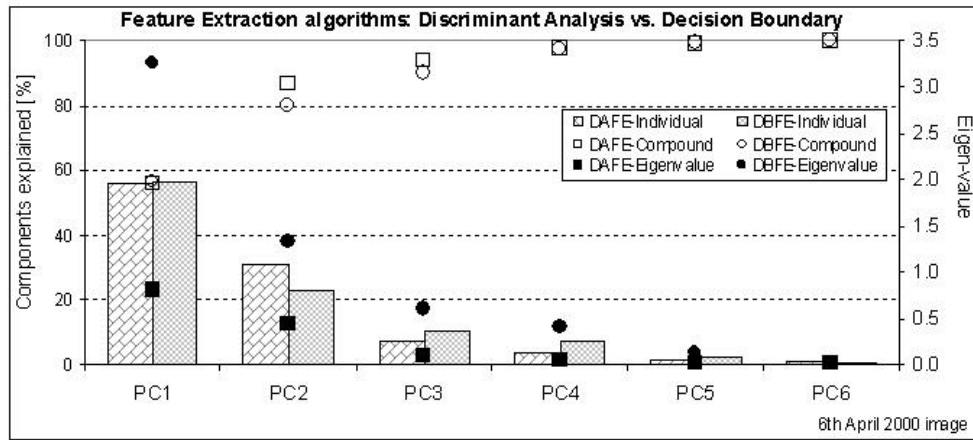


Figure 4.6 A comparison of feature extraction algorithms (DAFE vs. DBFE) for 6<sup>th</sup> April 2000 image

Table 4.9 Eigenvalues of covariance matrix obtained for 6<sup>th</sup> April 2000 image using discriminant analysis and decision boundary feature extraction algorithms

PC	FE-A	Channel					
		1	2	3	4	5	6
PC1	DAFE	0.1609	-0.7677	0.4452	0.0556	0.3287	-0.2743
	DBFE	-0.0131	0.6935	-0.2733	-0.4689	-0.3544	0.3138
PC2	DAFE	0.2287	-0.3373	-0.1555	0.7372	0.1887	-0.4802
	DBFE	-0.5543	-0.2420	0.5989	-0.4566	-0.0997	0.2384
PC3	DAFE	0.1655	-0.1443	-0.3235	0.8285	-0.2951	0.2712
	DBFE	0.0729	0.3599	0.2189	-0.4101	0.5818	-0.5572
PC4	DAFE	0.7905	-0.5917	0.1188	-0.0028	-0.0803	0.0662
	DBFE	-0.7777	0.3450	-0.1437	0.4411	0.0131	-0.2463
PC5	DAFE	-0.2809	0.8939	-0.3308	0.0044	0.0663	-0.0893
	DBFE	-0.2432	-0.2299	-0.5394	-0.2122	0.6194	0.4107
PC6	DAFE	-0.7207	0.1008	0.4952	0.3455	-0.3195	0.0608
	DBFE	0.1538	0.3985	0.4549	0.4046	0.3768	0.5502

Terms refer here to; PC= Principal component; FE-A= Feature Extraction Algorithms, DAFE= Discriminant Analysis Feature Extraction, DBFE= Decision Boundary Feature Extraction.

#### 4.6.2 Classification of training fields

The training class performance for three classification algorithms such as maximum likelihood, Fisher's linear discriminate analysis, ECHO classifier are compared. The results



for training classes using unequal weights and homogeneous cell likelihood threshold (in case of ECHO classifier) of the 6<sup>th</sup> April 2000 image are listed in table 4.14.

Table 4.14 Training class performance (redistribution method)

Classification algorithm →	Maximum likelihood		Fisher's linear discriminate		ECHO classifiers	
	Reference accuracy [%]	Reliability accuracy [%]	Reference accuracy [%]	Reliability accuracy [%]	Reference accuracy [%]	Reliability accuracy [%]
Class name						
Water bodies	75.0	94.1	68.8	95.6	88.0	97.2
River	57.1	79.1	39.6	93.4	66.5	95.8
Forest	91.5	80.3	41.8	71.3	94.7	91.1
Range land	57.9	81.1	0.6	16.7	79.3	94.9
Built-up area	61.2	78.9	44.6	82.7	79.9	90.9
Agriculture	93.7	79.5	94.7	46.5	95.8	83.5
Barren land	97.6	89.8	98.6	61.6	99.3	97.0
Overall class performance		80.3		59.2		88.6
Kappa index or statistics		76.4		50.4		86.4

The class distribution of image area is also given in table 4.15.

Table 4.15 Class distribution for image area

Classification algorithm →	Maximum likelihood		Fisher's linear discriminate		ECHO classifiers	
	Total sample	%	Total sample	%	Total sample	%
Class name ↓						
Water bodies	52344	1.4	25635	0.7	28764	0.7
River	170947	4.4	30842	0.8	182523	4.7
Forest	830077	21.4	458532	11.8	609627	15.7
Range land	456985	11.8	26652	0.7	405510	10.5
Built-up area	273282	7.1	142428	3.7	511463	13.2
Agriculture	1741010	45.0	2835143	73.2	1688830	43.6
Barren land	113797	2.9	265789	6.9	51721	1.3

#### 4.6.3 Comparison of image classification results

Extraction and classification of homogeneous objects (ECHO), a spatial pre-processing algorithm was proposed by Kettig and Landgrebe (1976). In this approach homogeneous regions are identified before classification. The classifier first divides the scene into homogeneous image segments and classifies them using an extended version of Gaussian maximum likelihood algorithm. The classification results for the 6<sup>th</sup> April 2000 image obtained using maximum likelihood and ECHO classification are shown in figure 4.7a and 4.7b respectively.

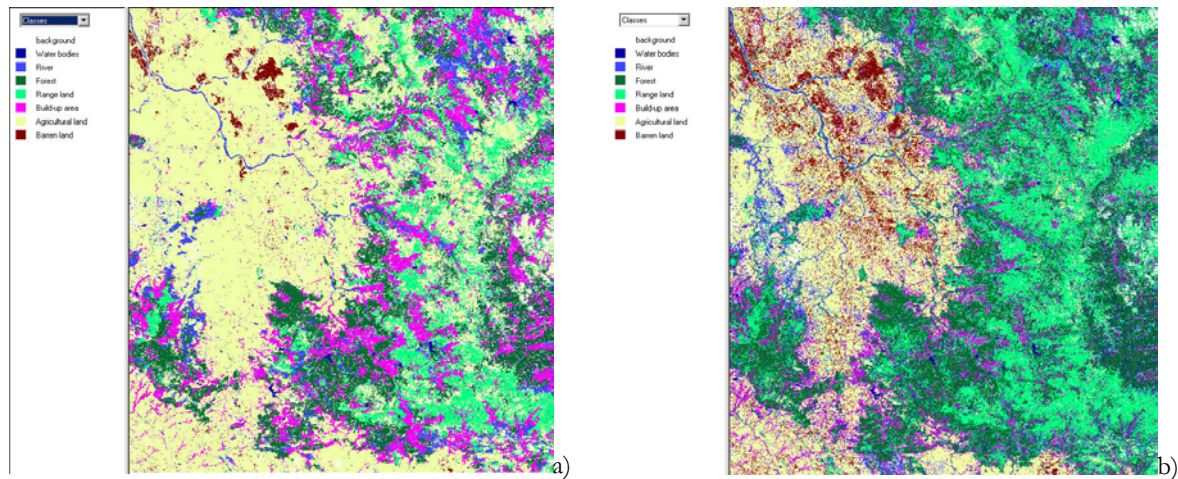


Figure 4.7 Results obtained from a) **ECHO classifier** and b) **Maximum-likelihood classifier** for 6<sup>th</sup> April 2000 image

#### 4.7 Image Integration in GIS

The integration of classified satellite imagery data and thematic feature data is usually done by using GIS techniques. One of the most important benefit of a GIS is its ability to spatially interrelate multiple type (images, grids, themes or coverages) if found to have same projection system. GIS is capable of handling both location data and attribute data in a multiple features. It also provides rational database capability for recording and characterisation of hydrological similar units (HSU's) of descriptive features. Here our focus is on merging land-use data soil map for determination of HSU's, representing areas of equal hydrological behaviour due to their similar land use classes and soil type.

The followings steps are performed:

1. Convert image format into GIS format.
2. Convert image into grid using the AML sub-routine in Arc/Info
3. Convert Arc/Info grid into vector coverage format
4. Clip the coverage using watershed boundary as clip coverage.
5. Convert the Arc/Info coverage into Arc-View shape format (as shown in figure 4.8)
6. Import data into ACCESS database and perform analysis

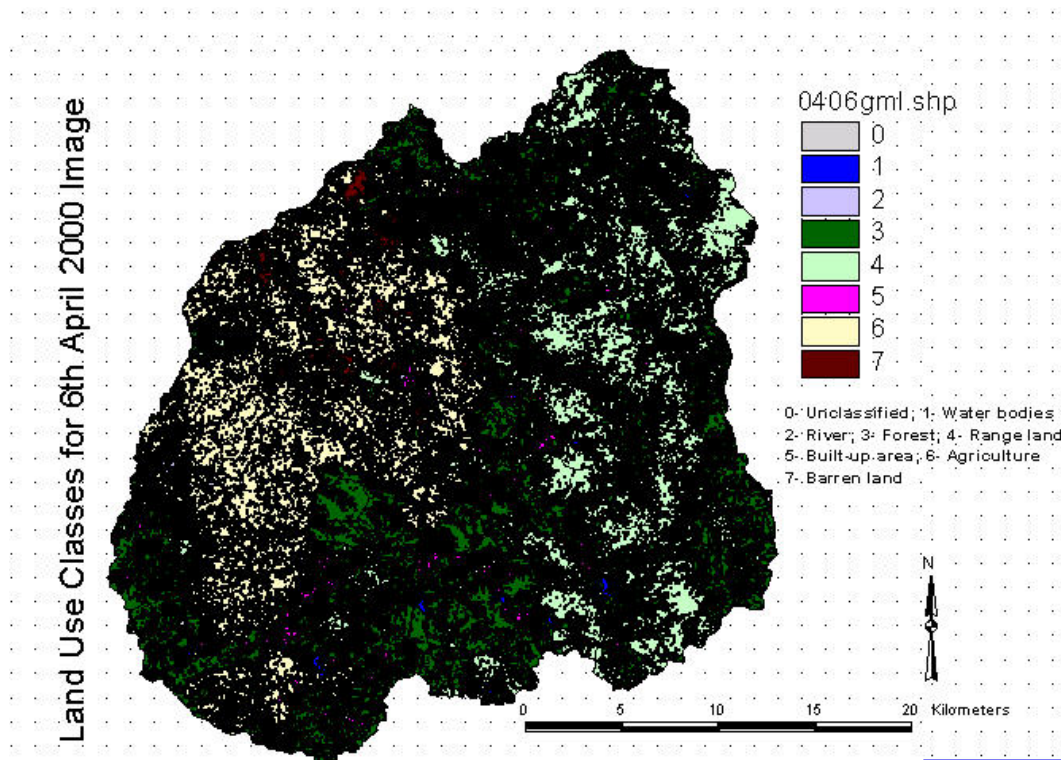


Figure 4.8 Land use classes derived from 6<sup>th</sup> April 2000 image

Table 4.18 Distribution of land use classes in each watershed for 6<sup>th</sup> April 2000 image

ID	Water bodies	River	Forest	Range land	Built-up area	Agriculture	Barren land	Un-classified
101	5.70	7.71	44.45	20.06	23.86	28.91	3.05	5.12
102	3.24	5.52	26.57	5.61	12.32	27.58	3.63	3.38
103	1.16	9.61	20.92	9.35	5.39	26.72	1.27	3.53
104	1.36	10.07	18.18	6.25	6.50	60.91	7.35	1.95
105	0.26	1.22	1.95	0.69	1.82	21.80	4.64	1.76
106	0.99	5.28	1.64	3.52	3.71	53.08	13.78	2.55
201	2.50	2.44	33.41	16.04	6.84	0.94	0.04	1.19
202	4.04	4.50	52.50	32.36	14.67	7.46	0.67	2.51
203	4.47	3.56	35.88	52.13	9.54	1.80	0.45	2.92
204	1.91	2.57	29.30	37.59	7.50	4.11	0.49	3.19
205	2.26	4.25	22.64	24.05	11.37	35.34	6.68	3.78
206	4.51	3.57	43.03	44.88	6.09	4.70	0.38	4.72
207	2.12	5.23	26.98	52.10	10.89	10.72	1.52	2.36
208	1.29	2.63	20.93	40.58	9.25	5.37	0.57	2.44
209	0.95	1.74	14.43	42.87	4.54	3.56	1.37	1.59
210	2.35	5.24	20.53	48.78	7.22	2.87	0.63	2.09
211	1.52	3.32	24.94	27.79	10.90	11.29	3.84	1.83
212	0.79	3.29	5.10	8.84	4.93	39.12	9.94	1.75
213	2.13	7.69	12.86	6.53	7.07	48.55	16.15	2.29
Sum	43.62	89.52	456.30	480.11	164.50	394.89	76.51	51.02
[%]	2.48	5.10	25.98	27.33	9.37	22.48	4.36	2.90

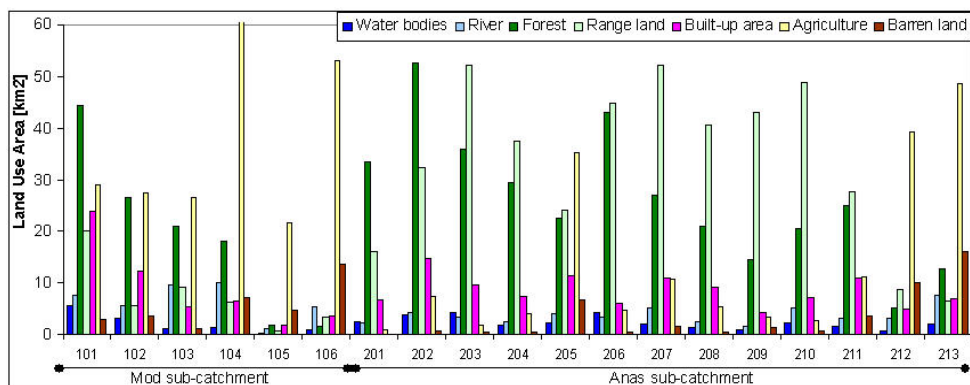


Figure 4.9 **Distribution of land use classes** in each watersheds for April 2000 image

Once the land use types for each sub-catchment or segment are analysed. Runoff curve number for each segment can be calculated. Although the advantage of such technique is not so much on model accuracy but rather on the potential to compute runoff discharge at all the node locations for un-gauged basins (Schultz 2000) and possibility to predict impact of land use change on future water resources planning. A detailed analysis for rainfall-runoff modelling in un-gauged catchment is given in chapters 3 and 6.

#### 4.8 Results and Discussion

The use of Landsat-TM data for land-use classification have been investigated using various classifiers to ensure the accuracy of images classification. The performance of ECHO classifier has been better due to cell likelihood threshold for each class. A combined classification accuracy of 84.6% for ECHO classifier shows good performance as compared to others. The training class performance for individual classes found to be varying between 50% to 95% which is mainly due to low class separability index.

For the selection of classification algorithm it should be based on class accuracy as well as on application. ECHO classifier offers an advantage over GML classifier if classification results are to be used for water resources assessment or rainfall-runoff modelling for medium to large scale catchments (larger than 500 km<sup>2</sup>). There is a possibility that similar pixels are merged into one object which may have different hydrological responses. GML algorithms still have an advantage of being able to define distinct classes for distributed locations and

can be interesting for flood forecasting in small catchments (smaller than 50 km<sup>2</sup>). It will be the further work of this research to verify the above statements.

Remote sensing has high technical potential for land use assessment and change detection for regions with limited amount of spatial and temporal data. This has given a basis for calculation of runoff curve number for SCS-CN runoff model as explained in chapter 3. Integration of remote sensing with GIS offers additional advantage for database development and analysis. A technical consensus on use and optimise digital processing of remote sensing data is still a subject of discussion among experts. Intense processing and ground surveys are needed to calibrate the remote sensing data.



## **5. RAINFALL PREDICTION BASED ON ATMOSPHERIC CIRCULATION**

One of the main objectives of this research work has been rainfall prediction and forecasting which is one of the important factors for catchment level water resources management decision making. This is particularly of high relevance under the semi-arid agro-climatic conditions where water supply is most often in short and agriculture and ecosystem are solely dependent on the rainfall. The monsoon variations, particularly unanticipated, impart significant economic and social consequences for the region. The monsoon variability often brings drought and famine during some years and devastating flood-like situations during the other years. The global climate change is likely to have a direct effect on the shifting of monsoon season, available soil moisture, reduced water levels and desertification hazards. The Indian ocean atmospheric circulation influences more than 1.5 billion people in arid and tropical Asia. Semi-arid regions of India generally display strong climate variability temporally and spatially (DWC 2003). This makes rainfall modelling rather a complex process but prediction of rainfall becomes an essential input parameter for decision support modelling and hydrological impact assessment studies (both in short and long term).

Accurate and reliable prediction of monsoon rainfall at regional or local scale can improve planning to mitigate the adverse impacts of droughts or floods and to take the advantage of early warning systems not only for water resources operations but also for agriculture where more than 70% of the total work force is still employed in this sector (Clark et al. 1999). Thus a better understanding of monsoon rainfall for arid and semi-arid India is clearly of a scientific and social value. Siddiq (1999) is of the view that enhancement of food production will result from tailoring of management strategies to rainfall variability rather than changes in crop varieties for the complex rainfed ecologies in India. Thus the importance of issuing reliable monsoon rainfall prediction on the likelihood of good or bad rainfall season is indispensable for farming risk reduction.

Modelling the dynamics of atmospheric circulation is sensitive to small changes in local rainfall. Statistical techniques have been developed to construct area-average means from observed precipitation data for use in GCM validation (Goodess 2000, Osborn and Hulme 1997). It is evident that large scale weather indices can also be downscaled for seasonal forecasting of hydro-meteorological variables at catchment scale (Clarke et. al 2001, Wilby 2001). The growing demand for climate scenarios for future hydrological and flood forecasting impact studies has created a need for downscaling methods which are relatively simple to apply and do not require large amounts of observed data and are transferable between regions (Goodess 2000).

Several downscaling models for rainfall prediction have utilised indicators of geo-potential heights at 500hPa or 700hPa, sea level pressure (SLP), sea surface temperature (SST) and land surface conditions (humidity, temperature and wind component). Gowariker et al. (1991) developed a regional scale power regression models for rainfall forecasting in selected regions of India based on time domain approach. Time domain approach for modelling daily rainfall typically involve vectors of time series for example the multivariate autoregressive (AR) type of models. Woolhiser and Roldan (1982) used direct numerical maximum likelihood estimates of Fourier coefficients to describe the seasonal variations of parameters in a stochastic model of daily precipitation. They used first-order Markov chain as the occurrence process and a mixed exponential distribution for daily precipitation. Bardossy and Plate (1992) developed a multi-dimensional stochastic model for space time distribution of daily precipitation. The rainfall is linked to atmospheric circulation patterns using conditional distributions and conditional spatial covariance functions. Wilby (2001) obtained the summer rainfall in U.K. from north Atlantic ocean temperatures using conditional probability for wet-days and dry-days. A linear regression model based on singular value decomposition to estimate rainfall in the Chikugo river basin at half day duration have been used by Uvo et. al. (2001) in Kyushu Island, Japan. Stehlik and Bardossy (2002) used multivariate stochastic downscaling model by means of maximum likelihood method to predict rainfall.



## 5.1 Downscaling Approaches

von Storch et al. (1999) in the review of empirical downscaling techniques is of the opinion that regional climate is conditioned by climate on larger scales. The multivariate downscaling seeks to derive the rainfall information from the large scale geo-potential heights using a fuzzy based random function. There are three major downscaling approaches which have been categorised based on specific field of applications and authors background (Bardossy et al. 2002, Fuentes and Heimann 2000, Wilby and Wigley 1997, Wilby et al. 1982) that counter the scale deficiency.

### 5.1.1 Dynamic downscaling

The dynamic downscaling also referred as physically based approach involves the general atmospheric circulation models (GCM) at the local scale that are derived by boundary conditions nested with regional climatic models. Dynamic downscaling using regional climatic models delivers meteorologically consistent variables, however is computationally expensive, not error free due to limited spatial resolution and non-uniqueness of the parameterisation solution (Salathe 2003, Bardossy et al. 2002). A spectral nudging techniques for dynamic downscaling at regional scale have been employed by von Storch et al. (2000). In other research work Kunstmann and Stadler (2003) used coupled hydro-meteorological simulations for alpine catchment of the river Mangfall in Germany. For forecasting the river discharge Anderson et al. (2002) coupled HEC-HMS with meso-scale model in Sierra Nevada mountains of California.

### 5.1.2 Statistical downscaling

The statistical downscaling approach also known as empirical downscaling use regional observations to derived statistical relations between regional scale anomalies and corresponding anomalies on a scale large enough to be resolved by GCM. Observed rainfall levels in space and time are modelled as joint realisation of a collection of space-indexed time series. Empirical downscaling can be performed using regression methods or nearest neighbourhood or circulation pattern approaches. They can generate a large number of realisations thus the assessment of the uncertainty of the prediction is possible. Further the local details which can not be reflected by the dynamic models are considered in these methods.

Empirical downscaling can be done either using regressive techniques or conditional probability approaches. The regressive method defines the relationship between large-scale and local information by means of an explicit function. The form of the function is usually selected so that parameters can be estimated without major numerical difficulties (Bardossy et al. 2002). Thus the concept may be written as

$$Z(t, u) = f\{W(t, u)\} \dots\dots\dots (5.1)$$

where  $Z(t, u)$  represents the local predictand (rainfall, temperature, humidity),  $W(t, u)$  is the large scale predictor (geo-potential heights, sea surface temperature, wind velocity) and  $f$  is a deterministic function conditioned upon  $W(t, u)$ . Then the statistical downscaling is done by using multivariate stochastic models with parameters dependent on the large scale atmospheric circulation pattern (CP) type. Bardossy and Plate (1992) used this techniques for predicting daily series of rainfall in Ruhr catchment in north Germany.

### 5.1.3 Statistical-dynamic downscaling

The statistical-dynamic downscaling approach links global and regional model simulations through statistics derived for large scale weather type. A regional scale model is run only once for each weather type. This method is based on the disaggregating multi-year time series of large scale meteorological data into multi-day episodes of quasi-stationery circulation. The episodes are subsequently grouped into a defined number of classes. A regional model is used to simulate the evolution of weather during the most typical episodes of each class. The model output are weighted with the climatic frequencies of the circulation classes in order to provide regional climate patterns. Fuentes and Heimann (2000) applied statistical-dynamic downscaling approach for predicting alpine precipitation climatology in Austria.

A comparison on strengths and weaknesses of dynamic versus statistical downscaling techniques are given in appendix 5.1. The literature review of atmospheric downscaling techniques shows that statistical downscaling have lot more advantages and simplicity over dynamic downscaling, so our focus for this research work remain on statistical downscaling. Thus the term downscaling will be referred as statistical downscaling through out the document.

## 5.2 Atmospheric Circulation and Statistical Downscaling

### 5.2.1 CP based approach to downscaling

As has been described in equation 5.1, the atmospheric circulation based approach relates large scale patterns of a daily predictor variable to local values of daily rainfall at a given station. The large scale daily 500hPa geo-potential height patterns are defined using circulation type for the yearly series of daily data. While using downscaling for rainfall prediction or local climate change detection it is postulated that;

- a) a relationship exist between atmospheric circulation pattern and observed station rainfall and
- b) the local rainfall changes are driven largely by changes in circulation patterns and not due to change in local meteorological conditions.
- c) the transfer function is also valid under altered climatic conditions (after Goodess 2000, von Storch et al. 1999).

Figure 5.1 below shows a typical form of statistical downscaling model along with model components at various spatial scale from GCM to RCM and local. Annex 5.2 shows the recent research techniques used for downscaling precipitation using various predictors are summarised along with their respective sources.

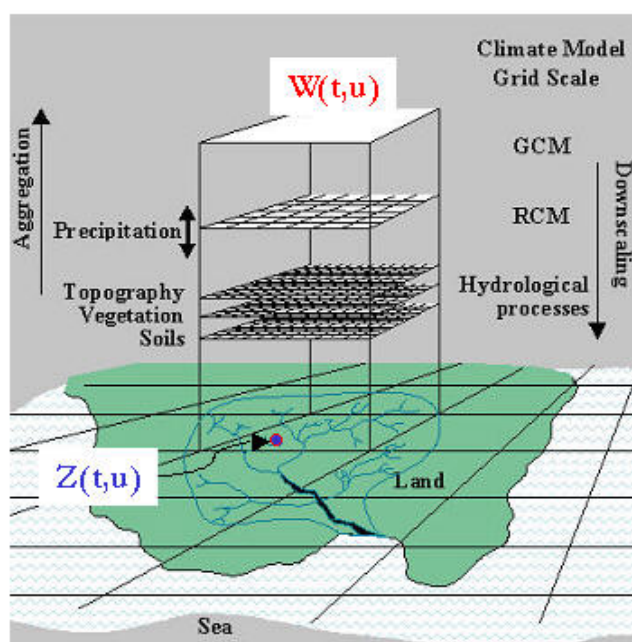


Figure 5.1 A typical representation of statistical rainfall downscaling model (modified anonymous)

### 5.2.2 State-of-art on CP based downscaling

For the river basin studies focusing on hydrological responses, Gutowski et. al. (1999) studies the performance of the statistical and dynamic downscaling for hydrological simulations in Animas river basin, USA. The runoff simulations for both methods produced relatively close results. Empirical approaches are relatively fast, allowing the user to develop ensembles of climate realisations, and thus obtain confidence interval estimates. Research studies conducted by Yoshino (1975), Bardosy and Plate (1992), Wilson et. al. (1992), Wilby and Wigley (1997), Wilby et al. (1998), Goodess and Palutikof (1998), Bardosy and Mierlo (2000) shows that changes in atmospheric circulation pattern affect rainfall. It is with this belief the statistical downscaling model will be tested for developing a decision support model for watershed management in Anas catchment, India.

It is widely accepted that GCM output from environment and climate studies are at a resolution (say 300km x 300km) that is too coarse to represent the regional climate variations for hydrology and water resources projects (Bardosy, 2002). To over come such mis-match problems various techniques needs to be developed with the help of predictor variable such as atmospheric circulation patterns. Hulme (1991) derived the rainfall change from global temperature data set for a period from 1901-1995 at 5° x 5° grid scale. There seems a

positive increase of approx. 20% for western India where the research area is situated (IPCC 1998). Thus it becomes much more important and interesting to research into this phenomena by undertaking a detailed study on rainfall downscaling as it will influence the basin hydrology and seasonal water availability within the Anas catchment.

The fuzzy rule based model used for the prediction of seasonal monsoon rainfall in Anas catchment is based on atmospheric circulation pattern of 500 hPa geo-potential heights from NCEP/NCAR data at  $5^\circ \times 5^\circ$  grid and daily station rainfall measurements from Department of Land Records. This model is an improved version of stochastic downscaling model proposed by Bardossy, Stehlik and Caspary (2002). The model computes distributed rainfall for the monsoon season at any point within the Anas catchment independent of point measurements on a known grid scale. A detailed description of the stochastic fuzzy model for the Anas catchment has been presented under section 5.3.

### **5.3 Modelling Methodology and Structure of Downscaling Model**

The circulation pattern classification technique was developed with the aim to serve as a basis for subsequent rainfall downscaling. The modelling code algorithms are written in Digital Visual FORTRAN which consists of a series of coupled sub-programmes for CP optimisation, CP classification, estimation of spatial and temporal co-relations using Fourier series and rainfall prediction using External-Drift-Kriging method. The modelling methodology and various steps used for analysis are described below;

#### 5.3.1 Classification of circulation type

An objective automated fuzzy rule based optimised method have been used for circulation type classification (other possible methods include neural network, K-means clustering). The CP type explains dependence between large scale atmospheric geo-potential heights at 500hPa and station rainfall through a random process. The model uses fuzzy-rule based logic concept for CP definitions. The days with similar range of geo-potential heights are assigned the same CP type. The classification is carried out using normalised pressure anomalies

$g(i, t)$  of daily geo-potential height data at a given station  $i$  and for a day  $t$ . The normalised pressure anomalies  $g(i, t)$  can be defined as:

$$g(i, t) = \frac{P(i, t) - \bar{P}}{\sigma_p} \dots\dots\dots (5.2)$$

where  $\bar{P} = \frac{\sum P(i, t)}{N}$  average pressure during time  $t$  having  $N$  number of observations.

and  $\sigma_p = \sqrt{\frac{\sum (P(i, t) - \bar{P})^2}{N}}$  is the standard deviation of daily pressure data.

Bardossy et. al. (2002) described every CP with a fuzzy rule  $k$  represented by a vector  $v(k)$ , thus

$$v(k) = \{v(1)^{(k)} \dots\dots\dots v(n)^{(k)}\} \dots\dots\dots (5.3)$$

where  $n$  are number of grid points for which the pressure data are available.

The rules for CP classification is that locations with anomalies  $v(k)$  may be high or low, depending upon the definition of threshold value. The term  $v(i)^{(k)}$  are the indices of the membership function corresponding to the selected locations. Five possible classes of membership function  $v$  were defined as triangular fuzzy numbers:

- $v = 1$ , very low:  $(-\infty, -1, -0.2)_T$
- $v = 2$ , medium low:  $(-1.4, -0.6, 0)_T$
- $v = 3$ , medium high:  $(0, 0.6, 1.4)_T$
- $v = 4$ , very high:  $(0.2, 1, +\infty)_T$  and
- $v = 5$ , the membership function is the constant.

These membership values are combined to calculate the degree of fulfilment (DOF) of the rule:

$$DOF(k, t) = \prod_{i=1}^4 \left[ \frac{1}{N\{v(i)^{(k)} = 1\}} \sum_{v(i)^{(k)}=1} \mu(i, k)^{P_i} \right]^{\frac{1}{P_1}} \dots\dots\dots (5.4)$$

where  $N$  is the number of grid points classified by class  $l$ , and  $P_l$  is the parameter which allows one to emphasise the influence of selected classes on the DOF. The  $k$  for which  $DOF(k, t)$  is maximal is selected as CP for day  $t$ .

The performance of a classification is measured by its conditional rainfall frequencies and conditional rainfall amounts for given CP type. First the probability of the rainfall on a given day is calculated by considering the threshold  $\mathcal{G}$  for the daily rainfall amount. Thus the objective function  $O_1(\mathcal{G})$  can be defined as:

$$O_1(\mathcal{G}) = \sum_{i=1}^S \sqrt{\frac{1}{T} \sum_{t=1}^T \{p(CP(t))_i - \overline{p_i}\}^2} \dots\dots\dots (5.5)$$

where  $S$  is number of stations,  $T$  number of days,  $p(CP(t))_i$  is the probability of rainfall exceeding the threshold  $\mathcal{G}$  on a day with given CP at station  $i$ ,  $\overline{p_i}$  is the probability of a day with rainfall exceeding  $\mathcal{G}$  for all days without classification and within the time period  $T$ .

Second for the amount of rainfall, the following objective function is defined:

$$O_2 = \sum_{i=1}^S \frac{1}{T} \sum_{t=1}^T \left| \left( \frac{z(CP(t))_i}{\overline{z_i}} \right)^{1.5} \right| \dots\dots\dots (5.6)$$

where  $z(CP(T))_i$  is the mean rainfall amount on a day with a given CP at station  $i$  and  $\overline{z_i}$  is the mean daily rainfall without classification at the same station. Higher values of  $O_1(\mathcal{G})$  and  $O_2$  indicate a better classification. It is possible to combine more objective functions by taking a weighted sum:

$$O = a_1 O_1(\mathcal{G}_1) + \dots\dots\dots + a_n O_n(\mathcal{G}_n) + a_{n+1} O_2 \dots\dots\dots (5.7)$$

where  $a_1 \dots\dots\dots a_{n+1}$  are weights. The weights are selected in order to express the importance of the different objective functions and to correct for the different ranges of the functions.

### 5.3.2 Downscaling of rainfall

The fuzzy based stochastic model for rainfall simulation has parameters which dependent on the actual CP-type on that day of the year. The seasonal cycle of the parameters such as mean and standard deviation, spatial and temporal correlations are modelled by applying Fourier series as described in Bardossy and Plate (1992). This algorithm aims to introduce a

transformation of the rainfall amount in order to replace the skewed probability density function by a normal distribution function. The transformation can be expressed as:

$$Z(t, u) = \left\{ \begin{array}{ll} \bar{W}^\beta(t, u) & \text{for } \bar{W}(t, u) > 0 \\ 0 & \text{for } \bar{W}(t, u) \leq 0 \end{array} \right\} \dots\dots\dots (5.8)$$

where,  $\beta$  is an appropriate positive exponent.  $Z(t, u)$  is a vector with daily rainfall amount on day  $t$  at location  $u$ . The relationship between  $\bar{W}(t, u)$  and  $\tilde{A}_t$  circulation pattern is obtained through rainfall process  $Z(t, u)$ .

The probability of rainfall at time  $t$  and location  $u$  depends on circulation pattern  $\tilde{A}_t$  and can be expressed as:

$$P[\bar{W}(t, u) > 0 \mid \tilde{A}_t = a_i] = P[Z(t, u) > 0 \mid \tilde{A}_t = a_i] = p_{\alpha_i}(u, t) \dots\dots\dots (5.9)$$

The distribution of daily rainfall amount at location  $u$ ,  $F_\alpha(z \mid u)$  also depends on circulation pattern  $\tilde{A}_t$  and time  $t$  which can be expressed as:

$$P[Z(t, u) < z \mid \tilde{A}_t = \alpha_i, Z(t, u) > 0] = F_{\alpha_i} z(t, u) \dots\dots\dots (5.10)$$

The multi-dimensional vector of transformed daily precipitation amounts at locations  $\bar{W}(t, u_1), \bar{W}(t, u_2) \dots \dots \bar{W}(t, u_n)$  can be described as random first order autoregressive (AR1) process. Thus the model parameters, mean transformed precipitation and standard deviation are estimated with the help of Fourier series. The spatial structure of the rainfall is described using a circulation pattern  $\tilde{A}_t$  dependent covariance structure.

$$\text{cov}(z(x), z(y)) = c_0 e^{-d(x, y)a} \dots\dots\dots (5.11)$$

where,  $d$  is the distance and parameters  $c_0$  and  $a$  are function of time.

For estimating the areal precipitation at unobserved points within the catchment external-drift-Kriging method has been applied. The method assumes the interpolated parameter  $Z(x)$  being correlated to a known parameter  $Y(x)$ . The relation can be expressed as:

$$E[Z(x) \mid Y(x)] = a + bY(x) \dots\dots\dots (5.12)$$



where  $a$  and  $b$  are unknown parameters. The elevation has been used as external drift parameter for interpolation on a 500 x 500m grid size.

The prediction at new location can be made by

$$\hat{Z}(x) = \sum_{i=1}^n w_i \cdot Z(x_i) \quad \dots\dots\dots (5.13)$$

The weighting factors  $w_i$  ( $i = 1, 2, \dots, n$ ) can be obtained by the following minimisation

$$error = E\left[\{Z(x) - \hat{Z}(x)\}^2\right] \sim \text{minimum} \quad \dots\dots\dots (5.14)$$

On the condition that  $\sum_{i=1}^n w_i = 1$  and  $\sum_{i=1}^n w_i \cdot Y(x_i) = Y(x)$   $\dots\dots\dots (5.15)$

## 5.4 Materials and Database

### 5.4.1 Large scale circulation data

The large scale circulation type approach described in this research work requires daily time series of mean geo-potential heights at 5° x 5° grid resolution for selected window between 05°N40°E and 35°N95°E over Indian sub-continent (refer Figure 5.2). The data-sets were obtained from the National Meteorological Centre for Atmospheric Research (NCAR) on CD-ROM for a period of 1962-94 (i.e. for 33 years period) by Institute of Hydraulic Engineering, University of Stuttgart. From the data-set 500hPa geo-potential heights has been taken for CP classification and rainfall downscaling purpose. Since the daily rainfall time series for all the stations within the Anas catchment have data set between 1985-99 thus a common data set period for geo-potential heights and rainfall during January 1985 to December 1994 has been found to be suitable.

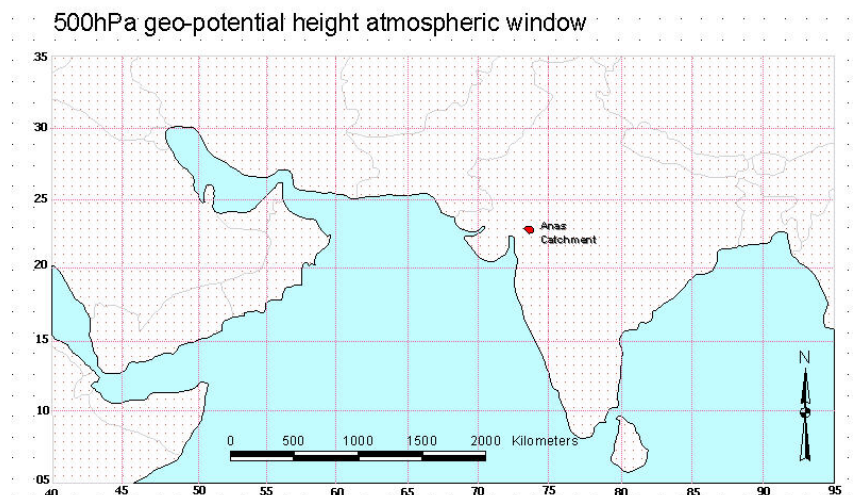


Figure 5.2 Location of Anas catchment (dark red) in **atmospheric circulation window** (05°N40°E and 35°N95°E) at 5° x 5° grid selected for downscaling over Indian ocean

#### 5.4.2 Station rainfall data

Long term daily rainfall data record for 10 rainfall stations has been collected from the Office of the Land Records Jhabua and State Water Data Centre Bhopal. Almost all the data were in paper form which have been converted into electronic format. The daily rainfall data available for various stations differ in quality but also in their temporal coverage. The rainfall stations Jhabua and Sardarpur have longest records 1957-99 followed by Thandla and Petlabad for a period of 1964-99. Rest of the stations have daily rainfall records between 1984-99 which are available for present analysis. The daily rainfall were recorded at 8:00 hr morning each day for all stations mainly during monsoon season. Seasonal variation play an important role for absolute rainfall amount as well as the number and probability of rainy days. Thus the year has been divided into two seasons namely monsoon season between 152<sup>nd</sup> to 304<sup>th</sup> days of the year and non-monsoon season rest day after this period. For rest of the period fictitious rainfall data were assumed from other stations in order to fill the yearly data series. Since 80-90% of the rainfall falls during monsoon season which has been responsible for runoff generation and hydrological modelling.

#### 5.4.3 Spatial database

The spatial database for the Anas catchment has been developed from topographic maps at 1:50000 using Arc/Info and Arc-View GIS software. The six maps were geo-referenced and later digitised to get various thematic coverages such as location of rain-gauge and discharge stations, contour lines and elevation points, stream network and land use. A detail description of GIS database development is explained in chapter 3 of this research work.

#### 5.4.4 Rainfall data characteristics

Due to the convective natures of the rainfall there are great differences on rainfall amounts at different stations during same season and also on same day. The main advantage of the automated classification is that it takes each individual station behaviour into account. The statistical properties of the monsoon season (June to October) data for a period of 1985-1994 were used in the analysis (refer table 5.1). The daily mean rainfall vary between station to station as the case with Meghnagar (4.8 mm) and Petlabad (6.6 mm). Although both stations are just 20 km apart but the mean rainfall variability is more than 37%. Similarly the stations Jhabua and Rama being 12 km away a mean rainfall variability of 17% has been calculated. The maximum daily rainfall also vary greatly between stations. The extreme daily rainfall statistic shows that station Sardarpur received maximum daily rainfall of 173mm while the station Rama 318mm.

Table 5.1 Statistical properties of daily rainfall data for various stations of Anas catchment during the monsoon season

Rainfall station Name	WMO-ID	Mean	Rainfall [mm]			Variance	Standard Deviation	Skewness
			Confidence	Min.	Max.			
			[95%]					
Jhabua	427531	5.2	5.9	0.0	226.8	253.3	15.9	6.31
Ranapur	427532	5.1	5.9	0.0	222.0	267.3	16.3	6.29
Udaigarh	427533	5.3	6.1	0.0	207.2	218.9	14.8	5.82
Amba	427534	5.6	6.4	0.0	200.0	279.4	16.7	5.32
Rama	427535	6.1	7.1	0.0	318.0	386.9	19.6	6.76
Meghnagar	427536	4.8	5.5	0.0	193.0	222.3	14.9	5.79
Thandla	427529	5.7	6.6	0.0	225.8	310.1	17.6	5.88
Bhabra	427537	5.2	5.9	0.0	210.0	216.4	14.7	5.58
Sardarpur	427528	5.0	5.7	0.0	173.0	221.6	14.8	5.08
Petlabad	427527	6.6	7.6	0.0	212.0	358.2	18.9	5.39

#### 5.5 Sensitivity Analysis for Rainfall Model

The sensitivity analysis for fuzzy based model has been conducted for various set of model parameters. The performance of rainfall downscaling model has been assessed in terms of how well they reproduce the statistical features such as conditional rainfall probability and conditional rainfall amount of the observed time series. The parameters used in the sensitivity analysis includes adjusting circulation pattern window, types of circulation patterns and varying the downscaling exponent ( $\beta$ ). The effect of shifting circulation window on the

conditional rainfall probability and average probability (see figure 5.3a) and conditional rainfall amount and average amount (see figure 5.3b) have been conducted. In case of rainfall probability distribution for both windows strong co-relation coefficient of 0.98 have been found as compared to 0.87 for rainfall amount. This shows that downscaling model predicts high conditional probability but lower amount of rainfall for atmospheric window  $0^{\circ}\text{N}45^{\circ}\text{E}$  and  $30^{\circ}\text{N}100^{\circ}\text{E}$ .

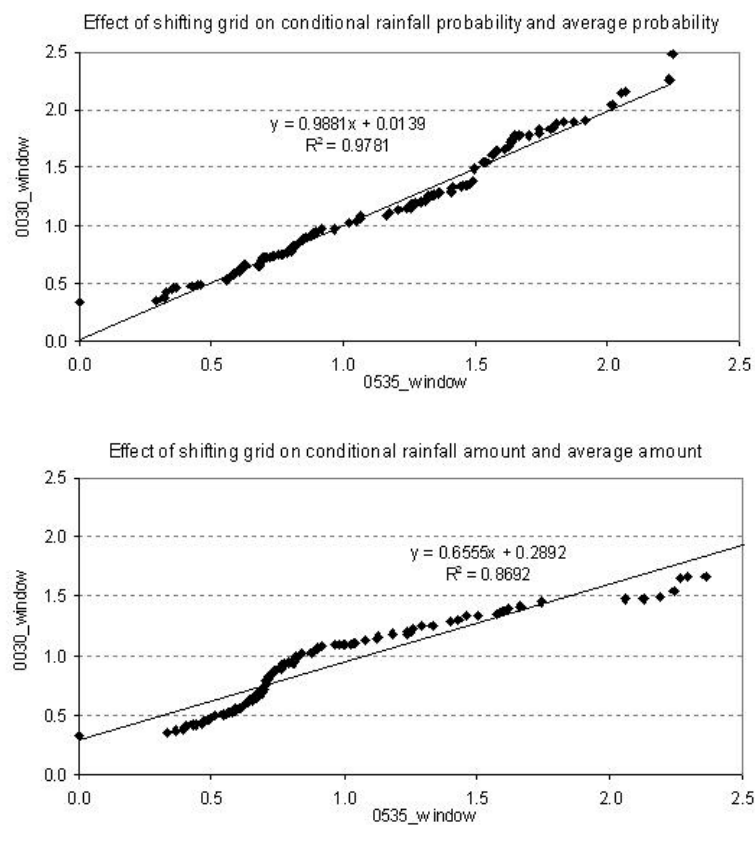


Figure 5.3 Model **sensitivity analysis for the effect of shifting atmospheric circulation window** on the a) rainfall probability and b) rainfall amount

The model results are further analysed for circulation pattern types, and the rainfall downscaling exponent ( $\beta$ ). The simulation results thus obtained are displayed in table 5.2 below.

The terms rainfall probability index\* is the ratio of conditional rainfall probability to the average rainfall probability and rainfall amount index\*\* is the amount rainfall to the average amount of rainfall for all CP types on all the years for a given station. Thus higher the value of rainfall probability and rainfall amount index better the circulation pattern classification.

Although the mean and maximum value of rainfall probability and rainfall amount index look somewhat closer but they have great bearing on the prediction of rainfall later. It is clear from the table 5.2 that atmospheric circulation window 5°N40°E and 35°N95°E with 12 CP types and linear downscaling exponent ( $\beta = 1$ ) found to be the best choice.

Table 5.2 Sensitivity analysis of parameters affecting the rainfall probability and rainfall amount

Model parameters	Sensitivity to			
	Rainfall probability index*		Rainfall amount index**	
	Mean	Maximum	Mean	Maximum
a. Atmospheric circulation window (with 12 CP's)				
5°N40°E and 35°N95°E	1.09	1.88	0.95	2.13
0°N45°E and 30°N100°E	1.07	1.84	0.90	1.84
b. Circulation pattern types (with 5°N40°E and 35°N95°E)				
12 CP types	1.08	1.91	0.95	1.73
10 CP types	1.03	1.60	0.92	1.82
08 CP types	0.96	1.38	0.97	1.19
c. Downscaling exponent (with 12 CP's and 5°N40°E and 35°N95°E window)				
$\beta = 1.0$	1.08	1.91	0.95	1.73
$\beta = 1.5$	1.01	1.56	0.98	1.26

## 5.6 Model Simulation Results

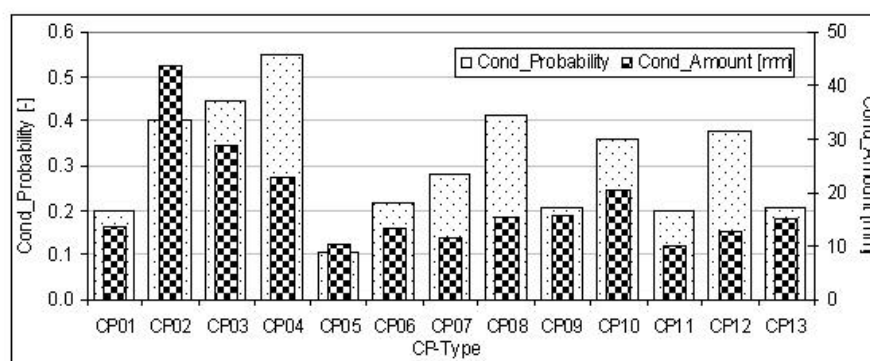
Twelve circulation pattern (CP) types have been defined based on automatic objective optimisation procedure, to allocate each day in the year to one of these twelve CP type. For CP-type classification it was found that atmospheric circulation window between 05°N-40°E and 35°N-95°E at 5° x 5° grid over Indian sub-continent produces better results as compared to other alternatives (refer section 5.5). Thus the circulation window 05°N-40°E, 35°N-95°E with twelve CP-types and linear exponent has been selected for rainfall downscaling using 500haP geo-potential heights (refer Figure 5.2). The rainfall downscaling model results are simulated for two objective functions namely conditional rainfall probability and conditional rainfall amount which are obtained from wet and dry circulation types. The results thus obtained for the optimum window and optimum number of circulation types are discussed below.

### 5.6.1 Conditional probability and conditional rainfall amount

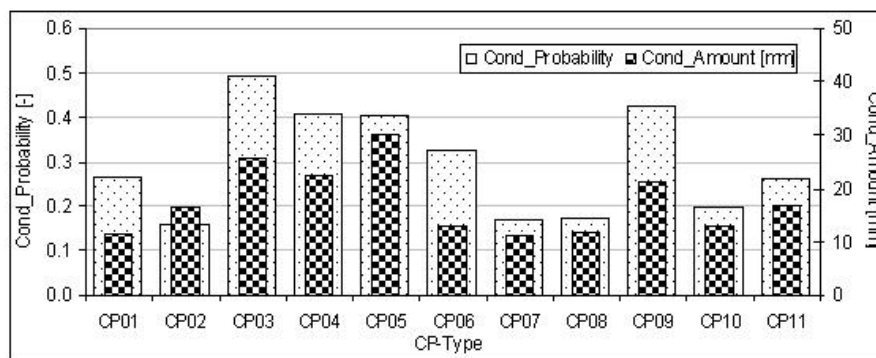
Conditional rainfall probability and conditional rainfall amounts were used as model parameters to predict the model goodness and well as to evaluate the performance of CP-classification routine. First the CP-statistics has been derived from circulation pattern

classification series and secondly the probability and amount of rainfall at given station are predicted. Monsoon is the most important season for an Indian farmer, the location specific predictions for rainfall probability and amount for a given season become important. The computed conditional mean probabilities and conditional mean rainfall amounts for all ten stations in Anas catchment during 1985-94 monsoon season are displayed in figure 5.4 below.

As shown in the figure 5.4a for 12 CP-type the conditional rainfall probability of the CP04 has been observed to be 0.54 with a conditional rainfall amount of 22.7 mm per day. Although the conditional rainfall probability ( $\sim 0.40$ ) for CP02 found to be low but the conditional amount (43.89 mm/day) estimated to be high as compared with CP04. Also CP04 has showed relatively very high conditional wet-day fraction (0.57) but low frequency of occurrence (just 5.8%). This shows that CP04 has been responsible for few large rainfall events as compared to CP02 where number of events of good rainfall amount do often occur. In case of CP03 and CP08 who have higher conditional probability (between 0.45 to 0.41) with a conditional daily rainfall amount of 28.6 mm and 15.4 mm respectively. The wet-day fraction for CP03 (0.39) has been found below the wet-day fraction of CP08 (0.46). This can be concluded that CP04 is the wettest CP followed by CP08 and CP03. Although CP02 observed to be responsible for higher conditional rainfall amount (43.89 mm per day) but has lower conditional probability and wet-day fraction. This type of circulation pattern may be termed as cyclonic weather type which may be occurring often during the monsoon season each year.



a.



b.

Fig. 5.4 Conditional **rainfall probability and rainfall amount** for all the stations in Anas catchment, a) for 12 CP-type and b) for 10 CP-type.

In the case of dry circulation types which have low wet-day fraction such as CP06 (0.16) and CP05 (0.22) but the frequency of occurrence of individual CPs found to be very high (between 13.4% to 16.1%). Similarly the conditional rainfall probability (0.217 and 0.106) and conditional rainfall amount (13.51 and 10.22 mm/day respectively) for CP06 and CP05 were observed to be low. CP06 has low conditional rainfall probability (0.106) having 10.2 mm of mean day rainfall amount and 0.211 a wet-day fraction. Low value for wet-day fraction indicates that CP06 contribute little to the rainfall as compared to high value (0.573) for CP04 with higher rainfall probability and rainfall amount. A low percentage of rainfall contribution from CP06, CP05, CP09 and CP11 may be due to the fact that there are many dry days with a small amount of rainfall falling on that day.

For most of the rainfall stations CP04 and CP08 were responsible for the higher conditional probability and conditional rainfall amount while the CP06 and CP05 found to be dry. Also the geographical distribution of CP-type shows that in northern part of catchment have been responsible for higher amount of rainfall. The distribution of CP-type statistics on conditional probability and conditional rainfall amounts for various stations is given in annex 5.6 of this chapter. A general observation between conditional frequency and conditional rainfall amount shows that CP06, CP05, CP09 and CP11 are associated with low rainfall amount for the Anas catchment as whole. The station-wise conditional probability and conditional amount index for all stations are depicted in figure 5.5.

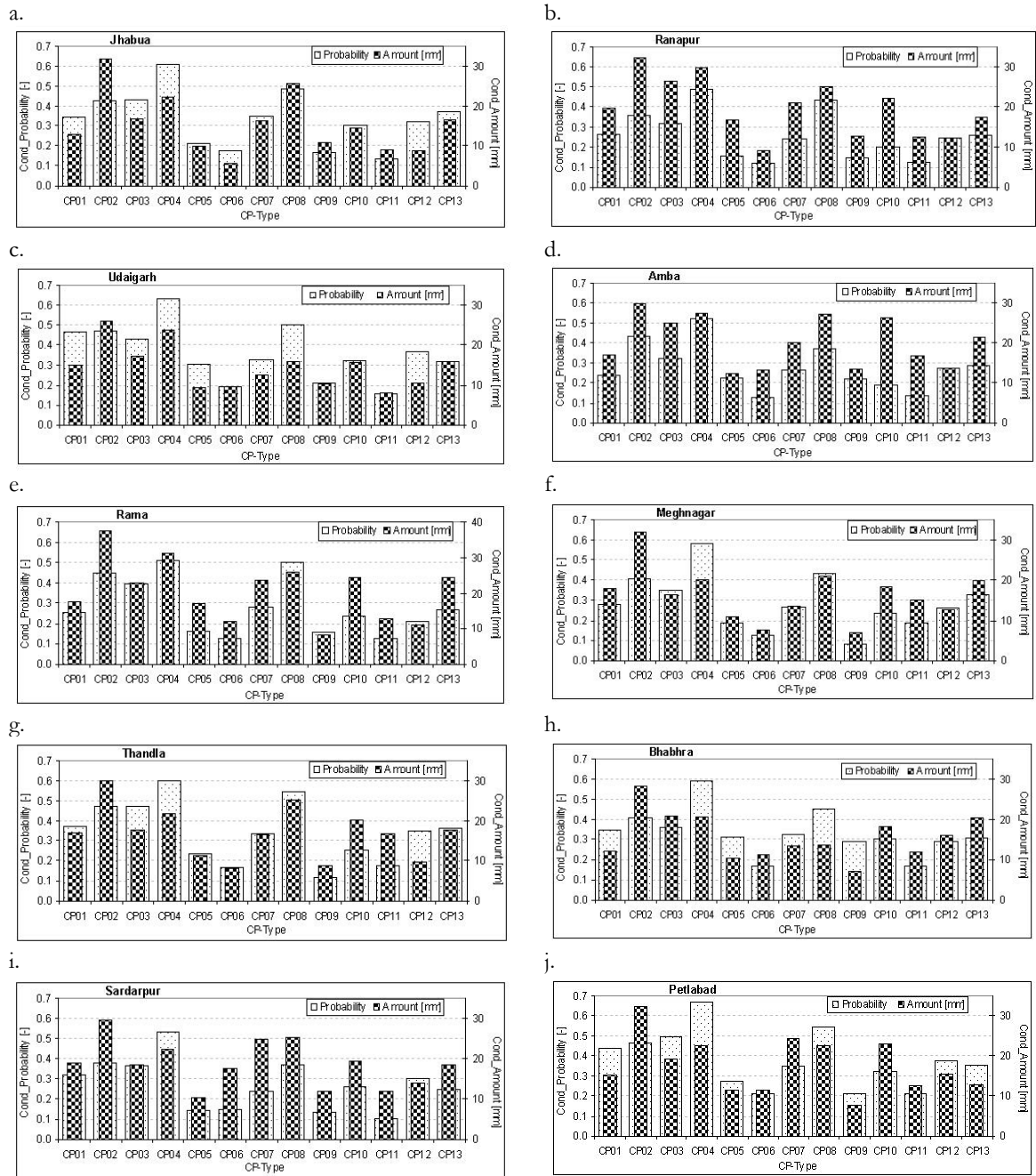


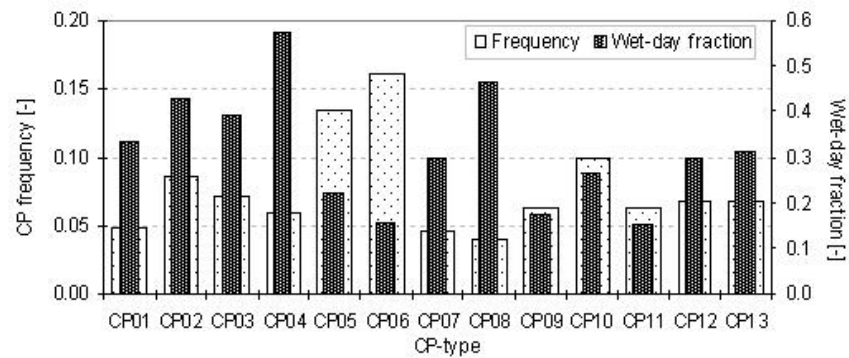
Figure 5.5 Analysis on conditional rainfall probability and conditional rainfall amount for all stations a) Jhabua, b) Ranapur, c) Udaigarh, d) Amba, e) Rama, f) Meghnagar, g) Thandla, h) Bhabhra, i) Sardarpur and j) Petlabad in Anas catchment India.

### 5.6.2 CP-Frequency analysis

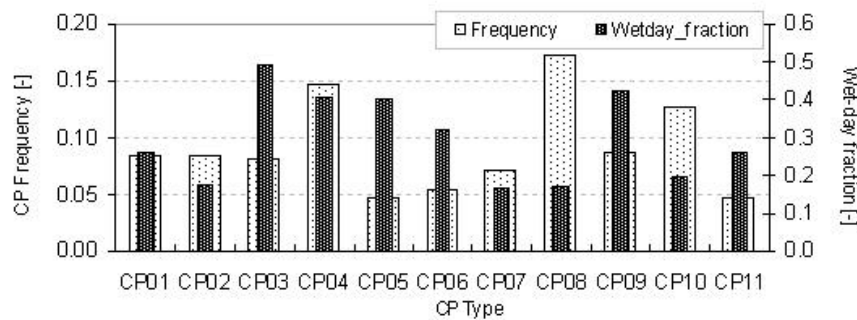
The results for the mean frequency of occurrence and mean of wet-day fraction analysis performed for daily geo-potential heights are described in figure 5.6 below for monsoon season (June-October) during 1985-94. The results for occurrence frequency for various CP-



types vary considerably from mean occurrence frequency of 0.07 for 12 CP-types to 0.09 for 10 CP-types. Similarly the mean wet-day fraction of 0.31 and 0.29 have been observed for 12 CP-types and 10 CP-types respectively. In case of 12 CP-types the circulation type CP06 and CP05 found to have very strong frequency of occurrence as compared to circulation type CP08 and CP04. The CP06 reported high mean occurrence frequency ( $\sim 0.16$ ) followed by CP05 ( $\sim 0.13$ ) and CP10 (0.10) while low mean occurrence frequency have been observed for CP08 ( $\sim 0.04$ ) and CP04 ( $\sim 0.06$ ). On the other hand the wet-day fraction for CP04 (0.57) and CP08 (0.47) have much dominated a compared to CP06 (0.16) and CP05 (0.22) wet-day fractions. It may be stated that both groups of circulation patterns produced rather different weather conditions in the Anas catchment.



a.



b.

Figure 5.6 shows the **mean frequency of CP-type occurrences and mean wet-day fraction** for various CP-types a) for 12 CP-types and b) for 10 CP-types during the monsoon season for the period between 1985-94 for 10 stations. An additional CP-type is added in respective classes to group the missing data and unclassified circulation pattern types.

Annex 5.4 shows the mean yearly CP-types frequency occurrence for 12 CP-types in Anas catchment. The frequency of CP occurrence for a given year can be analysed based on wet and dry seasons. It may be observed that during the wet year (1994) CP06 has low frequency of occurrence (16.9%) as compared to dry year (1985) has high frequency of occurrence (20.2%). Also in case of CP04 during wet year has high frequency of occurrence (16.34%)

and compared to dry year has low frequency of occurrence (3.27%). After observing the behaviour of CP12 and CP08 similar trend have been found. The high frequency of occurrence have been observed for CP12 in dry year (1985) while for CP08 in wet year (1994) as well the low frequency of occurrence for CP12 in wet year and for CP08 in dry year. The observation shows that CP06 and CP12 can be classified as dry CP-type while CP04 and CP08 as wet CP-types (refer Table 5.3).

Table 5.3 The mean occurrence frequency, rainfall probability, rainfall amount and wetness index for the period 1985-94 of 12 CP-types during monsoon season in Anas catchment

<i>CP-type</i>	<i>Frequency of occurrence [%]</i>	<i>of Rainfall probability [%]</i>	<i>Rainfall amount [mm]</i>	<i>Wetness index [-]</i>
CP01	13.10	19.8	13.63	0.196
CP02	4.10	40.3	43.89	0.403
CP03	11.90	44.7	28.65	0.446
CP04	4.20	54.7	22.74	0.545
CP05	12.20	10.6	10.21	0.106
CP06	10.30	21.7	13.50	0.216
CP07	9.80	28.1	11.44	0.280
CP08	2.40	41.1	15.42	0.408
CP09	9.90	20.8	15.48	0.208
CP10	5.80	35.9	20.27	0.360
CP 11	4.60	19.8	10.01	0.196
CP 12	7.40	37.8	12.82	0.377
CP13	4.50	20.6	14.87	0.206

### 5.6.3 Objective circulation pattern

The spatial distribution of mean pressure pattern anomalies for large scale 500hPa geopotential heights over Indian ocean further explains the phenomena of wet and dry CP-types responsible for rainfall and drought in the Anas catchment. The wet circulation pattern types (such as CP04 and CP08) which are the cause for major rainfall in the research area are influenced by high pressure over bay of Bengal and low pressure over Arabian sea. This forms a vortex kind effect over Indian sub-continent and thus responsible for the heavy monsoon rainfall. On the contrary the low pressure over bay of Bengal and high pressure over Arabian sea and south Plateau of China gave very little rainfall in the area. The high pressures in both the regions act as border to hinders the movement of clouds to the research area and on the land surface of Indian sub-continent as whole.

A comparison between 12 CP-types and 10 CP-types for wet and dry circulation patterns such as wet CP04 and CP03, and dry CP09 and CP07 for 12 CP-type and 10 CP-type

respectively shows a great coherence of pressure pattern distribution. The spatial distribution of circulation pattern for wet CP04 and dry CP09 are shown in figure 5.7 below.

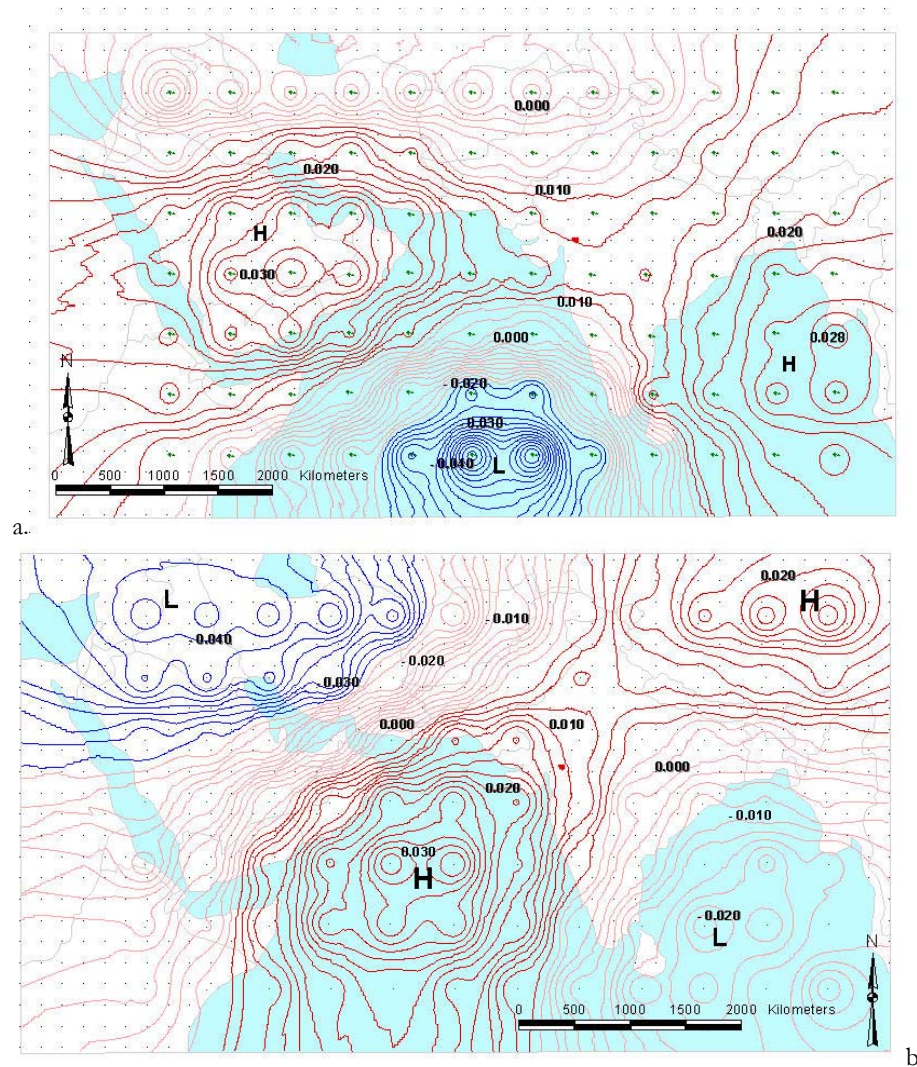


Figure 5.7 Spatial distribution of mean **500hPa geo-potential height anomalies** over selected atmospheric pressure window during 1985-94 for a) wet CP04 and b) dry CP09 for 12 CP-types. High pressure anomalies are shown in solid dark red lines while low pressure anomalies in solid blue lines.

#### 5.6.4 Observed and simulated rainfall

The mean seasonal frequencies and wet-day fraction for each CP-type has been calculated in section 5.6.1 above. It has been observed that some of the circulation-types appear seldom thus to make them statistically significant twelve similar CP-types have been regrouped into five major-groups based on their conditional average wet-day fraction and product factor (which is a function of conditional probability to mean probability and conditional rainfall amount to mean rainfall amount). The five major groups consist of wettest CPs (CP04, CP02

and CP08), wet CPs (CP03, CP13 and CP01), wet-dry CPs (CP07, CP10 and CP12), dry CPs (CP05, CP09) and driest CPs (CP11, CP06). The newly created major groups has been used to obtain statistical parameters such as auto-correlation coefficients and to generate the daily rainfall amount conditioned on each CP-type.

The temporal time series of daily rainfall for ten stations have been generated for a 10 year period between 1985-94 based on the multivariate random process. The statistics of monsoon season mean observed and simulated yearly rainfall totals for all the stations in Anas catchment are predicted as given in Table 5.4. The mean value shows a best compromise with an average error of 2.5%. The highest error has been calculated for Udaigarh (10.6%) and Jhabua (9.1%) while the lowest for Rama (1.2%) followed by Bhabhra (2.3%). In addition the results from statistical downscaling for predicting number of wet-days at each station have not been so promising as an average error of 24.6% have been calculated. For all the stations model always simulated more number of rainy days then as observed. This has been as high as 47.9% error for station Rama and lowest for Udaigarh with a error magnitude of 3.3% just keeping it very tight.

Table 5.4 Statistics of observed and simulated seasonal (June-October) rainfall totals for various stations (1985-94) in Anas catchment, India

Stations	Mean rainfall amount		Standard deviation		Number of wet days	
	Observed [mm]	Simulated [mm]	Observed [mm]	Simulated [mm]	Observed [No.]	Simulated [No.]
Jhabua	787.0	715.8	109.9	97.7	47.0	54.6
Ranapur	780.1	760.7	113.7	115.3	35.6	48.7
Udaigarh	817.3	729.8	98.2	99.9	52.0	53.7
Amba	852.3	873.9	129.9	120.1	39.2	55.3
Rama	934.3	922.8	127.5	110.0	39.4	58.3
Meghnagar	728.3	705.6	107.3	99.6	40.1	51.2
Thandla	881.1	844.1	116.5	115.6	48.3	55.7
Bhabhra	795.9	777.9	99.5	97.0	47.9	52.4
Sardarpur	769.2	775.4	93.2	79.5	38.7	51.9
Petlabad	1016.2	983.0	127.5	125.3	54.1	62.0

The long term time series of mean monthly rainfall totals for observed and simulated rainfall for stations Ranapur, Rama Meghnagar and Sardarpur shows good fit as shown in figure 5.5 below. The observed and simulated mean rainfall totals for other stations are given in annex 5.9. For most of the rainfall stations the difference between observed and simulated rainfall totals is under 15% limit except in October month where model was not found to have good fit. The monthly cycle of rainfall totals for observed and simulated rainfall data have been found to be highly correlated. The order of Pearson-type correlation vary between 0.99 for

station Amba and Meghnagar while 0.85 for station Petlabad. The correlation for other stations as depicted in table 5.5 and figure 5.9 vary between these threshold values.

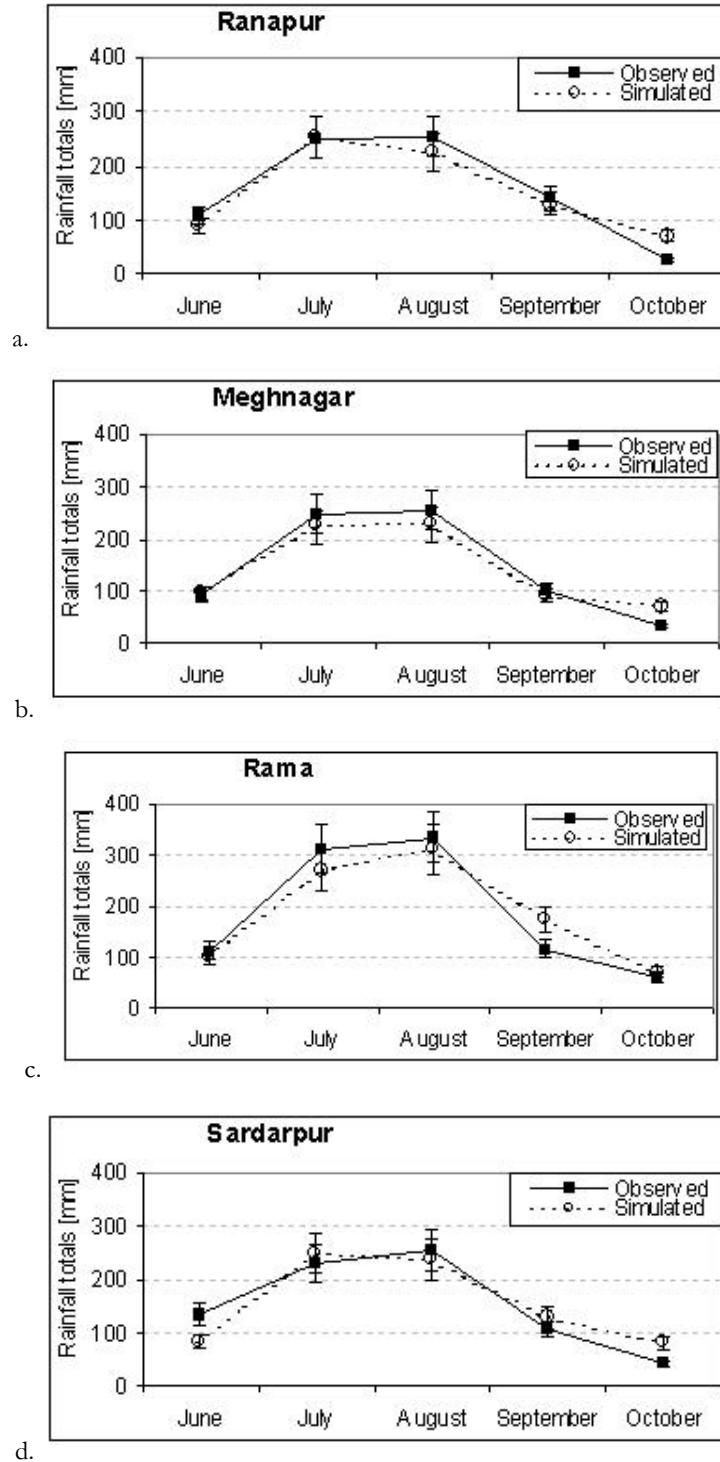


Figure 5.8 Mean monthly observed and simulated rainfall for selected stations in Anas catchment shows a good fit. The 15% error bars for mean rainfall at each month are also drawn for observed and simulated rainfall.

Table 5.5 Correlation between observed and simulated monthly rainfall totals

Station	Jhabua	Ranapur	Udaigarh	Amba	Rama
Correlation	0.94	0.96	0.88	0.99	0.96
Station	Meghnagar	Thandla	Bhabhra	Sardarpur	Petlabad
Correlation	0.99	0.96	0.98	0.91	0.85

A high spatial variability of rainfall totals between stations within Anas catchment have been found. This may be due to the fact that monsoon rains are produced by local convective system in semi-arid regions. The graph of monthly rainfall during monsoon season (June-October) both for observed and simulated series have been described in table 5.4 of this chapter. As the case with number of wet days in the season which are relatively over estimated for all the stations. The range wet-days over estimation varies between 1.7 days for Udaigarh and as high a 19 days for station Rama.

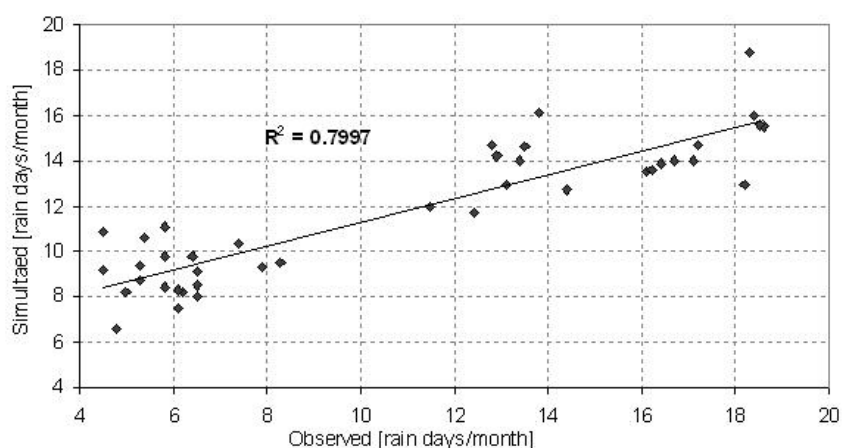


Figure 5.9 A comparison between **observed and simulated number of rain-days during monsoon season** of 1985-94

A detailed analysis for number rain-days in the monsoon season shows a higher co-relation coefficient of 0.80 between observed and simulated data (refer Figure 5.9). The monthly analysis as given in figure 5.10 shows mix degree of variability. For the month of July the number of rain-days found within the range of 2-3 days. A similar trend for all the stations have been observed for the month of August except one station showing higher variability.

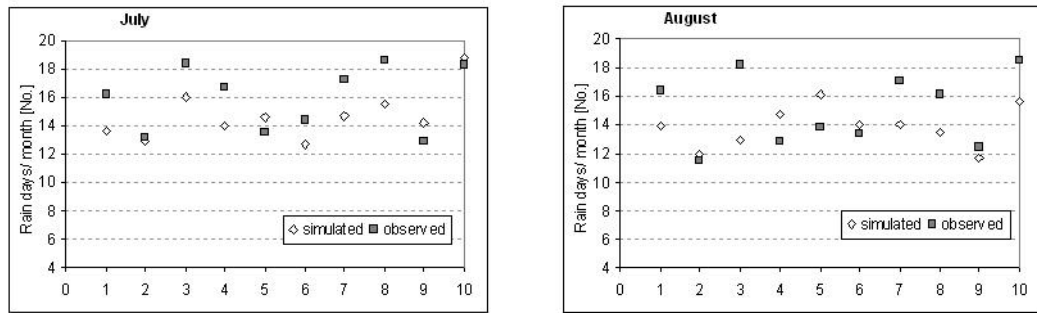
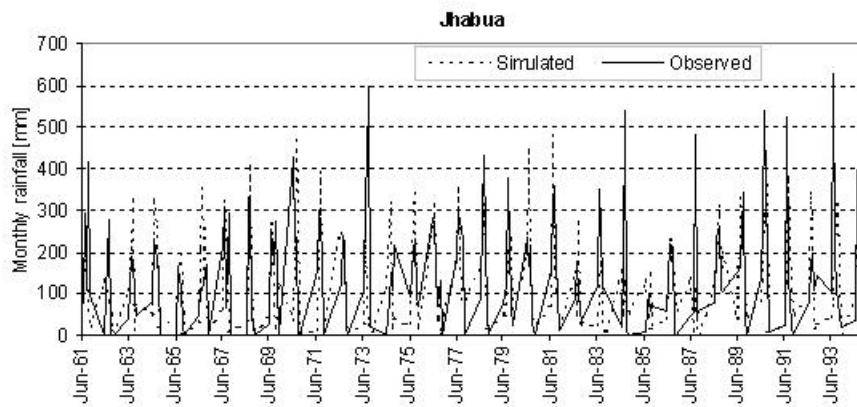


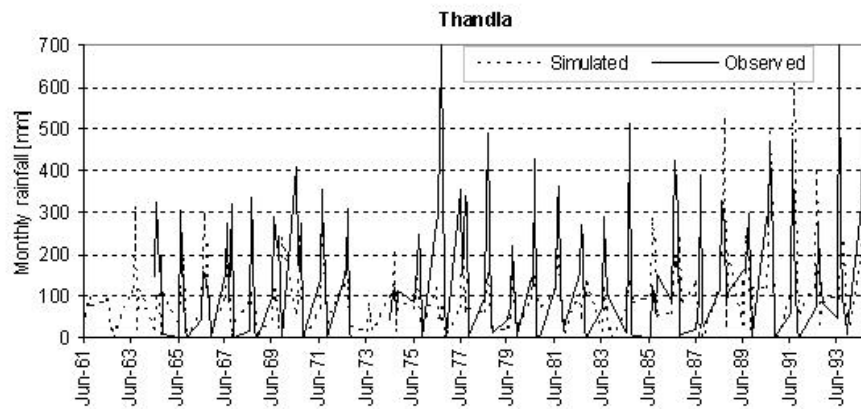
Figure 5.10 Observed and simulated **number of rain-days for all the stations** for the month of a) July and b) August during 1985-94

### 5.7 Prediction of Long Term Rainfall

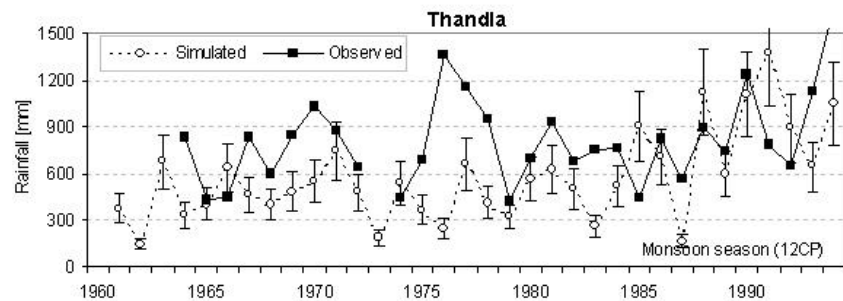
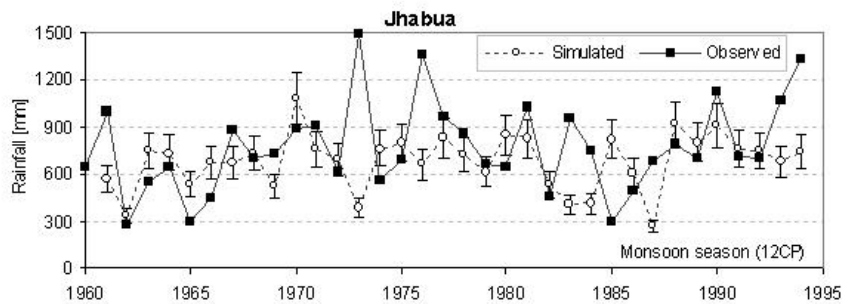
The model parameters obtained from 1985-94 daily rainfall time series have been used for predicting the long term monthly rainfall for a period 1961-94 during monsoon season. As the daily rainfall data from Jhabua and Thandla are available which can be used as an indicator of model performance. The rainfall time series thus generated for monthly data during monsoon season for a period of 1961-94 are listed in figure 5.11 below.



a.



b.  
Figure 5.11 Observed and simulated **monthly rainfall time series for 1961-94 for monsoon season** at station a) Jhabua and b) Thandla



a.  
b.  
Figure 5.11 **Simulated and observed monsoon season rainfall totals** for a.) Jhabua and b.) Thandla stations for a period between 1961-94

The overall correlation coefficient for observed and simulated monthly rainfall are calculated for station Jhabua and Thandla. A correlation coefficient of 0.40 for Jhabua and 0.32 for Thandla have been found which are not so bad given the stochastic nature of rainfall. In general model reproduced good fit in observed and simulated seasonal rainfall totals with a cross-correlation coefficient as high as than 0.90 for Jhabua during 1964, 1975, 1978 and for Thandla during 1966, 1971, 1978, 1979, 1981 years. Poor fit in observed and simulated rainfall totals were also discovered which have been limited to few years 1962, 1974, 1993 for Jhabua and 1964, 1977, 1993 for Thandla station. Except for few outliers total seasonal



rainfall amount found to be in the range of 25% seasonal variability. As a rule model gave relatively consistent results and could simulate the sinusoidal pattern of yearly rainfall variability with relatively small degree of certainty.

The analysis of mass-curve for monsoon season rainfall for observed and simulated values have not revealed any consistent changes in the precipitation series during last 40-years at station Jhabua. The linear trend analysis for observed and simulated rainfall found to be consistent and related through out the prediction period.

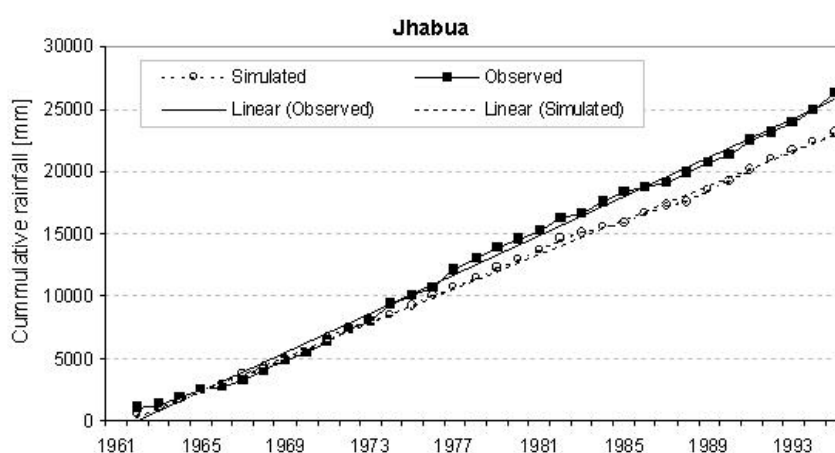


Figure 5.12 Mass curve for observed and simulated seasonal rainfall at station Jhabua

## 5.8 Results and Discussions

This research work demonstrates the benefit of using statistical downscaling model for rainfall prediction based on daily atmospheric circulation pattern in a semi-arid region of India. The model calibration parameters have been obtained from a daily rainfall time series just limited for a 10-years period between 1985-94. The period of analysis has been restricted due to availability of daily data both for the geo-potential height as well as the station rainfall data.

A conditional weather generator in which rainfall occurrence is conditional on the CP-type of each day and daily sequence of CP-type is modelled as fuzzy-rule based process, is used to simulate the number of rainy days for all the stations. The model has overestimated the total

number of rainy days for each station. So it is difficult to compare the future changes in rainy days frequency and occurrence which may be an indication of climate change impact. The distinct pattern of rainfall emerged from correlating CP-type with station rainfall amount. In arid and semi-arid regions of the world since most of the wet-days falls during monsoon (June-October) season thus the downscale modelling exercise is done for one season only. Some of the CP-types are combined and re-grouped in order to calculate rainfall occurrence and amount to make them statistical significant as few of them may show very low rainfall probability of occurrence.

Transferability of model parameters obtained from 1985-94 circulation pattern and rainfall time series has seen to be associated with larger uncertainty due to extreme high inter-annual variability and lower percentage of rainy intervals. Mean seasonal rainfall totals found to be an appropriate measure to cross-correlate the observed and simulated time series for model performance assessment. It can be stated that rainfall downscaling model has been successful for circulation pattern type classification and rainfall generation based on 500hPa geopotential height. In short model gave sound explanation for development of monsoon system and its dependence on wet and dry periods in Anas catchment. The future potential of the model is to test additional predictors such as sea surface temperature (SST) or air flow indices for rainfall generation. Thus the model performance can be compared by using distinct predictors and improving the rainfall prediction accuracy range.

The extension of point station rainfall statistics to unobserved points by using external-drift-Kriging (Ahmed and de Marsily 1987 as quoted in Bardossy et al. 2001) for downscaling model is one of the important advantage of the downscaling model used here. Thus the simulated rainfall results can be of direct interest for hydrological modelling and hydrological process identification during the years where data has been unavailable.

Hydrological extremes such as drought or flood are not properly addressed by the time scale of monthly or seasonal data. There is an urgent need for inter-comparison of different downscaling methods for hydrological models. Further, there is need for high quality meta-data since realistic hydrological scenarios and forecasting are based on meteorological data. A wide interest in the El-Nino and La-Nino implies that day to day decisions are influenced by seasonal climate outlook but the progress in systematic predictability and quantification is

limited to few regions (Goddard et al 2003). This research work is an interesting initiative for prediction in un-gauged or poorly gauged catchment. Generally decision support system studies have concentrated mainly on ecological and socio-economic impacts with little work on system modelling.

In future research will focus on coupling the statistical rainfall downscaling prediction model to distributed hydrological model as seen in chapter 6 for forecasting the runoff generation and future water availability in various sub-catchments of Anas catchment. The relevance of such model becomes very important for impact assessment of climate change on water resources availability as well as planning the water resources development measures.



## **6. RUNOFF MODELLING FOR PREDICTION IN UN-GAUGED CATCHMENTS**

Drainage basins in many parts of the world are un-gauged or poorly gauged and in some cases the existing measurement network are declining (Sivapalan 2003). In many river basins, the increased human activities have disturbed not only the hydrological regime but also threatened the sensitivity to flood and drought and natural ecology at large. Thus hydrological modelling, identification of model parameters, model sensitivity analysis and water resources impact assessment in un-gauged catchments remain to be an important issues. The recent decadal (2003-2012) initiative by International Association of Hydrological Sciences (IAHS) towards achieving major advances, to make prediction in un-gauged or poorly gauged basins become vibrant issue. This research work is an attempting to answer some of the interesting questions on modelling needs, model type, model parameters, application of modern technologies, predictive uncertainty of model, effect of input parameters variability and up-scaling for model validation will be discussed in this chapter.

Hydrological models have been developed to improve our knowledge for understanding the rainfall-runoff generation process and water availability within a complex watershed where data availability is limited. In recent years the advances in geographical information system (GIS) and remote sensing have opened many opportunities for enhancing hydrological modelling and decision support for catchment systems. During early 1990's most of the hydrological models used the lumped parameter approach in modelling the discharge from a catchment or part of it. In late 1990's the quality of hydrological models improved significantly by incorporating spatial characteristics of catchment in modelling process. Singh (1995) classified watershed models into three categories based on process, scale and solution.

- a) Process based classification: There may be two types of models based on process description such as lumped models includes HEC-HMS (Hydrologic Engineering

Centre 2000) and Tank model (Sugawara 1995), and distributed models such as SHE model (Abbott et. al 1986) and SLURP model (Kite 1995).

- b) Scale based classification: The scale based model can be distributed event based models such as GAWSER (Ghate et. al 1977) and ZIN (Lange et al. 1999), and continuous models such as HBV model (Bergstrom 1992) and PRMS ( Leavesley et al. 1995).
- c) Solution technique based classification: The solution based model can be numerical or analytical models and vary from finite element to boundary element and mixed types. The model in this category is GRAM++ (CSRE 2001) developed at Indian Institute of Technology Bombay.

Lumped parameter models integrate watershed characteristics over a given area, means spatial variations are averaged, thus resulting in simplified runoff conditions (Molnar et al. 2000). In addition the problem with using measured parameter values for the physically based model is that the scales at which models are performed are typically too small to enable incorporation of spatial variability into the models (Dunne 1982, James & Berger 1982, Beven 1983).

Distributed parameter models represent the variability in physical watershed characteristics in a different way than lumped parameter. The use of distributed models is complicated by the need to establish an appropriate scale to be used for watershed characterisation (Molnar et al. 2000) such as topography, drainage condition, geomorphology, transmission losses, surface water storage and rainfall pattern. Geographical information system (GIS) provide an unique environment that increases the potential for describing spatial variability.

In past few decades have seen increasing interest in arid and semi-arid hydrology which cover nearly 50% of the worlds land and 20% population (UNEP 1992). Despite increasing interest some of our understanding on dry land hydrological process is derived from humid regions and then transferred to dry land settings (Nanson et al. 2002). Thus a fresh look on runoff generation process and appropriate models for semi-arid regions are immediate need of this hour. It should be kept in mind that flexible tools are required which can cope with limited input data and extract maximum information out of available data type (Lange and Singh 2003). Many studies on runoff generation in semi-arid catchments have demonstrated the

complexity of the controlling processes and non-linear dependency on the antecedent wetness. Nicolau et al. (1996) have conducted field experiments in the Almeria Spain and found that threshold of storm rainfall with a particular rainfall may yield very wide range of runoff coefficients. This complex variability is a function of antecedent wetness, storm duration and the pattern of rainfall intensities (Beven 2002). Figure 6.1 below shows the strong non-linearity in the hydrological response measured for field plots at L'Avic (52 ha) and La Teula (39 ha) in Spain.

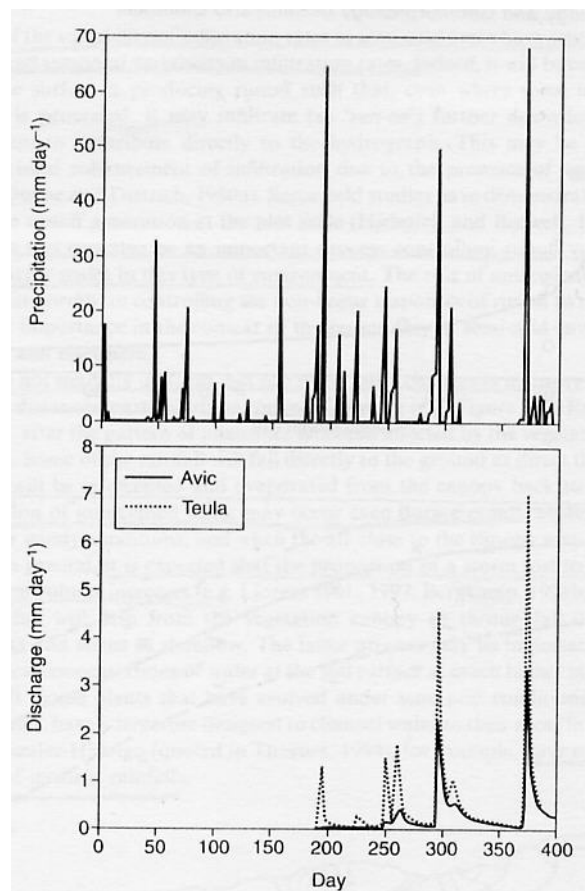


Figure 6.1 Rainfall and runoff in the L'Avic and La Teula catchments in Spain (adopted from Pinol et al. 1997 as referred in Beven 2002)

For runoff generation process in semi-arid catchment Lane (1982) developed a simplified conceptual rainfall-runoff model approximating the runoff response by runoff volume, transmission losses, peak rate and duration of flow. Sharma and Murthy (1995) used a flow-routing technique in arid ephemeral channels of Luni river basin, India. Sharma et al. (1996) incorporated remotely sensed data into a GIS based rainfall-runoff model for a small arid catchment in India. Lange et al. (1999) has developed a distributed non-calibrated rainfall-

runoff model for the 1400 km<sup>2</sup> arid catchment of Nahan Zin, Israel. The model simulates only the two major processes, namely runoff generation on the terrain and transmission losses into dry channel alluvium.

### **6.1 Modelling with the ZIN Model**

The distributed physically-based non-calibrated ZIN model developed (Lange et al. 1999) for event oriented rainfall-runoff modelling for a large arid catchment in Israel. Model uses spatially distributed sub-catchments determined by topographical analysis and digital elevation model. The model parameters are obtained through GIS database analysis and field measurements. The typical spatial units for different parameter groups include runoff generation based on terrain types, runoff concentration based on mean response function of tributary catchments, channel routing and transmission losses based on channel segments are estimated. The ZIN is distributed model in the sense that catchment can be sub-divided into smaller geographical segments in order to account for the variability of hydrological behaviour. In addition it is a process based model that all water fluxes represented in the model are assigned from field based hydrological processes. Figure 6.2 provides the schematic representation of the ZIN model and its hierarchical structure at spatial scale.

In addition the model uses a catchment with a grid of rainfall intensities interpolated from a network of rain-gauge stations in and around the catchment. The original model code of ZIN catchment has been modified in a joint-effort for the Anas catchment (Lange & Singh 2003) to incorporate the effect of cloud velocity and movement, the effect of reservoir storage and transmission losses and later for this research study the effect of runoff coefficients derived using Landsat 7ETM+ remote sensing data. The model is “field based” since not a single parameter has been forced to fit by calibration with measured discharge (Lange 1999). This methodology makes it very much suitable for runoff prediction in un-gauged catchments or catchment with limited data without model calibration.

Rainfall patterns over each of the sub-catchments were determined for each event separately using the AML sub-routines written for Arc-Grid and then distributing at sub-catchment level. Parameters controlling initial losses, runoff configuration, channel routing and



transmission losses were suitably identified. The Calibration of ZIN model was limited by the general lack of accurate stream-flow data. The selected rainfall events each for small, medium and large sizes were considered in order to understand the rainfall-runoff mechanism. The effect of cloud velocity from satellite data, infiltration for terrain types and wetting front for channel sections were simulated to understand the discharge mechanisms. A detailed model structure for ZIN model has been described in figure 6.2 above.

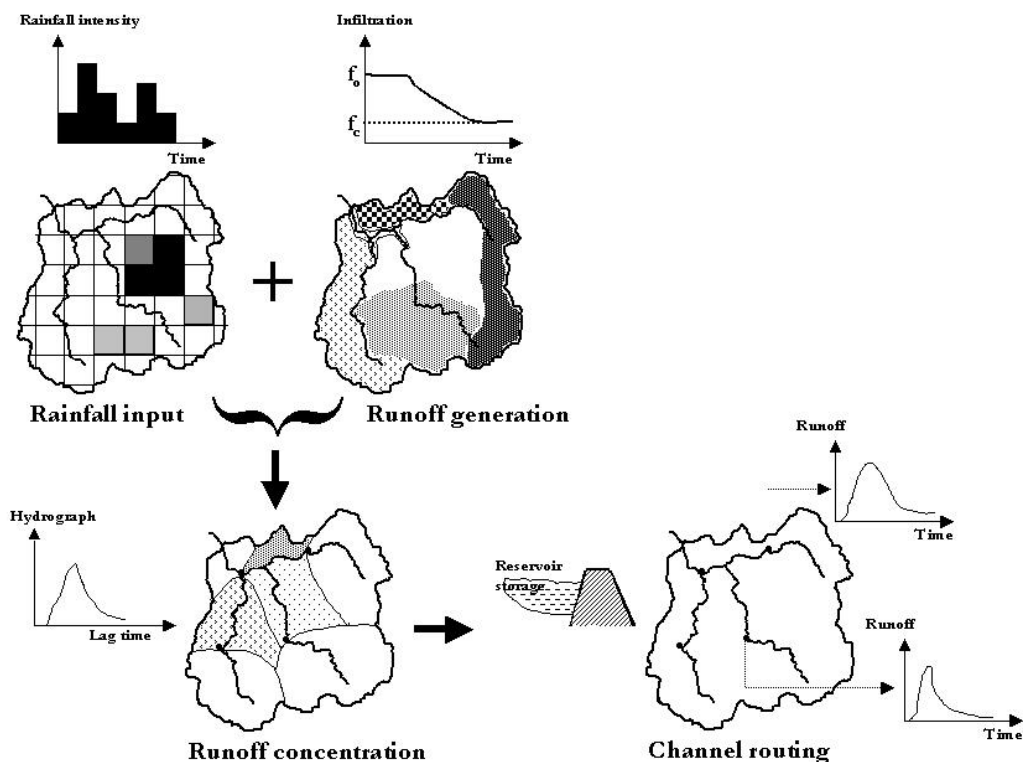


Figure 6.2 The schematic representation of ZIN model (modified Lange 1999), spatial sub-division and hydrological process

### 6.1.1 Development of catchment database

A digital elevation model at 50m cell size has been developed for the Anas catchment, details are given under section 3.6 of chapter 3. The spatial extent of river bed alluvium was digitised from the topographical maps of 1:50 000 scale in Arc/Info (see Figure 6.3). The river bed alluvium is considered as main morphological units for runoff process modelling. The map units have been transformed in a Universal Transverse Mercator (UTM) coordinate system which is described in chapter 3 of this research report.

### 6.1.2 Rainfall parameter

The sub-catchments are delineated from topographic maps at 1:50 000 scale which are assigned with an unique segment number. The catchment rainfall is measured from 10 rainfall stations located uniformly across the Anas catchment. The distribution of daily rainfall at 50m cell size for several segments is calculated using an inverse distance weighting (IDW) method based on station rainfall data. A special Arc Macro Language (AML) subroutine program written for Arc-Grid has been used to calculate rainfall for each sub-catchment. The process is described in the following steps:

- Step 1: Interpolate the station rainfall using inverse distance weighting method at grid with 50m x 50m cell size.
- Step 2: Overlay the rainfall grid over the sub-catchment grid having same spatial extent and cell size.
- Step 3: Calculate the sum over the zones for both the grids after overlaying the sub-catchment grid and combine the rainfall for each sub-catchment.

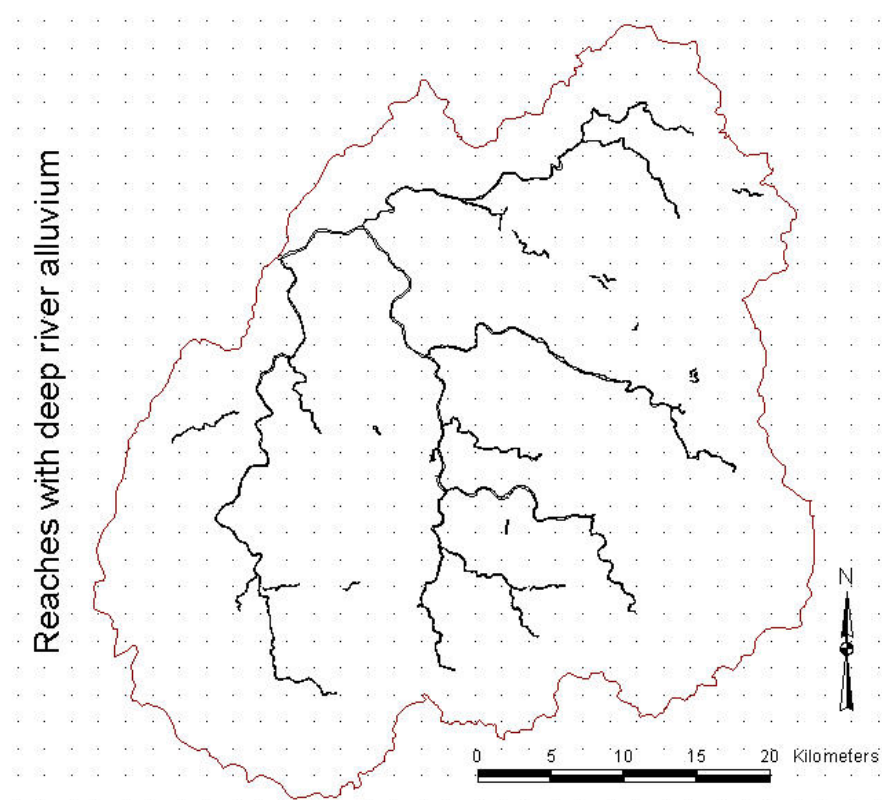


Figure 6.3 Spatial locations of reaches with deep river alluvium

Figure 6.4 shows the spatial distribution of rainfall volume [in litres/m<sup>2</sup>] over 50m raster cell for a rainfall event of 02.08.1994. The average rainfall volume for 50m raster cell has been 228500 litres/m<sup>2</sup> with minimum and maximum varying between 8184 litres/m<sup>2</sup> and 1535057 litres/m<sup>2</sup> respectively. The histogram analysis of rainfall classes shows that almost 50% belong to rainfall class one (8000 to 153600 litres/m<sup>2</sup>), 28% to rainfall class two (153600 to 307100 litres/m), 12% to rainfall class three (307100 to 460600 litres/m) and the other 10% to higher classes. A skew-ness coefficient for rainfall class variability of 2.43 has been calculated for the 02.08.1994 event. Similarly the rainfall distribution for other events such as 06.09.1994 and 07.09.1994 were also calculated. A typical rainfall intensity at a 5 minute interval was considered for discharge forecasting.

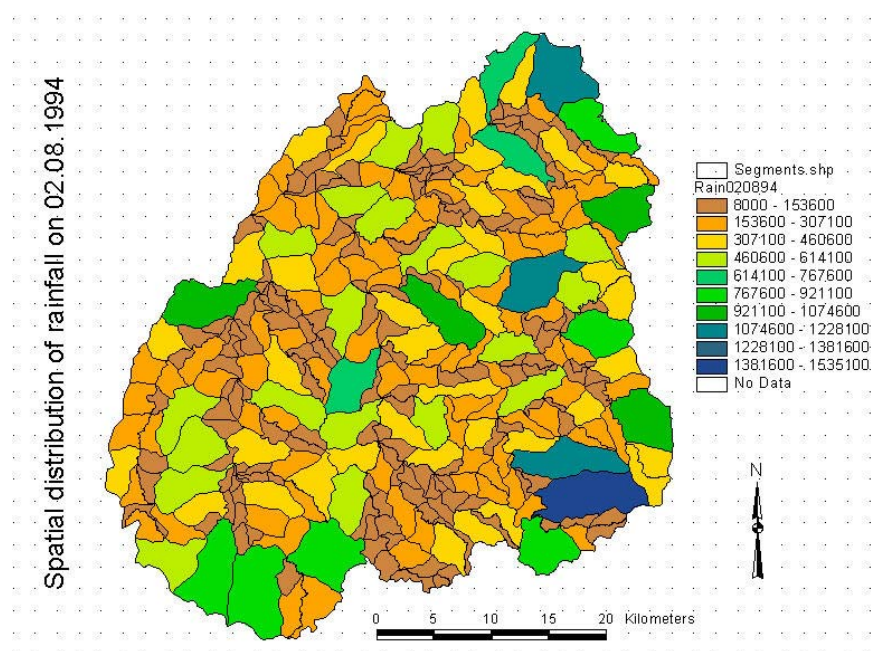


Figure 6.4 Spatial **distribution of rainfall volume** for 02.08.1994 event

The Anas catchment may be considered as an un-gauged catchment since not a single storm hydrographs has been measured directly at field. An alternative method of cloud movement captured from a sequence of satellite photographs has been used for local downscaling. A set of INSAT satellite imagery covering Central India (15°N 65°E to 25°N 110°E) for the year 1994 has been chosen on a day to day basis for quantification of cloud movement and calculation of cloud velocity. The evolution and movement of all the low pressure systems which appeared in satellite photographs as cloud clusters have been taken up for possible input in ZIN model using Hovmoller diagram (Sasidharan and Shukla 1994).

The Dvorak technique of locating a cloud system centre has been adopted by Sasidharan and Shukla (1999) for preparation of Hovmoller diagrams. The technique is based on the principle using enhanced visible or infra-red imagery to quantitatively estimate the intensity of a tropical system. The cloud pattern in satellite imagery normally shows an indication of cyclonic genesis before the storm reaches tropical storm intensity. Indications of development or weakening can also be found in the cloud features which refers to the intensity of rainfall falling over the catchment (refer Figure 6.5). This information is then standardised into an intensity code of rainfall (Dvorak 1984).

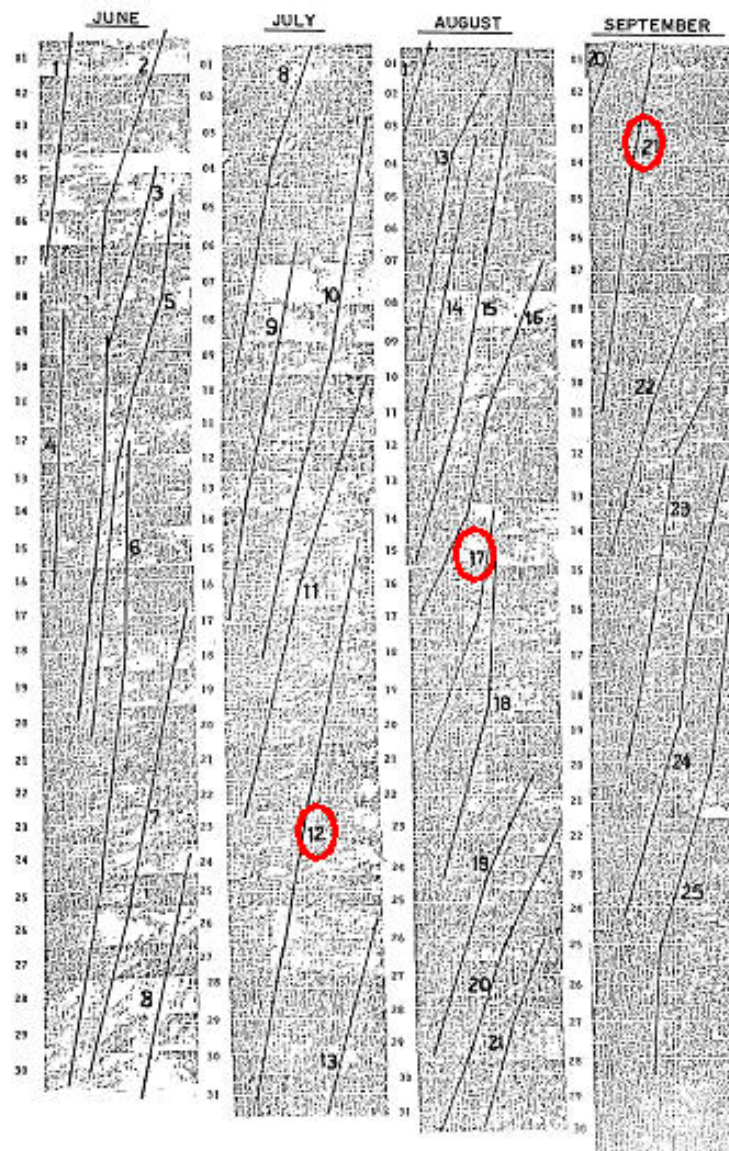


Figure 6.5 Hovmoller diagram derived from INSAT satellite images for 1994 monsoon season (Source: after Sasidharan and Shukla 1999)

Sasidharan and Shukla (1999) have analysed 14 different rainfall systems on a daily basis including 1 cyclonic storm and 1 depression during the period from 1<sup>st</sup> June to 30<sup>th</sup> September 1994. Figure 6.5 shows the cloud cluster movements associated with low pressures. The daily mean cloud movement calculated for various storms during 1994 monsoon season for ZIN model is given in Figure 6.6.

The movement of monsoon and cloud velocity differs daily which may effect the spatial extent of rainfall over the given catchment and time lag function for runoff generation process. It has been very useful to calibrate the station rainfall for understanding the rainfall-runoff process. The parameters of cloud movement for the Anas catchment have been found in the range of 1.75 m/s to 7.00 m/s. For the individual rain-storms events of 02.08.1994, 20.08.1994 and 07.09.1994 the velocity of cloud movement has been taken as 1.75 m/s, 7.00 m/s and 3.75 m/s respectively. This affects the runoff generation and runoff formation process within the channel network and contribution from various sub-catchment segments.

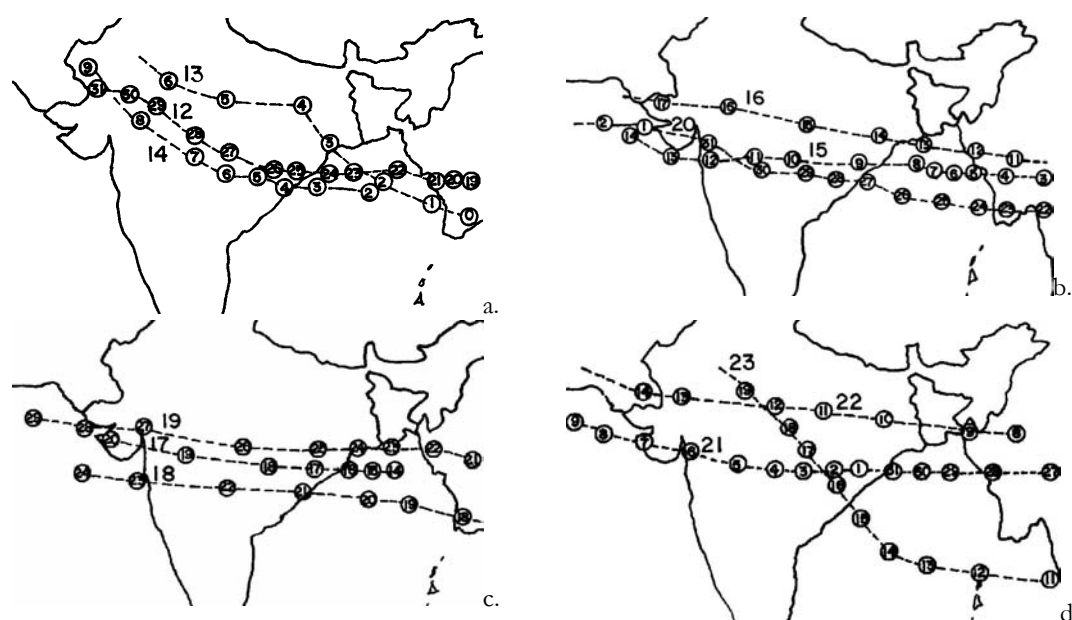


Figure 6.6 Movement of cloud from derived from INSAT cloud images a) for 02.08.1994, b) for 10.08.1994, c) for 20.08.1994 and for d) 07.09.1994 (Source: after Sasidharan and Shukla 1999)

### 6.1.3 Runoff generation parameters

There are three main possibilities of runoff generation for hill-slope hydrology, namely Horton overland flow, saturation overland flow and saturated flow through. Dunne (1978)

has surveyed the response of catchments size to hill-slope flow processes with lag time and peak-runoff rate for identification of runoff generation parameters. Thus the flow may be dominated by any one of several processes as shown in figure 6.7.

For each type of flow there is progressive change in response with the size of catchment area. The time to peak [hr] increases and peak runoff rate [mm/hr] decreases as catchment area become larger. It is clear that where peak flows are the main objective of forecasting, even a small amount of overland flow is able to dominate the hydrograph peak, so the models should be biased towards accurate assessment of overland flow occurrence (Dunne 1978) as the case with arid and semi-arid catchments.

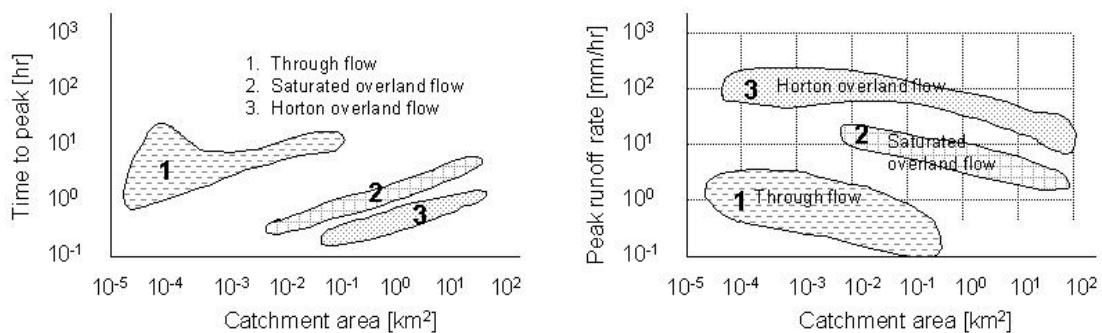


Figure 6.7 Response of catchment to **hill-slope flow process** (a) lag times and (b) peak runoff rates (Source: modified after Dunne 1978)

Furthermore, an analysis of rainfall intensity-duration-frequency relationships related to measured infiltration suggests that the infiltration excess runoff generation in semi-arid areas must be an important source of runoff (Kirkby 1978). Thus it is clear that the dominant process of runoff generation in semi-arid hydro-climate is Hortonian overland flow which is based on Horton's infiltration theory. It is based on the concept that when the initial infiltration rate is exceeded by accumulated rainfall the surface runoff generation process takes place. It had been agreed within the research community that Horton's infiltration theory is the dominant process for flood generation in arid and semi-arid catchments. In such climatic zones the groundwater tables are most often deep and the chances of direct infiltration may attribute to channel alluviums. Almost no sub-surface flow between soil mass and channel takes place due to limited soil depth and soil conductivity (Manning 1997). Even the time lag between sub-surface flow and surface flow are negligible as compared to time of concentration. A sketch of runoff generation and runoff formation for semi-arid climatic zone has been shows in Figure 6.8 below.

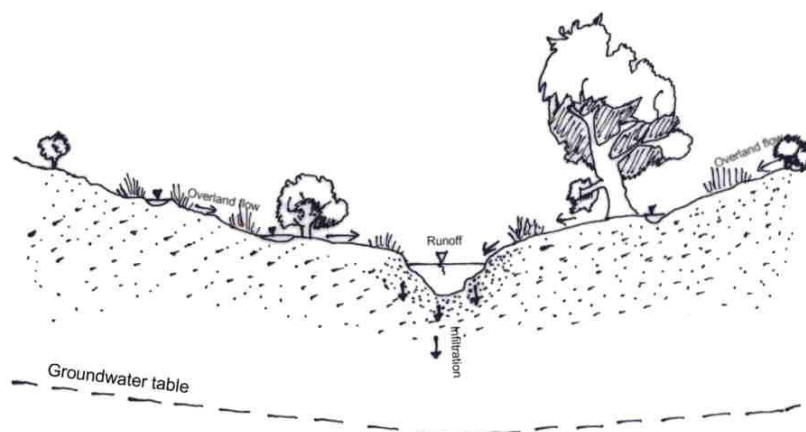


Figure 6.8 A sketch of **runoff generation process** (overland flow, infiltration) and bank-full storage in main channel with deep groundwater table (Source: modified Manning 1997)

Remote sensing imageries and the digital elevation model found to be a useful tool to study the hydrological characteristics and runoff generation process for a catchment having limited field data. Since not much information on infiltration rates for various terrain types in the Anas catchment are available alternative methods for runoff generation parameters have to be explored. In early models by Ross et al. (1979) soil type and land use parameters for overland flow routing using one-dimension kinematic wave model were considered. Kite and Kouwen (1992) described land-use characteristics such as grassland and forest for catchment differentiation. Flugel (1995) incorporated surface morphology, topography, soil and land-use parameters for runoff generation in the Brol catchment of Germany. Lange et al. (1999) have taken field experiment data for determination of initial loss and infiltration rate in Israel. Kottegods et al. (2000) took the curve number technique based on land-cover for calculation of infiltration for Arzino, Argentina and Tevere basins in Italy. Multiple-parameter landscape zones are used by Wooldridge and Kalma (2001) for developing a quasi-distributed water balance model in Australia.

A detailed land-use data classified from Landsat7ETM+ has been used as model parameters for the definition of terrain types and quantification of runoff coefficients for each sub-catchment. Seven major land-use classes such as forest, agriculture, range land, barren land, river and water bodies are obtained for each sub-catchment. The land-use class results are thus shown in section 4.6.9 of chapter 4. The data analysis and query building of land-use is undertaken using Microsoft ACCESS database system (refer chapter 3 section 3.6.2). The

model parameters for various terrain types are calculated based on land-use and slope analysis of each sub-catchment.

#### 6.1.4 Runoff concentration parameters

The channel network is divided into segments which are adjoined by small sub-catchments delineated according to catchment topography. Catchment wide information on the rainfall amount and runoff generation is distributed to various sub-watersheds. The lateral runoff flow from the model elements to the channel segments is considered as runoff concentration (Lange 1999). Figure 6.9 displays the general approach for the discretisation of an arbitrary catchment using catchment topography, stream network and channel nodes.

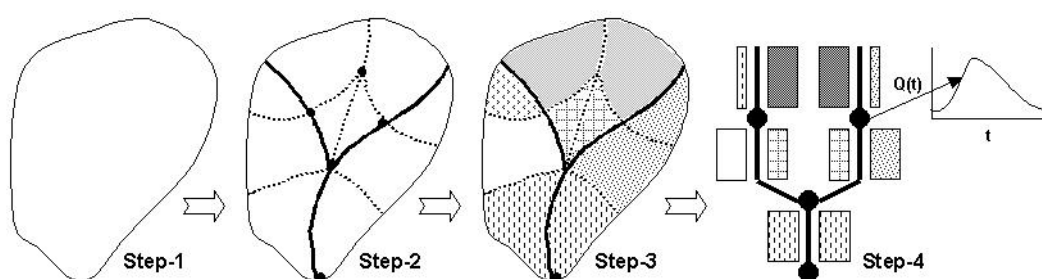


Figure 6.9 Discretisation scheme for **application of distributed model**. step1- catchment delineation, step 2- river network and channel nodes, step 3- allocation of sub-catchment based input data, step 4- connecting sub-catchment parameters to model (source: modified after Bogena 2001)

The similar scheme has been applied for delineation of spatial units for runoff concentration according to topography in the Anas catchment. The topographical maps at 1:50000 scale obtained from Survey of India have been used for this purpose. The model parameters such as sub-catchment area, flow path length, mean slope and area under alluvium were calculated for each sub-catchment or segment.

The entire Anas catchment has been divided into 330 sub-catchments, 144 nodes and 165 segments. Thus each sub-catchment has mean geographical area of 5.3 km<sup>2</sup> of size. The hydrological time lag response function derived by triangulated unit hydrograph for the Luni basin in arid-zone of India has been considered for the analysis (Sharma 1997). Figure 6.10 shows the location of nodes and spatial sub-division of the Anas catchment.



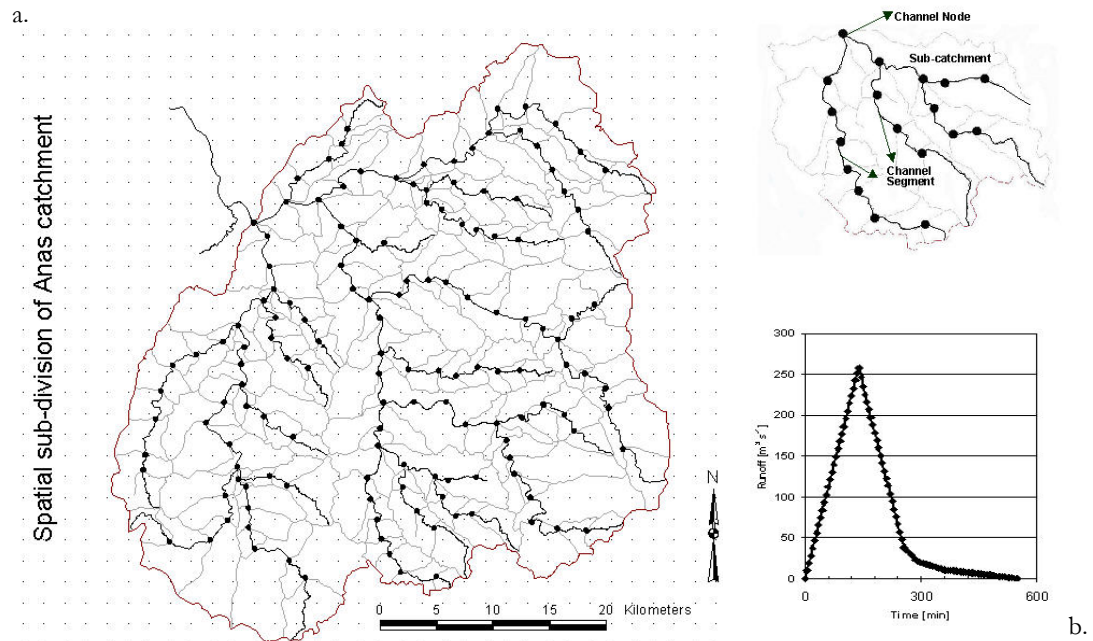


Figure 6.10 a.) Spatial sub-division of Anas catchment and b.) hydrological time-lag response function (Source: after Sharma, 1997)

For the determination of time step between channel nodes, the foremost condition is that the model should be stable. The stability of the model will depend on the way that the non-linear equations are linearised to obtain the solution at each time step which in turn be related to the spacing between nodes (Beven 1985). Approximate stability criteria for explicit scheme may use Saint-Venant equation for open channel flow which can be expressed in terms:

$$\Delta t \leq \Delta x / v_k \dots\dots\dots (6.1)$$

where  $\Delta x$  and  $\Delta t$  are the space and time step respectively,  $v_k$  is the kinematic wave celerity. It should be clear that the explicit scheme uses values of the coefficients and variables at the beginning of the time step to predict values of the dependent variables at the end of the time step.

In the case of Anas catchment model application a 5 minutes time step and a mean flow velocity of 3.5 m/s derived from INSAT satellite data (Sasidharan and Shulka 1994) has been used. The mean length of channel segments was about 3005 m which is greater than 1050m a space step derived from Saint-Venant equation for runoff concentration. The mean area of runoff generating sub-catchments found to be of 5.2 km<sup>2</sup> with lower and upper quartile ranging between 2.2 km<sup>2</sup> and 6.5 km<sup>2</sup> respectively. Since not much information on mean

response function or runoff hydrograph for sub-catchments in Anas catchment is available. A mean response function developed by Sharma (1997) for Luni catchment in Rajasthan India has been used for runoff concentration analysis in Anas catchment. This is a typical example of the application of model parameters for runoff prediction in un-gauged catchments.

6.1.5 Channel routing parameters

Channel routing is a mathematical model to predict the changing magnitude of flood wave as it propagates through reservoirs and river channels (Fread 1985). The basic channel routing model used in ZIN model has been based on Muskingum-Cunge technique applicable to single inflow routing and applying a modified three point variable parameter method (MVPMC3). Figure 6.11 below illustrates the linear form of kinematic wave propagation equation and the concept used for model development in Anas catchment in India.

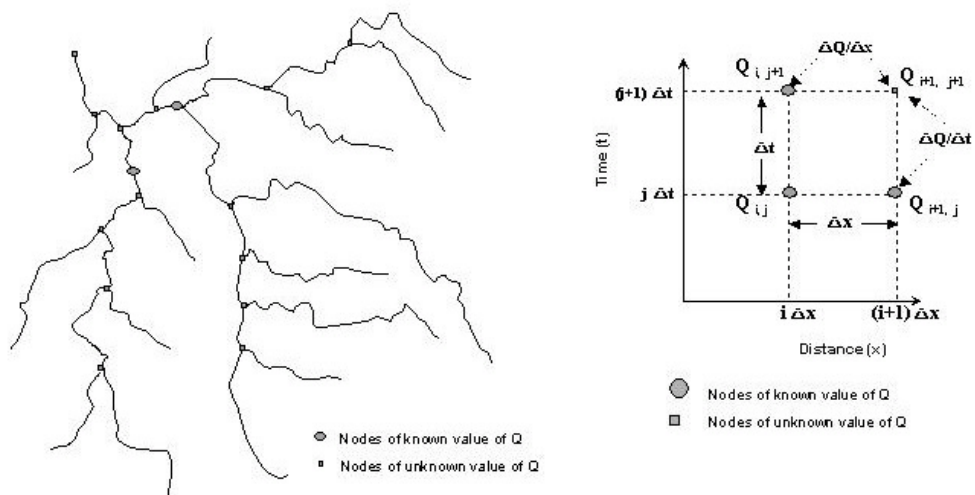


Figure 6.11 Illustration of **distributed flow routing model** using Muskingum-Cunge method

For a small routing interval  $\Delta t$ , let us assume that  $Q_{i,j}$  is the discharge at point  $i.\Delta x, j.\Delta t$ ;  $Q_{i+1,j}$  at point  $(i + 1)\Delta x, j.\Delta t$  and  $Q_{i,j+1}$  at point  $i\Delta x, (j + 1).\Delta t$ . Thus the relationship between inflow and outflow at point  $(i + 1).\Delta x, (j + 1).\Delta t$  can be written as:

$$Q_{i+1,j+1} = C_1 Q_{i,j+1} + C_2 Q_{i,j} + C_3 Q_{i+1,j} \dots\dots\dots (6.2)$$

where

$$C_1 = \frac{\Delta t - 2KX}{2K(1 - X) + \Delta t} \dots\dots\dots (6.3)$$

$$C_2 = \frac{\Delta t + 2KX}{2K(1 - X) + \Delta t} \dots\dots\dots (6.4)$$

$$C_3 = \frac{2K(1 - X) - \Delta t}{2K(1 - X) + \Delta t} \dots\dots\dots (6.5)$$

The term  $K$  is a storage constant having dimensions of time and  $X$  is a weighting factor expressing relative importance inflow and outflow have on storage. Note that sum of coefficients  $C_1 + C_2 + C_3 = 1$  should be unity. Cunge (1969) recommended following equation for an approximate solution of a modified diffusion equation.

$$K = \frac{\Delta x}{c_k} \dots\dots\dots (6.6)$$

$$X = 0.5 \left( 1 - \frac{Q_{ref}}{BC_k S_0 \Delta x} \right) \dots\dots\dots (6.7)$$

$$C_k = \beta \cdot (R^{2/3} S_0^{1/2} / n) \dots\dots\dots (6.8)$$

where  $\Delta x$  is distance step,  $c_k$  is kinematic wave celerity corresponding to reference discharge ( $Q_{ref}$ ),  $B$  width of water surface and  $S_0$  energy slope. For numerical stability it is required that  $0 \leq X \leq 0.5$  and  $\beta$  may have values in the range  $1 < \beta \leq 5 / 3$ . For wide channels where hydraulic radius approaches the flow depth the highest value of  $\beta$  ( $5/3$ ) is considered. The terms  $R$  and  $n$  are hydraulic radius and Manning's roughness coefficient respectively.

A non-linear modified three-point variable parameter method (MVPMC3) suggested by Ponce and Chaganti (1994) is applied for the Anas catchment. In the MVPMC3 method the routing parameters  $K$  and  $X$  for each computation cell are based on the average unit-width discharge at three know grid points:

$$Q_{ref} = (Q_{i,j} + Q_{i,j-1} + Q_{i+1,j-1}) / 3 \dots\dots\dots (6.9)$$

The kinematic wave celerity ( $c_k$ ) is calculated with equation 6.8 while the discharge is computed with equation 6.9. The physical geometry of the channel is represented by approximating wetted perimeter (see Figure 6.12) and thus calculating part of transmission

losses by multiplying constant infiltration rate within channel section. Surface water storage in the small reservoirs is also added in revised model code to obtain gross transmission losses. The following channel parameters such as channel length [m], percentage covered by inner channel [%], channel width [m], bank-full stage [m], infiltration rate [mm/m] for inner channel, width and depth of the active alluvium [m] are selected.

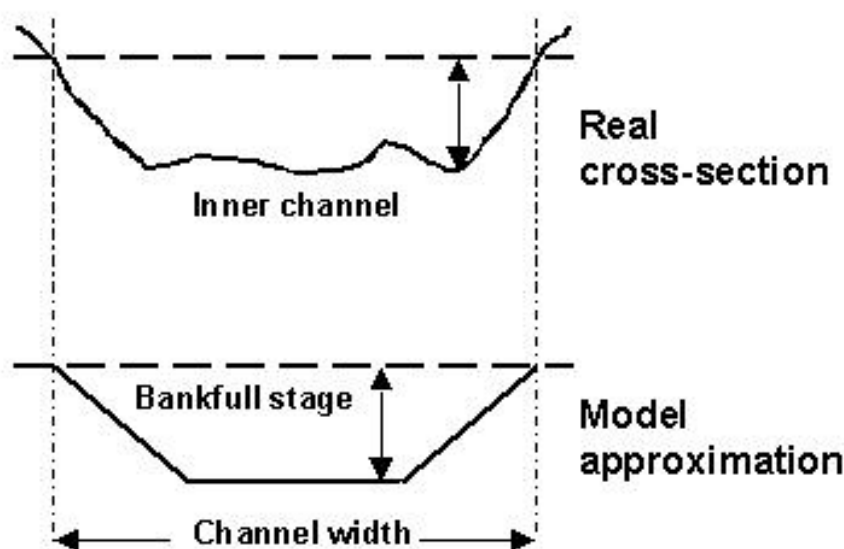


Fig. 6.12 A simplified representation of cross-section geometry

The channel parameters such as flow length, mean slope and alluvium storage are derived from topographic maps using GIS. Satellite images from Landsat have been used to derive channel width after making selected field measurements for the entire catchment (see figure 6.13). The total parameters are reduced to six channel types were considered depending upon channel width, bank-full stage, wetted perimeter and percentage of alluvium. The infiltration losses to the channel bed and banks are known as transmission losses. The form and structure of ephemeral stream channels are related to the rates and amount of stream flow experienced by following infrequent rainfall events. Given the semi-arid conditions of the Anas catchment it may be assumed that recharge of the alluvium aquifers could be approximated by transmission losses arising from infiltration throughout the stream reaches. Since limited information on channel type and infiltration characteristics for Anas catchment are available, a uniform infiltration coefficient for the all channel types has been considered.

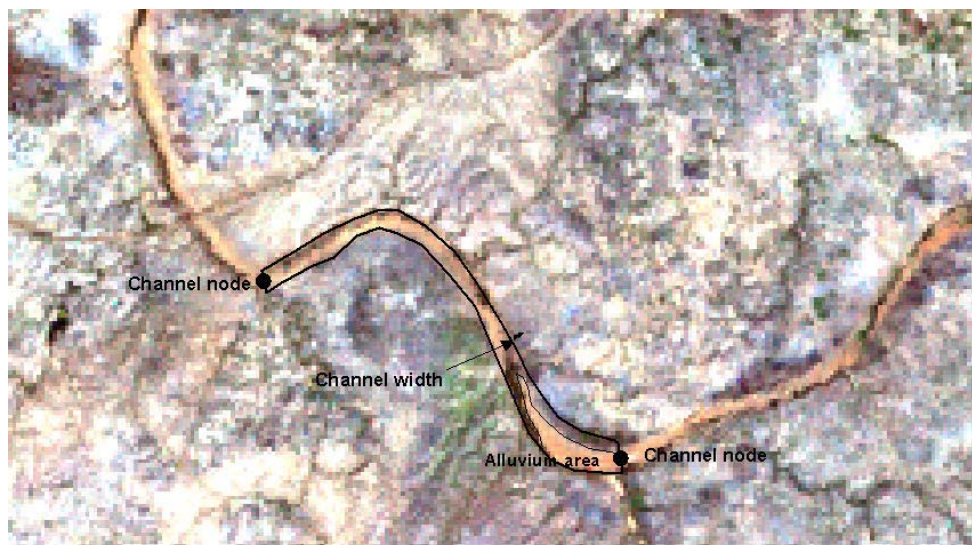


Figure 6.13 Determination of **channel parameters** from Landsat 7ETM+ remote sensing image

For the determination of depth of active alluvium a value between 2m to 4m has been considered depending upon channel type, channel width and percentage of alluvium. The wider channels with loessial alluvium, soft sediments and vegetation have contain larger depth of active alluvium than rocky fall channel. The characteristics of various channel types for Zin catchment have been defined in table 6.3 (Lange 1999).

Table 6.3 Characteristics of the different channel types

Type	Description	Manning $n$	Infiltration rate Channels [mm/h]	Bars [mm/h]	Depth of alluvium [m]	Covered by inner channel [%]
1	Channel on loessial alluvium with vegetation	0.050	44	44	2	20
2a	Confined channel entrenched into hard rock	0.030	420	110	1	45
2b	Confined channel entrenched into soft sedimentary rock	0.030	420	110	2	45
3	Wide braided channel system	0.045	420	110	2	20
4	Rocky channel, waterfalls and boulders	0.070	0	0	0	100

Source: after Lange 1999

The Manning's roughness coefficient has been commonly associated with channel flow and is the best fit for the uniform steady state. The Manning equation is still used to model discharge where conditions are relatively steady and have relatively constant cross-section for a long enough distance that the depth remains fairly constant. The approximate value of Manning's roughness coefficient for various channel types (surface roughness, vegetation,

channel irregularity, channel alignment, silting and scouring, size and shape of channel) has been given in annex 6.2 of this chapter. Once Manning's roughness coefficient is known, the channel routing parameters such as hydraulic radius  $R$  and channel energy slope  $S_o$  can be easily determined. Table 6.4 below depicts the mean statistics for 165 channel segments and their parameters adopted for Anas catchment.

Table 6.4 Statistics on segment parameters and their variability range

	Length [m]	Slope [%]	Storage [m <sup>3</sup> ]	Alluvium [m <sup>2</sup> ]	Width [m]	Time lag [min]	Runoff coefficient
Mean	3005	0.6	143820	111790	59.7	62.3	0.3
Median	2812	0.5	0	97558	43.6	60.0	0.3
Lower (25%)	3511	0.7	0	0	40.0	36.0	0.3
Upper (25%)	2265	0.3	0	184970	70.0	84.0	0.4
SD	1110	0.6	693010	122230	27.5	31.2	0.0
Skewness	1.4	2.3	8.8	0.9	1.7	0.0	1.4

## 6.2 Sensitivity Analysis for ZIN Model

In order to examine the effects of input parameter variations upon the model output a sensitivity analysis of the ZIN model was undertaken. The important procedure for the sensitivity analysis to follow is to run a set of simulations where the system parameter is changed by a given amount for each model run. The aim of such simulation has been to test whether model is sensitive to particular parameter. De Roo (1993) used a simple index for describing the sensitivity of a variable in following form:

$$S = \frac{|R_i - R_d|}{R_b} \dots\dots\dots (6.10)$$

where  $S$  is the sensitivity,  $R_i$  and  $R_d$  are model results with a variable being increased or decreased by 10% and  $R_b$  is the base line simulation. This method has been unable to reproduce the non-linear relationship between variables but gave good idea on model results range. Lange (1999) for rainfall-runoff modelling study in Israel took  $\pm 20\%$  error as the sensitivity range for most of the channel parameters and hydrograph shape.

Table 6.5 Sensitivity index of parameters affecting peak discharge and time to peak

Model parameters	Sensitivity range	Sensitivity to peak discharge		Sensitivity to peak time	
		[m <sup>3</sup> /s]	[%]	[min]	[%]
a. Terrain characteristics					
Initial loss	± 2.5 mm	± 77	± 4.5	± 0	± 0
Infiltration rate	± 20%	± 45	± 2.6	± 15	± 3.4
b. Runoff concentration					
Hydrologic time lag	± 10 min	± 35	± 2.0	± 60	± 13.8
Shape of response function	± 20%	± 374	± 21.7	± 70	± 16.1
c. Routing parameters					
Channel length	± 200 m	± 14	± 0.8	± 45	± 10.3
Channel slope	± 20%	± 34	± 2.0	± 70	± 16.1
Channel width	± 20%	± 17	± 0.9	± 45	± 10.3
Manning's coefficients	± 0.01	± 14	± 0.8	± 70	± 16.1
Bank-full stage	± 0.5 m	± 28	± 1.6	± 70	± 16.1
Percentage inner channel	± 20%	± 3	± 0.2	± 5	± 1.2
d. Transmission losses					
Depth of alluvium	± 2 m	± 36	± 2.1	± 5	± 1.2
Infiltration rate of alluvium	± 100 mm/h	± 340	± 19.7	± 10	± 2.3
Runoff coefficient	± 20%	± 330	± 19.2	± 15	± 3.4

The sensitivity analysis has been undertaken for ZIN model based on equation 6.10 for Anas catchment by simulating the effects of transmission losses, the effect of cloud movement and the effect of alluvium. Two aspects such as peak discharge and time to peak discharge from base for 12 parameters have been scrutinised. The uncertainty for initial loss have been taken as ± 2.5 mm while the infiltration has been increased or decreased by ± 20%. A hydrological time lag of ± 10 minutes for 1150 km<sup>2</sup> Anas catchment have been justified. Lange (1999) argued that to keep the mass conservation of water balance in the hydrograph shape first part was raised 20% while the second was lowered by ± 20%. The most of the physical parameters for routings have been run for an uncertainty range of ± 20% from the basic parameter range. A range of 0.5 m for the bank-full stage and Manning's coefficient ± 0.01 has been assigned. Depth of active alluvium and infiltration rate have been 2.0 m and 100 mm/h assumed since not much field based information is known. The results of this analysis are presented in table 6.5.

The sensitivity analysis of various parameters to peak discharge shows that the amount of peak discharge are mainly influenced by shape of hydrograph and infiltration rate of alluvium. The reason being that in arid and semi-arid catchments the storm runoff is

absorbed into alluvium material of the stream bed and flood plain (Sharma and Murthy 1995, Abdulrazzak and Sorman 1994, Jordon 1977). The shape of the response hydrograph function also played an important role for peak runoff discharge and difference in time to peak. The channel routing appeared to be decisive for defining the time to peak and occurrence of peak. The parameters for transmission losses have not shown significance for time to peak but found greater importance in peak discharge uncertainty.

### 6.3 Model Simulation Results

As described above in modelling methodology the Anas catchment has been split into hydrological units known as segments or sub-catchments. Each segment has been treated as hydrological unit where a lumped model is applied. Once the segment runoff is computed it is routed to the outlet following a response function of the hydrograph generation process. At the outlet, the sum of all the hydrological units provide the total discharges. In each hydrological unit the rainfall input has been different and been derived from station rainfall using IDW interpolation method and AML sub-routines in Arc-Grid functions.

The available river discharge data for the Anas catchment has been limited to three years from 1992-94 and just during rainy seasons from June to October only. The discharge have been measured at 6 hr interval using manual records and has been calibrated with current meter (refer chapter 2 for details). The several rainfall storms for the year 1994 have been selected based on constant cloud front velocity and consistency in discharge measurements. As a result the following four rainfall-runoff events were selected to check the model simulations during the middle and at the end of monsoon season (refer table 6.6).

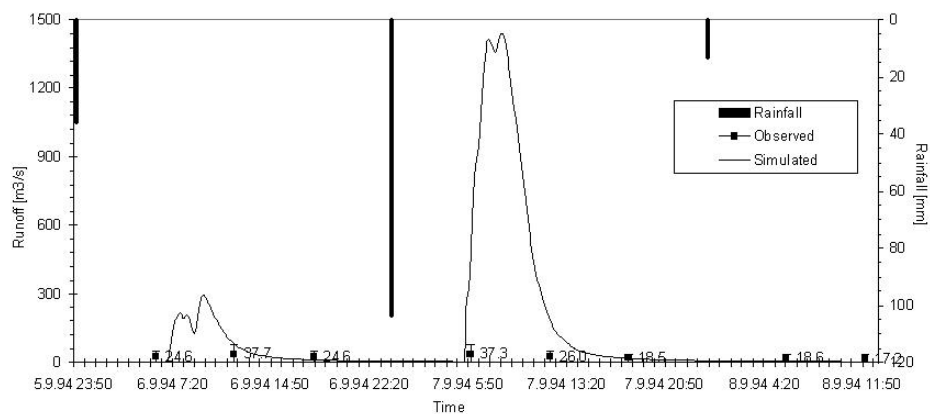
Table 6.6 Rainfall-runoff events selected for ZIN model run in Anas catchment

Event Date	Cloud velocity [m/s]	Rainfall depth at [mm]		Peak discharge observed at [m/s]	
		Anterbeliya	Mod	Anterbeliya	Mod
02.08.1994	1.75	104.5	87.5	6.90	98.5
20.08.1994	7.50	80.2	121.5	646.9	96.2
06.09.1994	3.50	35.9	21.2	37.3	4.2
07.09.1994	3.50	103.8	135.3	37.3	4.1

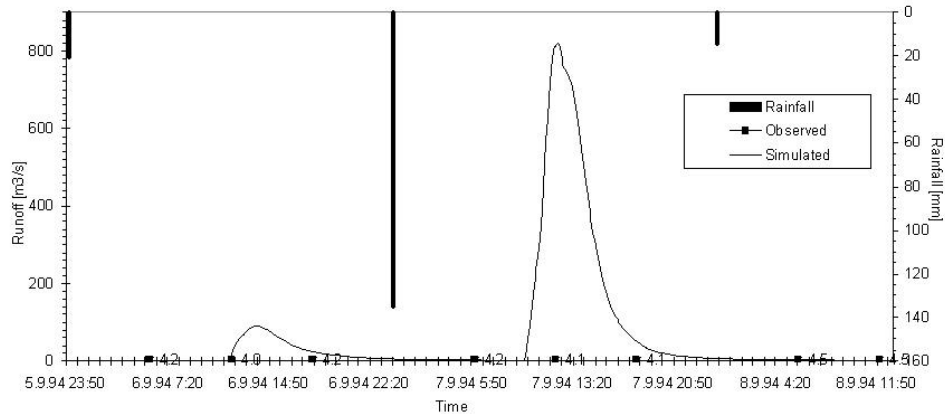


### 6.3.1 Model run for 07/09/1994

The ZIN model result on runoff simulation obtained for the 06-07/09/1994 event for the stations Anterbeliya and Mod are displayed in figure 6.14 below. There tend to be some degree of fit between observed and simulated discharge but the peak wave passed the measurement record of 6hr. The daily volume of surface water discharge at station Anterbeliya for 07/09/1994 event have been observed  $1.42 \text{ Mm}^3$  against the simulated volume of  $22.1 \text{ Mm}^3$ .



a.



b.

Figure 6.14 Results obtained in the **simulation for 06-07/09/1994** event; a.) discharge station at Anterbeliya and b.) discharge station at Mod

Similarly for the Mod station, the observed and simulated discharge differ significantly in peak discharge as well as in daily discharge volume (refer Figure 6.14b). The daily discharge volume for observed and simulated are found in the order of  $0.18 \text{ Mm}^3$  and  $8.6 \text{ Mm}^3$  respectively. There is significant difference in the observed and simulated discharge magnitudes (peak discharge as well as discharge volume). Almost no fit have been found between the observed and simulated discharge volume at both stations. It seems that either the observed discharge have been under-sampled or observed discharge data are erroneous.

### 6.3.2 Model run for 06/09/1994

Once again to check our apprehension, the model was run for a relatively small event of 06/09/1994 both for Anterbeliya and Mod discharge stations. The results are presented in the figure 6.15 which shows that the observed and simulated peak discharge could not be compared. The hydrological time scale resolution of 6 hours measurements have not been enough to compare the occurrence of simulated peak discharges.

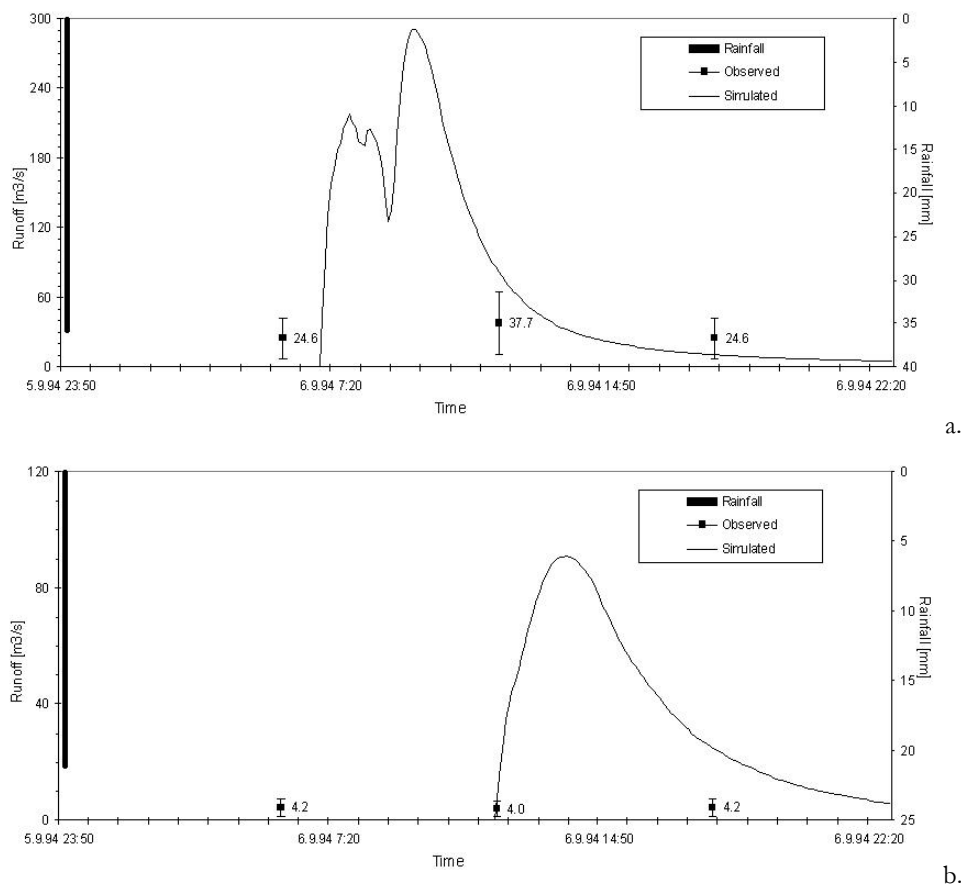


Fig 6.15 Results obtained in the **simulation for 06/09/1994** event; a.) discharge station at Anterbeliya and b.) discharge station at Mod

### 6.3.3 Analysis of volume check

The daily discharge volume checks are performed for station Anterbeliya to compare the amount of rainfall over catchment volume with simulated runoff volume at the outlet. The results obtained for three independent events are presented in table 6.7 below. It is interesting to learn that basin has a mean runoff coefficient of 0.19 and 0.20 depending upon the event type. The mean runoff coefficient of 0.20 for Anas catchment seems a typical

value. It can be concluded with some degree of reliability that simulated discharges are correct and the observed discharge are under sampled. The simulation results for 02.08.1994 event are presented in Annex 6.3.

Table 6.7 Volume check for simulated runoff at Anterbeliya for three independent events

Event →	02.08.1994	20.08.1994	07.09.1994
Daily rainfall volume [million m <sup>3</sup> ]	132.2	110.8	113.4
Daily simulated discharge [million m <sup>3</sup> ]	26.6	21.6	22.1
Mean runoff coefficient [-]	0.20	0.19	0.19
Daily observed discharge [million m <sup>3</sup> ]	0.46	0.43	2.43
Uncertainty observed vs. simulated [%]	98.3	98.0	89.0

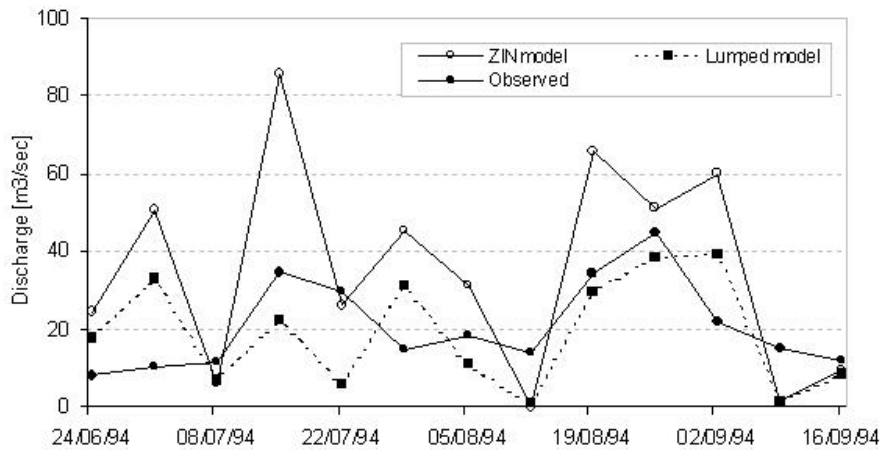
The ZIN model is field based and its performance depends on the quality of field data and its spatial and temporal availability. Even the model can't be independently validated at given time scale given the doubtful observed discharges both for the Anterbeliya and Mod stations. Nonetheless the calculation of discharge using physically based model are encouraging so it can be assumed that model is able to simulate the discharge rather in a satisfactory way.

#### 6.4 Model Validation: Up-scaling Discharge

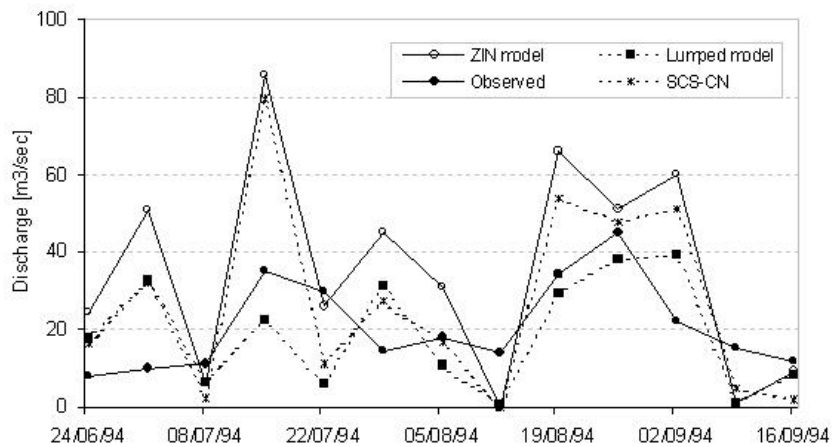
Figure 6.14 and 6.15 presents the model run for 2 rainfall events on 07/09/1994 and 06/09/1994 for Anterbeliya and Mod stations respectively. Data shows a very high degree of unreliability which is a typical case for rainfall-runoff modelling under un-gauges catchments. Now the questions are, how to validate the model results? What is the optimal time scale and spatial scale for discharge measurements? What are alternative methods for model validation? What is the reliability of our results under no validation since model parameters are within the range of  $\pm 20\%$  error?

In an attempt to validate the mean discharge parameter at the weekly scale two different set of models having different runoff process are used (a simple lumped water-balance model and SCS-CN runoff model). The model structure and characteristics of simple-lumped water balance model and SCS-CN runoff model have been discussed in chapter 3 in detail. Figure 6.16a presents the weekly discharge which shows that closeness of fit is rather unsystematic between ZIN model simulations and observed discharge. Rather a more coherent pattern

between ZIN model and simple lumped model have been found except that lumped model has simulated lower discharge. The simulated discharge using SCS-CN runoff model has better agreement with ZIN model results (refer Figure 6.16b).



a.



b.

Figure 6.16 Up-scaling model time scale to compare simulation results a) with ZIN model and simple lumped model and b) with ZIN model, lumped model and SCS-CN runoff model

The simulated results have been further up-scaled at monthly time step as shown in Figure 6.17 below. The simulated results from ZIN model are high as compared to observed discharge, simple lumped model and SCS-CN runoff model. The inter model comparison shows that ZIN model contains the most relevant elements of the runoff generation processes that cause the higher discharge even for up-scale. It may be further stated that the observed discharge data are under sampled.

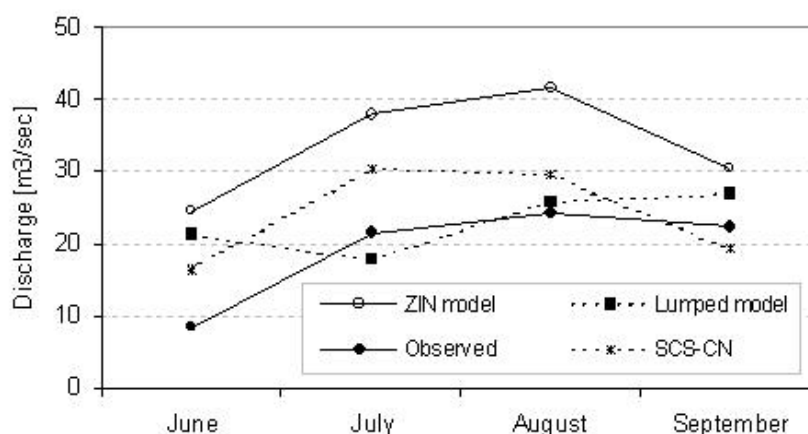


Figure 6.17 Comparison between simulated and observed discharge at monthly up-scale

## 6.5 Effect of Input Parameters Variability

The previous sections generated understanding on physically based distributed model run for rainfall excess and runoff process in Anas catchments. This section will show how the input parameters variability may affect the runoff generation process namely, peak discharge and discharge volume. In section 6.3 the model sensitivity analysis has been conducted for the various model parameters within a possible range of  $\pm 20\%$  from mean. The sensitivity results are site specific and may vary with locations of different catchment size, soil types, land-use distribution and slope (Liu 2003) but for the same site produce good results for change detection. Since the observed discharge data are erroneous, the effects of parameter sensitivity can be an important indicator for variability. The effect of important parameters such as cloud velocity, infiltration rate and reservoir storage have been studied for runoff generation.

### 6.4.1 Effect of cloud velocity

Instead of using a constant cloud velocity to calculate the flow path response the concept of cloud-front movement has been applied to calculate discharge flow at given node. The flow velocity for various rainfall events were derived from Sasidhran and Shukla (1999) based on daily INSAT images over Central India. Three alternative options on cloud velocity such as 7.00 m/s, 3.50 m/s and 1.75 m/s have been tested for runoff response at stations Anterbeliya and Mod respectively.

For large rainfall event of 07.09.1994 changing the cloud velocity from 7.00 m/s to 3.5 m/s decreased the peak discharge from 1437 m<sup>3</sup>/s to 697 m<sup>3</sup>/s for Anterbeliya and from 819 m<sup>3</sup>/s to 505 m<sup>3</sup>/s for Mod stations. The time to peak discharge also delays from 2 hours for Anterbeliya to more than 7 hours for Mod station. Clearly a double discharge peak have been observed in slow moving cloud-front. It is logical that the big rainfall events lead to higher peak discharges and shorter time of concentration. Further decreasing the cloud velocity until 1.75 m/s multiple-peaks and larger translation of travel time have been obtained.

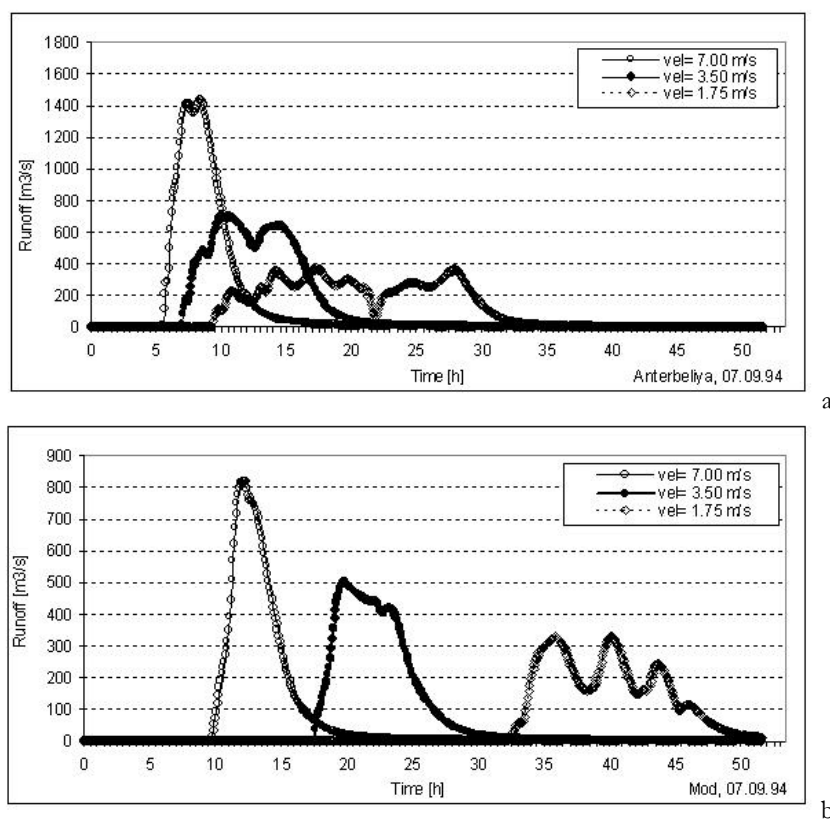


Fig 6.18 Modelling the **effects of cloud velocity** for a large size event of 07/09/1994 at a.) Anterbeliya and b.) Mod stations

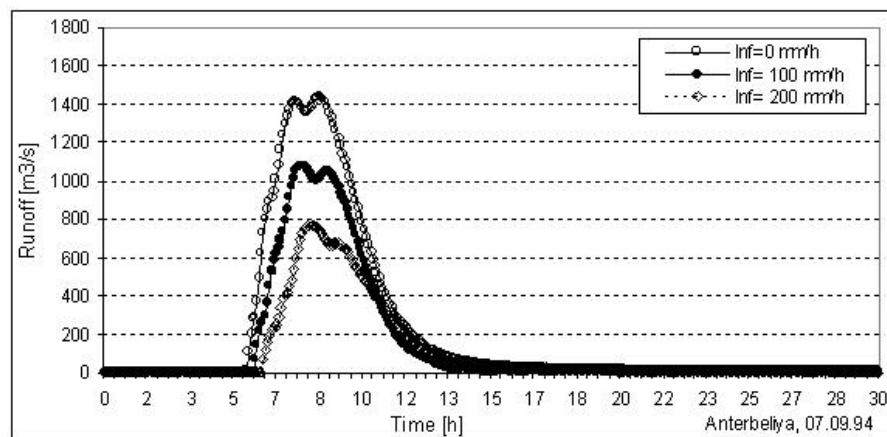
The effect of cloud velocity for smaller event of 02.08.1994 shows almost similar pattern on runoff generation and time of concentration. The discharge hydrographs are shown in Annex 6.4 of this chapter.

#### 6.4.2 Effect of alluvium infiltration rate

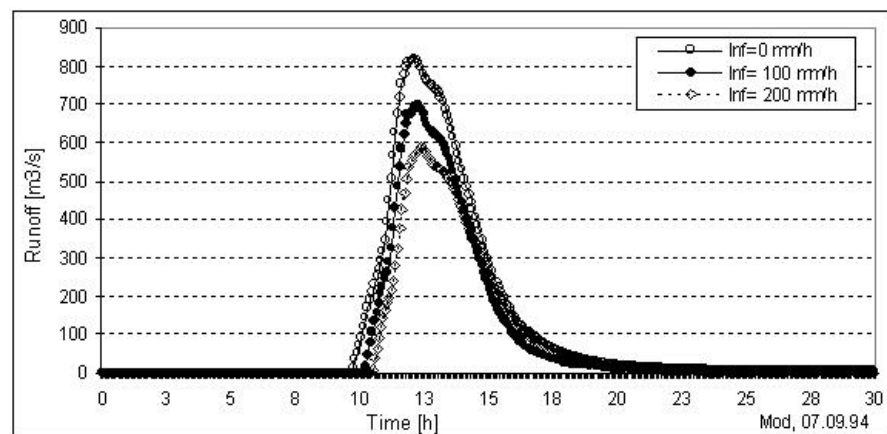
Since surface runoff from each catchment segment will contribute to stream flow, infiltration or transmission losses within the channel network have direct impact on runoff generation

and channel routing. The infiltration within the alluvium plain are estimated based on percentage of channel alluvium and bank-full depth. In principal it is higher for downstream and lower for upstream due to the phenomena of soil erosion and deposition. For the convenience of comparison and model computation a constant infiltration rate has been assumed for all the alluviums.

Fig 6.19 depicts the effect of infiltration rate on runoff hydrograph for 07.09.1994 event. Three alternative options for alluvium infiltration parameter (such as no-infiltration, infiltration of 100 mm/h and infiltration of 200 mm/h) were considered for the model run. In case of station Anterbeliya it is found that peak discharge decreased by 25% and peak time somewhat delayed by 15min after increasing the transmission losses by 100 mm/h. Further peak discharge decreased by 35% and delayed by 20min once infiltration rate changed from 100 mm/h to 200 mm/h. The reduction in peak discharge and time to peak are followed by reduction in surface runoff flowing in the channel.



a.



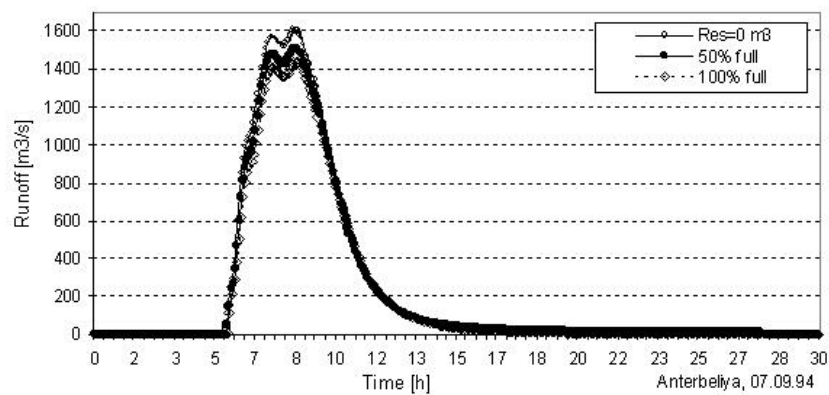
b.

Fig 6.19 Modelling the **effects of transmission losses** for a large size event of 07.09.1994 at a.) Anterbeliya and b.) Mod stations respectively

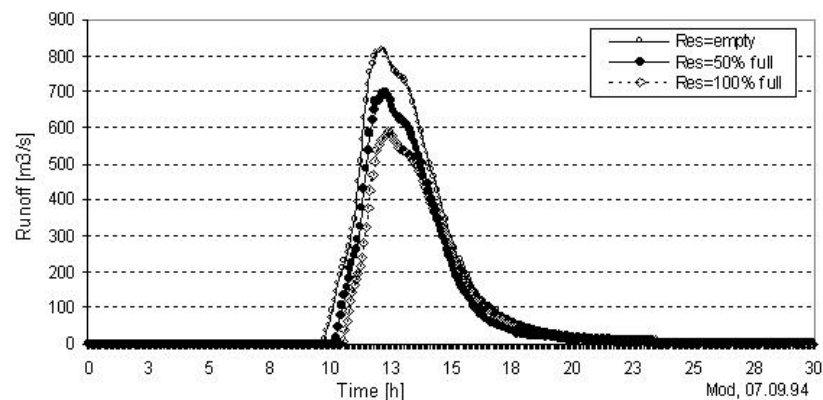
Similar phenomena has been observed for the discharge station Mod where increase in infiltration rate or losses with channel sections reduced the discharge peak by 16% for both the cases. Not much significant translation for time to peak has been found. This attribute to the fact that Mod sub-catchment has rather complex geomorphology and stream network pattern.

#### 6.4.3 Effect of reservoir storage

The model approach considers the changes in reservoir volumes with respect to their role in surface runoff routing. There are more than 140 small size reservoirs with an average storage capacity of 200,000 m<sup>3</sup> which are used for irrigation. The presence of reservoirs may have impact on runoff generation process once they are empty or filled or half-filled. Three alternative scenarios can be considered namely no-reservoir storage, 50% reservoir storage or full reservoir storage. The storage in reservoir may reduce the flood wave generating from a segment or routing through channel.



a.



b.

Fig 6.20 Modelling the **effects of reservoir storage** for a large size event of 07/09/1994 at a.) Anterbelya and b.) Mod stations respectively



Figure 6.20 depicts the model run for 07.09.1994 event for Anterbeliya and Mod stations. It is found that peak discharge decreased and time to peak increased just slightly by increasing the reservoir storage volume. This is because that reservoir storage will reduce the flood wave celerity ( $v_k$ ) which may cause decrease in peak volume and increase in travel time. In case of Anterbeliya, peak discharge decreased by 6% and time to peak by 1% while for Mod, the peak discharge decreased by 3% and time to peak by 2% for scenarios when reservoirs are 50% full. For second option by increasing reservoir storage from 50% to 100%, the peak discharge have been reduced to 5% and 2% for Anterbeliya and Mod stations respectively. This shows that reservoir storage volume has not significant effect on peak discharge and flood wave formation for channel routing.

## 6.6 Results and Discussion

A physically based single event distributed model derived from unit hydrograph response function has been presented partially using GIS based modelling approach. The model differs from original ZIN model code in that additional parameters such as reservoir storage as transmission losses, runoff coefficients from satellite data, station rainfall calibration for INSAT were added. The basic modelling approach used GIS modelling for rainfall distribution analysis, delineation of sub-catchments and segments, delineation of reaches with deep alluviums and definition of channel nodes. The model parameters such as sub-catchment area, mean slope, channel properties have been calculated in Arc/Info GIS environment. The flow velocity for each sub-catchment has been estimated based on Manning's equation which is a function of slope, roughness coefficient and channel properties. The time lag or travel time from each sub-catchment has been integrated to obtain the cumulative time lag at each station.

The mean runoff coefficients for each sub-catchment are derived from Landsat images at 30m x 30m raster cell size. Runoff is routed over surface flow path and accounts for model parameters. The final discharge at station has been obtained by superimposing all the

contributing discharges from all segments. Most of the physically distributed model parameters can be derived using standard GIS procedure and AML macros in Arc/Info.

The modified 3-point variable parameter method of Muskingum-Cunge for river routing is a viable alternative for un-gauged catchments where stream flow data are not available. But the hydraulic data such as channel geometry, channel cross-section and channel slopes can be readily ascertained from satellite images and/or topographic maps in GIS. The non-linear features of the variable parameter Muskingum-Cunge method makes it the method of choice in hydrologic flood routing.

Since most of the countries have topographical and spatial maps at an appropriate scale (1:50,000 or larger), either on paper or in electronic format. The integration of electronic data in GIS format with hydrological modelling holds the key promise for cost effective alternatives for studying the watersheds and their hydrological behaviour. The ability of GIS to perform spatial analysis for development of lumped hydrologic parameters can not only save time and efforts, but also can improve accuracy over traditional methods.

The modified ZIN model has been tested for un-gauged Anas catchment in India where limited discharge data just for three monsoon seasons are available. Model check against observed and simulated discharge illustrate considerable uncertainties in the observed discharge. This is particularly due to the fact that observed series is under sampled, even the 6 hr time step not found to be sufficient. The model volume check run for selected events shows uncertainty limit between 89.0% to 98.3% for 07/09/1994 and 02/08/1994 large and small size events respectively. The assessment and estimation of water resources potential based on observed data records are highly uncertain. Thus, the physically based distributed model offers an advantage over lumped method to check the observed discharge records.

Since model parameters are field based in general no calibration is needed. But the model calibration for Anas catchment has been hampered due to general lack of field observations and the under sampled gauged discharge data. Even the measured stream flow discharge data were found un-sufficient to perform a model validation. The model up-scaling shows an interesting cross-comparison between various model types and runoff generation process

involved in them. This is of particular interest when our main objective remain water resources planning and development.

A sensitivity analysis for model have been conducted to review the effect of cloud velocity, alluvium infiltration and reservoir storage on catchment discharge. It has been found that cloud velocity and alluvium infiltration are the most sensitive parameters. The effect of reservoir storage has not been significant due to small storage volume as well percentage of area under alluvium. The modelling experiences (Sharma et al. 1995, Abdulrazzak et al. 1994, Lange et al. 1999, Gheith et al. 2002) in arid and semi-arid catchments shows that alluvium infiltration always dominate the runoff generation and river routing process. More reliable results may be obtained when the different stream-order and geometry are assigned different Manning's roughness coefficients.

The catchment scale water resources scenarios for storage in alluvium aquifer (infiltration) and reservoirs (surface storage) were analysed. Despite the simple model structure the distributed ZIN model illustrated catchment scale recharge dynamics for medium and small size events. All reservoirs were filled mostly during large events, but the alluvium aquifers are replenished during small events too. With limited field-based efforts the reliability and the quality of the ZIN model simulations can be increased significantly. Thus further field measurements and investigations are needed for optimal hydrological modelling in order to make water resources assessment much reliable.



## 7. CONCLUSIONS AND PERSPECTIVES

### 7.1 Catchment decision support models

The decision support models are in much need when water resource is limiting the economic development and river basins are vulnerable to sudden drought and flood. This becomes essential for both the precision and timely decision making to avoid negative effects of drought. The main aim of this research study has been to understand the methodology inherited in decision support system and test the application of few modelling modules (rainfall modelling, rainfall-runoff modelling) for an un-gauged Anas catchment.

The utilisation of field based spatial and temporal data for decision making purposes helps to define future needs and strategies to improve assessment decisions. Thus based on the research findings from Anas catchment it may be stated that decision support model deal primarily with the data manipulation, simulation modelling, results analysis and setting decision criteria rules. It is hoped that once each module have been coupled may be used for long-term as well as short-term planning.

### 7.2 Hydrological modelling and database development

Incorporation of watershed models into GIS has improved matters by streamlining data input and providing better interpretation of hydrological output. The development of spatially distributed hydrologic model and stochastic rainfall model have led to improved model forecasting at the cost of more detailed spatial information. The hydrological model parameterisation for segments and channel routing as well rainfall model parameterisation for use in external-drift-Kriging have been of special interest. The GIS has tools to assist in

selecting a watershed and/or segment for analysis, removing depressions, development of DEM and enforcing drainage pattern so that model operates without problem.

The integration of GIS in catchment models provides a better interface and visualisation capacity in a user-friendly environment. The model described in chapter 6 has been used to perform sensitivity analysis on different model parameters which may help in assessing the impact of various management options. But building a tightly coupled interface between GIS and hydrologic model is a much complex and time consuming task which may be a subject of later research.

### 7.3 Remote sensing for hydrological model parameterisation

Achieving more reliable land-use classification by making use of decision boundary feature extraction (DBFE) algorithm for feature extraction and ECHO for image classification has been a major focus of chapter 4. Recent methodological developments in pattern recognition, image classification and GIS integration have been tested for improvements in land-use classification and hydrological regionalisation.

A newly developed DBFE algorithm has been used instead of classical DAFE. The results obtained from image classification shows that DBFE explained eigen-value components better as compared to DAFE. Decision boundary feature extraction uses all the six principal components as against DAFE which uses only three.

For training class performance the image classification algorithm ECHO found to be more reliable and accurate as compared to classical maximum-likelihood or fisher's linear discriminant. The overall class performance has been found to be much higher as compared to both methods. The new algorithm found to be more homogeneous with respect to Gaussian maximum-likelihood. The automatic digital image transformation program has been written in Arc/Info language AML to convert into GIS compatible format. Data has been transferred into database system (Microsoft ACCESS) for identification of similar hydrological response units.

#### 7.4 Rainfall prediction based on GCM

The prospects of atmospheric circulation taking geo-potential height as predictor for rainfall downscaling has been important for semi-arid Anas catchment where distinct seasonal climate pattern is dominating. An automated fuzzy-rule based model has been used to classify the circulation pattern on daily basis using geo-potential heights as predictor and station rainfall as the predictand. The circulation pattern anomalies are conditioned upon station rainfall to derive rainfall amount and probability.

The classification performance of automated fuzzy method have been influenced by; a) reliability of GCM grid data obtained from NCEP, b) spatial and temporal distribution of station rainfall and c) stationarity of rainfall time series. In general daily rainfall time series >30 years may yield stationarity in model parameter identification. The model produced good results for mean monthly rainfall amount and frequency but under-performed the daily low frequency processes. However a moderate degree of consistency in the characteristics of circulation types for Jhabua and Thandla stations over predicted rainfall time period of 1960-1994 have been observed.

Being the typical semi-arid climate a small rainfall and circulation type database size (limited to 10 years 1985-1994) for model parameters determination may be less reliable for description of conditional rainfall amounts and frequencies. Studies by Wilby and Wigley (1997) shows that observed rainfall relationship are not well simulated for all regions or for all GCM. Thus it is not clear whether database stationarity has been a limiting factor for enhanced forecasting.

The monsoon season (June-October) rainfall in Anas catchment have been convective events associated with frontal system from South-East or East direction. High cross-correlation (>0.60) have been found not only during heavy rainfall season but also during low rainfall year. During the frontal system all stations received similar magnitude of rainfall but several time it was confined to few stations only. This demonstrate that there are differences in the spatial extent of rainfall and in CP-type vs. rainfall relationship between wet and dry years during the monsoon season. Further research is needed to define the relationship between

circulation type and convective events in a more physically realistic manner. This will be a possible input to couple atmospheric model with hydrological forecasting as an input for event based ZIN model.

In future the fuzzy classification method may be improved for long-term prediction such as yearly series by using sea-surface temperature (SST) or sea-level pressure (SLP) as an additional predictor. The additional predictor may further guide in parameter identification that CP-type has not been only parameter for rainfall changes. This may improve the forecasting of rainfall amount as well as number of rainy days. It is further of the view that Markov-chain model for rainfall downscaling in which rainfall occurrence is conditioned upon the CP-type has to be improved using a new approach. In this approach the pair of circulation states are identified from the pattern of rainfall occurrence which may describe a more continuous description of circulation regime.

#### 7.5 Runoff modelling for prediction in un-gauged catchments

The structure of ZIN model for rainfall-runoff modelling combines the process based hydrological models at watershed scale and linking them for runoff routing. In general the Anas catchment modelling process is represented by; a.) Hortonian overland flow and b.) transmission losses (infiltration, percolation, storage). The hydrological response units which represents the spatial scale of hydrological process, have been classified based on terrain and landscape units. The simple model structure and the lateral distribution of sub-catchments/segments has been linked to topographic position and thus to runoff generation and river routing relationships. This has been important in view of incorporating sub-scale processes in efficient and flexible way for a large scale catchment under limited data availability.

Due to limited data availability for Anas catchment, the model parameters have been kept to minimum number. All the parameters have been determined from field conditions and none was determined by model calibration. The hydrograph response curve has been adopted from nearby Luni basin while the rainfall time lag has been derived from INSAT images. The flow velocity in each sub-catchment has been calculated by Manning's equation which depends upon the slope, channel roughness and hydraulic radius. The direct discharge has



been routed over the surface flow path, and account for the differences in runoff and velocities due to changing slope, soil and land-use type, and sub-catchment surface conditions. The total discharge at given node has been obtained by superimposing all contribution from surface flow paths for each sub-catchment based on runoff and velocities.

The spatial sub-catchment parameters such as mean slope, channel length and width, and runoff coefficient have not been bound to calibration data-sets. All model parameters are field based and do neither bound to specific model nor to calibration datasets as the case with most hydrological models. An independent model validation at catchment scale have been hindered due to low and poor quality of discharge data availability.

But the model has great advantage due to its flexibility to incorporate any hydrological and spatial information without much modifications in model code. The spatial information on rainfall distribution has been extracted using daily station rainfall and mean rainfall intensities using Arc/Info and Arc-View GIS tools. At sub-catchment or segment scale the variability of parameters limit has been considered at mean for all runs as no independent discrete data to verify this hypothesis have been available. The spatial scale of hydrograph response curve has been between 3-4 km<sup>2</sup> for runoff generation, the initial infiltration losses have been increased for larger catchment area. The hydrograph response curve has been adopted from field based study conducted by Sharma (1997) in Luni basin of western India. The mean size of sub-catchment and mean channel flow length have been of the order of 4 km<sup>2</sup> with mean flow length around 3 km long.

The sensitivity analysis for model parameters shows that model results are mainly influenced by hydrograph response curve and infiltration losses for an uncertainty range of  $\pm 20\%$ . But it does not address model structure and process uncertainties which may arise due to variability of spatial scale (sub-catchments between 2-8 km<sup>2</sup>) using single hydrograph response curve. The independent verification of model uncertainties has not been possible due to limited hydrological data.

Although large events have been mainly responsible for flood runoff and recharge dynamics within the catchment. The use of satellite data for rainfall monitoring such as weather radar offer new avenues not only for catchment monitoring but also for early warning during

drought or floods. In future the efforts will be made to validate the model with measured field data. Extended possibility of model validation will be an essential step for improvement of hydrological process in semi-arid catchments. Discharge measurements at various spatial scale ranging from plot scale to sub-catchment scale using pressure sensors. Since the spatial structure has been the main basis in this model, the transferability of the approach to un-gauged basins can be well extended.

#### 7.6 Application towards decision support models

The primary motivation for decision support models used in this research work has been the desire to reduce uncertainty in the decision making where the climate fluctuation and water resources availability may pose enormous costs for river basin management. Decision can range from simple choices about the priorities for a farmer's crop-calendar or operation of storage reservoirs. Although the simulation models used here have been simple, less data dependent, limited spatial and temporal range but found to be effective in conveying their usefulness. However the major issue has been how to develop the decision support modelling methodology for un-gauged catchments with limited database. This methodological approach can be helpful to conceptualise and assess the potential consequences of decisions. Finally it is necessary to go beyond the basic research and undertake demonstration project for possible application in Anas catchment.

## 8. REFERENCES

### 8.1 References for chapter 1

- Abbott M.B., Bathurst J.C., Cunge J.A., O'Connell P.E., Rasmusson L. 1986. An introduction to the European Hydrological System: 2. structure of physically based distributed modelling system. *Journal of Hydrology*, Vol. 87: 61-77.
- Adelman L. 1992. *Evaluating decision support and expert systems*. John Wiley & Sons, New York, USA.
- Adinarayana J., Maitra S., Venkatraman G. 2000. Spatial decision support system for rural land use planning. In: *Proceedings of Internet Workshop on Asia Pacific Advanced Networks and its Application*, Takakuba, Japan 15-17<sup>th</sup> Feb. 2000, p. 73-81.
- Andreu J., Capilla J., Sanchis E. 1996. AQUATOOL- a generalised decision support system for water resources planning and operational management. *Journal of Hydrology*, Vol. 177: 269-291.
- Bardosy A., Plate E.J. (1992). Space-time model of daily rainfall using atmospheric circulation patterns. *Water Resources Research*, Vol. 28, No. 5: 1247-1259.
- Bell P.C. 1992. Decision support systems- past, present and prospects. *Revue des systemes de decision*, Vol. 1, No. 2-3 : 126- 137.
- Billib M., Boochs P.W., da Silva T.C., de Silans A.P. 2003. Decision support system fuer die Wasserwirtschaftsplanung im semiariden Nordost-Brasilien. *KA-Wasser Abfall*, Vol. 50, No. 2: 172-176 (in German)
- Bothale V.M., Bhatwadekar S., Bothale R.V., Sharma J.R., Adiga S. 2002. Geo-Smart: A generic decision support system for resources planning and management. In: *Proceedings ISPRS Commission Symposium on Resource and Environmental Monitoring*, Hyderabad, India 3<sup>rd</sup> -6<sup>th</sup> December 2002.
- Breuer L., Bach M., Frede H-G., Eckhardt K. 2003. Konzeption eines integrierten Modellsystems als Spatial Decision Support System fuer Wassereinzugsgebiete. *KA-Wasser Abfall*, Vol. 50, No. 2: 189-194 (in German)

- Centre for Development of Advanced Computing (C-DAC). 2003. Decision support system using geomatics technologies. Centre for Development of Advanced Computing, Pune, India. <http://www.cdacindia.com/html/>
- Crausaz P.-A., Musy A. 1997. GESREAU an institutional GIS for integrated water management. IAHS Publ. No. 242: 33-41.
- Davis D. 1999. Integrated information management. World Meteorological Organisation, Geneva, Switzerland. Technical Report 71, 23 pp.
- De May M. 1992. The cognitive paradigm. The University of Chicago Press, Chicago, USA.
- Dhar V., Stein R. 1997. Intelligent decision support- the science of knowledge work. Prentice Hall, New Jersey, USA.
- Dunn S.M., Mackay R., Adams R., Oglethorpe D.R. 1996. The hydrological components of the NELUP decision support system: as appraisal. Journal of Hydrology, Vol. 177: 213-235.
- Emery J.C. 1987. Management information systems- the critical strategic resource. Oxford University Press, New York.
- Food and Agriculture Organisation (FAO). 1993. Guidelines for economic appraisal of watershed management projects. FAO, Rome, Italy, 152p.
- Food and Agriculture Organisation (FAO). 1977. Guidelines for watershed management. FAO, Rome, Italy.
- Fedra K., Jamieson D.G. 1996. The WaterWare decision support system for river basin planning. 2-planning capability. Journal of Hydrology, Vol. 177: 177- 198.
- Fedra K., Jamieson D.G. 1996. An object-oriented approach to model integration a river basin information system example. IAHS Publ. 235: 669-676.
- Fedra K, Reitsma R.F. 1990. Decision support and geographical information system. In: H.J. Scholten and J.C.H. Stillwell (eds.), Geographical Information System for Urban and Regional Planning, Kluwer Publishers, Boston, pp. 177-188.
- Gijsbers P.J.A. 1998. Decision support for water allocation. In: Brouwer R., Heijstek D.E.P., Huisman P., Kramer M.W., van der Stelt M.L. (eds.), Informatics in Operation Water Management, ICID Water-day Proceedings , Delft, pp35-42.
- Government of India. 1987. National water policy. Ministry of Water Resources, New Delhi, India.
- Haan C.T., Johnson H.P., Brakensiek D.L. 1982. Hydrological modelling of small watersheds. American Society of Agricultural Engineers, Michigan, USA.

- IPCC. 2001. Climate change- Impacts, adaptation and vulnerability. 3<sup>rd</sup> Assessment Report of Intergovernmental Panel on Climate Change, Cambridge University Press, UK.
- Jacucci G., Kabat P., Pereira L.S., Verrier P., Steduto P., Uhrík C., Bertanzon G., Huygen J., Van den Broek B., Teixeira J.L., Fernando R., Giannerini G., Carboni F., Todorovic M., Toller G., Tziallas G., Fragaki E., Vera-Munoz J., Carreira D., Yovchev P., Calza D., Valle E., Douroukis M. 1994. The HYDRA project- A decision support for irrigation water management. In: Proceedings Land and Water Resources Management in the Mediterranean Region, 4-8<sup>th</sup> Sept., 1994, Bari, Italy. Vol. 6: 1-18.
- Jamieson D.G., Fedra K. 1996. The WaterWare decision support system for river basin planning. 1-conceptual design. *Journal of Hydrology*, Vol. 177: 163- 175.
- Jamieson D.G., Fedra K. 1996. The WaterWare decision support system for river basin planning. 3-example application. *Journal of Hydrology*, Vol. 177: 199- 211.
- Kersten G. E. 2000. Decision Making and Decision Support. In: Kersten, G. E., Z. Mikolajuk, A. G. Yeh (eds.) *Decision Support Systems for Sustainable Development: A Resource book of methods and applications*. International Development Research Center, Canada. pp. 29-51.
- Krejčík J., Vanecek S. 1999. Application of decision support system for development of accession strategies in the water sector in Czech Republic. In: Proceedings, Participatory Process in Water Management, UNESCO Paris, 28-30 June.
- Lange J., Singh A.K. 2003. Water resources assessment in dry catchments by hydrological modelling adopted to limited data availability river Anas India. *Geophysical Research Abstracts*, Vol. 5, 02521, European Geophysical Society.
- Lange J. 1999. A non-calibrated rainfall-runoff model for large arid catchments, Nahal Zin, Israel. *Institute of Hydrology, Freiburg im. Br., Band 9*.
- Letcher R. 2002. Issues in integrated assessment and modelling for catchment management. Unpublished (Ph.D. thesis), Australian National University, Sydney, Australia. [http://icam.anu.edu.au/research/letcher\\_thesis.pdf](http://icam.anu.edu.au/research/letcher_thesis.pdf)
- Little, J. D. C. 1970. Models and Managers: The concept of a decision calculus. *Management Science*, Vol. 16, No. 8: 35-43.
- Moore J.H., Chang M.G. 1980. Design of decision support system. *Database*, Vol. 12, No. 1-2: 8-14.
- National Centre for Human Settlements and Environment. 1993. Sustainable utilisation of natural resources in Jhabua district. NCHSE Bhopal, India. 298 pp.

- Ninan K.N. 1998. An assessment of European-aided watershed development projects in India. Centre for Development Research, Copenhagen. CDR Working Paper 98.3, 49 pp.
- Prastacos P. 2003. ANFAS- A decision support system for simulating river floods. Concept Paper, Institute of Applied and Computational Mathematics, Herakleion, Greece, 14pp., <http://www.iacm.forth.gr/old/regional/papers/prastacos-ANFAS.pdf>
- Simonovic S.P., Bender M.J. 1996. Collaborative planning support system: an approach for determining evaluation criteria. *Journal of Hydrology*, Vol. 177, No. 3-4: 237-251.
- Sivapalan M., Takeuchi K., Franks S.W., Gupta V.K., Karambiri H., Lakshmi V., Liang X., McDonnell J.J., Mendiondo E.M., O'Connell P.E., Oki T., Pomeroy J.W., Schertzer D., Uhlenbrook S., Zehe E. 2003. IAHS decade on predictions in un-gauged basins 2003-2012- shaping an exciting future for the hydrological sciences. *Hydrological Sciences Journal*, Vol. 48, No. 6 : 857-880.
- Todini E., Zamboni L., Catelli C., Adorni G., Neri P., Brozzo G. 1999. FLOODSS- a flood operation decision support system. In: *Proceedings 2<sup>nd</sup> Inter-regional Conference on Environment and Water*, EPFL Lausanne, Switzerland, 1-3 September.
- Ubbels A., Verhallen J.M. 2000. Suitability of decision support tools for collaborative planning processes in water resources management. Institute for Inland Water Management and Waste Water Treatment (RIZA), The Netherlands, p.47, Report 99.067
- Vellekoop, A.H.; C.G.E. Boender; A.H.G. Rinnooy Kann. 1987. The Design of Interactive Decision Support Systems. In: Lewandowski A., Stanchev I. (eds.) *Methodology and Software for Interactive Decision Support*. Springer. pp 234-241.
- Welp M. 2000. The use of decision support systems in participatory river basin management. Vol. 2, European Geophysical Society, Nice France.

## 8.2 References for chapter 2

- Ananthakrishna R., Soman M.K. 1989. Statistical distribution of daily rainfall and its association with the coefficient of variation of rainfall series. *International Journal of Climatologic* Vol. 9: 485-500.
- Awulachew S.B. 2001. Investigation of water resources aimed at multi-objective development with respect to limited data situation: The case of Abaya-Chamo Basin, Ethiopia. Heft 19, Institut für Wasserbau u- Technische Hydromechanik, TU Dresden.

- ESRI. 1997. Understanding GIS: The Arc/Info method. Environmental System Research Institute Inc., USA.
- Haan C.T., H. P. Johnson, D. L. Brakensiek (eds.). 1982. Hydrologic Modelling of Small Watersheds. ASAE Michigan, USA.
- IARI. 1983. Resource analysis and plan for efficient water management: Mahi right bank canal command area. Water Technology Centre, Indian Agricultural Research Institute, New Delhi.
- Maidment D. 1999. GIS Hydro' 99. <http://www.ce.utexas.edu/prof/maidment/new.html> July 24, 1999.
- National Centre for Human Settlements and Environment. 1993. Sustainable utilisation of natural resources in Jhabua district. NCHSE Bhopal, India. 298 pp.
- Pichamuthu C.S. 1967. Physical Geography of India. National Book Trust India, New Delhi. pp. 212.
- Rosegrant M.W., Cai X., Cline S.A. 2002. World water and food to 2025: Dealing with scarcity. International Food Policy Research Institute (IFPRI), Washington D.C.
- Sivaramakrishnan K.C. 1993. Managing urban environment in India- water supply and sanitation. Times Research Foundation, Calcutta, India.
- Soman M.K., Krishnakumar K. 1990. Some aspects of daily rainfall distribution over India during the south-west monsoon season. International Journal of Climatologic, Vol. 10: 299-311.
- Subramanya K. 1994. Engineering Hydrology. Tata McGraw-Hill New Delhi.
- Velayutham M., Mandal D.K., Mandal C. and Sehgal J. 1999. Agro-ecological sub-regions of India for planning and development. NBSS Pub. 35, Nagpur, National Bureau of Soil Science and Land Use Planning.
- Yair A. and H. Lavee. 1985. Runoff Generation in Arid and Semi-arid Zones. In: Anderson M.G. and Burt T.P. (Eds.) Hydrological Forecasting. John Willey & Sons Ltd.. pp 183-220.

### 8.3 References for chapter 3

- Ananthakrishna R., Soman M.K. 1989. Statistical distribution of daily rainfall and its association with the coefficient of variation of rainfall series. International Journal of Climatologic Vol. 9: 485-500.

- Awulachew S.B. 2001. Investigation of water resources aimed at multi-objective development with respect to limited data situation: The case of Abaya-Chamo Basin, Ethiopia. Heft 19, Institut für Wasserbau u- Technische Hydromechanik, TU Dresden.
- Baker M.D., Carder D.R. 1976. An approach for evaluating water yield and soil loss model. As quoted in Haan C.T., H. P. Johnson, D. L. Brakensiek (eds.). 1982. Hydrologic Modelling of Small Watersheds. ASAE Michigan, USA.
- Band L.E. 1993. Effect of land-surface representation on forest water and carbon budget. *Journal of Hydrology*, Vol. 150: 749- 772.
- Bardossy A., Plate E.J. 1992. Space time model for daily rainfall using atmospheric circulation patterns. *Water Resources Research*, Vol. 28, No. 5, 1247-1259.
- Becker R., Nestmann F. 2001. Datenbank und Informationssystem des Verbundprojekts. In: Nestmann F., Buechle B. (eds.), *Morphodynamic der Elbe*. Institute für Wasserwirtschaft u- Kulturtechnik, Karlsruhe, pp. 415-430.
- Berndtsson R., Larson M. 1987. Spatial variability of infiltration in semi-arid environment. *Journal of Hydrology*, Vol. 90: 177-133.
- Beven K.J. 2002. Runoff generation in semi-arid areas. In: Bull L.J., Kirkby M.J. (eds.), *Dryland Rivers- Hydrology and geomorphology of semi-arid channels*. John Wiley & Sons, Chichester, pp57-105.
- Beven K.J., Moore I.D. 1993. *Terrain Analysis and Distributed Modelling*. John Wiley, Chichester, England.
- Beven K.J. 1985. Distributed models. In: Anderson M.G. & Burt T.P. (eds.), *Hydrological Forecasting*, John Wiley & Sons, Chichester, pp405-435.
- Black P.E. 1991. *Watershed hydrology*. Prentice Hall, London, UK, 408p.
- Blosch G., Sivapalan M. 1995. Scale issues in hydrological modelling- a review. *Hydrological Processes*, Vol. 9: 251- 290.
- Casenave A., Valentin C. 1992. A runoff capability classification system based on surface features criteria in semi-arid of West Africa. *Journal of Hydrology*, Vol. 130: 231-249.
- Duckstein L. 1974. Trade-off between models and information in river basin planning. Fall annual meeting of AGU, San Francisco, USA.
- ESRI. 1997. *Understanding GIS: The Arc/Info method*. Environmental System Research Institute Inc., USA.
- Gupta V.K., Rodriguez-Iturbe I., Wood E.F. 1986. Scale problems in hydrology: Runoff generation and basin response. Dordrecht u.a., Reidel, The Netherlands.



- Haan C.T., H. P. Johnson, D. L. Brakensiek (eds.). 1982. Hydrologic Modelling of Small Watersheds. ASAE Michigan, USA.
- Hatfield J.L., Allen R.G. 1995. Evapotranspiration estimates under deficient water supplies. *Journal of Irrigation and Drainage Engineering*, Vol. 122, No. 5: 301- 308.
- Horton R.E. 1933. The role of infiltration in the hydrologic cycle. *Geophysical Union Transactions*, Vol. 14: 446-460.
- Jackson T.J. 1982. Application and selection of hydrologic models. In Haan C.T., H. P. Johnson, D. L. Brakensiek (eds.), *Hydrologic Modelling of Small Watersheds*. ASAE Michigan, USA.
- Jennings M.E., Shearman J.O., Bauer D.P. 1976. Selection of streamflow and reservoirs-release models for river quality assessment. USGS, Reston, No. 715E.
- Kisiel C.C., Dukstein L., Fogel M.M. 1971. Analysis of ephemeral flow in dry-lands. *Journal of Hydraulics Division*, Vol. 97: 1699-1717.
- Kite G.W., Kauwen N. 1992. Watershed modelling using land classification. *Water Resources Research*, Vol. 28, No. 12: 3193- 3200.
- Knighton A.D., Nanson G.C. 1997. Distinctiveness, diversity and uniqueness of arid zone river systems. In: Thomas D.S.G. (ed.), *Arid Zone Geomorphology*. John Wiley & Sons, Chichester, pp185-203.
- Lane L.J. 1982. Distributed model for small semiarid watershed. *Journal of Hydraulics Engineering*, Vol. 108, No. 10: 1114-1131.
- Lange J., Leibundgut C., Greenbaum N., Schick A.P. 1999. A non-calibrated rainfall-runoff model for large arid catchments. *Water Resources Research*, Vol. 35, No. 7: 2161-2172.
- Larson C.L., Onstad C.A., Richardson H.H., Brooks K.N. 1982. Some particular watershed models. In: Haan C.T., Johnson H.P., Brakensiek D.L. (eds.), *Hydrologic Modelling of Small Watersheds*, American Society of Agricultural Engineers, 533p.
- Leibundgut Ch. 1975. Tracer technology for hydrological systems. IAHS Publ. 199, 311p.
- Lovell R.E. 1975. Hydrological model selection in decision making context. Technical Report 26, Dept. of Hydrology and Water Resources, University of Arizona, Tucson, USA.
- Maidment D.R. 2002. Arc Hydro GIS for water resources. Environmental System Research Institute, Reedlands, 203 pp .
- McCuen R.H. 1989. Hydrologic analysis and design. Prentice Hall, Englewood Cliffs, New Jersey.

- Mengelkamp H.-T., Warrach K., Raschke E. 1997. A land surface scheme for atmospheric and hydrological models. GKSS-Forschungszentrum, Geesthacht, Germany, 40p.
- Merwade V., Maidment D.R. 2002. Hydrological modelling. In : Maidment D.R. (ed.), Arc Hydro GIS for water resources. ESRI, Reedlands, USA.
- Miller R. L., Kahn J.S. 1962. Statistical analysis in the geological science. John Wiley, London.
- Moore I.D., Grayson R.B., Ladson A.R. 1993. Digital terrain modelling: A review of hydrological, geomorphological and biological applications. In: Beven K.J., Moore I.D. (eds.), Terrain Analysis and Distributed Modelling. John Wiley, Chichester, England.
- Pilgrim D.H., Chapman T.G., Doran D.G. 1988. Problems of rainfall-runoff modelling in arid and semi-arid regions. Hydrological Sciences Journal, Vol. 34, No. 4, pp379-400.
- Podobnikar T., Stancic Z., Ostir K. 2000. Data integration for the digital terrain model production. ISPRS Working Group VI/3, Ljubljana, 2-5 February. <http://www.zrc-sazu.si/pic/pub/dtm2/isprs.pdf>
- Renard K.G., Rawls W.J., Fogel M.M. 1982. Currently available models. In: Haan C.T., Johnson H.P., Brakensiek D.L. (eds.), Hydrologic Modelling of Small Watersheds, American Society of Agricultural Engineers, 533p.
- Schumann A.H. 1993. Development of conceptual semi-distributed hydrological models and estimation of their parameters with the aid of GIS. Journal of Hydrological Sciences, Vol. 38, No. 6: 519- 528.
- Shrama, K.D., Murthy J.S.R. 1995. Hydrologic routing of flow in arid ephemeral channels. Journal of Hydraulic Engineering, Vol. 121, No. 6: 466-471.
- Singh V.P. (ed.) 1995. Computer models of watershed hydrology. Water Resources Publications, Colorado, 1130p.
- Soman M.K., Krishnakumar K. 1990. Some aspects of daily rainfall distribution over India during the south-west monsoon season. International Journal of Climatology, Vol. 10: 299-311.
- Subramanya K. 1994. Engineering Hydrology. Tata McGraw-Hill New Delhi.
- Schultz G.A., Engman E.T. 2000. Remote sensing in hydrology and water management. Springer Verlag, Berlin.
- USGS. 2000. US Geo-data digital elevation models. US Geological Survey, download <http://erg.usgs.gov/isb/pubs/factsheets/fs04000.pdf> Fact sheet 040-00, April 2000.
- USGS. 1986. Urban hydrology for small watersheds. TR-55, US Department of Agriculture.

- Valentin C., Bresson L.M. 1992. Morphology, genesis and classification of soils in loamy and sandy soils. *Geoderma*, Vol. 55: 225- 245.
- Weber J., Kisiel C.C., Duckstein L. 1973. On the mismatch between data and models of hydrologic and water resources systems. *Water Resources Bulletin*, Vol. 9, No. 6:1075-1088.
- Woolhiser D.A., Brakensiek D.L. 1982. Hydrologic system synthesis. In Haan C.T., H. P. Johnson, D. L. Brakensiek (eds.), *Hydrologic Modelling of Small Watersheds*. ASAE Michigan, USA.
- Yair A. and H. Lavee. 1985. Runoff Generation in Arid and Semi-arid Zones. In: Anderson M.G. and Burt T.P. (Eds.) *Hydrological Forecasting*. John Willey & Sons Ltd.. pp 183-220.
- Ye W., Bates B.C., Viney N.R., Sivapalan M., Jakeman A.J. 1997. Performance of conceptual rainfall-runoff models in low-yielding ephemeral catchments. *Water Resources Research*, Vol. 33, No. 1: 153- 166.

#### **8.4 References for chapter 4**

- Baban S.M.J. 1997. Potential applications of satellite remote sensing and GIS in maximising the use of water resources in middle east: Examining Iraq as case study. *IAHS Publ.* 242, pp23-32.
- Bhaskar N.R., James W.P., Devulapalli R.S. 1992. Hydrologic parameters estimation using GIS. *J. of Water Resources Planning and Management*, Vol. 118, No. 5:492-512.
- Belz S. 2000. Nutzung von Landsat TM Daten zur Ermittlung hydrologischer Parameter. Heft 206, Institut für Wasserwirtschaft und Kulturtechnik, University of Karlsruhe, Germany.
- Biftu G.F., Gan T.Y. 2001. Semi-distributed physically based hydrologic modelling of the Paddle river basin Alberta using remote sensing data. *Journal of Hydrology*, Vol. 244: 137- 156.
- Campbell J.B. 1996. *Introduction to remote sensing*. Guilford Press, New York.
- Carlotto M.J. 1998. Spectral shape classification of Landsat-TM imagery. *ISPRS Journal of Photogrammetric and Remote Sensing*, Vol. 64, No. 9: 905- 913.
- Castleman K.R. 1996. *Digital image processing*. Prentice Hall, New Jersey.

- Cheng T., Molenaar M. 1998. The identification and monitoring of objects with fuzzy spatial extent. In: Schenk T. and Habib A. (eds.), Object recognition and scene classification from multi-spectral and multi-sensor pixels, ISPRS commission, Ohio, July 1998, pp. 207- 212.
- Congalton R. 1991. A review of assessing the accuracy of classification of remotely sensed data. *Remote Sensing of Environment*, Vol. 37: 35- 46.
- Crist E.P., Cicone R.C. 1984. Application of the Tasseled Cap concept to simulate Thematic mapper data. *Photogrammetric Engineering and Remote Sensing*, Vol. 50, No. 3: 343- 352.
- Dobson M.C., Ulaby F.T., Letoan T., Beaudoin A., Kasischke E.S. Christensen N. 1992. Dependence of radar backscatter on coniferous forest biomass. *IEEE Transaction on Geosciences and Remote Sensing*, Vol. 30, No. 2:412-415.
- ERDAS. 1997. ERDAS field guide. ERDAS International, Atlanta, USA.
- Fluegel W.A. 1995. Delineating hydrological response units by GIS analysis for regional hydrological modelling using PRMS/MMS in the drainage basin of the river Broel, Germany. *Hydrological Processes*, Vol. 9: 423- 436.
- Foody G.M. 1992. On the compensation for change agreement in image classification accuracy assessment. *Photogrammetric Engineering and Remote Sensing*, Vol.58, No.10 :1459-1560.
- Gibson P.J., Power C.H. 2000. *Introductory remote sensing: Digital image processing and applications*. Routledge, London.
- Gomer D., Vogt T. 2000. Physically based modelling of surface runoff and soil erosion under semi-arid Mediterranean conditions. In: Schmidt J. (ed.), *Soil Erosion- Application of Physically Based Models*, Springer Verlag, Berlin, pp59-78.
- Hsieh P., Landgrebe D.A. 1998. Linear feature extraction for multi-class problems. *International Geo-science and Remote Sensing Symposium*, Seattle, Washington, July 6-10.
- Kettig R.L., Landgrebe D.A. 1976. Classification of multi-spectral image data by extraction and classification of homogeneous objects. *IEEE Transactions on Geoscience Electronics*, Vol. 14, No. 1:19-26.
- Landgrebe D.A. 2003. *Signal theory methods in multi-spectral remote sensing*. John Wiley & Sons, New York.

- Landgrebe D.A. 1997. On information extraction principles for hyper-spectral data. SECE, Purdue University, West Lafayette.
- Landis J.R., Koch G.G. 1977. The measurement of observer agreement for categorical data. *Biometrics*, Vol. 33: 159-174.
- Lee C., Landgrebe D.A. 1993. Feature extraction based on decision boundaries. *IEEE transactions on Pattern Analysis and Machine Intelligence*, Vol. 15, No. 4:388-400.
- Lillesand T.M., Kiefer R.W. 2000. Remote sensing and image interpretation. John Wiley & Sons, New York, USA.
- Meijerink A.M.J., Mannaerts C.M.M. 2000. Introduction to general aspects of water management with the aid of remote sensing. In: Schultz G.A., Engman E.T. (eds.) *Remote sensing in hydrology and water management*. Springer Verlag, pp329-348.
- Mohan S. and Shrestha M.N. 2000. A GIS based integrated model for assessment of hydrological changes due to land use modifications. In proceedings: Lake 2000, Indian Institute of Science, Bangalore, November 27-29, 2000.
- Ott M., Su Z., Schumann A.H., Schultz G.A. 1991. Development of a distributed hydrological model for flood forecasting and impact assessment of land use change in the Mosel river basin. IAHS Publication 201, Vienna, Austria.
- Randy-Keller G., Harder V., Seeley J. 2003. Getting started with remote sensing. Internet download, May 2003. <http://nasa.utep.edu/paces/>
- Richards J.A. 1993. Remote sensing digital image processing: An introduction. Springer Verlag, Berlin.
- Salama R.B., Tapley I., Ishii T., Hawkes G. 1994. Identification of areas of recharge and discharge using Landsat-TM satellite imagery and areal photography mapping techniques. *Journal of Hydrology*, Vol. 162 :119-141.
- Schultz G.A. 2000. Potential of modern data types for future water resources management. *Water International, IWRA*, Vol. 25, No. 1:96-109.
- Schultz G.A. 1993. Application of GIS and remote sensing in hydrology: HydroGIS 93: IAHS Publication 211, Vienna, Austria.
- Schumann A.H. 1995. Remote sensing for parameterisation of hydrological models. *Sistema Terra: IV*, No. 3: 48-52.
- Schumann A.H. 1993. Development of conceptual semi-distributed hydrological models and estimation of their parameters with the aid of GIS. *J. of Hydrological Sciences*, Vol. 38, No. 6: 519-528.

- Sabins F.F. 1997. Remote sensing- Principles and interpretation. W.H. Freeman and Company, New York. 499 pp.
- Tauer W., Humborg G. 1992. Runoff irrigation in the Sahel Zone. CTA, Ede, The Netherlands.

### 8.5 References for chapter 5

- Ahmed S., de-Marsily G. 1993. Cokriging estimation of aquifer transmissivity as indirect solution of the inverse problem- a practical approach. *Water Resources Research*, Vol. 29: 521- 530.
- Anderson M.L., Chen Z.Q., Kavvas M.L., Feldman A. 2002. Coupling HEC-HMS with atmospheric models for prediction of watershed runoff. *Journal of Hydrologic Engineering*, Vol. 7, No. 4 : 312-318.
- Bardossy A., Stehlik J., Caspary H-J. (2002). Automated objective classification of daily circulation patterns for rainfall and temperature downscaling based on optimised fuzzy rules. *Climate Research*, Vol. 23 :11-22.
- Bardossy A., Stehlik J., Caspary H-J. (2001). Generating of areal precipitation series in the upper Neckar catchment. *Phys. Chem. Earth (B)*, Vol. 26, No. 9: 683-687.
- Bardossy A., van Mierlo J.M.C. 2000. Regional precipitation and temperature scenarios for climate change. *Hydrological Sciences Journal*, Vol. 45, No. 4: 559-575.
- Bogardy I., Matyasovszky I., Bardossy A., Duckstein L. (1994). A hydro-climatological model of areal droughts. *Journal of Hydrology*, Vol. 153 :245-264.
- Bardossy A., Plate E.J. (1992). Space-time model of daily rainfall using atmospheric circulation patterns. *Water Resources Research* Vol. 28, No. 5: 1247-1259.
- Clark C.O, Cole J.E., Webster P.J. (1999). Indian ocean SST and Indian summer rainfall: Predictive relationships and their decadal variability. *Journal of Climate*, Vol. 13, No. 14: 2503-2519.
- Clarke M.P., Hay L.E., McCabe G.J., Leavesley G.H., Serreze M.C., Wilby R.L. 2001. The use of weather and climate information in management of water resources in the western United States. *Proceedings of the Special Conference on Climate Variability and Water Resources*, NOAA, Boulder, USA.
- DWC. 2003. Climate changes and water rules. *Dialogue on water and climate*, Delft, The Netherlands.

- Fuentes U. and Heimann D. 2000. An improved statistical downscaling scheme and its application to the Alpine precipitation climatology. *Theoretical and Applied Climatology*, Vol. 65: 119-135.
- Goodess C.M. (2000). Rainfall scenarios for Mediterranean sites using a circulation-type approach to downscaling. Ph.D. thesis, University of East Anglia, 428p.
- Goodess C.M., Palutikof J.P. (1998). Development of daily rainfall scenarios for south-east Spain using circulation type approach to downscaling. *International Journal of Climatologic*, Vol. 18: 1051-1083.
- Gowarikar V., Thapliyal V., Sarkar R.P., Mandal G.S., Sen Roy N., Sikka D.R. 1989. Parametric and power regression models: New approach to long range forecasting of monsoon rainfall in India. *Mausam*, Vol. 40: 115-122.
- Gowarikar V., Thapliyal V., Kulshrestha S.M., Mandal G.S., Sen Roy N., Sikka D.R. 1991. A power regression model for long range forecast of south-west monsoon rainfall over India. *Mausam*, Vol. 42: 125-130.
- Gutowski W.J., Wilby R., Hay L.E., Anderson C.J., Arritt R.W., Clark M.P., Leavesley G.H., Pan Z., Silva R., Takle E.S. (1999). Statistical versus dynamic downscaling for hydrologic analysis. In: *Workshop on Regional Climate Prediction and Downscaling Techniques for South America*, Petropolis, Brazil.
- Hulme M. (1991). An intercomparison of model and observed global precipitation climatologies. *Geophysical Research Letters*, Vol. 18: 1715-1718.
- IPCC. 2001. *Climate change- impacts, adaptation and vulnerability. 3<sup>rd</sup> Assessment Report of the Intergovernmental Panel on Climate Change*, Cambridge University Press, UK.
- IPCC. 1998. *The regional impacts of climate change- an assessment of vulnerability. Assessment Report of the Intergovernmental Panel on Climate Change*, Cambridge University Press, UK.
- Kunstmann H., Stadler C. 2003. Coupled high resolution meteorological-hydrological simulations for the alpine catchment of the river Mangfall. *Hydrologie und Wasserbewirtschaftung*, Vol. 47, No. 4: 151-159.
- Osborn T.J., Hulme M. 1997. Evaluation of the daily precipitation characteristics of AMIP atmosphere model simulations over Europe. *Journal of Climate*, Vol. 10: 1885-1908.
- Salathe E.P. 2003. Comparison of various precipitation downscaling methods for the simulation of stream flow in a rain shadow river basin. *International Journal of Climatology*, Vol. 23: 887-901.

- Siddiq E.A. (1999). Rainfall prediction for rice growing areas. In : Abrol Y.P. and Gadgil S. (eds.), *Rice in a variable climate*, APC Publication Delhi, pp.107-123.
- Stehlik J., Bardossy A. (2002). Multivariate stochastic downscaling model for generating daily Rainfall series based on atmospheric circulation. *Journal of Hydrology*, Vol. 256: 120-141.
- Uvo C.B., Olsson J., Morita O., Jinno K., Kawamura A., Nishiyama K., Koreeda N. and Nakashima T. 2001. Statistical atmospheric downscaling for rainfall estimation in Kyushu Island, Japan. *Hydrology and Earth System Sciences*, Vol. 5, No. 2: 259-271.
- Von Storch H., Bruce H., Mearns L. 2000. Review of empirical downscaling techniques. In: *Proceedings ReClim Spring Seminar*, Jevnaker, Norway, 8-9 May, pp1-22.
- Wilby R.L. 2001. Downscaling summer rainfall in the UK from north Atlantic ocean temperatures. *Hydrology and Earth System Sciences*, Vol. 5, No. 2: 245-257.
- Wilby R.L., Wigley M.L. 2000. Downscaling general circulation model output: A reappraisal of methods and limitations. In: Sivakumar M.V.K. (Ed.), *Climate Prediction and Agriculture*, START/WMO workshop Geneva, Switzerland, 27-29 September 1999.
- Wilby R.L., Wigley M.L. 1997. Downscaling general circulation model output: A review of methods and limitations. *Progress in Physical Geography*, Vol. 21: 530-548.
- Wilby R.L., Wigley M.L., Conway D., Jones P.D., Hewitson B.C., Main J. and Wilks D.S. (1998a). Statistical downscaling of general circulation model output: a comparison of methods. *Water Resources Research*, Vol. 34, No. 11: 2995-3008.
- Wilby R.L., Hassan H., Hanaki K. (1998b). Statistical downscaling of hydro-meteorological variables using general circulation model output. *Journal of Hydrology*, Vol. 205: 1-19.
- Wilby R.L., Hay L.E., Gutowski W.J., Arritt R.W., Tackle E.S., Pan Z., Leavesley G. H. and Clark M.P. (2000) Hydrological responses to dynamically and statistically downscaled climate model output. *Geophysical Research Letters*, Vol. 27:1199-1202.
- Woolhiser D.A., Roldan J. 1982. Stochastic daily precipitation models- A comparison of distribution of amounts. *Water Resources Research*, Vol.18, No. 5: 1461-1468.
- Yoshino M. 1975. *Climate in a small area*. University of Tokyo Press.

### **8.6 References for chapter 6**

- Abdulrazzak M.J. and Sorman A.U. 1994. Transmission losses from ephemeral stream in arid zone. *Journal of Irrigation and Drainage Engineering*, Vol. 120(3) : 669-675.



- Abbott M., Bathurst J.C., Cunge J.A., O'connell P.E., Rasmussen J. 1986. An introduction to the European Hydrologic System. 1- The history and philosophy of a physically based distributed modelling system. *Journal of Hydrology*, Vol. 87: 45-59.
- Abbott M., Bathurst J.C., Cunge J.A., O'connell P.E., Rasmussen J. 1986a. An introduction to the European Hydrologic System. 1- The history and philosophy of a physically based distributed modelling system. *Journal of Hydrology*, Vol. 87: 61-77.
- ACE. 2000. Hydrological modelling system. US Army Corps of Engineers, Technical reference manual, March 2000.
- Bergstrom S. 1995. The HBV model. In: Singh V.P. (ed.), *Computer Models of Watershed Hydrology*, Water Resources Publications, Colorado, USA. Pp443-476.
- Beven K. 2002. Runoff generation in semi-arid areas. In: Bull L.J., Kirkby M.J. (Eds.), *Dryland River- Hydrology and Geomorphology of Semi-arid Channels*. John Wiley & Sons, Chichester, UK, pp. 57-105.
- Beven K. 1985. Distributed models. In: Anderson M.G. and Burt T.P. *Hydrological Forecasting*. John Willey and Sons, New York, pp. 405-435.
- Beven K. 1983. Surface water hydrology: Runoff generation and basin structure. *Rev. of Geophysics*, 21(3): 721-729.
- Bogena H. 2001. Analysing and modelling solute and sediment transport at different spatial and temporal scales. Ph.D. thesis, University of Bonn, Germany, 182p.
- Chow V.T.; Maidment D.R.; Mays L.R. 1988. *Applied hydrology*. McGraw-Hill Book Company, New York.
- Cunge J.A. 1969. On the subject of a flood propagation method. *Journal of Hydrological Research*, Vol. 7: 205- 230.
- CSRE. 2001. GRAM++ GIS Modules. Indian Institute of Technology Bombay, India.
- De Roo A.P.J. 1998. Modelling runoff and sediment transport in catchments using GIS. *Hydrological Processes*, Vol. 12, No. 6: 905- 922.
- Dunne T. 1982. Models of runoff processes and their significance. *Scientific basis of water resources management*, National Academy Press, Washington, 17-30.
- Dunne T. 1978. Field studies on hill-slope flow process. In: Kirkby M.J.(ed.), *Hill-slope Hydrology*, John Wiley & Sons, pp. 227-293.
- Flügel W.A. 1995. Delineating hydrological response units by geographical analysis for regional hydrological modelling using PRMS/MMS in the drainage basin of the River Bröl, Germany. *Hydrological Processes*, Vol. 9: 423-436.

- Fread D.L. 1985. Channel routing. In: Anderson M.G. and Burt T.P. (eds.), *Hydrological Forecasting*. John Wiley & Sons, New York, p 437-503.
- Ghate S.R., Witeley H.R. 1977. *GAWSER model users manual*. University of Guelph, Guelph, Canada, TR: 126- 137.
- Gheit H., Sultan M. 2002. Construction of a hydrology model for estimating wadi runoff and groundwater recharge in eastern desert, Egypt. *Journal of Hydrology*, Vol. 263: 36-55.
- James L.D. and Burges S.J. 1982. Selection, calibration and testing of hydrologic models. In: *Hydrologic modelling of small watersheds*, C.T. Haan, H.P. Johnson, D.L. Brakensiek (eds.), American Society of Agricultural Engineers, St. Joseph, Michigan, Monograph 5, pp. 435-472.
- Jordan P.R. 1977. Streamflow transmission losses in Western Kansas. *Journal of Hydraulics*, Vol. 103(8) : 905-919.
- Kirkby M.J. 1978. *Hill-slope hydrology*. Wiley, Chichester, UK.
- Kite G.W., Kauwen N. 1992. Watershed modelling using land classification. *Water Resources Research*, Vol. 28, No. 12: 3193- 3200.
- Kite G.W. 1995. The SLURP model. In: Singh V.P. (ed.), *Computer Models of Watershed Hydrology*, Water Resources Publications, Colorado, USA. Pp521-562.
- Kottegoda N.T., Natale L., Raiteri E. 2000. Statistical modelling of daily streamflows using rainfall input and curve number technique. *Journal of Hydrology*, Vol. 234: 170-186.
- Lange J. and Singh A.K. 2003. Water resources assessment in dry catchments by hydrological modelling adopted to limited data availability river Anas India. *Geophysical Research Abstracts*, Vol. 5, 02521, European Geophysical Society.
- Lange J. 1999. A non-calibrated rainfall-runoff model for large arid catchments, Nahal Zin, Israel. *Institute of Hydrology, Freiburg im. Br., Band 9*.
- Lange J., Leibundgut C., Greenbaum N., Schick A.P. 1999. A non-calibrated rainfall-runoff model for large arid catchments. *Water Resources Research*, Vol. 35 (7): 2161-2172.
- Lane L.J. 1982. Distributed model for small semiarid watershed. *Journal of Hydraulics Engineering*, Vol. 108, No. 10: 1114-1131.
- Lane L.J. 1982. Development of a procedure to estimate runoff and sediment transport in a ephemeral stream. In: *Recent Developments in the Explanation and Prediction of Erosion and Sediment Yield*, IAHS Publication No. 137, pp. 275-282.

- Leavesley G.H., Stannard L.G. The precipitation runoff modelling system- PRMS. In: Singh V.P. (ed.), *Computer Models of Watershed Hydrology*, Water Resources Publications, Colorado, USA. Pp281-310.
- Liu Y.B., Gebremeskel S., Smedt F.De, Hoffmann L., Pfister L. 2003. A diffusive transport approach for flow routing in GIS-based flood modelling. *Journal of Hydrology*, Vol. 283: 91-106.
- Manning J.C. 1997. *Applied principles of hydrology*. Prentice Hall, New Jersey, p. 276.
- Molnar D.K., Julien P.Y. 2000. Grid-size effects on surface runoff modelling. *Journal of Hydrological Engineering*, Vol. 5, No.1: 8-16.
- Nanson G.C., Tooth S., Knighton A.D. 2002. A global perspective on dryland rivers: Perceptions, misconceptions and distinctions. In: Bull L.J., Kirkby M.J. (eds.) *Dryland Rivers- Hydrology and Geomorphology of Semi-arid Channels*. John Wiley and Sons, Chichester, pp. 17-54.
- Nicolau J.M., Sole-Benet A., Puigdefabregas J., Gutierrez L. 1996. Effects of soil and vegetation on runoff along a catena in semi-arid Spain. *Geomorphology*, Vol. 14: 297-309.
- Ross B.B., Contractor D.N., Shanholz V.O. 1979. A finite element model of overland and channel flow for assessing the hydrological impact of land-use change. *Journal of Hydrology*, Vol. 41: 11-30.
- Sasidharan N.V., Shukla H.P. 1999. INSAT cloud images based tracks of lows and depressions during south-west monsoon season. In: Gupta R.K. and Reddy S.J. (eds.), *Advanced Technologies in Meteorology*. Tata McGraw Hill, New Delhi, p. 570.
- Sharma K.D., Menenti M., Huygen J., Fernandez P.C. 1996. Distributed numerical rainfall-runoff modelling in an arid region using TM data and a GIS. *Hydrologic Process*, 10: 1229-1242.
- Shrama K.D., Murthy J.S.R. 1995. Hydrologic routing of flow in arid ephemeral channels. *Journal of Hydraulic Engineering*, Vol. 121, Vol. 6: 466-471.
- Sharma K.D., Murthy J.S.R., Dhir R.P. 1994. Streamflow routing in the Indian arid zone. *Hydrological Processes*, Vol. 8: 27-43.
- Singh V.P. (ed.) 1995. *Computer Models of Watershed Hydrology*, Water Resources Publications, Colorado, USA.
- Singh V.P. 1988. *Hydrologic systems- Rainfall runoff modelling*. Prentice Hall, Engelwood Cliffs, New Jersey, USA.

- Sivapalan M., Takeuchi K., Franks S.W., Gupta V.K., Karambiri H., Lakshmi V., Liang X., McDonnell J.J., MENDIONDO E.M., O'CONNELL P.E., OKI T., POMEROY J.W., SCHERTZER D., UHLENBROOK S., ZEHE E. 2003. IAHS decade on predictions in un-gauged basins 2003-2012- shaping an exciting future for the hydrological sciences. *Hydrological Sciences Journal*, Vol. 48, No. 6 : 857-880.
- Sugawara M. 1995. Tank model. In: Singh V.P. (ed.), *Computer Models of Watershed Hydrology*, Water Resources Publications, Colorado, USA. Pp165-214.
- Wooldridge S.A., Kalma J.D. 2001. Regional-scale hydrological modelling using multi-parameter landscape zones and a quasi-distributed water balance model. *Hydrology and Earth System Sciences*, 51(1): 59-74.
- Woolhiser D. A. and Brakensiek D. L. 1982. *Hydrologic system synthesis: Hydrologic modelling of small watersheds*. American Society of Agricultural Engineers (ASAE), St. Joseph, Michigan.
- UNEP. 1992. *World atlas of desertification*. Edward Arnold, Sevenoaks, UK.

## ANNEX

### Annex A.1

Annex 1.1 In depth overview of decision support model reviewed

Model name	Source	Model type	Components/ Modules	Variables	Strengths/ Weaknesses
AQUA-TOOL	Andreu et al. 1996	Distributed linear model	Basin model, aquifer flow model, risk assessment model	Rainfall and discharge, channel parameters, water demand, aquifer data	Integration of all the modules under single source
FLOODSS	Todini et al. 1999	Semi-distributed simulation model	Rainfall and hydrological model, hydraulic model, set of relational tools	Meta-data, channel parameters, land use, river DEM, decision criteria	Forecasting is linked with emergency support plan within DSS
GESREU	Cruasaz et al. 1999	Conceptual institutional model	GIS thematic layers, spatial objects	Water and land management input, stakeholder	Qualitative decision analysis at different spatial scales
HYDRA	Jacucci et al. 1994	Dynamic simulation model	Agro-meteorological model, crop growth and soil water balance model	Meta-data, land use, crop data, soil type, irrigation infrastructure, ground water,	Uses sets of empirical models, useful for regions of low quality data
NELUP	Dunn et al. 1996	Linear planning model	Hydrological model, Ecological and land use model	Soil, meteorological data, land use data	Uses land cover to link hydrology
WATER-WARE	Jamieson et al. 1996	1-D simulation models	Pollution control, hydrological process, demand forecasting, water resources planning	Land use, ground water and channel flow, crop data, irrigation practices, hydraulic data and velocity	Suitable for water resources planning and irrigation demand forecasting in un-gauged catchments
Geo-Smart	Bothale et al. 2002	Thematic linear model	GIS database, query builder	Topography, terrain and socio-economic data	Develop resources management plans using user specified queries

Annex A.2**Annex 2.1** Classification of major climatic zones, agro-ecological regions and sub-regions in India

1. Arid	101. Western Himalayas: cold arid eco-region	10101. Ladakh Plateau: cold, hyper-arid eco-sub region	
	102. Western plain, Kutchh and part of Kathiawar: hot arid eco-region	10102. Northern Kashmir Himalaya: cold typical arid eco-sub region	
		10203. Marusthali: hot hyper-arid eco-sub region	
		10204. Kutchh peninsula: hot hyper-arid eco-sub region	
		10205. Rajasthan Bagar, north Gujarat and s-w Punjab plain: hot typical arid eco-sub region	
		10206. South Kutchh and North Kathiawar peninsula: hot typical arid eco-sub region	
	103. Deccan plateau: hot arid eco-region	10307. Deccan plateau: hot arid eco-sub region	
	2. Semi-arid	204. Northern plain and central highlands	20408. North Punjab plain, Ganga-Yamuna Doab and Rajasthan uplands: hot dry semi-arid eco-sub region
			20409. North Punjab plain incl. of Aravali range and East Rajasthan: hot dry semi-arid eco-sub region
			20410. Ganga-Yamuna Doab, Rohilkhand and Avadh plain: hot moist semi-arid eco-sub region
20411. Madhya Bharat pathar and Bundelkhand uplands: hot moist semi-arid eco-sub region			
205. Central (Malwa) highlands, Gujarat plains, Kathiawar peninsula: hot semi-arid dry eco-region			20512. Central Kathiawar peninsula: hot dry semi-arid eco-sub region
206. Deccan plateau: hot semi-arid eco-region		20513. Madhya Bharat plateau, western Malwa, eastern Gujarat plain, Vindhya & Satpura range, Narmada valley: hot moist semi-arid eco-sub region	
		20514. Coastal Kathiawar peninsula: hot moist semi-arid eco-sub region	
		20615. Southern western Maharashtra and north Karnataka plateau: hot dry semi-arid eco-sub region	
		20616. Central & western Maharashtra and north Karnataka plateau & N-W Telengana: hot moist semi-arid eco-sub region	
		20617. Eastern Maharashtra plateau: hot moist semi-arid eco-sub region	
207. Deccan plateau and eastern Ghats: hot arid eco-region	20618. North Sahydris and western Karnataka plateau: hot dry sub-humid eco-sub region		
	20719. South Telengana (Rayalseema) plateau and Eastern Ghats: hot dry semi-arid eco-sub region		
	20720. North Telengana plateau: hot moist semi-arid dry sub-humid eco-sub region		
	20721. Eastern Ghats (south): hot moist semi-arid dry sub-humid eco-sub region		
	208. Eastern Ghats, Tamilnadu uplands, Deccan Karnataka plateau: hot semi-arid region	20822. Tamilnadu uplands and leeward flanks of south Sahydris: hot dry semi-arid eco-sub region	
3. Sub-humid	309. Northern plain: hot semi-arid dry eco-region	20823. Central Karnataka plateau: hot moist semi-arid eco-sub region	
		20824. Tamilnadu uplands and plains: hot moist semi-arid eco-sub region	
		30925. Punjab and Rohilkhand plains: hot moist semi-arid eco-sub region	
		30926. Rohilkhand, Avadh and south Bihar plains: hot dry sub-humid eco-sub region	
		310. Central highlands (Malwa, Bundelkhand and eastern Satpura): hot semi-humid eco-region	31027. Malwa plateau, Vindhya scarpland and Narmada valley: hot dry sub-humid eco-sub region
		31028. Satpura and eastern Maharashtra plateau: hot dry sub-humid eco-sub region	
		31029. Vindhyan scarpland and Baghelkhand plateau: hot dry sub-humid eco-sub region	
		31030. Satpura range and Waiganga valley: hot moist sub-humid eco-sub region	

	311. Eastern plateau (Chhattisgarh): hot semi-humid eco-region	31131. Moderately to gently sloping Chhattisgarh/ Mahanadi basin: hot sub-humid eco-sub region
	312. Eastern plateau (Chhotanagarpur), eastern Ghats: hot semi-humid eco-region	31232. Gujarat hills, Dandakaranya and eastern Ghats: hot moist sub-humid eco-sub region 31233. Eastern Ghats: hot moist sub-humid eco-sub region 31234. Chhotanagarpur plateau and Gujarat hills: hot dry moist sub-humid eco-sub region
	313. Eastern plains: hot moist sub-humid eco-region	31335. North Bihar and Avadh plains: hot dry moist sub-humid eco-sub region 31336. Foot hills of central Himalayas: warm to moist sub-humid eco-sub region
	314. Western Himalayas: warm sub-humid eco-region	31437. South Kashmir and Punjab Himalayas: cold and warm dry semi-arid eco sub-region 31438. South Kashmir and Kumaon Himalayas: cold and warm dry semi-arid eco sub-region 31439. Himalayas: warm humid eco sub-region 31440. Kumaon Himalayas: warm humid eco sub-region 31441. Foothills of Kumaon Himalayas: warm humid eco sub-region
4. Humid/ Per humid	415. Bengal and Assam plain: Hot sub-humid to humid eco-region	41542. Bengal and Assam plain: hot sub-humid to humid eco-region 41543. Middle Brahmaputra plain: hot humid eco-sub region 41544. Teesta, lower Brahmaputra plain and Barak valley: hot moist humid to per humid eco-sub region 41545. Upper Brahmaputra plains: warm to hot per humid eco-sub region
	416. Eastern Himalayas: warm per-humid eco-region	41646. Foothills of eastern Himalayas: warm to hot per-humid eco-sub region 41647. Darjeeling and Sikkim Himalayas: pre-humid eco-sub region 41648. Arunachal Pradesh: warm to hot per-humid eco-sub region
	417. North-eastern hills: warm per-humid eco-region	41749. Meghalaya plateau and Nagaland hill: warm to hot moist humid to per humid eco-sub region 41750. Eastern range: warm to hot per humid eco-sub region
5. Coastal	518. Eastern coastal plain: hot sub-humid to semi-arid eco-region	51851. South Tamilnadu: hot dry semi-arid eco-sub region 51852. North Tamilnadu plains: hot dry semi-arid eco-sub region 51853. Andhra coastal: hot dry sub-humid eco-sub region 51854. Utkal plain and east Godavari delta: hot dry sub-humid eco-sub region 51855. Gangetic delta: hot moist sub-humid eco-sub region
	519. Western Ghats and coastal plain: hot humid to per-humid eco-region	51956. North Sahydrus and Konkan coast: hot humid eco-sub region 51957. Central and south Sahydrus: hot moist sub-humid to humid eco-sub region 51958. Konkan, Karnataka and Kerala coastal plain: hot humid to per-humid eco-sub region
6. Island	620. Islands of Andaman-Nicobar & Lakshwadeep: hot humid to per-humid island eco-region	62059. Andaman & Nicobar group of island: hot per-humid eco-sub region 62060. Lakshwadeep and groups of islands: hot humid eco-sub region

Source: Indian Council of Agriculture Research, 2001

## Annex 2.2 Average monthly flow of selected major rivers in India

River	Tapti at Kathore	Wanganga at Ashti	Krishna at Almati	Bhima at Takali	Mahi at Sevalia	Godavari at Dhalegaon	Damodar at Rhondia	Narmada at Jamtara	Sabarmati at Ahmedabad
basin area [km <sup>2</sup> ]	61575	50990	36286	33916	33670	30840	19220	16576	12950
Data period	1940-79	1968-79	1971-79	1968-79	1968-79	1968-79	1934-79	1949-74	1968-79
Monthly Discharge [m <sup>3</sup> /sec]									
Jan	71.5	41.4	6.8	20.7	14.9	10.09	32.4	20.4	6.0
Feb	64.7	43.3	4.6	12.7	12.9	8.82	28.4	13.6	5.9
Mar	69.5	23.4	3.0	8.6	26.9	5.09	23.3	9.0	4.6
Apr	67.3	12.2	2.3	3.4	10.8	2.36	21.3	5.3	3.4
May	63.4	9.5	17.0	9.2	7.1	1.55	37.2	1.8	1.3
Jun	273.5	290.7	547.2	98.3	172.6	65.18	195.4	56.4	13.9
Jul	1035.3	1726.7	2339.1	528.5	719.0	274.82	698.5	764.6	47.1
Aug	1941.5	3305.6	2106.4	916.6	1667.1	466.73	1038.5	1397.7	137.5
Sep	1634.6	2075.6	1078.8	757.8	1802.7	480.36	941.4	1100.3	117.5
Oct	384.8	520.9	385.2	356.0	101.8	147.82	398.6	197.2	28.8
Nov	156.4	162.6	90.1	79.0	33.7	23.00	95.4	49.6	17.1
Dec	109.1	69.2	26.6	44.3	21.3	29.91	45.0	28.6	7.1
JS	m <sup>3</sup> 4611.5	7108.0	5524.4	2203.0	4188.8	1221.91	2678.5	3262.7	302.2
	/s								
	% 78.5	85.8	83.6	77.7	<b>91.2</b>	80.6	75.3	89.5	77.3
JO	m <sup>3</sup> 4996.3	7628.9	5909.6	2559.0	4290.6	1369.73	3077.0	3459.9	331.1
	/s								
	% 85.1	<b>92.1</b>	89.4	<b>90.2</b>	<b>93.5</b>	<b>90.4</b>	86.5	<b>94.9</b>	84.7

Source: Monthly river flow data obtained from <http://dss.ucar.edu/datasets>. Acronyms JS and JO refers to flow duration June-September and June-October respectively.

## Annex 2.3 Scenario narratives and definition of terms used under section 2.1.4

The digital atlas of the World Water Balance developed at the Centre for Research in Water Resources of the University of Texas at Austin features a compilation of global climate data in GIS format, for use in characterising the water balance of earth. The World Water and Climate Atlas developed at International Water Management Institute (IWMI) at Colombo, Sri Lanka is another global data source providing access to key climatic variables for agriculture and water resources management. The primary drivers used in the IMPACT-WATER model (Rosegrant et. al. 2000) for various scenarios are:

- Economic and demographic drivers including population growth, rate of urbanisation, rate of growth of GDP.
- Climate and hydrological parameters include rainfall, runoff, evapotranspiration, and groundwater recharge.
- Technological, management and infrastructure drivers include river basin efficiency, reservoir storage, water withdrawal capacity, potential physical irrigated area and crop yield.
- Policy drivers include water prices, water allocation priorities among sectors, committed water flows for environmental purposes, inter-basin water shares, commodity price policy as defined by taxes and subsidies.

The three scenarios can be described as:

- The business-as-usual (BAU) assumes a continuation of current trends and existing plans in water and food policy, management and investment.
- The water crisis scenario (CRI) examines the impact of a deterioration of current trends in water, food policy and investment. Moderate deterioration of many of these trends builds sufficiently to tip the scale to genuine water crisis.
- The sustainable water use scenario (SUS) explores the potential for dramatically increasing environmental water allocations and achieving full connection of all urban households to piped water and higher per capita domestic water consumption, while maintaining food production at business-as-usual level.



Annex A.3

## Annex 3.1

The following AML algorithm in Arc/Info has been used for projecting the survey of India decimal degree maps coordinate system to Universal Transverse Mercator (UTM) for zone 43.

```

/* Geographic Decimal Degree -> UTM Zone43
INPUT
projection geographic
units dd
parameters
OUTPUT
projection UTM
units meters
zone 43
parameters
END

```

## Appendix 3.2 Map elevation vs. DEM elevation

Point ID	UTM coordinates		Map elevation [m]	DEM elevation [m]	$(X_h - D_h)^2$
	X- coordinate	Y- coordinate	$X_h$	$D_h$	
93	473488.60	2537651.40	396.00	393.20	7.84
137	478177.60	2534628.50	470.00	470.00	0.00
154	466034.30	2532739.10	351.00	351.10	0.01
157	461328.30	2531519.70	331.00	331.20	0.04
161	453915.90	2530349.70	301.00	300.50	0.25
188	449420.00	2527953.30	313.00	310.80	4.84
192	458243.90	2525391.10	303.00	303.10	0.01
193	461103.30	2524716.50	335.00	330.00	25.00
204	469005.80	2527552.10	397.00	396.50	0.25
208	471977.20	2526057.80	444.00	442.90	1.21
211	478641.30	2527655.10	482.00	475.50	42.25
212	481320.70	2529733.40	507.00	504.20	7.84
284	442160.20	2513502.40	337.00	336.10	0.81
290	443929.30	2519428.00	330.00	329.90	0.01
301	460346.60	2516627.60	323.00	322.60	0.16
309	465069.40	2519367.40	390.00	390.00	0.00
311	469948.80	2519863.20	446.00	443.70	5.29
317	476717.60	2515013.90	465.00	463.90	1.21
353	480994.40	2510616.90	532.00	531.50	0.25
355	475841.70	2508779.10	481.00	479.50	2.25
365	467287.30	2513366.00	390.00	389.50	0.25
367	464939.00	2508956.30	368.00	368.30	0.09
379	453066.80	2511630.30	389.00	387.80	1.44
381	448446.50	2510342.10	365.00	363.30	2.89
389	439274.70	2508487.10	412.00	411.70	0.09
413	443895.00	2505636.00	376.00	375.30	0.49
418	450833.90	2502784.80	371.00	370.40	0.36
421	457223.30	2502733.30	430.00	426.20	14.44
425	464230.90	2500861.10	418.00	415.40	6.76
429	468473.30	2501342.00	517.00	514.60	5.76
435	476322.60	2502321.10	513.00	505.80	51.84
438	480101.20	2500723.70	554.00	558.80	23.04

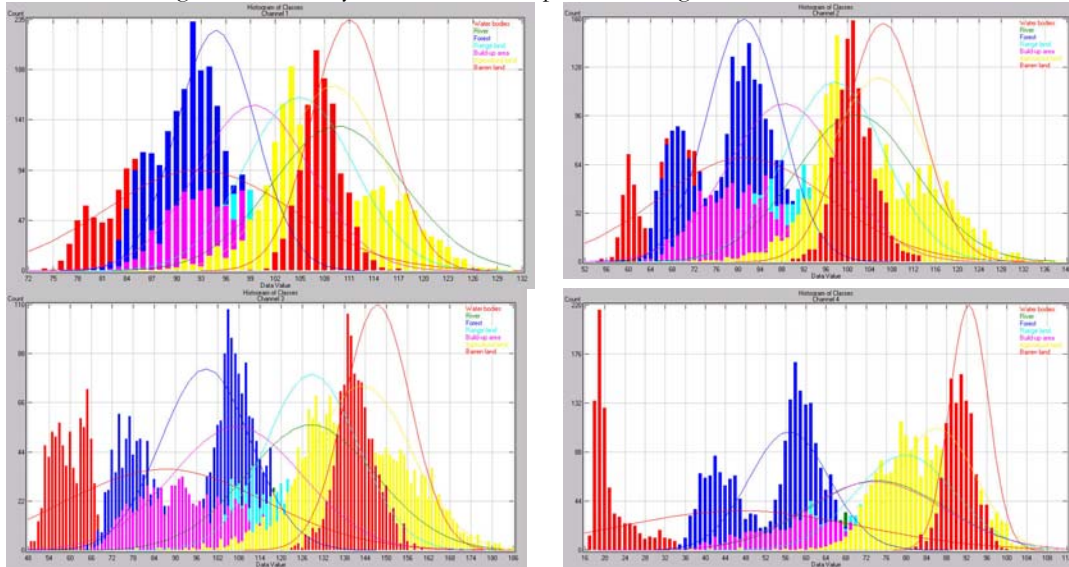
505	452328.20	2492101.50	442.00	440.50	2.25
508	444599.20	2494763.80	410.00	409.60	0.16
537	451538.10	2495330.60	404.00	403.60	0.16
552	442297.60	2489611.10	389.00	389.20	0.04
565	451469.40	2522571.10	310.00	310.00	0.00
566	458243.90	2525304.30	303.00	303.10	0.01
Root mean-square error (RMSE)					2.35

## Appendix 3.3 Comparing TIN and GRID/ Lattice

Factor	TIN	GRID/Lattice
Availability of terrain modelling data	Must be provided by user or extracted from a lattice	Generated from coverages, available from GTOPO30 database
Acceptable data source formats	Arc/Info coverages, ASCII files	ASCII files Arc/Info grids
Location of sample points	Samples located adaptively to fit the surface	Samples locations dictated by mesh point spacing
Representation of linear features	Yes	No
Allows break lines for defining surface smoothness and continuity	Yes	No
Ability to represent point samples at precise location	Yes	No, unless it happens to fall exactly on a mesh point
Ability to represent holes in the surface model where no interpolation can occur	Yes, with CLIP and ERASE polygon features	Yes, holes and mesh points outside the model are assigned the NODATA value
Allowance for samples without a z-value	No, all nodes in TIN must have a z-value	YES, mesh points without z-values are assigned the NODATA value
Cost of increasing the surface accuracy	Low, add new sample points representing important features	High, the accuracy of the surface is achieved by increasing the lattice resolution, but at the cost of increasing data redundancy
Relative number of points required to represent a surface	Few, depending in the spatial resolution of the surface	More to achieve the same degree of accuracy
Data redundancy	None	Moderate to high
Storage required for each sample point	Approx. 68 bytes (high cost per point is due to the cost of maintaining TIN topology)	Approx. 4 bytes (for floating point lattices)
How the model stored	A directory	Undefined for integer lattices.
How projection information stored	An ASCII file within the TIN directory	A directory
Computing cost of surface analysis	Moderate	An ASCII file within the GRID directory
Suitability for 3-D viewing	Must first be resampled to a lattice	Low
Types of interpolators	Linear, QUINTIC (smooth)	Lattice can be viewed directly, but can be resampled to an alternate resolution
Accuracy on the edge of the model in terms of defining the zone of interpolation	The zone of interpolation is precisely defined by the hull polygon	Bilinear
Coordinate precision	x,y double z single	The zone of interpolation is fuzzy near mesh points adjacent to NODATA mesh points
		x, y double z single or 32 bit INTEGER

Source: Arc/Info on-line help

## Annex A.4

Annex 4.1 Histogram and density function for 6<sup>th</sup> April 2000 image.

Annex 4.2 Weighted interclass distance measured between training class pairs for class separability decision making, 6th April 2000 image

Class pairs

Channels (1,2,3- visible range, 4,5- IR, 6- MIR)

	<b>6</b>	<b>5</b>	<b>3</b>	<b>2</b>	<b>1</b>	<b>4</b>
Min.	0.04	0.03	0.03	0.02	0.02	0.00
Mean	0.60	0.76	0.55	0.39	0.35	0.68
1-2	0.28	0.27	0.42	0.31	0.40	0.32
1-3	0.31	0.29	0.18	0.16	0.18	0.29
1-4	0.54	0.47	0.58	0.28	0.29	0.57
1-5	0.19	0.23	0.13	0.08	0.12	0.31
1-6	1.03	1.05	0.90	0.54	0.48	0.87
1-7	1.00	1.57	1.29	0.70	0.74	1.46
2-3	0.42	0.35	0.48	0.68	0.70	0.38
2-4	0.33	0.11	0.03	0.03	0.06	0.05
2-5	0.09	0.03	0.16	0.19	0.24	0.00
2-6	0.23	0.29	0.12	0.03	0.02	0.22
2-7	0.25	0.67	0.32	0.09	0.08	0.74
3-4	0.24	0.36	0.68	0.56	0.41	0.84
3-5	0.14	0.20	0.08	0.13	0.11	0.36
3-6	1.97	2.05	1.39	1.24	0.84	1.75
3-7	1.88	4.22	2.42	1.75	1.49	4.21
4-5	0.15	0.06	0.25	0.12	0.08	0.06
4-6	1.20	0.61	0.14	0.10	0.05	0.08
4-7	1.04	1.45	0.37	0.17	0.17	0.55
5-6	0.64	0.52	0.60	0.40	0.27	0.23
5-7	0.57	1.05	1.03	0.57	0.53	0.76
6-7	0.04	0.14	0.06	0.02	0.04	0.25

Note: for separability analysis equal weights for each class have been taken.

Class symbols: 1- water bodies, 2- river, 3- forest, 4- range land, 5- built-up area, 6- agricultural land, 7- barren land.

Annex 4.3 Separability index between training classes for 15<sup>th</sup> April 2000 image

Class name		Channel					
		<i>1</i>	<i>2</i>	<i>3</i>	<i>4</i>	<i>5</i>	<i>6</i>
Water bodies	River	0.83	0.83	0.94	0.98	0.88	0.87
	Forest	0.16	0.32	0.58	1.01	0.80	0.70
	Range land	0.43	0.57	0.82	1.30	1.11	0.90
	Built-up area	0.16	0.19	0.26	1.04	0.80	0.60
	Agriculture	0.81	0.92	1.07	1.76	1.64	1.45
River	Barren land	0.28	0.51	0.58	2.20	1.60	1.04
	Forest	0.89	0.77	0.47	0.15	0.50	0.54
	Range land	0.64	0.51	0.28	0.31	0.01	0.31
	Built-up area	0.77	0.81	0.83	0.16	0.33	0.50
	Agriculture	0.07	0.26	0.36	0.86	0.64	0.50
Forest	Barren land	0.70	0.51	0.45	1.17	0.46	0.06
	Range land	0.37	0.36	0.25	0.54	0.72	0.38
	Built-up area	0.03	0.15	0.39	0.32	0.18	0.03
	Agriculture	0.85	0.90	0.74	1.22	1.64	1.35
Range land	Barren land	0.18	0.29	0.01	1.79	1.58	0.67
	Built-up area	0.29	0.47	0.66	0.10	0.45	0.34
	Agriculture	0.64	0.70	0.61	0.61	0.86	1.06
Built-up area	Barren land	0.15	0.04	0.23	0.88	0.65	0.34
	Agriculture	0.76	0.93	1.01	0.59	1.26	1.20
Agriculture	Barren land	0.13	0.41	0.39	0.80	1.13	0.59
	Barren land	0.69	0.69	0.72	0.05	0.33	0.71

Annex 4.4 Training class performance (redistribution method) for 15<sup>th</sup> October 2000 image

Classification algorithm →	Maximum likelihood		Fisher's discriminate	linear	ECHO classifiers	
	Reference accuracy [%]	Reliability accuracy [%]	Reference accuracy [%]	Reliability accuracy [%]	Reference accuracy [%]	Reliability accuracy [%]
Class name						
Water bodies	75.3	91.4	48.8	84.8	80.6	97.2
River	39.7	49.0	15.0	35.3	57.3	95.8
Forest	72.5	73.1	73.9	64.4	81.0	91.1
Range land	52.1	87.3	40.6	84.1	60.3	94.9
Built-up area	95.1	57.4	89.5	58.2	100.0	90.9
Agriculture	45.8	44.4	50.0	42.4	79.9	83.5
Barren land	41.5	37.6	37.7	32.4	43.4	97.0
Overall class performance	61.2		53.3		72.1	
Kappa statistics	54.3		45.3		67.2	

Annex 4.5 Class distribution for image area of 15<sup>th</sup> October 2000

Classification algorithm → Class name ↓	Maximum likelihood		Fisher's discriminate	linear	ECHO classifiers	
	Total sample	%	Total sample	%	Total sample	%
Water bodies	31608	0.8	14458	0.4	20320	0.5
River	307720	7.9	70329	1.8	221838	5.7
Forest	896464	23.1	824642	21.3	681804	17.6
Range land	922139	23.8	1153080	29.8	971283	25.1
Built-up area	515740	13.3	574821	14.8	550008	14.2
Agriculture	626133	16.2	1073171	27.7	843762	21.8
Barren land	486934	12.6	20981	0.5	324921	8.4

Annex 4.6 Separability index between training classes for 6<sup>th</sup> April 2000 image

Class name		Channel					
		1	2	3	4	5	6
Water bodies	River	0.87	0.76	0.89	0.73	0.72	0.75
	Forest	0.13	0.00	0.28	0.30	0.36	0.39
	Range land	0.68	0.67	1.01	0.97	0.80	0.73
	Built-up area	0.37	0.28	0.44	0.71	0.61	0.53
	Agriculture	0.93	1.00	1.32	1.23	1.42	1.42
River	Barren land	1.14	1.12	1.60	1.63	1.77	1.36
	Forest	1.16	1.15	0.96	0.81	0.70	0.73
	Range land	0.32	0.19	0.01	0.23	0.13	0.40
	Built-up area	0.68	0.61	0.57	0.02	0.20	0.36
	Agriculture	0.04	0.21	0.45	0.55	0.61	0.48
Forest	Barren land	0.11	0.27	0.68	1.04	0.90	0.36
	Range land	0.89	1.05	1.17	1.29	0.85	0.68
	Built-up area	0.39	0.43	0.28	0.78	0.51	0.35
	Agriculture	1.29	1.57	1.16	1.87	2.03	1.99
	Barren land	1.72	1.87	2.21	3.01	3.00	1.94
Range land	Built-up area	0.41	0.48	0.67	0.26	0.13	0.10
	Agriculture	0.31	0.44	0.53	0.36	1.11	1.55
	Barren land	0.54	0.55	0.84	0.92	1.73	1.44
Built-up area	Agriculture	0.73	0.90	1.09	0.58	0.98	1.12
	Barren land	1.01	1.05	1.43	1.06	1.40	1.02
Agriculture	Barren land	0.19	0.05	0.19	0.55	0.28	0.24

Annex 4.7 Class distribution for image area of 6<sup>th</sup> April 2000 image for Anas catchment, India

Classification algorithm → Class name ↓	Maximum likelihood		Fisher's linear discriminate		ECHO classifiers	
	Total sample	%	Total sample	%	Total sample	%
Water bodies	52344	1.4	25635	0.7	28764	0.7
River	170947	4.4	30842	0.8	182523	4.7
Forest	830077	21.4	458532	11.8	609627	15.7
Range land	456985	11.8	26652	0.7	405510	10.5
Built-up area	273282	7.1	142428	3.7	511463	13.2
Agriculture	1741010	45.0	2835143	73.2	1688830	43.6
Barren land	113797	2.9	265789	6.9	51721	1.3

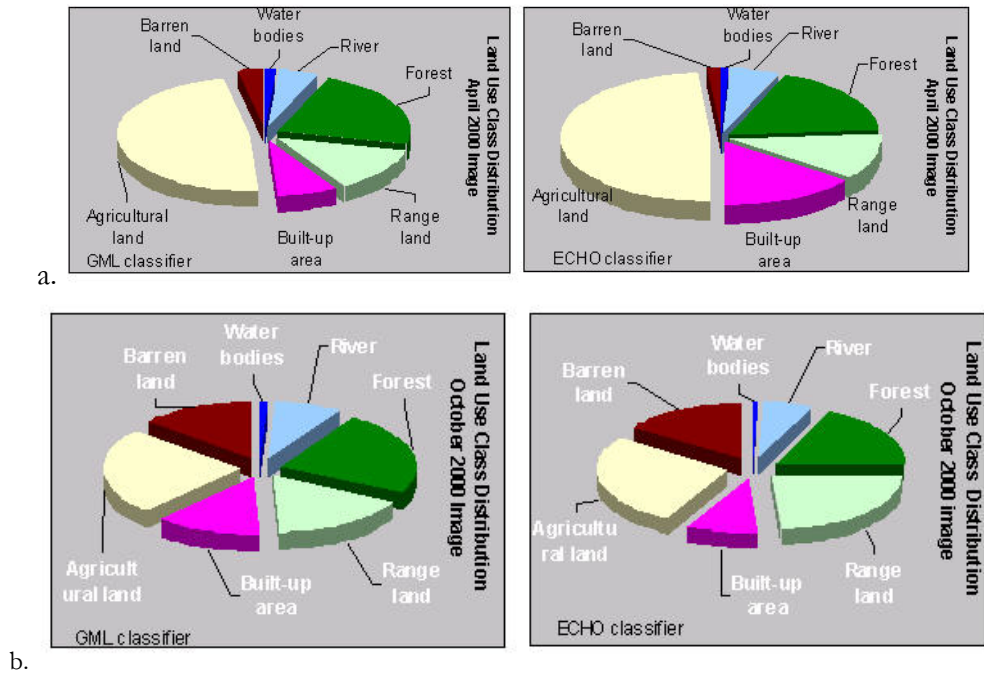
## Annex 4.8 Definition of Terms

<sup>1</sup>Feature extraction the process of studying and locating areas and objects on the ground and deriving useful information from images.

<sup>2</sup>Multi-spectral image classification is the process of identifying groups of pixels that represents a common characteristic of the image using spectral pattern recognition step (ERDAS 1997).

<sup>3</sup>False colour composite appear similar to an infrared photograph where objects do not have same colour or contrast as natural. In general false colour composite is prepared after projecting Landsat TM or ETM+ channel 4 (0.76-0.90  $\mu$  m) in red, channel 3 (0.63-0.69  $\mu$  m) in green and channel 2 (0.52-0.60  $\mu$  m) in blue. A detail on colour scheme and channel combinations is presented in table 4.1 (after Sabins 1997).

Annex 4.9 The land use class distribution using GML and ECHO classifiers a) for 6<sup>th</sup> April 2000 image and b) for 15<sup>th</sup> October 2000 image.



Annex A.5

## Annex 5.1 Comparison of main strengths and weaknesses of dynamic and statistical downscaling

Type →	<i>Dynamic downscaling</i>	<i>Statistical/empirical downscaling</i>
Strengths	10-50 km climate information from GCM-scale output Respond in consistent ways to different external forcing Resolve atmospheric processes such as orographic precipitation Consistency	Station-scale climate information from GCM-scale output Cheap, computationally undemanding and readily transferable Ensembles of climate scenarios uncertainty analysis Flexibility
Weaknesses	Dependent on the realism of GCM boundary forcing Choice of domain size and location affects results Requires significant computing power  Ensembles of climate scenarios seldom produced Initial boundary condition affect results	Dependent on the realism of GCM boundary forcing Choice of domain size and location affects results Requires high quality data for model calibration Non-stationery empirical relationships Choice of predictors affects results

Source: Compiled from various sources

## Annex 5.2 Predictor variables and techniques on downscaling daily precipitation

<i>Predictor variable(s)</i>	<i>Technique(s)</i>	<i>Source (authors)</i>
Geo-potential heights, specific humidity	Artificial neural networks	Crane and Hewitson (1998)
Sea level pressure, air flow indices	Weather classification	Goodess and Palutikof (1998)
Air flow indices	Weather classification	Wilby and Wigley (1997)
Sea level pressure anomalies	Stochastic	Katz and Parlange (1996)
Wind direction, cloud cover	Weather classification	Hay et. al. (1992)
Mean air pressure	Fuzzy based	Bardossy and Plate (1992)
Geo-potential heights, Sea level pressure, relative humidity	Principal component analysis and canonical correlation	Karl et. al. (1990)

Source: Compiled from various sources

## Annex 5.3 Topographic parameters of rain-gauge stations in Anas catchment, India

<i>Rain-gauge station</i>	<i>Station ID</i>	<i>UTM coordinates</i>		<i>Height [m] above MSL</i>
		<i>X</i>	<i>Y</i>	
Jhabua	427531	458011.03	2518470.23	333
Ranapur	427532	451584.54	2504745.49	369
Udaigarh	427533	452483.93	2492056.64	432
Amba	427534	470069.61	2505695.69	416
Rama	427535	470309.94	2518575.66	365
Meghnagar	427536	453690.90	2532890.70	315
Thandla	427529	456720.39	2543416.91	290
Bhabhra	427537	430887.00	2491134.19	375
Sardarpur	427528	498014.11	2506626.65	507
Petlabad	427527	479855.49	2543335.48	395

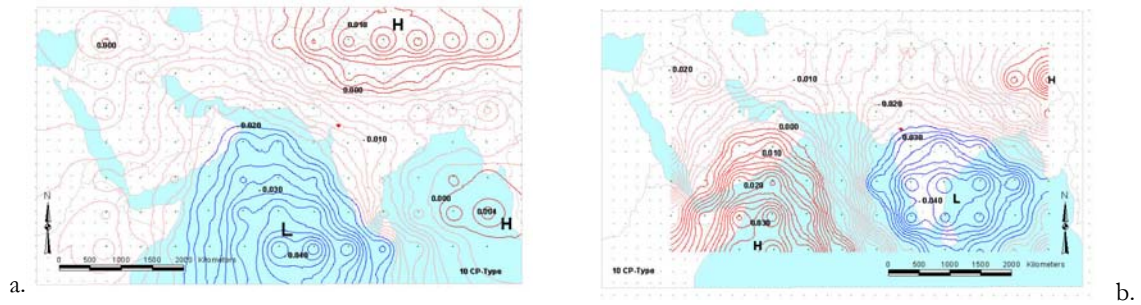
Source: Derived from GIS database of Anas catchment

Annex 5.4 Yearly frequency of CP occurrence [%] during monsoon season for 1985-94 period

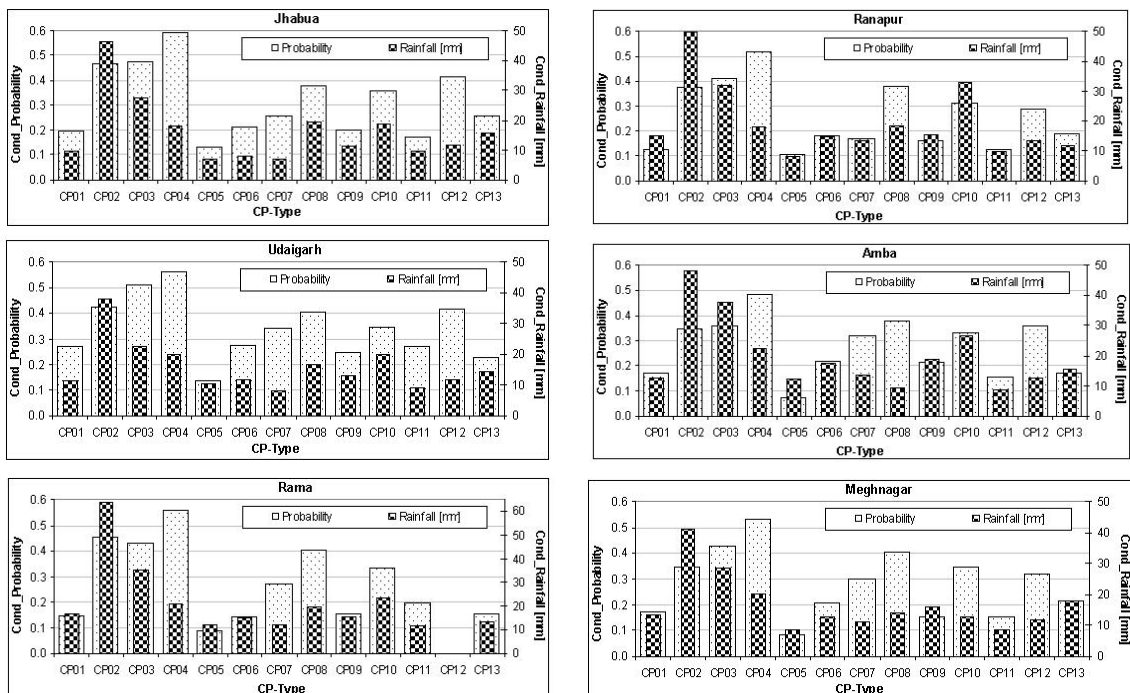
CP type	Frequency of occurrence [%]										
	1985	1986	1987	1988	1989	1990	1991	1992	1993	1994	
CP01	5.23	9.80	2.61	2.61	3.27	2.61	3.27	5.88	6.54	7.19	
CP02	2.92	5.23	5.23	12.42	6.54	21.57	9.80	8.50	6.54	3.27	
CP03	14.38	5.23	5.88	3.27	7.84	6.54	9.80	0.65	5.88	9.80	
CP04	3.27	7.84	2.61	4.58	5.23	11.11	1.31	4.58	1.31	16.34	
CP05	13.07	8.50	16.34	20.92	19.61	9.80	20.92	5.88	11.11	9.15	
CP06	20.26	23.53	11.76	3.92	7.84	16.99	13.07	17.65	28.10	16.99	
CP07	3.27	7.84	5.88	5.23	5.88	0.00	3.92	3.27	3.92	6.54	
CP08	0.65	3.27	2.61	1.31	5.23	5.88	3.27	5.88	1.96	8.50	
CP09	6.54	5.88	4.58	5.23	5.23	5.88	10.46	5.23	7.19	5.88	
CP10	2.61	3.27	15.03	17.65	15.03	5.88	5.88	18.30	9.80	7.19	
CP11	3.27	3.27	7.19	5.23	8.50	3.92	7.84	11.76	8.50	3.27	
CP12	16.99	8.50	13.07	9.15	2.61	7.19	5.88	0.00	4.58	1.31	
CP13*	6.54	7.84	7.19	6.54	7.19	2.61	4.58	12.42	4.58	4.58	

\*data which does not fall under any of these twelve CPs has been put separately into separate group.

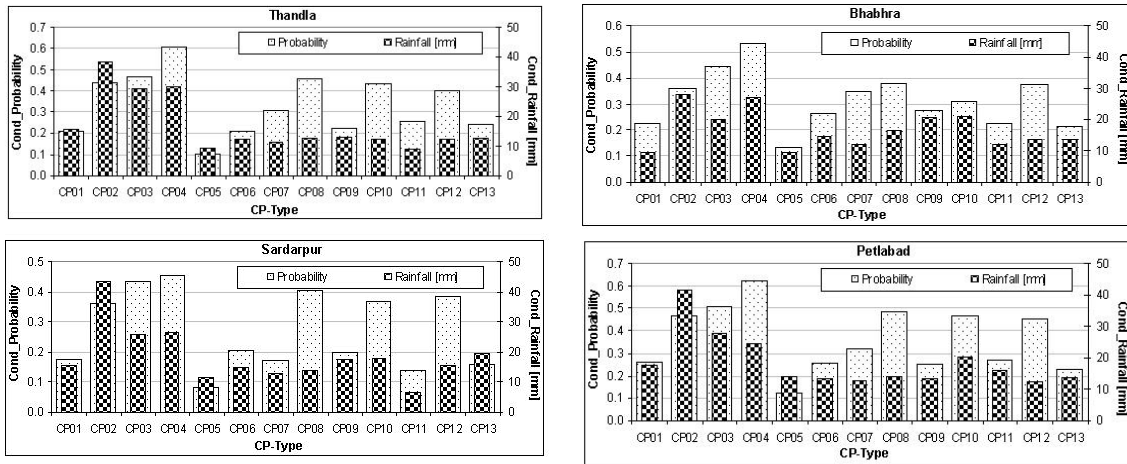
Annex 5.5 Spatial development of 500hPa geo-potential heights anomalies for a) for wet CP03 and b) for dry CP07 based 10 CP-types for Anas catchment, India.



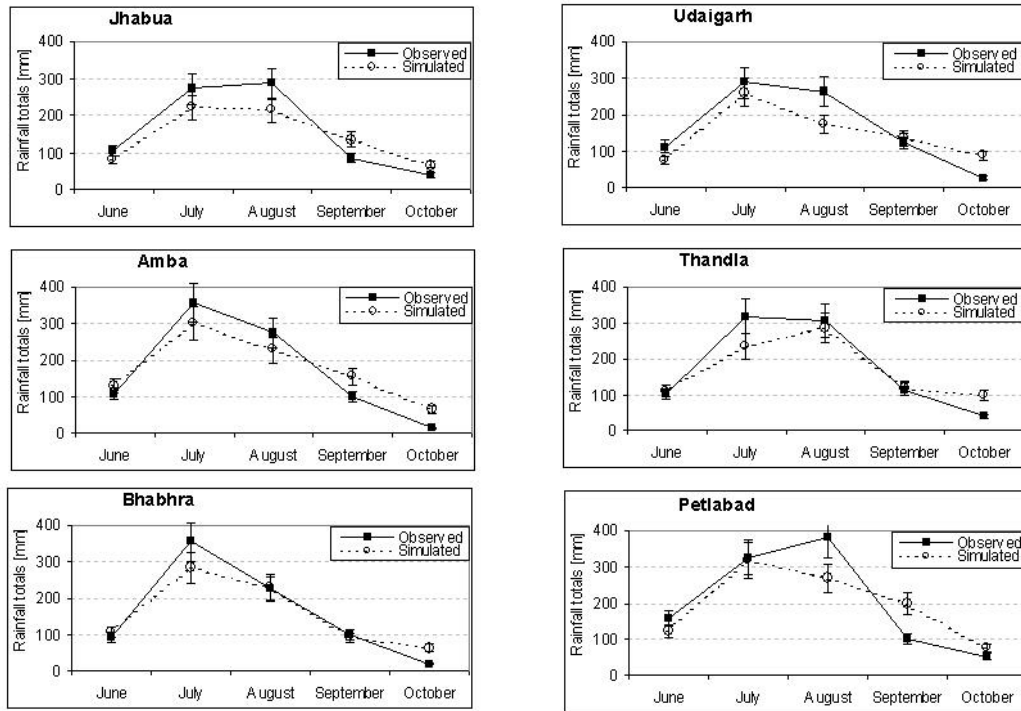
Annex 5.6 Conditional probabilities and conditional rainfall amount [mm/day] for various CP type at rainfall stations in Anas catchment







Annex 5.7 Long term mean (for 10 years) of monthly rainfall totals for observed and simulated series during 1985-94



Annex A.6

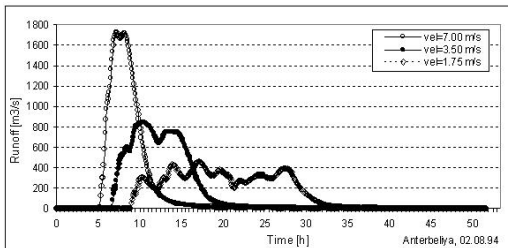
Annex 6.1 Land use classes, curve number and runoff coefficients derived from Landsat 7ETM+ satellite image of 15.11.2000

Grid_Code	Landuse name	Curve number (CN)		Runoff coefficients		Remarks
		Pervious area	Impervious area	Pervious area	Impervious area	
1.	Water body	95		1.00		
2.	River	81		0.20		
3.	Forest	65		0.25		
4.	Range land	86		0.30		
5.	Built-up area	79		0.40		
6.	Agriculture land	82		0.28		
7.	Barren land	91		0.32		
8.	Miscellaneous	60		0.25		

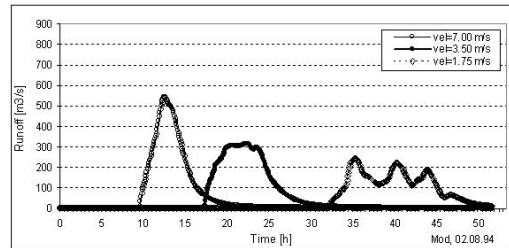
Annex 6.2 Manning roughness coefficients for various channel types

Channel types	Roughness coefficients
1. Concrete lining	0.011 to 0.013
2. Clay or earth channel in good condition	0.015 to 0.017
3. Straight unlined earth channels	0.020
4. Rivers and earth channels in fair conditions	0.025
5. Winding natural streams and canals in poor condition	0.035
6. Mountain streams with rocky beds and rivers with variable sections and some vegetation along banks	0.040 to 0.050
7. Alluvial channels, sand bed (lower regime)	0.017 to 0.028
8. Alluvial channels, sand bed (upper regime)	0.012 to 0.020

Annex 6.3 Modelling the effect of cloud velocity for small size rainfall event of 02.08.1994 on runoff generation at a.) Anterbeliya and b.) Mod stations respectively

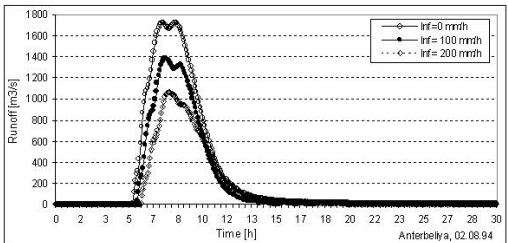


a.

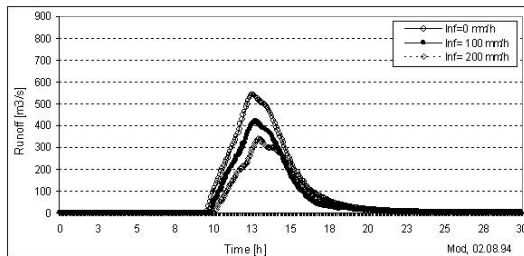


b.

Annex 6.4 Modelling the effect of infiltration rate for small size rainfall event of 02.08.1994 on runoff generation at a.) Anterbeliya and b.) Mod stations respectively



a.



b.

Lebenslauf

**Anupam K. Singh**

15.06.1967	Geboren in Kanasi/ Indien
07/1979 bis 05/1983	10+2 von Gymnasium Manjhana, Farrukhabad/ Indien
09/1983 bis 05/1985	Bakkalaureus im Science (B.Sc.) an der KN Institute of Science and Technology (Avadh University Faizabad)/ Indien
08/1985 bis 06/1989	Bauingenieurwesen (B.Tech.) an der KN Institute of Technology Sultanpur/ Indien
09/1989 bis 02/1991	Landesplanung (M. Planning) an der School of Planning and Architecture (Deemed University) New Delhi.
03/1991 bis 07/1992	Planner (Behörde) am Staatesbau u- Landesplanung, Amt der Ministerium von Gebäude u- Umwelt, Bhopal.
08/1992 bis 06/1995	Wissenschaftlicher Mitarbeiter am Zentrum für Ländliches Entwicklung, School of Planning and Architecture New Delhi.
01/1994 bis 06/1994	Stipendium zum P.G. Dipl. Studium an der Technische Universität Stettin, Polen.
07/1995 bis 06/1996	Manager bei Ingenieur u- Beratungsbüro, Development Management Group (India) Pvt. Ltd. New Delhi.
08/1996 bis 09/1998	Aufbaustudium des M. Sc. (Resources Engineering) an der Universität Karlsruhe (TH)
02/1997 bis 1999	Wissenschaftliche Hilfskraft (Abt. Kulturtechnik) am Institut für Wasserwirtschaft und Kulturtechnik, Universität Karlsruhe (TH)
09/1998 bis 03/2000	Mitarbeiter Ingenieurbüro Dr.-Ing. Klemm, Schollbronn
Seit 03/2000	Doktorand und Wissenschaftliche Mitarbeiter am Institut für Wasserwirtschaft und Kulturtechnik, Universität Karlsruhe (TH)

